ATRIAL ARRHYTHMOGENESIS IN A MURINE MODEL OF MITOCHONDRIAL INSUFFICIENCY

HASEEB VALLI

HUGHES HALL, CAMBRIDGE

January 2019

This dissertation is submitted for the degree of Doctor of Philosophy

Declarations

I declare that this thesis is the result of my own work and contains nothing that is the outcome of work done in collaboration with others, except as declared in the Preface and specified in the text. It has not been submitted for any other degree or qualification. It is not substantially the same as any that I have submitted, or, is being concurrently submitted for a degree or diploma or other qualification at the University of Cambridge or any other University or similar institution except as declared in the Preface and specified in the text.

I further state that no substantial part of my dissertation has already been submitted, or, is being concurrently submitted for any such degree, diploma or other qualification at the University of Cambridge or any other University or similar institution except as declared in the Preface and specified in the text

The dissertation does not exceed the word limit for the Degree Committee of the Faculty of Biology (word count 53410, excluding references).

All of the work from this thesis has been peer reviewed and published, and the relevant citations are listed in the following pages.

Haseeb Valli
January, 2019

Summary

Atrial arrhythmogenesis in a murine model of mitochondrial insufficiency

Haseeb Valli

Age-related atrial arrhythmias are frequently encountered in clinical practice and represent a major public health issue owing to evolving population demographics and rising prevalence of their respective risk factors. Of these, atrial fibrillation (AF) is the most common sustained arrhythmia affecting in excess of 8 million in Europe, and this figure is projected to rise to 18 million by 2060. AF, independent from other known predictors of mortality, doubles death rates, confers a five-fold increase in the risk of stroke, is associated with impaired left ventricular function and contributes to cognitive decline.

The trend in increasing incidence mirrors that of a number of the constituents of the metabolic syndrome, including obesity, insulin resistance and hypertension. There is increasing data implicating metabolic, and in particular mitochondrial, dysfunction as a central feature of the biochemical changes that characterise ageing as well as the conditions listed above, and may also underlie the susceptibility to AF that accompany these states. Abnormal mitochondrial structure has been noted in animal and human studies of AF. Whether the observed mitochondrial abnormalities are a cause or consequence of AF, or the mechanisms through which these changes occur remain largely unexplored.

A putative role for chronic mitochondrial impairment in the pathogenesis of such atrial arrhythmias was investigated here using a murine model with homozygous deficiency of the transcriptional coactivator peroxisome proliferator-activated receptor γ coactivator-1 β (*Pgc-1β*). *Pgc-1β* regulates mitochondrial biogenesis and function, and unlike other murine models of mitochondrial dysfunction *Pgc-1β*$^{-/-}$ mice have a mild cardiac phenotype, devoid of confounding contractile dysfunction.

As the sequelae of chronic mitochondrial dysfunction progress with age, all experiments were performed in young (12-16 weeks) and aged (>52 weeks) *Pgc-1β*$^{-/-}$ mice and compared to aged-matched wild type (WT) controls. The investigations were initially performed in the in vivo setting using electrocardiographic assessment of electrical properties at baseline and following β1-adrenergic (intraperitoneal dobutamine) challenge. *Pgc-1β*$^{-/-}$ animals displayed chronotropic incompetence suggesting sino-atrial node disease and a paradoxical negative dromotropic response to dobutamine

suggesting atrioventricular node dysfunction. The deficiency was also associated with evidence of slowed conduction, together alluding to underlying remodelling phenomena.

More detailed evaluation of the atrial phenotype associated with *Pgc-1β* deficiency was performed using sharp microelectrode recordings of cellular action potentials (AP) in a whole-heart Langendorff-perfused system during programmed electrical stimulation. The *Pgc-1β*$^{-/-}$ genotype was associated with an atrial arrhythmic phenotype that progressed with age. Young and aged *Pgc-1β*$^{-/-}$ hearts showed evidence of slowed AP conduction at the cellular level, through deficits in maximum rates of AP depolarization $(dV/dt)_{max}$, and at the tissue level through prolonged AP latencies. Action potential duration (APD) was also significantly shorter in *Pgc-1β*$^{-/-}$ hearts at high heart rates.

APD restitution has previously been linked to the pathogenesis of ventricular fibrillation and more recently AF. However in the present work the incidence of alternans or steepness of the restitution curves did not correlate with arrhythmic tendency, but rather ageing was associated with flattening of the APD restitution curve and reduced episodes of alternans. Arrhythmogenecity better correlated with reductions in AP wavelength parameters in *Pgc-1β*$^{-/-}$ hearts.

The mechanisms underlying the altered electrical properties were then investigated, firstly using a novel loose patch clamp technique permitting transmembrane current recordings in intact atrial preparations preserving the in vivo extracellular and intracellular conditions. *Pgc-1β*$^{-/-}$ atria had significantly lower inward Na^+ currents than that of WT preparations, correlating to the differences in $(dV/dt)_{max}$ values obtained. No differences in delayed outward (K^+) currents were evident. Morphometric analysis revealed that *Pgc-1β* deficiency was associated with accelerated fibrosis, with aged *Pgc-1β*$^{-/-}$ hearts displayed the greatest fibrotic change.

The *Pgc-1β*$^{-/-}$ murine model of chronic mitochondrial impairment results in an atrial arrhythmic phenotype that progresses with age. The transgenic mice develop progressive electrical and structural remodelling producing an atrial substrate promoting AP reentry and arrhythmia persistence. A number of the adverse remodelling phenomenon observed mirror those seen in human AF and therefore implicate mitochondrial impairment as a potential upstream mediator of age-related arrhythmogenesis.

إِنَّمَا الْأَعْمَالُ بِالنِّيَّاتِ، وَإِنَّمَا لِكُلِّ امْرِئٍ مَا نَوَى

لِكُلِّ دَاءٍ دَوَاءٌ

Contents

Publications

The following publications were achieved following peer review during the course of the PhD. Research publications 1 – 4 make up the main chapters (Chapters 3 – 6) of the thesis. Publication 1 was performed in collaboration with Dr Shiraz Ahmad.

1. *Ahmad S, *Valli H, Salvage SC, Grace AA, Jeevaratnam K & Huang CL-H (2018). Age-dependent electrocardiographic changes in *Pgc-1β* deficient murine hearts. *Clin Exp Pharmacol Physiol* **45,** 174–186.

2. Valli H, Ahmad S, Chadda KR, Al-Hadithi ABAK, Grace AA, Jeevaratnam K & Huang CL-H (2017*a*). Age-dependent atrial arrhythmic phenotype secondary to mitochondrial dysfunction in *Pgc-1β* deficient murine hearts. *Mech Ageing Dev* **167,** 30–45.

3. Valli H, Ahmad S, Fraser JA, Jeevaratnam K & Huang CL-H (2017*b*). Pro-arrhythmic atrial phenotypes in incrementally paced murine *Pgc1β* $^{-/-}$ hearts: effects of age. *Exp Physiol* **102,** 1619–1634.

4. Valli H, Ahmad S, Jiang AY, Smyth R, Jeevaratnam K, Matthews HR & Huang CL-H (2018*a*). Cardiomyocyte ionic currents in intact young and aged murine *Pgc-1β*$^{-/-}$ atrial preparations. *Mech Ageing Dev* **169,** 1–9.

5. Ning F, Luo L, Ahmad S, Valli H, Jeevaratnam K, Wang T, Guzadhur L, Yang D, Fraser J, Huang C-H, Ma A & Salvage S (2016). The RyR2-P2328S mutation downregulates Na(v)1.5 producing arrhythmic substrate in murine ventricles. *Pflugers Arch* **468,** 655–665.

6. Chadda KR, Ahmad S, Valli H, den Uijl I, Al-Hadithi AB, Salvage SC, Grace AA, Huang CL-H & Jeevaratnam K (2017). The effects of ageing and adrenergic challenge on electrocardiographic phenotypes in a murine model of long QT syndrome type 3. *Sci Rep* **7,** 11070.

7. Jeevaratnam K, Chadda KR, Salvage SC, Valli H, Ahmad S, Grace AA & Huang CL-H (2017). Ion channels, long QT syndrome and arrhythmogenesis in ageing. *Clin Exp Pharmacol Physiol* **44,** 38–45.

8. Valli H, Ahmad S, Sriharan S, Dean LD, Grace AA, Jeevaratnam K, Matthews HR & Huang CL-H (2018). Epac-induced ryanodine receptor type 2 activation inhibits sodium currents in atrial and ventricular murine cardiomyocytes. *Clin Exp Pharmacol Physiol* **45,** 278–292.

*Joint first author

Acknowledgments

As a recipient of the Wellcome Trust Clinical Research Training Fellowship, I would like to thank the Wellcome Trust for the generous support of this PhD project. I would also like to extend my gratitude to the Sudden Arrhythmic Death UK society and the NIHR BRC for supporting my research.

I am indebted to my supervisor Prof. Chris Huang for his tireless support and encouragement throughout my PhD. His immense patience, dedication, attention to detail, intellectual rigour and scientific direction has been inspirational during my research.

I would like to express my gratitude to my co-supervisor Dr Andrew Grace for his generous support and advice. I would also like to thank Dr Hugh Matthews for assistance in developing the loose patch clamp technique and providing relevant advice throughout this period. I am very grateful to Dr James Fraser for use of his laboratory space for various experiments.

I have been fortunate to have had the opportunity to work with some very talented individuals during this period. I am very thankful for being able to work and develop a friendship with Dr Shiraz Ahmad and Dr Kamalan Jeevaratnam, both of whom provided invaluable support through the duration of this fellowship and with whom I look forward to collaborating with in the years to come. I am grateful for the help given Ali Al-Hadithi, Anita Jiang, Robert Smyth, Karan Chadda, Sujan Sriharan, Lydia Dean, Vishal Vyas and James Cranley, and wish them all the best in their studies and future careers. Mr Alan Cattell, Mr Paul Frost and Ms Vicky Johnson's technical assistance, helpful anecdotes and biographical tails made difficult days more bearable.

Finally, words cannot describe the debt of gratitude I owe to various members of my family – my parents, siblings, and my wife for providing the foundation upon which all of these efforts are supported.

There are many more whom I have not been able to mention by name, but I am grateful to nonetheless.

Abbreviations

ADP	Adenosine diphosphate
AF	Atrial fibrillation
AFL	Atrial flutter
ANOVA	Analysis of variance
AP	Action potential
APD	Action potential duration
APD_{90}	AP durations at 90% repolarisation
AT	Atrial tachycardia
ATP	Adenosine triphosphate
AUC	Area under the curve
AV	Atrioventricular
AVN	Atrioventricular node
AVNRT	Atrioventricular nodal re-entrant tachycardia
AVRT	Atrioventricular re-entrant tachycardia
BCL	Basic cycle length
BDM	2,3-butanedione monoxime
BrS	Brugada syndrome
$[Ca^{2+}]_i$	Intracellular calcium concentration
CaMKII	Ca^{2+}/calmodulin dependent protein kinase II
CPVT	Catecholaminergic polymorphic ventricular tachycardia
CV	Conduction velocity
DAD	Delayed after-depolarisation
DI	Diastolic Interval
DI_{crit}	Critical diastolic Interval
DNA	Deoxyribonucleic acid

$(dV/dt)_{max}$	Maximum rates of AP depolarization
EAD	Early after-depolarisation
ECG	Electrocardiogram
Epac	Exchange protein directly activated by cAMP
ERR	Estrogen-related receptors
FOXO1	Forkhead box O1
HNF-4	Hepatic nuclear factor-4
I_{CaL}	L-type calcium current
I_{Cl}	Calcium-activated chloride current
I_{KUR}	Ultrarapid rectifier potassium current
I_{K1}	Inward rectifying K^+ channels (I_{K1}).
I_{Kr}	Rapid delayed rectifier potassium current
I_{Ks}	Slow delayed rectifier potassium current
I_{Na}	Fast inward sodium current
I_{to}	Transient outward potassium current
$I_{to,f}$	Fast transient outward potassium current
$I_{to,s}$	Slow transient outward potassium current
IR	Ischaemia-reperfusion
KH	Krebs-Henseleit
LA	Left atrium
LQTS	Long QT syndrome
MANOVA	Multiple analysis of variance
MEA	Multi-electrode array
MEF-2	Myocyte enhancer factor-2
mtDNA	Mitochondrial DNA
Nav	Voltage-gated sodium channel
NCX	Na^+/Ca^{2+} exchanger
NRF-1	Nuclear respiratory factor-1

NRF-2	Nuclear respiratory factor-2
PES	Programmed electrical stimulation
PGC-1	Peroxisome proliferator-activated receptor γ coactivator-1
PKA	Protein kinase A
PPAR	Peroxisome proliferator-activated receptors
PS	Phase singularity
PV	Pulmonary Vein
RMP	Resting membrane potential
RFA	Radiofrequency ablation
ROS	Reactive oxygen species
RyR2	Cardiac isoform of ryanodine receptor
SAN	Sino-atrial node
sarcK$_{ATP}$	Sarcolemmal K-ATP channel
SEM	Standard error of the mean
SERCA	Sarcoplasmic reticulum calcium ATPase
SNP	Single nucleotide polymorphism
SR	Sarcoplasmic reticulum
SREBP1	Sterol regulatory element-binding protein-1
Sox9	Sry-related HMG box-9
Tfam	Mitochondrial transcription factor A
TGF-β	Transforming growth factor-β
VF	Ventricular fibrillation
VT	Ventricular tachycardia
WT	Wild type

List of Figures

List of Tables

1 Introduction

1.1 Atrial Arrhythmias

Heart rhythm abnormalities involving the atria, whether presenting as pathological slowing of the atrial rate or non-physiological acceleration, are common and often symptomatic. While some forms of such atrial arrhythmias are benign, others are associated with significant morbidity and mortality.

Tachy-arrhythmias involving the atrioventricular junction include atrioventricular re-entrant tachycardia (AVRT) and atrioventricular nodal re-entrant tachycardia (AVNRT), both of which are characterised by the presence of anatomical pathways that provide a substrate for re-entry. As such these can be considered as being congenital in nature and accordingly are amongst the most prevalent forms of tachy-arrhythmias encountered in younger cohorts (Porter *et al.*, 2004).

Atrial tachy-arrhythmias include atrial flutter (AFL) and atrial fibrillation (AF), which in the majority of cases are acquired arrhythmias presenting later in life. Of these, AF has the highest prevalence and represents a significant clinical challenge. Consequently AF has been and remains the subject of intense study, and is accordingly the primary focus of the present work. However both arrhythmias share similar risk factors (Vidaillet *et al.*, 2002) and frequently co-exist in the same individual though their episodes may be temporally segregated (Halligan *et al.*, 2004). Amongst 110 individuals who underwent radiofrequency ablation (RFA) for typical AFL, 25% had documented AF during mean follow-up of 20.1 ± 9.2 months (Paydak *et al.*, 1998). In a separate study 31% of 333 patients undergoing RFA for AFL developed AF during mean follow-up of 29 ± 17 months (Hsieh *et al.*, 2002) and of those undergoing similar treatment at the Cleveland Clinic this figure was as high as 82% during a follow-up period of 39 ± 11 months (Ellis *et al.*, 2007). Thus these arrhythmias, together with some forms of focal atrial tachycardias (AT), may therefore represent varying manifestations of a common electrophysiological 'atriopathy'.

AFL, particularly in its most common form, is very amenable to curative treatment with RFA. In contrast, despite its high prevalence and significant clinical consequences, the efficacy of

therapeutic strategies for the treatment of AF remain modest. To a large extent progress on this front has been hampered by the limited understanding of the cellular and molecular mechanisms that govern its initiation and perpetuation. Animal models provide valuable platforms to characterise and sequence such changes, and identify new targets for intervention.

1.2 Cardiac Electrophysiology

1.2.1 The cardiac conduction system

Normal electrical excitation propagates through the heart as a wave of depolarisation, coupled to contraction, in a time ordered sequence to maintain cardiac output. Cardiac cells are anchored to an average of eight neighbouring cells via intercalated discs within which low resistance gap junctions electrically couple the cells, allowing rapid propagation of the depolarising wavefront.

In normal sinus rhythm, this electrical activity initiates in the sino-atrial node (SAN) located at the junction of the superior vena cava and right atrium. The SAN consists of a collection of specialised pacemaker cells that have an unstable resting membrane potential that decays during diastole, eventually reaching the threshold to trigger an action potential (AP). The electrical impulse generated rapidly traverses the atria, propagating to the left atrium through the Bachmann's Bundle, stimulating atrial contraction, and reaching the atrioventricular node (AVN) via internodal tracts. The AVN serves to retard the conduction of the electrical impulse to the ventricles, permitting atrial contraction to occur prior to the onset of ventricular systole thereby optimising ventricular filling. It also acts as a low pass filter, preventing rapid atrial rates being conducted to the ventricles. The nodal cells of the AVN are phenotypically similar to those of the SAN, with low expression of rapidly conducting voltage gated Na^+ channels (Nav1.5), responsible for the fast inward Na^+ current (I_{Na}), and instead their AP upstroke is driven by Ca^{2+} influx through the relatively slower L-type Ca^{2+} channels (I_{CaL}). These as well as other differences in ion channel expression give rise to the slower AP upstroke and relatively long action potential duration (APD) of the nodal cells, underlying the conduction delay and decremental properties of the AVN (Figure 1.1).

From the AVN, the electrical impulse rapidly conducts down the bundle of His, originally defined by Sunao Tawara in 1906, as the point at which the AVN fibres penetrate the central fibrous body (Tawara S, 1906). The His bundle bifurcates into the right and left bundle branches, transmitting the electrical impulse along the interventricular septum to the right and left ventricles respectively, and then through the Purkinje fibres to the endocardium at the apex. The wavefront can then spread through the ventricular myocardium from apex to base and from endocardium to epicardium. Repolarisation of the ventricles occurs in the reverse sequence, that is from base to apex and epicardium to endocardium. Accordingly, the APD at the base and epicardium are shorter than those at the apex and endocardium.

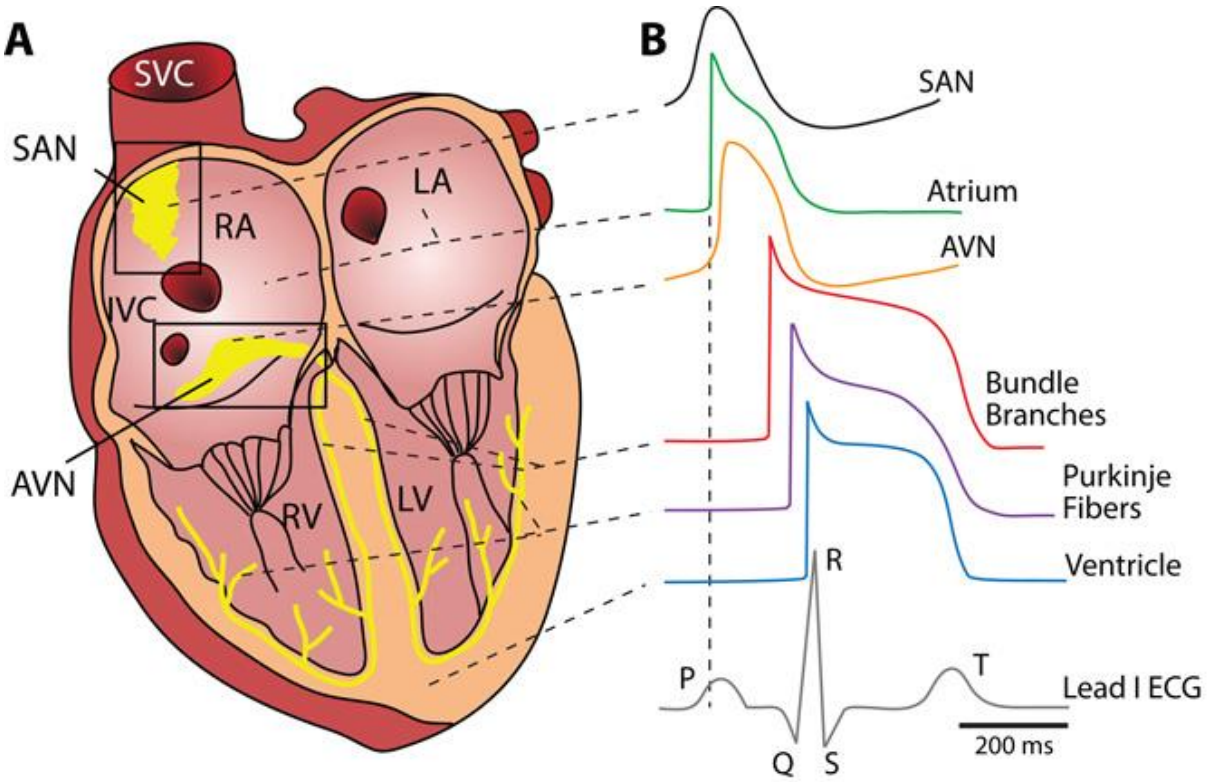

Figure 1.1 Anatomy of the cardiac conduction tissue

Schematic outlining the specialised conduction tissues in the mammalian heart (A) and their respective characteristic AP and surface electrocardiogram waveforms (B) (Adapted from Bartos et al., 2015)

1.2.2 The resting membrane potential

The resting membrane potential (RMP) is the potential difference across the cell membrane in the non-stimulated state and is determined by the ions present in each compartment (intracellular and extracellular), their valency and the membrane permeability to these. Where only a single ion is present and/or the membrane is exclusively permeable to a single ion, the potential difference measured across the membrane at equilibrium for given intracellular and extracellular concentrations can be determined through the Nernst equation:

$$E_X = \frac{RT}{zF} \ln\left(\frac{[X]_{out}}{[X]_{in}}\right)$$

where R is the ideal gas constant (8.31 J K^{-1} mol^{-1}); T is absolute temperature; z is the valency; F is Faraday's constant (9.65x10^4 C mol^{-1}); and E is the equilibrium potential for ion X.

The RMP of a cardiomyocyte is approximately -85mV, close to the Nernst potential of K^+, which was the basis of the Bernstein Hypothesis that *"the cell membrane is selectively permeable to K^+ at rest and hence the cell resting potential is the result of the Nernst potential for K^+"* (Bernstein, 1902). In reality the RMP is generally less negative than the equilibrium potential for K^+ and reflects the permeability of the membrane to additional ions, primarily Na^+ and Cl^-, and can be calculated from a more generalised form of the Nernst equation, the Goldman-Hodgkin-Katz equation:

$$E_m = \frac{RT}{zF} \ln\left(\frac{P_K\,[\mathrm{K^+}]_\mathrm{o} + P_{Na}\,[\mathrm{Na^+}]_\mathrm{o} + P_{Cl}\,[\mathrm{Cl^-}]_\mathrm{i}}{P_K\,[\mathrm{K^+}]_\mathrm{i} + P_{Na}\,[\mathrm{Na^+}]_\mathrm{i} + P_{Cl}\,[\mathrm{Cl^-}]_\mathrm{o}}\right)$$

where P_x represents the membrane permeability to ion X. As mentioned, pacemaker cells display a decaying RMP, termed the pacemaker potential, progressively rising from -60mV towards their threshold potential of between -50mV - -40mV.

1.2.3 The cardiac action potential

The unit per cell of cardiac excitation is the AP, a time-dependent voltage waveform that propagates along excitable tissues. It is generated through changes in membrane permeability, permitting a coordinated sequence of ion fluxes through their respective ion channels down their electrochemical gradients. The movement of each ion in or out of the cells biases the membrane potential towards its equilibrium potential.

Based in the Physiological Laboratory at the University of Cambridge, Draper and Weidmann published the first intracellular AP recordings from mammalian cardiac cells (Draper and Weidmann, 1951), adapting the microelectrode technique developed by Ling and Gerard to record skeletal muscle membrane potentials (Ling and Gerard, 1949). Interestingly Hodgkin, on visiting the University of Chicago from Cambridge, was introduced to the glass microelectrode technique by Gilbert Ling and adapted these methods to record fast events (Hodgkin and Nastuk, 1949). Hodgkin was focussed on skeletal muscle, training Weidmann in the protocol and remarking "*Here is a powerful tool. Prod round in nature, but keep the skeletal muscle reserved for me*" (Weidmann, 1993). Weidmann and Draper sampled isolated canine Purkinje fibre bundles owing to their weak contractions, thus obviating issues with electrode displacement or fracture, and provided the first details on the voltage-time course of the cardiac AP, the magnitude of the resting potential and the various phases of repolarisaton (Figure 1.2).

Figure 1.3 shows the prototypical human atrial and ventricular AP waveforms, and the various ionic currents that contribute to their formation. The *phase 0* upstroke is initiated by depolarisation of the membrane to its threshold value resulting in the activation of Nav1.5 voltage-gated Na^+ channels and influx of Na^+ into the cell along its electrochemical gradient. The α subunit of the Nav1.5 channel is encoded by the *SCN5A* gene, and the channel activates in a regenerative fashion that accounts for the fast inward Na^+ current, in the order of 400 $\mu A\ \mu F^{-1}$. The channels also rapidly inactivate, the entire process being completed in approximately 1 ms or less, and require the period of one absolute refractory period to elapse before being capable of further activation. This is followed by a period of relative refractoriness where a sub-population of the channels remain inactive and a larger than normal voltage excursion is required to bring the membrane to threshold for a second depolarisation.

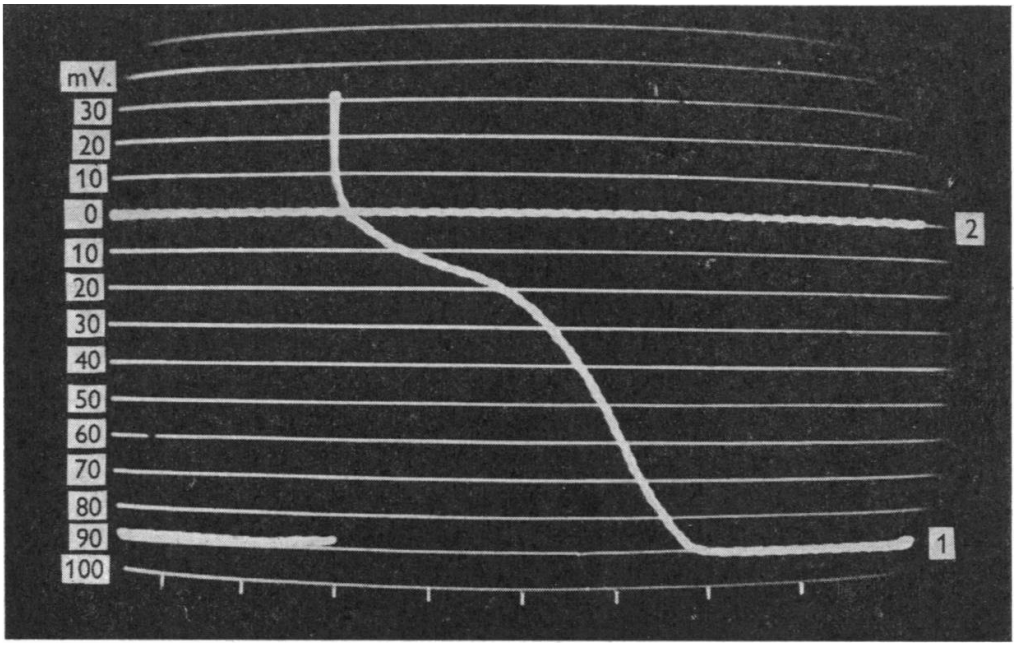

Figure 1.2 Canine Purkinje fibre action potential

First published intracellular cardiac action potential recording using glass microelectrodes in a superfused canine Purkinje fibre bundle preparation. The cells demonstrated automaticity, spontaneously contracting after being immersed in warm Tyrode's solution for 20-30mins. Note resting potential of -90mV and clearly demonstrating the now recognised phases of the cardiac action potential. (Adapted from Draper and Weidmann 1951))

A brief early repolarisation phase (*phase 1*) follows, mediated by opening of K^+ channels carrying the fast and slow transient outward currents, $I_{to,f}$ and $I_{to,s}$. $I_{to,f}$ activates and inactivates rapidly, with time constants in the range of 60 -100 ms, in a conventional voltage dependent manner (Näbauer *et al.*, 1996; Hoppe *et al.*, 1999). Its pore-forming (α) subunits are from the Kv4 subfamily, Kv4.2 and Kv4.3 encoded by *KCND2* and *KCND3* respectively (Nerbonne & Kass, 2005). $I_{to,s}$ is less well characterised and has greater variation between species. Its current is carried by the Kv1.4 channel encoded by *KCNA4* and is thought to activate in response to changes in the intracellular free Ca^{2+} concentration and has slower rates of recovery from inactivation, with time constants on the order of seconds (Fermini *et al.*, 1992; Papp *et al.*, 1995; Köster *et al.*, 1999). Though the function of this phase is not entirely clear, I_{to} currents shape the partial repolarisation in *phase 1* and set the initial plateau (*phase 2*) potential. They therefore influence the activity of voltage-gated Ca^{2+} channels and the balance between inward and outward currents during the plateau phase, thus tempering the duration and amplitude of

phase 2. One assumes in part, they prevent the Ca^{2+} current in *phase 2* from depolarising the membrane to E_{Ca}, which would reduce overall Ca^{2+} entry into the cell. In atrial cells the markedly higher densities of I_{to}, together with the expression of the ultrarapid delayed rectifier, accelerate the early phase of repolarization leading to lower plateau potentials and shorter APDs (Varró *et al.*, 1993; Amos *et al.*, 1996). In many species $I_{to,f}$ and $I_{to,s}$ are differentially expressed and contribute to regional heterogeneities in the AP waveform. $I_{to,f}$ is more prominently expressed in the epicardium and mid-myocardium, and underlies the spike and dome morphology of epicardial APs (Liu *et al.*, 1993).

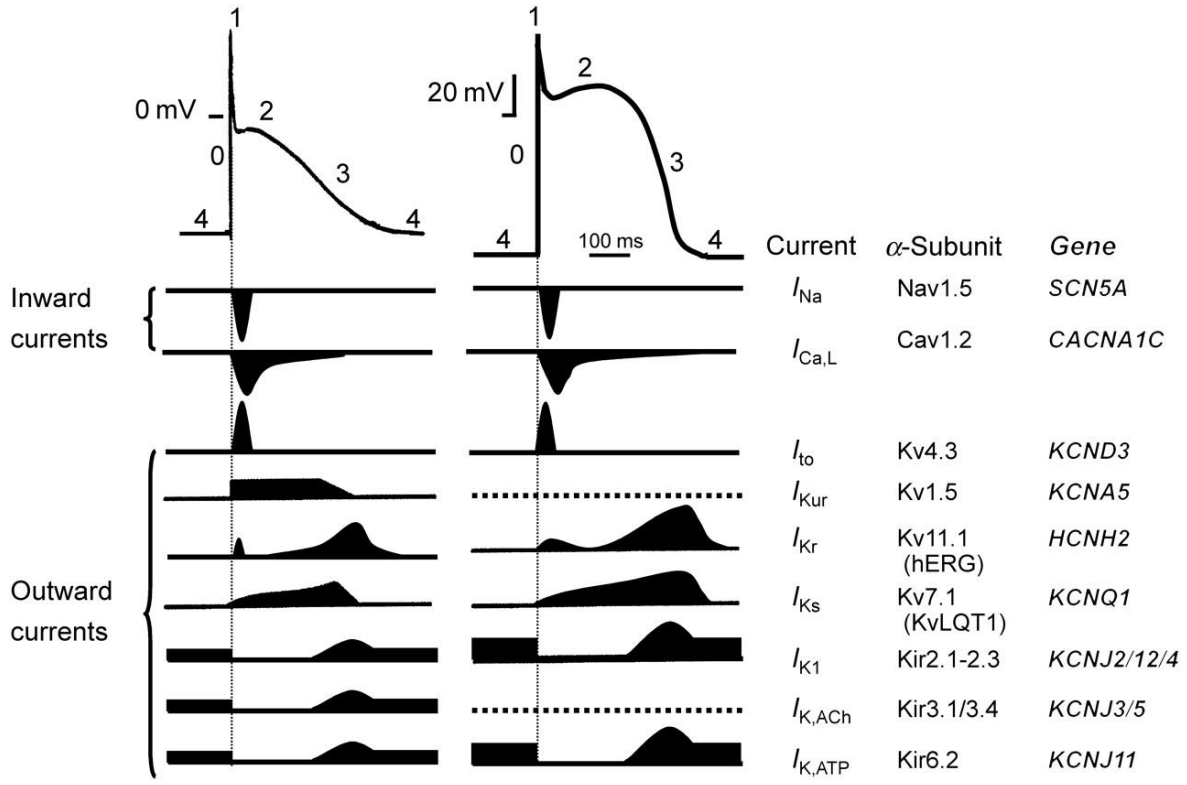

Figure 1.3 Cardiac action potential waveform and relevant currents

Typical action potential profiles from human atrial (left) and ventricular (right) cardiomyocytes. The time course of various ionic currents contributing to the phases of the respective action potentials are shown below the traces where shading above the baseline denotes outward current and shading below the baseline represent inward currents.

The *phase 2* plateau is attributable to a balance between inward currents carried by the L-type Ca^{2+} channel and Na^{+}/Ca^{2+} exchanger (NCX), and a collection of outward rectifying K^{+} currents. The L-type Ca^{2+} channel is a member of the high voltage activated Cav family

encoded by the *CACNA1C* gene, opening at membrane potentials of -25mV and remaining open for approximately 100msecs (Lee *et al.*, 1985). During the plateau phase, the NCX also produces a depolarising current, moving 3 Na^+ ions into the cell and extruding 1 Ca^{2+} ion. The influx of positive ions is counter-balanced by outward potassium currents carried principally by the rapid (I_{Kr}) and slow (I_{Ks}) delayed rectifier K^+ channels. Unlike I_{to}, these slower potassium channel currents persist through the plateau phase. The I_{Kr} current is carried by the Kv11.1 channel (also known as the hERG channel) encoded by the *KCNH2* gene, while the I_{Ks} current is carried by the Kv7.1 channel encoded by the *KCNQ12/3* genes. While both are activated by depolarising voltages during the plateau phase, I_{Kr} channels inactivate more rapidly, passing smaller currents as *phase 2* progresses, whereas I_{Ks} channels activate gradually and show little inactivation (Sanguinetti & Jurkiewicz, 1990). Additional K^+ efflux occurs through the K_{ATP} channel which adopts a closed state in the presence of ATP and so opens during cardiac contractions where intracellular ATP levels fall and ADP levels rise (Noma, 1983).

Late repolarisation in *phase 3* is mediated by the termination of inward movement of Ca^{2+} and continued K^+ efflux from the cell via I_{Kr} and I_{Ks}. I_{Kr} channels cycle through activation and inactivation more swiftly than those responsible for I_{Ks} thus although they inactivate during the *phase 2* plateau, they rapidly recover from inactivation producing a large resurgent outward current driving the membrane towards repolarisation in *phase 3* (Jeevaratnam *et al.*, 2018). I_{Ks} activates in a more gradual manner, accommodating larger outward currents at latter stages of the plateau and into *phase 3*. The additional contribution of the ultrarapid delayed rectifier $K_v1.5$ channel (I_{Kur}), encoded by the *KCN5A* gene, leads to more rapid repolarisation and therefore shorter APs in atrial cells. *Phase 4* reflects electrical diastole where the membrane is held stable at the resting potential, maintained by inward rectifying K^+ channels (I_{K1}).

Ion channel density and composition show distinct regional variation between cardiac chambers and are reflected in specific differences in their respective AP waveforms. Subtle differences also exist within the same chamber from endocardium to epicardium and apex to base. The typical APD of a ventricular cell is 300 - 350 ms, significantly longer than that of skeletal muscle or the nervous system, reflecting its involvement in processes beyond signal propagation. In keeping with the longer APDs, the refractory period is also longer which provides some protection against deleteriously rapid heart rates and also reduce the probability of reentrant excitation under normal conditions.

Atrial APs are shorter than that of ventricular cells, lasting on average 200 ms. The resting membrane potential is slighter higher in atrial cells owing to reduced activity of background inward rectifier K^+ currents. As a result the magnitude of I_{Na} and therefore rates of depolarisation are lower (150 - 300 VS^{-1} in atrial cells Vs. 300 - 400 VS^{-1} in ventricular cells). There is also a lesser role for the slow component of I_{to} in atrial cells, and instead I_{KUR} has a significant role, influencing both the *phase 2* plateau, *phase 3* repolarisation and the APD overall.

1.2.4 Excitation-contraction coupling

Cardiac excitation-contraction coupling is the physiological process through which depolarisation of the cardiomyocyte membrane elicits a mechanical response (Figure 1.4). Sidney Ringer first reported the central role of Ca^{2+} in this process, following a serendipitous mix up in the laboratory water supply (Ringer, 1883). The influx of extracellular Ca^{2+} into the cell during the AP plateau produces a small but significant increase in the intracellular Ca^{2+} concentration, $[Ca^{2+}]_i$. The subsequent binding of free Ca^{2+} to the cardiac ryanodine receptor (RyR2) located on the membrane of the sarcoplasmic reticulum (SR), triggers Ca^{2+} induced Ca^{2+} release from the SR stores. The resultant more pronounced increase in $[Ca^{2+}]_i$ promotes binding of Ca^{2+} to troponin C, causing a transformational change that facilitates actin-myosin cross bridge formation and ultimately muscle contraction. The systolic Ca^{2+} transient is followed by a return of $[Ca^{2+}]_i$ to diastolic levels, and muscle relaxation in preparation for the process to repeat. This restoration of diastolic Ca^{2+} levels occurs through extrusion to the extracellular compartment via NCX activity and action of the Ca^{2+} ATPase, or transfer into intracellular organelles by the SR Ca^{2+} - ATPase (SERCA) and the mitochondrial Ca^{2+} uniporter (Bers, 2002).

Unlike ventricular myocytes, atrial cells have a far less extensive T-tubule system. In its place, these cells have a highly convoluted arrangement of the SR with projections lying perpendicular to the sarcolemma, termed Z-tubules. They also have two separate populations of RyR2 channels, some located on the Z-tubules in close proximity to the sarcolemma mirroring the arrangement in the dyadic clefts of ventricular myocytes, and a further population is located more centrally within the cell. This arrangement results in a more heterogeneous calcium induced calcium release response in atrial cells than in ventricular

cells. Under basal conditions, the elevation evoked by depolarisation is largely limited to the periphery of the cell whereas the bulk of the protein filaments involved with contraction sit deeper within the cell. In certain conditions, for example with sympathetic stimulation, centripetal propagation of the Ca^{2+} transient is seen with activation of the inner population of RYR2 channels, greater recruitment of the contractile machinery and more pronounced atrial contraction (Bootman *et al.*, 2006).

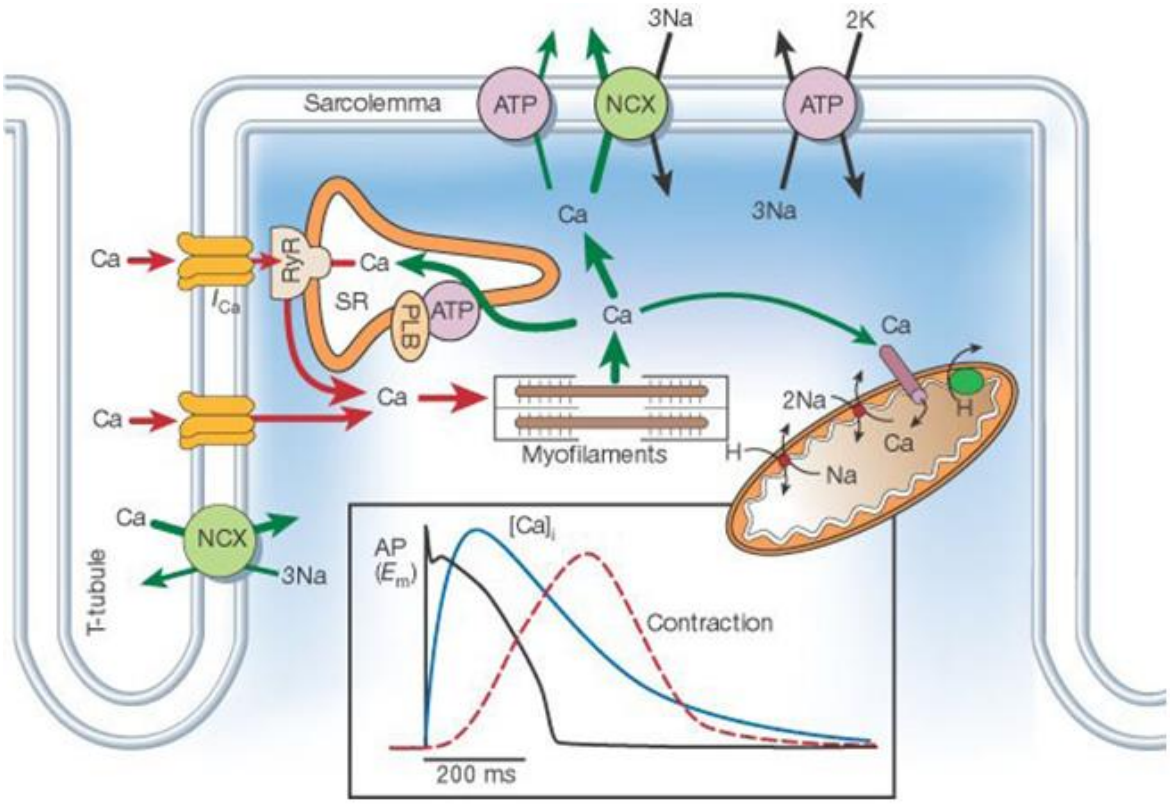

Figure 1.4 Excitation-contraction coupling

Pathways of Ca^{2+} entry into the myocyte (red arrows) and removal from intracellular compartment (green arrows). Inset displays time course of action potential, the Ca^{2+} transient and muscle contraction. (Adapted from Bers, 2002).

1.3 Mechanisms of arrhythmogenesis

Cardiac arrhythmias represent at the organ level, disruptions in the orderly process of myocardial excitation. They may be classified on a mechanistic basis as those arising through i) abnormalities in AP generation, ii) abnormalities in AP propagation (reentry) or iii) a combination of the two (Hoffman & Rosen, 1981).

1.3.1 Abnormal action potential generation

Inappropriate AP formation can be initiated through several mechanisms. These include the non-physiological acceleration of normal pacemaker cell automaticity, most commonly in response to significant hypokalaemia or drugs such as digitalis, and is termed enhanced normal automaticity. Furthermore, myocardial cells in the atrium and ventricle outside of the specialised conduction system do not display the spontaneous resting depolarisation observed in pacemaker cells and therefore lack this feature of automaticity. However 'abnormal automaticity' or depolarisation-induced automaticity is observed in such cells, most commonly under conditions of reduced RMP such as in ischaemia or infarction and may underlie certain arrhythmias (Katzung *et al.*, 1975; Ypey *et al.*, 2013).

The hierarchical organisation of the cardiac conduction tissue mean that the propagating wavefront of the dominant pacemaker, usually the SAN, resets other latent pacemaker sites and suppresses their activity. A region of conduction block near such subsidiary pacemaker tissue due to infarction or infection, can prevent the propagating wavefront from invading this focus, enabling the alternate pacemaker region to escape its usual censorship. This parallel activity of two (or more) pacemaker sites is termed parasystole.

Dysregulation of automaticity and instances of parasystole have classically been regarded as rare causes of tachy-arrhythmias, though depolarisation-induced automaticity has not been extensively studied and its contribution possibly under-represented. In contrast extra-systoles originating in regions outside of the specialised conduction system, referred to as triggered activity, are thought to have a more prominent role in arrhythmogenesis. They are usually a result of after-depolarisation phenomena, which are oscillations of the membrane potential that are a function of the preceding AP and if of sufficient amplitude can trigger a premature AP, and hence a triggered beat (Figure 1.5).

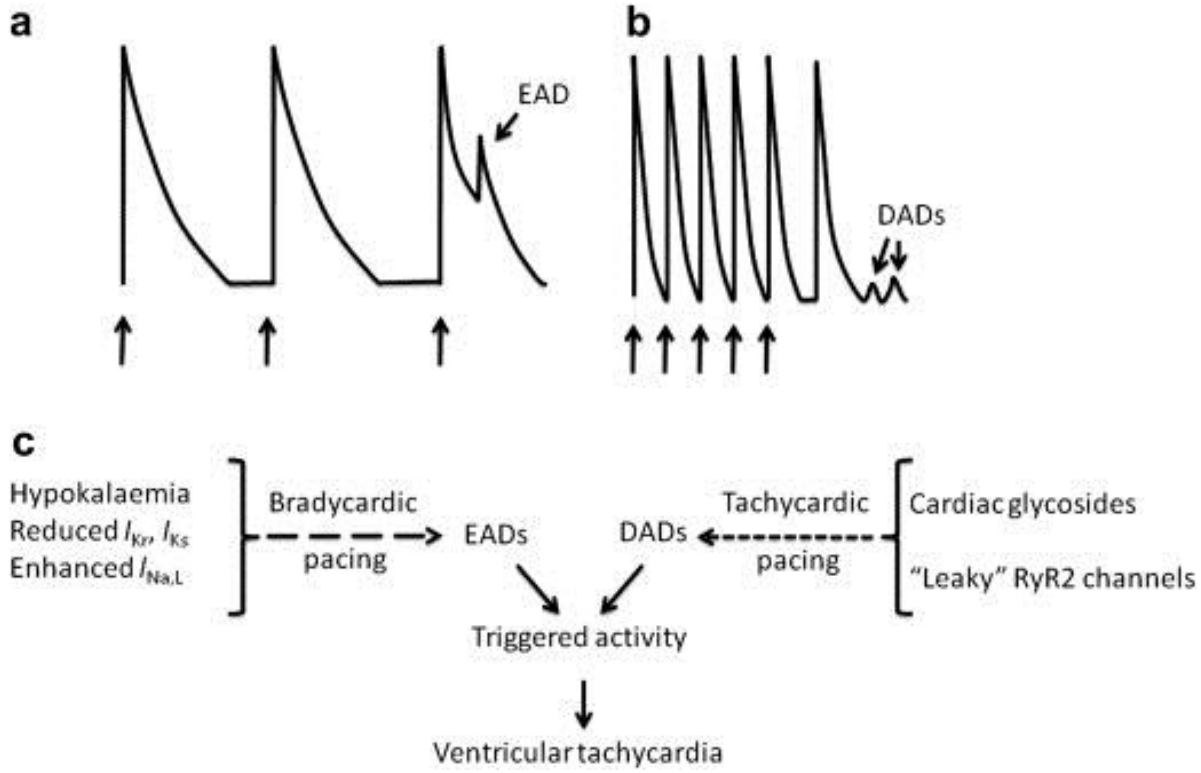

Figure 1.5 Representation of early- and delayed-afterdepolarisation phenoma

Arrhythmogenic triggers and conditions favouring their induction in the murine heart. (a) Early-after depolarisations (EADs) induce premature depolarizations in the otherwise monotonic repolarization phase. (b) delayed-after depolarisations (DADs) represent small, transient oscillations in resting membrane potential following full repolarization. (c) EADs are frequently observed in the setting of marked action potential prolongation, through compromised repolarization seen in LQTS and bradycardia. DADs typically occur in the presence of rapid pacing and conditions which favour diastolic leak of calcium through RyR2 channels, in catecholaminergic polymorphic ventricular tachycardia (CPVT) or cardiac glycoside toxicity. (Arrows in panels a and b represent pacing stimuli). (Adapted from Killeen et al., 2008)

After-depolarisation events that interrupt the phase 2 plateau or prior to repolarisation in phase 3 are termed early after-depolarisations (EADs). EADs generally occur in circumstances associated with prolongation of the APD, where the balance of active current during phase 2 or phase 3 of the AP is shifted in the inward direction. This may be a result of abnormalities in I_{Na} inactivation, a persistent late Na^+ current (I_{NaL}), or reductions in outward K^+ currents. Alternatively prolonged APD allows time for L-type Ca^{2+} channels to recover from inactivation with the resultant I_{CaL} depolarising the membrane and triggering an after-

depolarisation (January *et al.*, 1988; Zeng & Rudy, 1995; Weiss *et al.*, 2010). EADs have been demonstrated in models of arrhythmia associated with hypokalaemia and long QT syndrome (LQTS) (Fabritz *et al.*, 2003*b*; Killeen *et al.*, 2007). Delayed after-depolarisations (DADs) occur where repolarisation is complete (phase 4) or near complete and are observed under conditions that augment $[Ca^{2+}]_i$, which invoke diastolic Ca^{2+} discharge from the SR. The resultant inward current through activity of the NCX and/or calcium-activated chloride current, I_{Cl}, depolarises the cell triggering an AP (Venetucci *et al.*, 2007). Such arrhythmias have been observed in response to digitalis toxicity (Rosen *et al.*, 1973; Gold *et al.*, 2000) and catecholaminergic polymorphic ventricular tachycardia (CPVT) (Jiang *et al.*, 2005).

1.3.2 Cardiac reentry

Reentry refers to abnormal AP propagation where an AP wave fails to completely extinguish following normal activation and is able to re-excite regions that have recovered from refractoriness. John McWilliam was possibly the first to allude to reentry as a mechanism for arrhythmia, during experiments characterising the nature of abnormal ventricular rhythms. Commenting on a pacing induced atrial arrhythmia (which was most likely AFL), he remarked: "*The application of the current sets the auricles into a rapid flutter, the rapidity of which largely depends upon the excitability of the auricular tissue and the strength of current employed. The movements are regular; they seem to consist of a series of contractions originating in the stimulated area and thence spreading over the rest of the tissue. The movement does not show any distinct sign of incoordination; it looks like a rapid series of contraction waves passing over the auricular walls. The difference between this appearance and that seen in the ventricles probably depends on the simpler structure and arrangements obtaining in the auricles. The persistence of the movement after the discontinuance of the stimulating current varies according to the excitability of the auricular tissue and strength of current employed"* (McWilliam, 1887).

Subsequently, in a series of elegant and insightful experiments, Alfred Mayer provided a clearer demonstration of reentry and also highlighted the importance of unidirectional block (Mayer, 1906). In studying the rhythmic pulsation of the jellyfish, *Cassiopea xamachana*, the marginal sense organs were removed and incisions were made in the subumbrella to form circuits, the most simple being a ring (Figure 1.6(a - c)). Where two waves were stimulated either side of a permanent line of block created by an incision, they would travel in opposite

directions and extinguish at the point of collision, producing a single contraction. Similarly a single impulse could traverse circumferentially around the ring but not cross the line of block (Figure 1.6(d)). In contrast, where the ring was intact, if an impulse could be induced to propagate in one direction only (by applying mechanical pressure preventing bidirectional conduction i.e. unidirectional block), the wave would return to the original focus and continue to circulate indefinitely without the need for further stimulation. Beyond these crucial observations, he also highlighted the importance of the refractory period, enabling the tissue to *"recover and regain its sensibility to the stimulus which calls forth the contraction"*.

It was Georges Mines however who extended the application of this concept of reentry as a clinically relevant phenomenon, coining the phrase circus movement, and suggesting that such reciprocating rhythms were responsible for *"some cases of paroxysmal tachycardia as observed clinically"* (Mines, 1913). Mines, through studies on two-chambered electric ray and frog hearts, noted the ability to initiate a perpetual cycle of excitation consistent with a reentry circuit between the atrium and the ventricle. He tested this further by creating a ring preparation in a tortoise heart by making a longitudinal incision extending from the atrium to the ventricle and observed more definitively circus movement of the impulse sequentially through the four component chambers (Figure 1.7(a)). Moreover not only did he propose the novel concept of anatomic reentry but also suggested reentry required differential electrophysiological properties in the two limbs of the circuit and was facilitated by slow conduction and/or a short refractory period (Figure 1.7(b)). These observations provided the foundations for the principal requirements for the initiation of re-entrant arrhythmia (Allessie *et al.*, 1973, 1977):

- An obstacle around which the AP wavefront is able to circulate.
- A conduction velocity sufficiently slow such that each region recovers excitability prior to the wave returning.
- The existence of unidirectional block, preventing the wave from self-extinguishing.

In the clinical setting, the anatomical obstacles around which the reentrant circuit forms may be through the congenital presence of two or more connections between regions such as in AVNRT or AVRT. Alternatively myocardial scars formed following an infarct can form such an obstacle and therefore act as a substrate for reentry. The simplified circuit around such an obstacle is shown in Figure 1.8. In normal rhythm, the AP wavefront conducts through both

limbs (A and B) and collide at the bridge of tissue connecting the two limbs distally (C) causing the wavefront to extinguish within the circuit. If an impulse such as an extrasystole arrives at a time where branch B is refractory or has unidirectional block, the impulse can travel down branch A, across the common distal path and retrograde into the branch B crossing the area of unidirectional block. If on exiting the area of unidirectional block, the AP finds excitable tissue, it can reenter branch A and thus continue on a circular path at high frequency causing a tachy-arrhythmia.

(a – c)

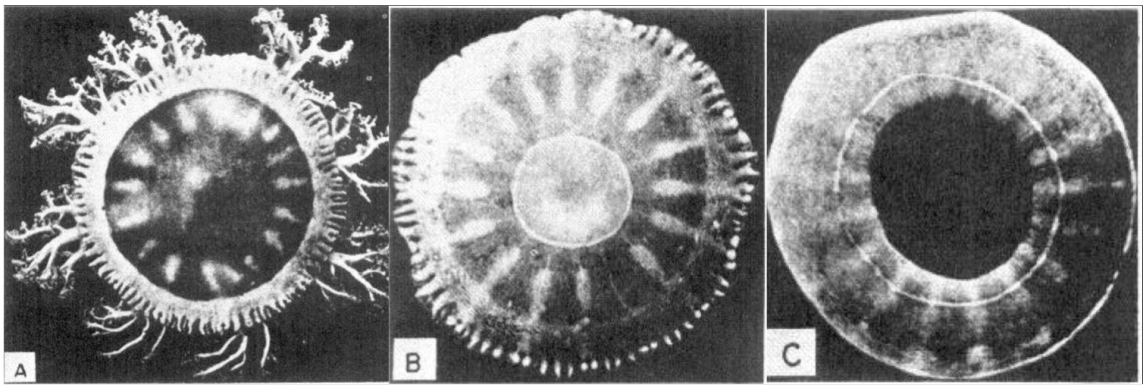

(d)

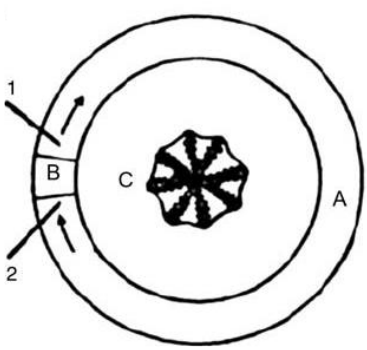

Figure 1.6 Ring preparation from Cassiopea xamachana

Circus movement of pulsations were demonstrated by Mayer in the subumbrella of the jellyfish, Cassiopea xamachana. (a) Aboral view of the Cassiopea. (b) Oral view with stomach and mouth-arms removed. (c) Ring preparation after removal of the marginal sense organs which normally trigger contractions of the subumbrella. (d) Schematic where A represents intact segment of the ring and B is a length of tissue which has been isolated by cutting from A. Stimulation at either points 1 or 2 triggers a wave of contraction passing through the length of segment A but unable to cross the interruption at B therefore producing a solitary contraction. Arrows show passage of pulsation from 1 clockwise to 2 before blocking at the mechanical obstacle at B. (Adapted from Mayer, 1917)

(a)

(b)

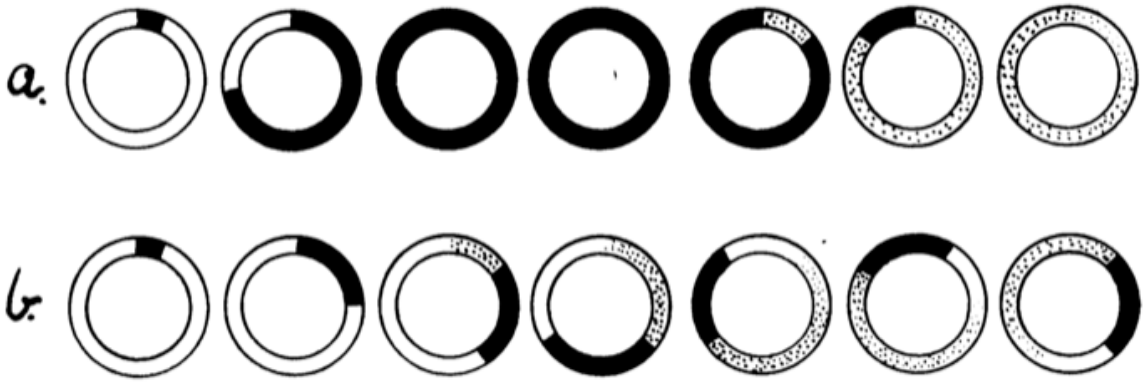

Figure 1.7 Demonstration of reciprocating rhythms by G.R. Mines

Diagrams from Mines' seminal paper identifying reentry as a mechanism of arrhythmogenesis. (a) Diagram of the tortoise heart preparation with a central longitudinal incision forming an anatomical obstacle for the wave of excitation to circulate. Following the application of an external stimulus, contractions were seen sequentially in chamber V1, V2, A1, and A2 then continuing in that order. (b) Mines' proposal for the principle requirements of a reentry circuit. In the upper schematic, beginning from the left, a wave of depolarisation is initiated at the apex of the ring (shown in black) and moves in a clockwise direction. As the conduction velocity is fast and refractory period long, the leading edge of the wave meets the tail while it is still refractory and therefore the circuit is extinguished. In the lower series, the conduction velocity is slow and/or the refractory period is short such that when the wave of excitation returns to the site of initiation the area has recovered from refractoriness and can be re-excited setting up a reentrant circuit. (Adapted from Mines, 1913)

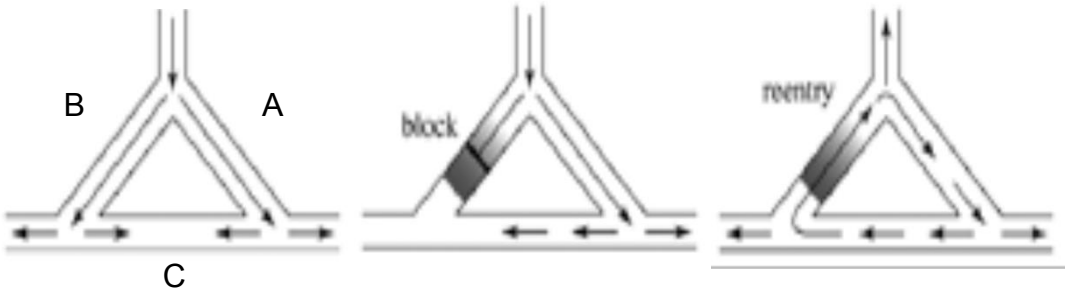

Figure 1.8 Mechanism of reentry

Diagram represents muscle fibres bifurcating into two tracts, A and B, connected distally by a common pathway C. In normal circumstances an AP wavefront (shown by arrows) conducts along A and B simultaneously and collide causing the wavefront to extinguish within the circuit in C (left panel). If an AP arrives when branch B has unidirectional block (may be refractory from previous impulse), the AP conducts along A and through C unobstructed (middle panel). It may conduct along branch B retrograde through the areas of block and down branch A setting up a reentrant circuit and manifesting as a tachycardia. (Adapted from Den Ruijter et al., 2007)

Reentry can also occur in the absence of an anatomically defined circuit or scar. Regional differences in electrophysiological properties such as conduction and/or repolarisation can give rise to areas of unidirectional block and provide a substrate for reentry, termed functional reentry (Allessie *et al.*, 1973).

1.3.3 Spatial heterogeneity

The effective uniform pumping function of the heart is contingent upon well-coordinated myocardial heterogeneity at the cellular level. This complex spatial heterogeneity in cellular electro-mechanical properties has been most extensively characterised in left ventricular tissue. For example, following rapid propagation of excitation through the endocardially sited Purkinje network, ventricular depolarisation proceeds from endocardium to epicardium whereas the reverse is true for repolarisation. In keeping with this, APs recorded from the left ventricular epicardial surface are significantly shorter than those measured in endocardial regions in murine (Milberg *et al.*, 2005), rabbit (Wang *et al.*, 2006) and canine (Yan & Antzelevitch, 1998) hearts. These spatial differences in APD are largely established by regional differences in repolarising K^+ currents. Epicardial myocytes from both murine (Nerbonne &

Guo, 2002) and canine (Litovsky & Antzelevitch, 1988) hearts have higher densities of I_{to}, accounting for the differences observed.

Disruption of these gradients may allow a depolarising region to re-excite areas that have repolarised and serve as a substrate for reentry. Transmural gradients are thought to be particularly important in this regard, as differences in repolarisation are exerted over a relatively short distance. Indeed alterations in transmural gradients have been correlated with arrhythmic tendencies in a number of animal models of Brugada Syndrome (BrS) and long QT syndrome (LQTS) (Antzelevitch & Oliva, 2006; Martin *et al.*, 2011*a*), as well as a murine model of heart failure (Wang *et al.*, 2006). Heterogeneities are also observed from apex to base accounting for the differential activation and repolarisation of these regions. In a cohort of patients with cardiomyopathy, greater dispersion in repolarisation gradients was associated with episodes of T wave alternans and ventricular tachycardia (VT) (Chauhan *et al.*, 2006).

The role of spatial heterogeneity in atrial tissue is less well studied, and given its thin-walled structure g76uy the significance of transmural gradients is less clear. Electrophysiological heterogeneity of atrial myocytes has predominantly been studied in pathological states, chiefly AF, and is reported to have an important role in the vulnerability to AF induction and maintenance (Fareh *et al.*, 1998).

1.3.4 Temporal heterogeneity

Microvolt T wave alternans is a repolarisation phenomenon manifesting as beat-to-beat variation in the amplitude of the T wave and ST segment on the surface electrocardiogram (ECG), and has long been recognised as a harbinger for malignant arrhythmias in a wide range of experimental (Verrier & Nearing, 1994; Pastore *et al.*, 1999; Euler, 1999) and clinical settings (Nearing *et al.*, 1991; Rosenbaum *et al.*, 1994; Armoundas *et al.*, 1998). It is thought to reflect spatiotemporal heterogeneity in repolarisation due to beat-to-beat alternation in the duration and/or amplitude of the AP at the cellular level. Several hypotheses exist for the cellular and molecular mechanisms underlying alternans with the prevailing theories being founded upon the APD restitution hypothesis and abnormalities in calcium handling. Evidence for either is conflicting, and it is likely that they are not mutually exclusive.

APD restitution refers to the normal attenuation of the APD in response to increasing heart rates, which is thought to be a physiological mechanism to preserve diastole and therefore diastolic filling and coronary perfusion. At the cellular level, modest increases in heart rate are perceived by shortening of the diastolic interval (DI) and are briskly accommodated for by a like response in the APD. At greater increases in the heart rate, this adaptation may involve transient oscillations or 'alternans' in the DI and APD before a new steady state between the respective intervals is reached. At even faster heart rates, the time in alternans may be more protracted and above a threshold rate, become sustained. Classically, the rate-dependent adaption of APD and the tendency to alternans has been analysed using the dynamic APD restitution curve, plotting APD as a function of the preceding DI (Nolasco & Dahlen, 1968) (Figure 1.9). According to the restitution hypothesis, APD alternans is governed by the gradient of the restitution curve, where alternans will occur when the slope exceeds unity. Where the gradient is steep, small changes in the DI are associated with larger magnitude changes in APD, amplifying heterogeneities in repolarisation and predisposing to wave break and arrhythmia.

Concordant alternans, where neighbouring cells alternate in phase is intrinsically not arrhythmogenic, but is a prerequisite for discordant alternans where neighbouring regions alternate out of phase (Watanabe *et al.*, 2001). The onset of discordant alternans significantly alters the spatial organization of repolarization across the tissue by markedly amplifying pre-existing heterogeneities, producing a substrate prone to conduction block and reentrant excitation. The utility of APD restitution in elucidating the mechanisms underlying ventricular arrhythmias has attracted much interest. Restitution profiles have correlated with propensity to alternans and arrhythmia in animal models of LQTS and BrS (Moss & Kass, 2005; Sabir *et al.*, 2008*c*; Matthews *et al.*, 2010). More recent reports have also highlighted steeper restitution curves in left atria of humans with AF (Kim *et al.*, 2002; Narayan *et al.*, 2008; Krummen *et al.*, 2012).

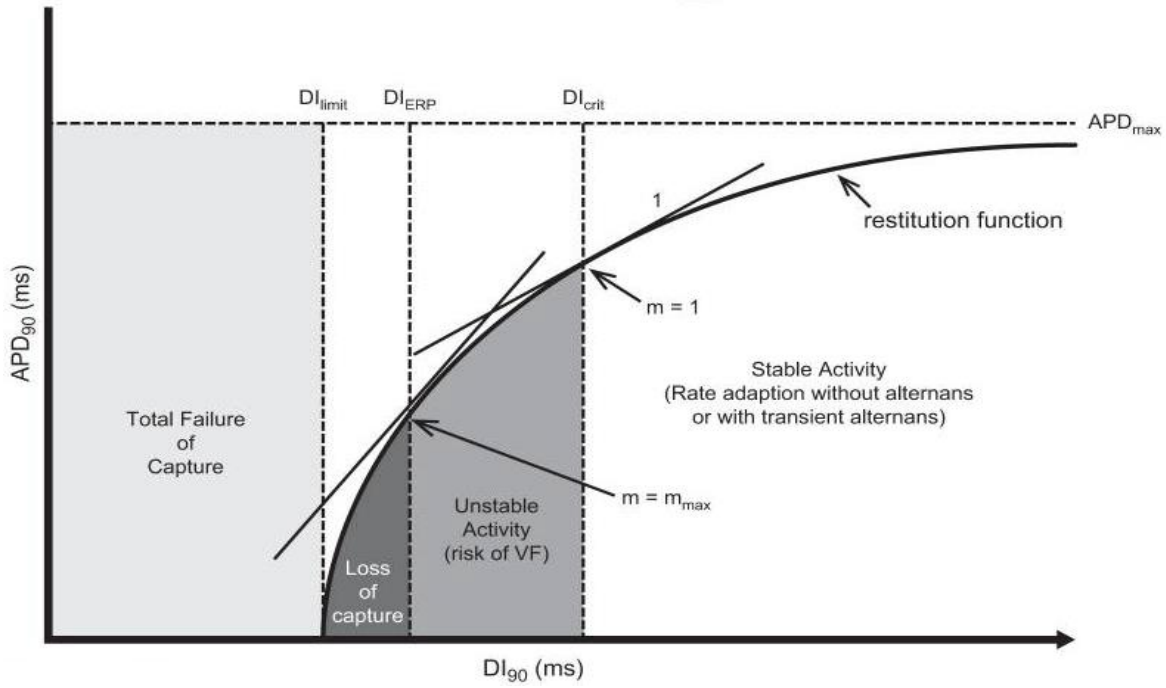

Figure 1.9 Idealised restitution curve

Generic restitution function relating APD90 corresponding to the action potential duration at 90% recovery to the corresponding diastolic interval (DI90) for a paced heart. The graph highlights the critical diastolic interval (DI_{crit}) where gradient (m) is 1 and represents threshold for onset of alternans, maximum gradient (m_{max}) corresponding to steepest point of the curve, maximum APD (APD_{max}) at low heart rates, DI90 at the effective refractory period (DI_{ERP}), and the horizontal axis intercept of the restitution function (DI_{limit}) corresponding to absolute refractoriness. This permits definition of conditions for stability (unshaded), instability (gray), as well as relative (dark shading) and complete loss of capture (left shaded area). (Adapted from (Huang, 2017*a*)

Interestingly cardiac ischaemia, recognised to provoke T wave alternans, was associated with paradoxical flattening of the restitution curve, albeit in a small cohort of human subjects (Taggart *et al.*, 1996). Additionally APD restitution was reported to have a limited role in a canine model of AF, which was found to be associated with abnormalities in Ca^{2+} dynamics (Burashnikov and Antzelevitch 2006). Consistent with this, depletion of SR Ca^{2+} stores suppresses alternans (Saitoh *et al.*, 1988) while delayed decay of the Ca^{2+} transient renders the tissue more susceptible to alternans phenomena (Wan *et al.*, 2005). Finally, isolated cardiomyocytes under voltage clamp conditions to prevent repolarization alternans continue to exhibit Ca^{2+} alternans suggesting the latter can arise independent of APD alternans and support a possible primary role for altered Ca^{2+} dynamics in the alternans events (Chudin *et*

al., 1999). Thus maladaptive changes in Ca^{2+} handling could give rise to such temporal susceptibility to arrhythmia in both ventricular and atrial tissue.

1.4 Atrial Fibrillation

1.4.1 Definition of atrial fibrillation

AF is a supraventricular tachy-arrhythmia with uncoordinated atrial activation and consequently ineffective atrial contraction. Characteristics on an electrocardiogram (ECG) include 1) irregular R-R intervals (when atrioventricular [AV] conduction is present), 2) absence of distinct repeating P waves, and 3) irregular atrial activity.

2014 ACC/AHA/HRS Guideline for the Management of Patients with Atrial Fibrillation

1.4.2 A historical perspective

"I have tremor cordis on me: My heart dances; But not for joy; not joy".

[The Winter's Tale, William Shakespeare, 1610]

References to irregularities in the pulse that we would now consider to be consistent with AF can be found in the works of numerous physicians throughout history, the earliest of which pre-dating classical antiquity. Emperor Huang Ti, the legendary Chinese sovereign reputed to have ruled from 2696 to 2598 BC, reported in The Yellow Emperor's Classic of Internal Medicine: *"When the pulse is irregular and tremulous and the beats occur at intervals, then the impulse of life fades; when the pulse is slender (smaller than feeble, but still perceptible, thin like a silk thread), then the impulse of life is small".* William Harvey penned the first written account describing the appearance of the fibrillating atrium in the heart of a horse approaching death, commenting on the chaotic *"undulation/palpitation"* of the right auricle (atrium) in his seminal work "Concerning the motion of the heart and blood" (more commonly known as De motu cordis, published 1628) (Lip & Beevers, 1995). Following on from Harvey's assertions John Baptiste de Senac, the 18th century physician to Louis XV, while investigating the cause of palpitations, related obstructive lesions of the mitral valve with dilatation of the atria, making them agitated and prone to abnormal heart rhythms. His recognition of their origin being distinct from the normal heart beat, presaged the association of atrial arrhythmias with mitral stenosis (McMichael, 1982). Around the same time William Withering, a physician and avid

botanist, used digitalis to treat fluid overload in a series of patients, noting in some cases the weak and irregular pulse became "*more full and more regular*" (Silverman, 1989).

In the nineteenth century, following Rene Leannec's invention of the stethoscope, Adams (1827) and Bouilland (1835) linked mitral stenosis to an irregular pulse. The latter referred to it as "*ataxia of the pulse*", suggesting this state of anarchy of the heart was akin to delirium of the brain. In 1876 Nothnagel, using the then recently-developed kymograph to record graphical representations of the pulse, published arterial traces of the irregular pulse he termed delirium cordis and highlighted complete irregularity as a defining feature of the arrhythmia. Believing meticulous examination of the arterial and venous pulse could help prognosticate cardiac disease Sir James Mackenzie, a general practitioner in the north of England, would follow his patients with serial venous and arterial recordings, initially with a modified sphygmograph and later the ink-writing polygraph which he had invented. He published the first of his polygraphic studies in 1894, advancing the notion that the initial wave of the venous pulse reflected atrial contraction and the second wave was due to ventricular contraction (Mackenzie, 1894). He later published similar traces from patients with mitral stenosis, demonstrating that in advanced stages when the irregular pulse supervenes, no signs of atrial activity are visible in the venous recordings, only to return when the pulse regains its regularity (Figure 1.10) (Mackenzie, 1904, 1905). MacKenzie initially postulated the loss of atrial activity was a result of atrial paralysis with the surviving ventricular contraction driven by the AV node, but later corrected this view as the origins of fibrillation were unearthed.

In parallel to the clinical reports of arrhythmias, pioneering work from Carl Ludwig's laboratory demonstrated canine hearts could be made to fibrillate and ultimately arrest with the application of an electrical stimulus (Flegel, 1995). In 1874, Vulpian reported similar behaviour in the atria with more localised faradization of the chambers referring to it as "fremissement fibrillaire" (from which the term fibrillation is derived). Arthur Cushny conducted similar studies on anaesthetised dogs at the end of the nineteenth century and commented on the remarkable similarity between the arterial traces of "*clinical delirium cordis*" and "*physiological delirium auriculae*" though he stopped short of suggesting they were the same entity (Cushny, 1899). Hering made similar suggestions in 1903, referring to the arrhythmia as pulsus irregularis perpetuus, and Cushny reinforced his view after publishing

the first correlative clinical report of the pulse in a female patient with the condition (Cushny and Edmund, 1907).

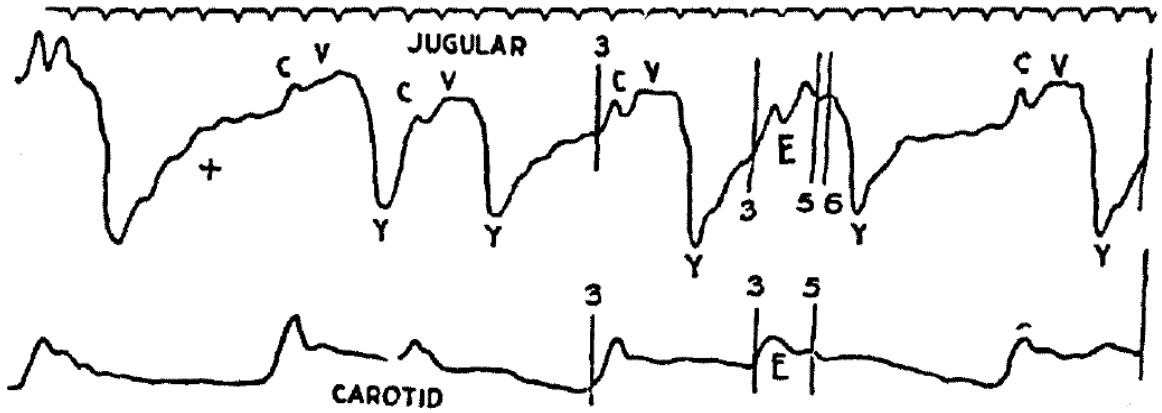

FIG. 17.—Simultaneous tracings of the jugular and the carotid pulses. The jugular pulse is now of the ventricular type. Note the irregularity and the small ripples in the tracing at the long pause +, due in all likelihood to fibrillary contraction of the auricle.

Figure 1.10 Arterial and venous pulse recorded with the polygraph

Simultaneous jugular venous (upper trace) and carotid artery (lower trace) pulse waveforms recorded by MacKenzie using the ink-writing polygraph from a patient with atrial fibrillation, along with his own figure legend, noting the absence of the 'a' wave and irregular rhythm. He also speculates the fluctuations in the baseline may be due to 'ripples' of the atria. (Adapted from Silverman, 1994)

Stimulated by Cushny's intimation, MacKenzie encouraged his colleague Sir Thomas Lewis to take advantage of Einthoven's recently developed string galvanometer to record the ECG in an attempt to elucidate the underlying pathology. Interestingly Einthoven, in 1906, had already published the first ECG illustrating AF (he referred to it as pulsus inaequalis et irregularis) but had not recognised its significance (Figure 1.11a) (Silverman, 1994). Hering had also reported on ECGs of similar patients, concluding that one could see no sign on the ECG of the activity of the auricles, though on closer inspection F waves are evident (Figure 1.11b). In October 1909, Lewis applied the string galvanometer to a patient with pulsus irregularis perpetuus, demonstrating the fine diastolic oscillations corresponded to the fibrillatory movements of the auricles seen in the experimental preparations. Lewis described

the classic absence of P waves and irregularity of the F waves that define AF. In the same year, Rothberger and Winterberg, based in Vienna, undertook similar recordings and independently came to the same conclusion thus connecting the irregular pulse that had for a long time intrigued many physicians and typical ECG finding, with disarray in atrial activity.

(a)

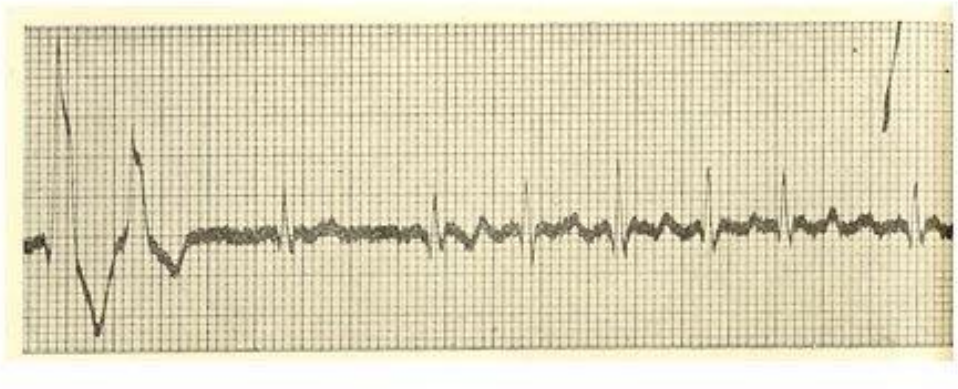

(b)

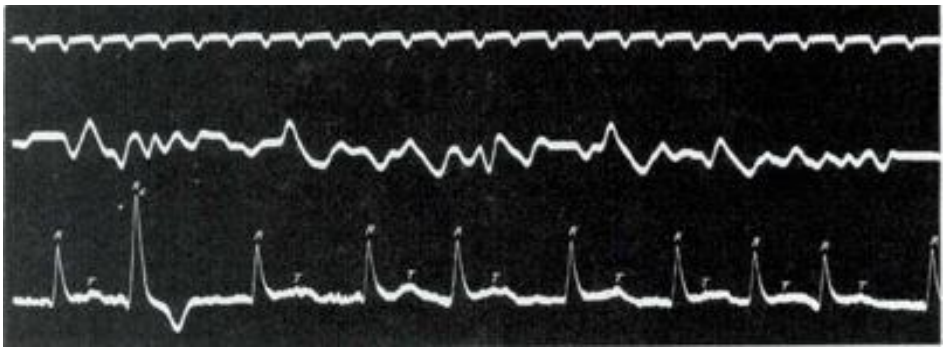

Figure 1.11 Early electrocardiogram recordings of atrial fibrillation

(a) First electrocardiogram of atrial fibrillation recorded by Eintohoven after inventing the string galvanometer. He referred to the rhythm as "pulsus inaequalis et irregularis. (Adaped from Fye, 2006). (b) Hering's simultaneous recording of "pulsus irregularis perpetuus" with the sphygmograph and electrocardiogram with the string galvanometer. Hering speculated the clinical arrhythmia correlated with auricular fibrillation but felt no evidence of atrial activity was evident on the ECG. (Adapted from Silverman, 1994)

1.4.3 Epidemiology of atrial fibrillation

AF affects 1-4% of the population in the developed world (Majeed *et al.*, 2001; DeWilde *et al.*, 2006; Friberg & Bergfeldt, 2013) and accounts for 1 in 3 of all arrhythmia-related hospital attendances (Wu *et al.*, 2005*a*). The overall number of individuals with AF, as estimated by the

2010 Global Burden of Disease study, was 20.9 million males and 12.6 million females, with approximately 5 million new cases of AF annually (Chugh *et al.*, 2014). These figures could conceivably be an underestimate, given a significant proportion of those affected are undiagnosed. Additionally the data largely reflect figures from Western Europe and the USA, as data from other regions, particularly the developing world, is sparse.

Given the progressive improvements in AF surveillance, coupled with shifting population demographics and the growing burden of risk factors, the prevalence of AF is predicted to rise significantly in the coming decades. Approximately 3.5 million individuals in the USA have AF and this is expected to exceed 8 million by 2050 (Colilla *et al.*, 2013). Similarly in excess of 8 million individuals were estimated to be living with AF in Europe in 2010, and this figure is projected to rise to 18 million by 2060 (Krijthe *et al.*, 2013). UK specific data suggest the prevalence is a little under 2%, and according to The Office of Health Economics estimates for 2008, the direct cost of AF to the NHS was £429 million; there were approximately 851,095 GP visits attributable to AF and patients with primary or secondary diagnoses of AF occupied an estimated 5.7 million bed-days (The Office of Health Economics, 2009). The prevalence of AF appears to a great extent to be a function of age, affecting 0.1 % under the age of 55 and approaching 15 - 20 % above the age of 80 (Go *et al.*, 2001*b*; Krijthe *et al.*, 2013; Zoni-Berisso *et al.*, 2014). Based on the Framingham cohort, the lifetime risk of AF for men and women reaching the age of 40 is 1 in 4, and in the absence of cardiovascular or other comorbidities the lifetime risk is 1 in 6 (Lloyd-Jones *et al.*, 2004).

Traditionally rheumatic heart disease and associated mitral valve lesions were a major cause of AF. The advent of early antibiotic treatment for streptococcal infections in the western world has relegated its contribution, though its prevalence remains an impressive 30 – 60 % in AF populations in developing countries (Bhardwaj, 2012; Hersi *et al.*, 2015). In contrast, hypertension is the most common medical condition associated with AF, affecting up 70 % of patients with AF (Kakkar *et al.*, 2013). Diabetes mellitus is also increasingly recognised as a risk factor for AF (Aksnes *et al.*, 2008; Chiang *et al.*, 2012), though data from earlier studies is conflicting (Ruigómez *et al.*, 2002; Schnabel *et al.*, 2009). Interestingly the odds ratio for AF in patients with type 2 diabetes mellitus appears to increase with increasing hemoglobin A1c levels and each year with diabetes mellitus confers a 3 % increased risk of developing AF (Dublin *et al.*, 2010). Several studies have also highlighted an association between obesity and

AF. The risk of AF in obese individuals is approximately 1.6 times that of counterparts with normal BMI (Wanahita *et al.*, 2008; Watanabe *et al.*, 2008; Zhang *et al.*, 2009*a*) and an elevated BMI is a strong predictor of AF recurrence following treatment with catheter ablation (Guijian *et al.*, 2013; Middeldorp *et al.*, 2018). AF frequently complicates recovery from myocardial infarction with rates being highest in peri-infarct period and an elevated risk persisting for several years after the event (Jabre *et al.*, 2011). Similarly, the risk of developing AF is increased multiple fold in the presence of heart failure (Schnabel *et al.*, 2009).

Early insights into the heritability of AF were gained from cases of early onset AF or families in which AF segregates as a Mendelian trait. These patient groups have a high *a priori* likelihood of a genetic aetiology of AF, with an expectation that this is primarily due to single rare variants of large effect size. Further analyses have highlighted variants in genes encoding ion channels, transcription factors and structural proteins (Bapat *et al.*, 2018), though it is unclear whether all of the putative "AF genes" are truly causative of AF. The susceptibility to AF is evidently complex and multifactorial, reflecting probable epistatic effects from a combination of genetic variants and the imprint of environmental factors on this underlying inherited susceptibility. It is likely that the latter to some degree provide an explanation for the ethnic variation in prevalence. Rates of AF are significantly lower in individuals of non-European ancestry despite higher rates of AF risk factors in what has been termed the race-risk AF paradox (Lip *et al.*, 1998; Jensen *et al.*, 2013; Dewland *et al.*, 2013).

1.4.4 Mortality and morbidity

Though often asymptomatic and frequently an incidental finding, AF is far from benign. AF, independent from other known predictors of mortality, is associated with a two-fold increased risk of death (Miyasaka *et al.*, 2007). Additionally the arrhythmia confers a five-fold increase in the risk of stroke (Wolf *et al.*, 1978), and cerebral events in this context are associated with greater mortality and morbidity than those in its absence (Jørgensen *et al.*, 1996). Heart failure and AF frequently coexist and each predisposes to the other. AF is also associated with a 2 - 3 fold increased risk of heart failure (Wang *et al.*, 2003) and the presence of both conditions confers significantly elevated mortality risk than either in isolation (Chamberlain *et al.*, 2011; McManus *et al.*, 2013). There is increasing evidence linking AF with

cognitive decline (Kalantarian *et al.*, 2013). In the ONTARGET and TRANSCEND studies, patients with AF showed more brisk worsening of Modified Mini-Mental State Examination and Digit Symbol Substitution Test scores over the subsequent 5 years than did patients without AF (Marzona *et al.*, 2012).

1.5 Early concepts of atrial arrhythmogenesis

More than a century has passed since the nature of AF, as a clinical entity, was elucidated and debate regarding its electrophysiological basis has existed since that time. Our current understanding remains very much rooted in the rudiments of those original concepts.

1.5.1 The multiple heterotopous centres theory

The earliest theory regarding the mechanism of AF was proposed by Theodor Englemann (1894), who believed that each heart fibre became independently rhythmic, discharging simultaneously as a result of increased excitability (Wit & Cranefield, 1978). The theory, which became known as the multiple heterotopous centres theory, was later espoused by Winterberg (1906) who reasoned that activity from one or more heterogeneous centres would account for regular and irregular atrial arrhythmias. Lewis (1912) initially shared this view, following experiments evaluating electrical currents on strips of myocardium. Winterberg, along with Rothberger, subsequently presented a variation on the theory, suggesting that a single ectopic focus firing at a markedly accelerated rates (3000 per minute for AF and 500 per minute for AFL) accounted for such arrhythmias.

1.5.2 Circus movement theory

Building on the work of Mayer, Mines in Cambridge and Walter Garrey, an American physiologist at Tulane University, both performed similar studies and independently published reports demonstrating reentry as a mechanism for arrhythmia (Mines, 1913; Garrey, 1914). In investigating mechanisms of fibrillation, Garrey cut a fibrillating chamber into 4 four pieces and observed that each sample continued to fibrillate, undermining the theory that fibrillation could be driven by a single tachysystolic focus as suggested by

Rothberger. He then cut the fibrillating tissue into several small pieces and observed that the individual pieces ceased to fibrillate. He concluded that individual fibres could therefore not be independently rhythmic thus disproving the multiple heterotopous centres theory. Moreover he demonstrated that if the tissue was cut into a ring of appropriate size, the fibrillatory activity would organise into a rotating wave of contractions. He therefore reasoned that fibrillation was contingent upon a critical mass of tissue and involved a complex circuit of reentry with potentially multiple waves of activity moving in different directions and bound by transitory areas of conduction block, remarking: *"The impulse is diverted into different paths weaving and interweaving through the tissue mass, crossing and recrossing old paths again to course over them or to stop short as it impinges on some barrier of refractory tissue*".

1.5.3 Mother wave theory

In 1921 Lewis published results postulating AFL was a reentrant arrhythmia, characterised by circus movement of an impulse limited by anatomical structures, and activating the rest of the atrial tissue through centrifugal conduction from this central ring (Lewis, 1921). The experimental protocol involved in vivo bipolar recordings from the surface of the right atrium in an anaesthetised canine model using a modified string galvanometer. Lewis also observed rhythms which he termed "impure flutter", which in some cases had exceptionally variable cycle lengths and resembled AF on the surface ECG. He, having abandoned the concept of heterotropic centres of activity, surmised that AF originated from a central 'mother' wave rotating through a smaller circuit than that of AFL, emitting centrifugal or 'daughter' waves along its course, which passively activate the remaining atrial mass in a disorderly fashion owing to regional heterogeneities in the electrophysiological properties.

1.5.4 Multiple wavelet theory

Repetitive discharge from ectopic foci and circus reentry remained the prevailing theories explaining the pathogenesis of AF for several decades. Gordon Moe, a physiologist in New York, found both difficult to countenance, suggesting that neither could sufficiently explain the sustained nature of AF (Moe, 1956). In 1959, Moe and Abildskov published details of a novel canine model using atrial pacing and simultaneous vagal stimulation, that could sustain

AF for long periods (Moe and Abildskov, 1959). Moe contended that since vagal stimulation significantly increases the dispersion of refractoriness, a single wave of activation would unlikely remain intact. Rather he envisioned that AF was a result of multiple randomly wandering wavefronts, conducting through an inhomogeneous repolarisation milieu. He subsequently postulated the multiple wavelet hypothesis where the initial central wave fragments into an increasing number of independent daughter wavelets as it divides about strands of refractory tissue, and provided that a sufficient number of wavelets had formed the atria would continue to fibrillate. The hypothesis was further supported by an early computer model of AF developed by his group, highlighting key contributions of enlarged atrial size and electrophysiological heterogeneity, and demonstrated that it was probabilistically unlikely that a large number of wavefronts would all extinguish simultaneously (Moe et al., 1964). According to this model the critical number of wavefronts for perpetuation of AF was between 15 and 30.

1.6 The electrophysiological basis of AF

Atrial fibrillation appears to be a progressive disorder, which at its inception is characterised by fleeting episodes which spontaneously terminate (termed paroxysmal AF). With time these episodes become increasingly frequent and more protracted, and eventually persistent. A multiplicity of electrophysiological abnormalities are known to contribute to the genesis of AF, and the relative contribution of each is likely to vary with time, reflected in the spectrum of manifestations. Understandably the efficacy of any single therapeutic intervention is not uniform across this continuum.

1.6.1 Trigger versus substrate

In early animal models, AF was induced through high rate atrial pacing however the bouts of AF would terminate fairly briskly. The issue restricted detailed analysis of the underlying mechanisms. Moreover, this tendency to spontaneously cardiovert reinforced the perception that continued focal discharge was essential in sustaining AF, underpinning the multiple heterotopous centres or tachysystolic theories of arrhythmogenesis. These schemes of AF

however were considered less relevant in light of Lewis' demonstration of re-entry, which became the most widely accepted position for several decades.

The role of reentry in maintaining AF was later challenged by Scherf and colleagues, deeming such activity to be epiphenomena not involved in its perpetuation (Scherf & Terranova, 1949). Sustained AF could be induced in canine hearts through injections of the alkaloid aconitine into the right atrial appendage. The arrhythmia could consistently be terminated by cooling the tissue, but would promptly reinitiate upon rewarming. They reasoned that termination would imply interruption in any reentrant circuit(s) present thus reentry could not precipitate the spontaneous recurrence when the preparation was warmed, and therefore supported a pivotal role of ectopic activity in driving AF (Scherf et al., 1953). Similar assertions were made by Prinzmetal who failed to demonstrate circus movement or daughter waves using high-speed cinematography and multi-channel electrocardiography in the same canine model of sustained AF (Prinzmetak and Corday, 1950). Sustained AF in Moe's canine model was achieved through high rate pacing from the right atrial appendage and simultaneous vagal stimulation (Moe and Abildskov, 1959). The latter posited that once established, AF could persist without the agency of the initiating mechanism. In their model, following the onset of AF, the appendage was clamped and electrically isolated from the atrial body. On cessation of pacing, fibrillation was no longer evident in the atrial appendage but persisted in the remaining atrial mass, disaffiliating the mechanisms underlying the initiation of AF from those involved in its maintenance, and implying roles for both ectopic activity and reentry.

Definitive evidence supporting a role for ectopic activity in the pathogenesis of AF was demonstrated in a landmark study by Haïssaguerre et al., who reported spontaneous activity from sites within the right or left atria triggered the arrhythmia in a cohort of patients with drug-refractory paroxysmal AF (Haïssaguerre *et al.*, 1998). In all 45 patients enrolled in the study, AF was initiated by ectopic activity from a small number of foci, 94% of which were located at the ostia of the pulmonary veins (PV) (Figure 1.12). Elimination of this ectopic discharge through RFA was effective in preventing recurrence in two thirds of cases during the follow-up period. Techniques for PV isolation have evolved significantly since this report of its utility in managing AF, and has become the primary invasive intervention for the treatment of AF. However, despite significant technical advances in ablation methods, outcomes from AF ablation remain suboptimal. Success rates vary between 60% to 80% for

paroxysmal AF, depending on ablation strategies, and between 50% to 60% for persistent AF (Brooks *et al.*, 2010; Ganesan *et al.*, 2013; Verma *et al.*, 2015). AF recurrence may be attributable, in part, to reconnection of the PVs or the presence of non-pulmonary vein triggers, however processes beyond triggered activity are likely to contribute.

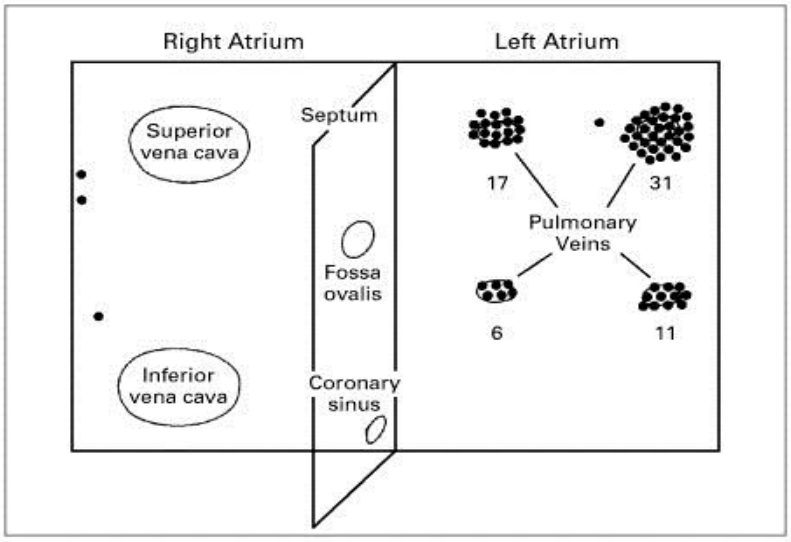

Figure 1.12 Foci of ectopic activity

Schematic diagram identifying sites of ectopic activity seen to trigger atrial fibrillation in 45 patients with drug-refractory paroxysmal atrial fibrillation. Of the 69 sites identified, 94% were at the ostia of the pulmonary veins. (adapted from Haïssaguerre et al., 1998)

Several studies have identified the AF type (paroxysmal or persistent) and duration as sensitive predictors of long term outcome (Tutuianu *et al.*, 2015; Sultan *et al.*, 2017). The poorer outcomes in patients with persistent AF have served to highlight differing mechanisms underlying AF in its early stages to that when more established and has led to the trigger-substrate model of AF. For the arrhythmia to be sustained, ectopic activity must encounter tissue with electrophysiological properties that promote reentry. In the early stages of AF, ectopic activity emanating from the PVs or alternative foci precipitate AF which sustains for variable amounts of time. As the disease progresses, progressive electrical, mechanical and structural alterations in the atria generate a substrate promoting the perpetuation of AF, hence a trigger-targeted therapy such as PV isolation is less likely to be effective (Iwasaki *et al.*, 2011).

1.6.2 Triggers for AF

There is general consensus that sites of high frequency ectopic activity play a prominent role in initiating episodes of paroxysmal AF, and such abnormal discharges have been recorded from a number of structures including the left atrial appendage (Di Biase et al., 2010), superior vena cava (Tsai *et al.*, 2000), ligament of Marshall (Katritsis *et al.*, 2001), coronary sinus (Johnson *et al.*, 1986) and the crista terminalis (Nanthakumar *et al.*, 2004). These however account for a fraction of all such cases with the PVs being implicated in the overwhelming majority. Reasons behind this predilection for the PVs or indeed the mechanisms driving the rapid discharge from any of these structures remain yet to be elucidated. Venous structures feeding into the atria such as the PVs and superior vena cava are known to be in electrical continuity with the heart through extensions of the myocardium from the embryological atrial antrum into these veins. Aberrant activity within these structures can therefore conduct along these muscular sleeves and invoke reentry.

Genome-wide association studies have demonstrated a consistent and robust association between AF and single nucleotide polymorphisms (SNPs) in proximity to the PITX2 gene. A comprehensive understanding of the function of the PITX2 family of transcription factors is at present lacking, but they are recognised to have a diverse range of roles during both embryological development and in adulthood. PITX2 was initially described in the context of embryological development of left-right asymmetry of internal organs (Ryan *et al.*, 1998). The development of cardiac left–right specific characteristics such as the restriction of the SAN to the right atrium is critically dependent on asymmetrical organ morphogenesis, and is subject to PITX2 expression in the left-sided cardiac chambers. Loss of PITX2, in some cases at least, could result in incomplete suppression of pacemaker activity in the left heart and give rise to foci of ectopic activity (Wang *et al.*, 2010). Interestingly, there is progressive loss of left atrial PITX2 expression with advancing age in murine hearts, and may have some bearing on the age-related incidence of AF (Wang *et al.*, 2010). Further, risk variants at the PITX2 locus have been reported to predict AF recurrence in patients undergoing PV isolation (Husser *et al.*, 2010). Both under- and overexpression of PITX2 have been linked to AF in humans suggesting a critical level of expression is required for normal atrial function (Chinchilla *et al.*, 2011; Pérez-Hernández *et al.*, 2016). In animal models, PITX2 deficiency was associated with shortening of

the APD and higher susceptibility to inducible atrial arrhythmias including AF (Kirchhof *et al.*, 2011).

Several lines of evidence suggest PVs harbour cells with pacemaker-like activity, and that enhanced automaticity in these cells underpin PV based triggers for AF. Masani and colleagues identified sinus-node like cells (P cells) interspersed between normal atrial myocytes in the pre-terminal segment of the PVs using electron microscopy (Masani, 1986). Further histological studies from explanted human hearts have reported cells with morphological characteristics reminiscent of P cells, transition cells, Purkinje cells and Cajal cells (Perez-Lugones *et al.*, 2003; Gherghiceanu *et al.*, 2008). A number of these cell types express ion channels usually found in nodal tissue further raising the potential for a role in PV based triggers (Morel *et al.*, 2008; Nguyen *et al.*, 2009), however studies characterising their electrophysiological properties or exploring mechanisms by which they may contribute to atrial arrhythmias are lacking.

The architectural arrangement of myocardial fibres within the muscles sleeves are rather complex and may influence their arrhythmic potential. Myocyte bundles appear to be arranged in a variety of orientations, with circumferentially orientated bundles interconnected to those running in longitudinal and more oblique trajectories (Ho *et al.*, 2001). Such an arrangement of fibres may lead to anisotropic conduction properties between bundles and predispose to reentry. Additionally, the muscle sleeves are not uniform across their length, varying in depth and displaying fibrous gaps between neighbouring myocytes with inter-pulmonary interconnections/bridges between bundles within veins and between adjacent veins (Cabrera *et al.*, 2009). Although such findings are not limited to patients with a history of AF, histological analysis does suggest myocardial extension is significantly increased in the context of AF (Hassink *et al.*, 2003). Furthermore AF is associated with higher frequency of discontinuity and a greater degree of fibrosis when compared to muscle sleeves from control groups, potentially supporting micro-reentry (Saito *et al.*, 2000).

Evidence of reentry within the PVs has been reported in several animal models and human studies of AF. PVs in a canine left atrial preparation demonstrated slowed conduction and heterogeneous electrical properties along their length, predisposing to re-entry (Hocini *et al.*, 2002). Optical mapping studies of canine and sheep preparations have also shown conduction

slowing, with areas of conduction block and re-entry in the proximal segments of the PVs in response to pacing (Arora *et al.*, 2003; Yamazaki *et al.*, 2012). Canine PVs also appear to have anisotropic conduction with a propensity for reentry following rapid pacing. Here, reentry circuits localised to the venoatrial junction and corresponded to areas displaying abrupt changes in fibre orientation (Chou *et al.*, 2005). Furthermore, using high density mapping of human PVs, anisotropic conduction and heterogeneity in repolarisation properties is evident within the PVs and at their insertion in the LA (Kumagai *et al.*, 2004), and these features appear significantly more pronounced in PVs from patients with AF compared to those in sinus rhythm (Jaïs *et al.*, 2002).

Interestingly, pulmonary myocardial cells do not develop from atrial cells, but rather *de novo* at the junction of the common PV and LA, and display distinct electrophysiological properties (Webb et al., 2001; Sherif 2013). Indeed, PV cardiomyocytes have distinct ionic currents to those of LA cells, with characteristically shorter APDs and particularly brief ERPs (Tada *et al.*, 2002; Melnyk *et al.*, 2005). They also develop enhanced automaticity and frequent after-depolarisations, both early and delayed, in response to rapid atrial pacing (Chen *et al.*, 2001). There are therefore numerous mechanisms through which aberrant activity in the PVs may originate, and in the appropriate conditions, trigger AF.

1.6.3 Atrial substrate in AF

The canine model of AF described by Moe (Moe and Abildskov, 1959) suggested that once initiated, AF could sustain for long periods of time in the absence of on-going trigger activity. Their computer simulations suggested AF arose from a rapid succession of impulses, and would persist when such impulses encountered partially and irregularly excitable tissue that would promote reentry (Moe *et al.*, 1964). Allessie et al., provided the first actual demonstration of such functional reentry, that is reentry in the absence of an anatomical obstacle, thus displaying many of the phenomena hypothesised by the likes of Garrey and Moe (Allessie *et al.*, 1973, 1976, 1977). Using multi-electrode array recordings in an isolated rabbit atrial preparation, heterogeneous repolarisation properties gave rise to unidirectional block and clockwise spread of excitation, with the impulse returning to the initial site of block once excitability had recovered and then could continue to circulate for many revolutions (Figure 1.13). The pathway could have a circumference of as small as 6-8mm and was

described as the 'leading-circle model' of reentry. In this model, the dimensions of the circuit are determined by the electrophysiological properties of the tissue, where the circumference would be the minimum length at which the leading edge of the wave approaches but does not encroach upon its refractory tail. The circus movement results in constant centripetal activation of the centre of the circuit rendering it continuously refractory, thus forming a functional barrier that can sustain reentry in a way similar to a fixed anatomic barrier such as a scar. Centrifugal impulses emanating from the circuit would activate the remaining atrial tissue. Later mapping studies on cholinergically induced AF in isolated canine hearts provided more direct support for Moe's multiple wavelet hypothesis (Allessie *et al.*, 1996). Using similar MEA recordings, reentrant activity was seen in both atria and they estimated that a critical number of 3-6 wavelets were required for perpetuation of AF.

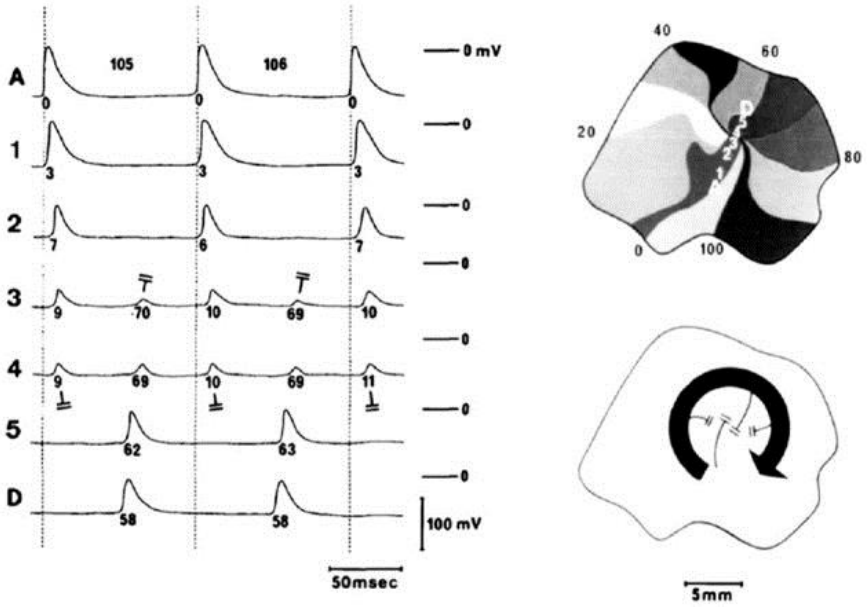

Figure 1.13 Circus reentry in rabbit atria during sustained tachycardia

Multi-electrode array recordings from isolated rabbit left atrial preparation during pacing induced tachycardia. Points are taken from fibres along a straight line as labelled in top right diagram. Fibres 3 and 4 are located at the centre of the circuit, being of lower amplitude and activate twice as frequently as peripheral points due to repetitive stimulation. Activation times of these fibres suggest centripetal activation. The tachycardia appeared to rotate clockwise as shown by activation times (top right) and shown in schematic (bottom right). (Adapted from Allessie et al., 1977)

Although functional reentry seems to be a critical feature in the mechanisms underlying AF, it appears to be significantly more complex than described by the leading circle model. The leading circle concept implies that the refractory central region prevents the excitation wave from invading it, thus representing a central core of functional block that fixes the circulating wavefront to a unique location. This model however appeared to be incongruent with studies investigating the dynamics of ventricular fibrillation (VF) and spiral waves have been suggested to better characterise the nature of reentry in VF as well as AF (Davidenko *et al.*, 1990; Jalife *et al.*, 1998; Pandit *et al.*, 2005). Spiral waves represent a specific form of functional reentry that exhibit a curved wavefront, which is most pronounced at its core (Figure 1.14). Importantly, the wavefront velocity is not uniform, instead varying along different points owing to the differing degrees of curvature and consequent current source-sink mismatch. The extreme curvature in the central region creates an area of exceptionally slow conduction, thus rendering the core excitable but extremely difficult to penetrate. The repolarisation tail follows the course of the activation front, meeting the latter at a focal point termed the phase singularity (PS). This PS point is able to precess and meander about the core, thus behaving differently to the defined course in the leading-circle model. Rotors may be initiated when a wavefront encounters some form of barrier, either due to a structural obstacle such as a scar, electrophysiological inhomogeneity or anisotropy. As a wavefront passes through the barrier it can, under certain conditions, fragment into daughter wavelets by a process called vortex shedding. As the rotating wavefronts spread away from the PS and core, they interact with other areas inhomogeneity fragmenting further, giving rise to multiple wavelets manifesting as fibrillation. Crucially the multiple waves arise from a small number of principle rotors, which may provide discrete targets for therapy (Narayan *et al.*, 2012).

Whether the leading-circle model or spiral wave concept best describes the nature of fibrillating myocardium remains an area of debate and ongoing investigation, however both are contingent upon reentry of a propagating wavefront. Functional reentry is generally thought to arise through maladaptive changes in electrophysiological properties resulting in slowed conduction and/or shortening of the ERP. These alterations reduce the AP wavelength, defined as the distance travelled by the depolarising wave during one refractory period and calculated as the product of conduction velocity (CV) and ERP, permitting the formation of reentrant circuits (Allessie *et al.*, 1977). The longer the wavelength, the less likely that areas of depolarisation and repolarisation will meet, passing over areas of intrinsic

heterogeneity without incident. Shortening of the wavelength to values smaller than the dimension of the available circuits or limits of heterogeneity increases the probability of reentry and wavebreak.

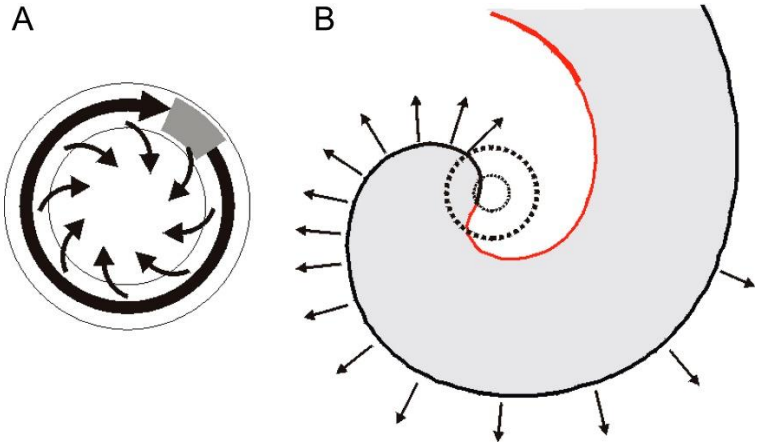

Figure 1.14 Representation of leading-circle and spiral wave reentry

A) The leading circle concept: Activity establishes itself in the smallest pathway that can support reentry, shown as a large black arrow. Inside the leading circle, centripetal wavelets (small arrows) emanating from it constantly maintain the central core in a refractory state. B) Spiral wave mode: Schematic diagram of a spiral wave with the activation front shown in black and the repolarization front in red. The point at which the red and black curves meet has an undefined voltage state and is usually referred to as the phase singularity point. The phase singularity point is not anatomically fixed and so can pivot around the core, thus precessing and meandering within the tissue. (Adapted from Comtois et al., 2005).

Evaluation of the electrophysiological properties of atria in both animal models and patients with AF reveal features that would shorten the AP wavelength and predispose to re-entrant arrhythmia. Pacing-induced AF in a canine model was associated with reduction in the atrial ERP and correlated with the inducibility of AF (Morillo *et al.*, 1995; Elvan *et al.*, 1996; Goette *et al.*, 1996). Nattel's group performed various measurements in a similar pacing-induced canine AF model, reporting that AF was associated with increased heterogeneity of refractoriness in addition to overall shortening of the atrial ERP, and it was the former that appeared to be a better independent determinant of AF inducibility (Fareh *et al.*, 1998). Reduction in atrial

refractory periods is similarly seen in human hearts with AF (Daoud *et al.*, 1996). Additionally, loss of rate adaptation of the ERP has also been associated with vulnerability to AF in canine hearts (Lee *et al.*, 1999) and these findings have been corroborated in human studies (Attuel *et al.*, 1982).

While attenuation of the APD and concomitant shortening of the atrial ERP significantly contribute to AF initiation and maintenance, the propensity for the atrium to fibrillate does not entirely parallel changes in repolarisation properties, and in fact some studies have noted prolongation of atrial ERPs in patients with chronic AF (Stiles *et al.*, 2009). In this study, patients with chronic AF displayed marked conduction slowing. Kumugai et al., investigated electrophysiological properties in patients with chronic AF, immediately following cardioversion (Kumagai *et al.*, 1991). P wave duration on the surface ECG was taken as a surrogate of atrial conduction time and was longer in AF patients during premature atrial beats but not during normal sinus beats indicating abnormal anisotropic conduction properties in the atria. These patients also showed shortening of refractory periods. In contrast, overall intra-atrial conduction times in young patients with a history of lone AF did not differ significantly from those of control patients however there was greater heterogeneity in conduction properties across the atria in those with AF (Holmqvist *et al.*, 2011). The conduction velocity of a wavefront across the atria is determined not only by the ion channel properties of individual cardiomyocytes, but also the architectural composition of the atria that influence their ability to function as a syncytium. Transgenic mice carrying a mutation in the connexin 40 gene were no more susceptible to AF than wild-type control animals, however once induced, AF would persist for significantly longer durations, emphasising the importance of conduction properties in creating a substrate favouring reentry (Lübkemeier *et al.*, 2013).

Static properties such as intrinsic heterogeneities that exist across normal atria may promote wavebreak and degeneration to fibrillation, however these do not sufficiently account for development of AF since the majority of premature ectopic beats do not initiate AF. While the initiation of AF is underpinned by localised phenomenon chiefly originating from the PVs, adverse electrical, contractile and structural remodelling is fundamental in the formation of an arrhythmogenic atrial substrate that permits AF to persist. The relative contribution of each in the evolution of AF, and the upstream processes driving this remodelling are yet to be fully

elucidated. Fascinatingly, AF itself appears to induce atrial remodelling, thereby facilitating its own persistence.

1.6.4 Electrical remodelling in AF

The notion that AF itself results in remodeling of atrial properties such that AF becomes more likely was elegantly shown by the Allessie laboratory (Wijffels *et al.*, 1995). In normal goat hearts, short-lived paroxysms of AF were observed following burst pacing from the atrium. Artificially maintaining AF for increasing periods of time resulted in enhanced inducibility of AF and prolongation of these episodes. Following 2-3 weeks of pacing, AF became sustained in the majority of animals (Figure 1.15). At the same time, Morillo and colleagues independently performed similar studies in a canine model and reported development of sustained AF following 6 weeks of rapid atrial pacing (Morillo *et al.*, 1995). Marked reductions in the atrial refractory period and reverse adaptation of repolarisation to rate, in the form of greater shortening of the ERP at slower heart rates, were observed in both studies, matching the altered repolarisation properties seen in human hearts with AF (Attuel *et al.*, 1982; Daoud *et al.*, 1996; Pandozi *et al.*, 1998). These studies provided valuable insights into the pathogenesis of AF and led to the concept of *'AF begets AF'*.

The clinical course of AF is epitomised by initially brief bouts of the arrhythmia, progressing with time to more frequent and protracted episodes, and eventually becoming persistent. The reductions in atrial ERP certainly serve to increase the probability of AF being sustained, however in isolation are unlikely to fully account for the progressive nature of AF. The alterations in repolarisation characteristics occur early in AF implying acute changes in ion channel expression and function, however the time course of these changes in atrial refractoriness do not parallel the propensity of the atria to fibrillate. In the goat model described by Wjiffels *et al.*, (1995) significant shortening of the atrial ERP was seen within 24 hours of AF and appeared maximal at 2-3 days, however several further days of rapid pacing was required for AF to become persistent. Additionally these changes appeared to be eminently reversible, returning to baseline values within 1 week following restoration of sinus rhythm. Yu et al., (1999) demonstrated shorter ERPs with impaired rate adaptation in patients following cardioversion for long-standing persistent AF, with the ERP increasing after 4 days of maintenance of sinus rhythm (Yu *et al.*, 1999). AF in its paroxysmal form is typified by long

periods of sinus rhythm variably punctuated with episodes of AF. Where the intervening period in sinus rhythm is sufficiently long enough to allow reversal of such electrical remodelling, it is challenging to explain how these transient changes have a bearing on the subsequent AF recurrence and protraction as observed in the clinical setting. In fact, following successful cardioversion from AF, atrial ERPs are surprisingly longer than in control subjects (Stiles *et al.*, 2009). The long term effects of repeated episodes of AF were evaluated in the pacing induced goat model (Garratt *et al.*, 1999). Here AF was induced for 3 consecutive 5-day periods, each interrupted by 2 days of sinus rhythm. Each episode of AF was associated with marked alterations in refractory properties, which appeared to normalise within 2 days of AF termination. There were no additive changes to the spectrum of electrical remodelling following successive episodes of AF and no difference in the susceptibility to AF was seen. A similar protocol was employed by Hobbs and colleagues, who allowed episodes of AF to continue for a month before cardioversion was performed (Hobbs *et al.*, 2000). Features of electrical remodelling were allowed to normalise before a further 1-month episode of AF was induced. The sequence and time course of remodelling events did not vary between episodes of AF, however a time-dependent increase in AF susceptibility was observed. Taken together, these findings support a role for altered refractory properties in sustaining AF, however the increased susceptibility following longer periods of AF hint towards additional and possibly more enduring remodelling phenomena being involved in this 'domestication' of AF.

Slowed conduction is recognised to reduce the AP wavelength and has been demonstrated in AF as described previously. Conduction slowing was not highlighted as a prominent feature of remodelling in AF in several early models (Ausma *et al.*, 1997*a*; Neuberger *et al.*, 2005). However, conduction slowing was observed following progressively lengthening episodes of AF in a canine model (Gaspo *et al.*, 1997*b*). The attenuation of conduction velocity was maximal at 6 weeks, lagging behind the reduction in atrial ERPs and rate adaptation, which peaked within 7 days suggesting these abnormalities are potentially mediated by different mechanisms. Indeed, conduction slowing can arise through fibrotic change disrupting the arrangement of myocyte bundles and such structural remodeling may be less likely to reverse. Atria from a canine model of congestive cardiac failure displayed marked interstitial fibrosis, heterogeneous conduction, and prolongation of atrial ERP, but were susceptible to sustained periods of AF (Li *et al.*, 1999). Similarly canine hearts modeling mitral regurgitation showed

abnormalities in conduction, significant structural remodeling and an increased propensity to AF despite prolongation of the ERP from baseline values (Verheule *et al.*, 2004).

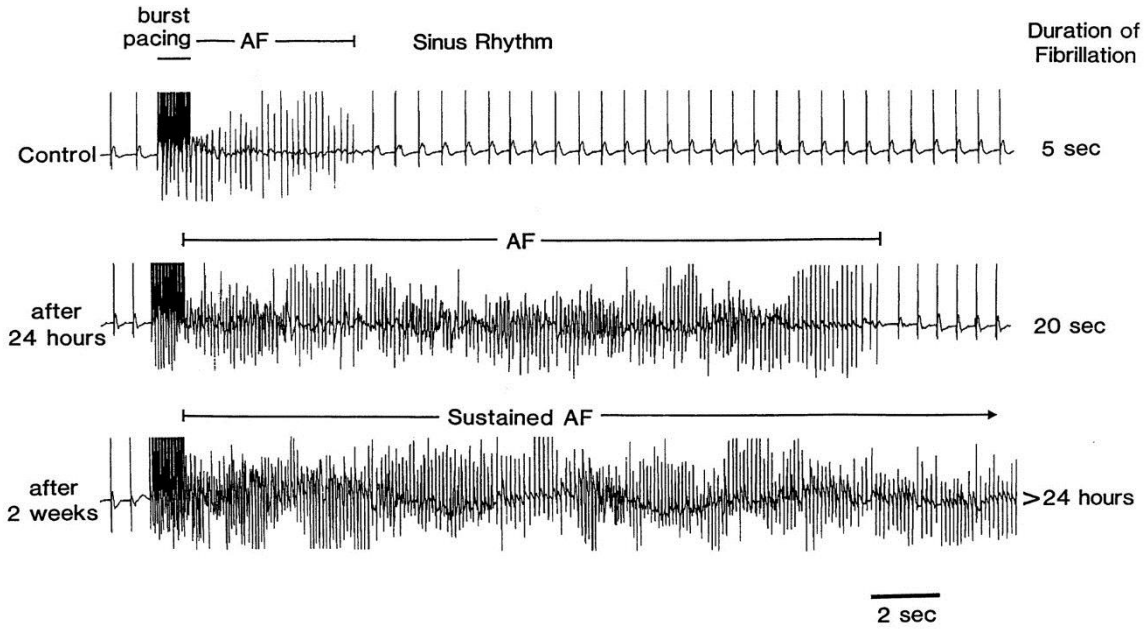

Figure 1.15 'AF begets AF'

Traces represent ECG recordings from a pacing-induced goat heart model of AF. Short burst of rapid atrial pacing would instigate brief episodes of AF on termination of pacing (top trace). If AF was maintained with continuous pacing for 24 hours, upon termination the AF would continue for 20 seconds before spontaneous cardioversion to sinus rhythm. If pacing was maintained for 2 weeks, sustained episodes of AF were observed in over 80% of the study animals, reflecting remodelling processes that supported persistence of AF. (Adapted from Wijffels et al., 1995)

Finally AF induced remodeling would not account for antecedent events that contribute to AF at its very inception. It is likely to alterations in cardiac physiology associated with ageing, underlying cardiac pathology and/or those conditions known to increase the risk of AF contribute to the initiation and maintenance of AF. Additionally AF is a progressive condition, underpinned by seemingly unrelenting remodeling, even when in sinus rhythm. Indeed, early and repeated cardioversion to minimise the time in AF in an effort to avert the AF induced remodeling failed to prevent AF progression suggesting that sinus rhythm does not beget sinus rhythm (Fynn *et al.*, 2002). Importantly these finding may intimate that the processes

underlying its genesis and progression are, to some degree, distinct from the arrhythmia itself and identification of these upstream instigators may represent sensitive therapeutic targets.

Studies investigating the molecular correlates of electrical remodelling in AF have suggested a panoply of potential mediators, however much of the data is conflicting and often difficult to reconcile. It remains unclear as to what extent such differences reflect species specific variations in ionic fluxes and indeed differences due to the method used to induce AF, and therefore how representative any abnormality is to human AF. A consistent finding in both animal models of AF (Wijffels *et al.*, 1995) and human specimens is a reduction in the APD (Van Wagoner *et al.*, 1999), a change attributed to a reduction in I_{Ca}, secondary to reduced expression of L-type Ca^{2+} channels (Lai *et al.*, 1999; Brundel *et al.*, 1999). This reduction in gene expression however becomes apparent after approximately three months of being in AF, suggesting against this being an instigating insult in the genesis of AF. The reduction itself has been postulated to be an adaptive phenomenon, in response to cellular calcium overload due to rapid atrial rates at the onset of AF (Van Wagoner *et al.*, 1999). The majority of intracellular calcium is derived from the sarcoplasmic reticulum (SR); it is released into the cytosol through RyR2 and levels are returned to their baseline during diastole through uptake into the SR by SERCA and extrusion out of the cell by NCX. Supra-normal intracellular Ca^{2+} concentrations augment activity of the NCX, the resultant net inward positive current if of sufficient magnitude depolarizes the cell causing delayed after-depolarisations.

Analysis of specimens from a murine model of AF (Li *et al.*, 2014) and atria of humans with AF demonstrate increased frequency of spontaneous diastolic SR Ca^{2+} leaks (Hove-Madsen *et al.*, 2004). Atrial cells from patients with AF demonstrate comparable SR Ca^{2+} levels to that from patients in sinus rhythm suggesting against excessive Ca^{2+} release being due to SR Ca^{2+} overload, but rather altered activity of the proteins involved in its release and re-uptake (Liang *et al.*, 2008; Neef *et al.*, 2010). Hyperphosphorylation of the RyR2 has been noted in atrial cells from a canine model of AF and cells from right atria of humans with AF, and this was associated with increased diastolic open probability (Vest *et al.*, 2005). In this study, the phosphorylation was protein kinase A (PKA) dependent. In a separate study, hyperphosphorylation of RyR2 in human atrial cells with noted at Ca^{2+}/calmodulin dependent protein kinase II sites (CaMKII), and CaMKII expression levels was also increased in these cells (Neef *et al.*, 2010). Furthermore, pharmacological or genetic inhibition of CaMKII

prevented AF in a murine gain-of-function RyR2 model of AF (Chelu *et al.*, 2009), suggesting CaMKII activity is required for the development of AF in this setting. The relative importance of either of these kinases in human AF remains open for discussion. Impaired Ca^{2+} re-uptake into the SR may also contribute to the mishandling of Ca^{2+} seen in AF. In keeping with this, expression of SERCA was reduced in human atrial tissue from individuals with AF. Little data exist as to the functional changes in AF or indeed the time course of this, particularly in relation to the alterations in RyR2 function mentioned above.

CaMKII may exert further arrhythmogenic effects through modulation of atrial K^+ transients. I_{to} density is significantly diminished in chronic AF (Caballero *et al.*, 2010) with corresponding downregulation in the expression of its α subunit Kv4.3 (Brundel *et al.*, 2001*b*). Acute over-activity of CaMKII actually increases I_{to} (Tessier *et al.*, 1999), however transgenic mice over-expressing CaMKII display downregulation of I_{to} (Wagner *et al.*, 2009). Reductions in gene expression and currents have also been reported for I_{KUR} (Van Wagoner *et al.*, 1997; Christ *et al.*, 2008) and the ATP sensitive K^+ channel (K_{ATP}) (Brundel *et al.*, 2001*b*; Balana *et al.*, 2003), however conflicting evidence exist for both (Bosch *et al.*, 1999; Wu *et al.*, 2005*b*) and their respective contributions to the genesis of AF remains unclear.

The evolution of AF is characterized by electrical and structural remodeling, producing an inhomogeneous atrial substrate permissive to AF maintenance. CPVT is characterized by episodic ventricular arrhythmias during periods of adrenergic stress. It is associated with genetic abnormalities in the cardiac RyR2, or proteins that interact with it. Interestingly murine models of CPVT demonstrate increased susceptibility to AF (Shan *et al.*, 2012). Similarly, an increased incidence of atrial tachy-arrhythmias has also been documented in human series of CPVT (Bhuiyan *et al.*, 2007). Huang & colleagues reported evidence of reduced ventricular conduction velocities in the *RyR-P2328S* murine model of CPVT, providing a substrate for reentry (Zhang et al., 2013). Moreover similar reductions in maximal upstroke of depolarization and conduction velocity were seen in the atria (King *et al.*, 2013*c*), providing some insights into alterations that underlie susceptibility to AF. Such changes in depolarization rate and conduction velocity are predominantly a function of Nav. In keeping with this, they demonstrated reduced Na^+ channel expression and function (King *et al.*, 2013*b*), highlighting downstream electrical remodelling from an isolated genetic abnormality in RyR2. Furthermore reduced I_{Na} could be recapitulated to some degree in wild type atria

following acute increases in intracellular Ca^{2+} concentration. The C-terminal of Na^{+} channel constructs have been shown to contain two Ca^{2+} sensitive regions that may explain their sensitivity to acute disturbances in Ca^{2+} homeostasis. Taken together, these observations provide some insight into acute and more chronic remodelling events that follow RyR2 dysfunction, and are implicated in the perpetuation of AF. Interestingly, previous studies had failed to identify any changes in I_{Na} or its channel expression (Bosch et al., 1999; Brundel et al., 2001b) however more recent patch clamp studies in atrial myocytes suggest such reductions in Nav function (Sossalla *et al.*, 2010).

1.6.5 Structural remodelling in AF

Early evidence of AF-related adverse structural remodelling was presented by Davies & Pomerance (1972), who reported on post-mortem examination findings on 100 patients with AF (Davies & Pomerance, 1972). Chronic AF was associated with fibrotic replacement of normal atrial myocardium in the region of the SAN and inter-nodal tracts in addition to nodal artery stenosis, compared to patients with AF onset within the final two weeks of life. This absence of fibrosis in early AF suggests the initiation of AF is not dependent upon it and also raises the possibility that it too may be an AF-induced remodelling phenomenon. Importantly, characterisation of atrial tissue from patients with a history of long standing AF who were undergoing cardiac surgery revealed evidence of apoptosis, suggesting a degree of irreversibility in this remodelling process that may underpin the progressive and increasingly intractable nature of AF with time (Aimé-Sempé *et al.*, 1999).

The progressive ultra-structural changes in atrial tissue related to AF were assessed by electron microscopy in the pacing-induced goat (Wijffels *et al.*, 1995) and canine (Morillo *et al.*, 1995) models of AF. Early changes included loss of the myocardial structural protein cardiotin, initially thought to have a role in linking the SR to sarcomeric proteins but more recent studies rather suggest a role in supporting cardiac mitochondrial function (Driesen *et al.*, 2009). Accordingly abnormal enlargement of mitochondria and fragmentation of the SR closely succeed these changes in cardiotin. The early period of AF is further typified by overall increase in atrial cell size, perinuclear accumulation of glycogen, progressive myolysis and alterations in the connexin composition and distribution (Ausma *et al.*, 1997*b*; Kostin *et al.*, 2002). Histological analysis form human atrial samples suggest progressive non-specific

patchy fibrosis with severe hypertrophy, vacuolar degeneration and necrosis of myocytes (Frustaci *et al.*, 1997).

The disruption of gap junction activity through fibrotic change within the atrium and altered connexin expression/distribution is likely to impact upon conduction properties within the atria and support reentry, even in the absence of cellular AP characteristics. Levels of both connexin 40 and connexin 43 are found to be reduced in AF and their location less limited to the intercalated discs as predominantly observed in sinus rhythm (Kostin *et al.*, 2002). Moreover these structural changes do not resolve at the same rate, if at all, as those that reflect electrical remodelling. Following 4 months of maintained sinus rhythm, atrial cell size and connexin expression patterns appear to normalise, however evidence of a degree of myolysis persist, albeit less severe, as well as the alterations in the extracellular matrix fraction (Ausma *et al.*, 2003). Thus structural abnormalities, which appear more gradually than electrical remodelling, may play a greater role in sustaining AF over longer periods, and determine the likelihood of AF progression with time.

1.6.6 Mitochondrial dysfunction and AF

The incidence of AF increases steeply with age, and there are now established associations between AF and a number of the constituents of the metabolic syndrome, including obesity, insulin resistance and hypertension (Asghar *et al.*, 2012; Isik *et al.*, 2012). The aetiological significance of these observations remain yet to be resolved. There is increasing data implicating general metabolic dysfunction, and in particular mitochondrial dysfunction, as a central feature of the biochemical changes that characterise ageing as well as the conditions listed above, and may also underlie the susceptibility to AF that accompany these states. Abnormal mitochondrial structure has been noted in animal models of AF (Morillo *et al.*, 1995; Ausma *et al.*, 1997*b*). In these models, mitochondrial abnormalities became apparent early following the induction of AF. Analysis of mitochondria in cardiomyocytes from human subjects with atrial fibrillation demonstrate greater degrees of DNA damage (Tsuboi *et al.*, 2001; Lin *et al.*, 2003), structural abnormalities (Bukowska *et al.*, 2008) and evidence of impaired function (Lin *et al.*, 2003; Ad *et al.*, 2005). Atrial tissue from patients with longstanding AF demonstrate altered transcription of mitochondrial oxidative phosphorylation-related proteins and increased myofilament oxidation (Mihm *et al.*, 2001;

Lamirault *et al.*, 2006). Also mitochondrial Complex II/III activity is decreased in permeabilised atrial fibres obtained from patients who developed post-operative AF, corresponding to decreased expression of the gene cluster for mitochondrial oxidative phosphorylation (Montaigne *et al.*, 2013). Additionally studies similarly analysing right atrial tissue from patients undergoing cardiac surgery also demonstrated downregulation of electron transport chain activity and proton leakage in patients with a history of AF (Seppet *et al.*, 2005; Emelyanova *et al.*, 2016).

Normal cardiomyocyte function is dependent upon a number of energy-intensive processes, in human hearts this amounts to kilogram quantities of adenosine triphosphate (ATP) daily (Leone & Kelly, 2011). This energetic cost is defrayed by a rich network of mitochondria. Mitochondria occupy up to 30% of cardiomyocytes cell volume and produce over 90% of cellular ATP (Schaper *et al.*, 1985; Barth *et al.*, 1992). Approximately 60-70% of cellular ATP is utilised in cardiac muscle contraction; the remainder is required for efficient calcium cycling as well as maintaining plasma gradients of other ions. It stands to reason that inefficient or mismatched energy supply will impact upon these processes. Accordingly, the sarcolemmal K-ATP (sarcK_{ATP}) channel is tightly coupled with mitochondrial energy state, its open probability increases with ATP depletion or rising levels of adenosine diphosphate (ADP) (Akar & O'Rourke, 2011). Activity of this channel causes efflux of potassium from the cell, which in cardiac tissue is associated with shortening of the APD and consequently the ERP (Fosset *et al.*, 1988; Faivre & Findlay, 1990), a state conducive to re-entrant arrhythmia. Inhibition of this channel in Langendorff-perfused rabbit hearts exposed to ischaemia-reperfusion (IR) was associated with reduced incidence of VF (Fischbach *et al.*, 2004). Similarly, inhibition of sarcK_{ATP} was associated with a reduction in VF and mortality in rats subjected to IR (Vajda *et al.*, 2007). Interestingly, Lin and colleagues recently demonstrated increased ectopic activity, burst firing and APD shortening in PVs and left atria of rabbit hearts subjected to IR, and this was attenuated with sarcK_{ATP} inhibition (Lin *et al.*, 2012). Whether such observations would be replicated with more subtle impairments of mitochondrial function associated with chronic disease has hitherto not been established.

In addition to receding provisions of ATP, uncoupling of mitochondria is also associated with increasing formation of reactive oxygen species (ROS) (Siasos *et al.*, 2018). In normal physiology, low levels of ROS play an important role in a variety cellular process by

modulating the activity of signalling molecules or assuming the role of signal molecules themselves. These effects may be transient by altering the activity of cellular proteins, or more enduring through their effects on transcription factors and gene expression.

The ability of ROS to influence the excitability of cardiomyocytes was first posited by Manning & colleagues, who demonstrated reduced incidence of malignant ventricular arrhythmias in rats following IR when pre-treated with the xanthine oxidase inhibitor, allopurinol (Manning *et al.*, 1984). Several studies have expanded on the role for oxidative stress in models of ventricular arrhythmia and more recent reports suggest a role in AF. Rapid-pacing induced AF in a canine model was associated with increased protein nitration in atrial tissue, reflecting formation of peroxynitrite (formed through the reaction of nitric oxide with superoxide anion), implicating a role for increased ROS production (Carnes *et al.*, 2001). Here rapid pacing resulted in shortening of the atrial ERP, a change that was attenuated by pre-treatment with the anti-oxidant ascorbate. A later study in a porcine model of rapid atrial pacing demonstrated, through direct measurements, augmented superoxide production from the left atria of animals that developed AF (Dudley *et al.*, 2005). Moreover, markers of oxidative stress are increased in right atrial appendage of patients with AF (Mihm *et al.*, 2001; Emelyanova *et al.*, 2016). Analysis of atrial specimens from patients with AF show reduced levels of glutathione, the most prominent endogenous anti-oxidant (Carnes *et al.*, 2007). Additionally genetic studies of atrial tissue from patients with AF suggest a shift towards a pro-oxidant state (Kim *et al.*, 2003). Amongst the several sources of ROS within cardiomyocytes, mitochondria are the most prominent (Siasos *et al.*, 2018), and have been implicated as an important source of ROS in AF in human atrial specimens (Reilly *et al.*, 2011).

Where in the pathogenesis of AF ROS reside – either cause or consequence - or the precise mechanisms by which abstraction of ROS production from the usual stringent controls confers increased susceptibility to arrhythmia remains an area of much debate. Indeed, oxidative stress has been shown to influence I_{Na}, I_K and I_{Ca} within cardiomyocyes, however the precise alteration in ion current function observed in studies demonstrate a significant degree of variability and indeed in some cases are contradictory. This conflicting data may reflect species dependent differences in the effect of ROS, or variability through differences in concentrations of ROS used, or the duration of exposure to ROS, and understandably poses a challenge to gaining clear mechanistic insights.

Dysregulated Ca^{2+} handling has been strongly linked to various phases of AF progression and may be influenced by ROS. CaMKII appears to be redox sensitive, its oxidation resulting in kinase activity resembling that of well characterized auto-phosphorylated CaMKII (Erickson *et al.*, 2008) and pharmacological inhibition of CaMKII can prevent H_2O_2 induced ventricular arrhythmias (Xie *et al.*, 2009). ROS have also been shown to oxidize and activate PKA (Eager & Dulhunty, 1998). Moreover, Terentyey and colleagues recently demonstrated ROS mediated changes in RyR2 function associated with ageing in rabbit ventricular myocytes were primarily through thiol oxidation of the RyR2 molecule itself and treatment with a mitochondrial specific ROS scavenger dithiothreitol returned RyR2 function to control levels, implicating direct alterations in RyR2 function may underlie the abnormalities seen rather than through the intermediacy of serine kinases (Terentyev *et al.*, 2008). Additionally, oxidative stress has been shown to reduce SERCA mediate calcium re-uptake, through thiol oxidation (Kukreja *et al.*, 1988). Little data exist as to the functional changes in AF or indeed the time course of this, particularly in relation to the alterations in RyR2 function mentioned above. Interestingly, reductions in cardiac Na^+ channel expression have also been reported following dysregulated ROS production (Liu *et al.*, 2010) as well as tentative links to increased cardiac fibrosis through fibroblast activation and production of transforming growth factor-β (TGF-β) (Friedrichs *et al.*, 2012).

Mitochondrial dysfunction in animal models of AF is seen following the induction of AF and so it is clear that rapid atrial rates certainly have a negative impact on mitochondrial function. Similarly, human studies of AF have generally involved obtaining atrial tissue for analysis from patients with established AF. Thus it remains difficult to differentiate whether such mitochondrial abnormalities represent bystander anomalies in the maelstrom of abnormalities that arise as a result of the atrial arrhythmia, or have a more direct role in the pathogenesis. If the latter were true, the available evidence would suggest a role in sustained AF. However given the proposed involvement of mitochondrial dysfunction in ageing and other conditions known to predispose to AF, one cannot discount a putative role in the instigation of AF however to date this has not been investigated.

1.7 Murine models for arrhythmia

Despite the clear difference in size, the basic cardiac structure between all mammals, including mice, is well conserved. Like human hearts, the murine cardiac system is organised within a dual circulation network where the right and left ventricles are structurally homologous between the species. The murine atria appear as two distinct chambers with prominent appendices, overlying the respective ventricles and contribute significantly to ventricular filling (Rentschler *et al.*, 2001). Structurally the murine SA node, AV node and AV bundles are similar to those in the hearts of larger mammals including humans (Rentschler *et al.*, 2001), while there are notable differences in basal heart rate (Vaidya *et al.*, 1999).

Species specific differences in the cardiac AP are also recognised. The murine AP has a less prominent contribution from the L-type Ca^{2+} current and therefore lacks a prolonged AP plateau, with corresponding reductions in APD from 150 – 400 ms in humans to 30 – 80 ms in mice (Danik *et al.*, 2002). In rodents, high I_{to} densities dominate all phases of repolarization and account for the significantly abbreviated APs, and absence of a clear plateau phase (Gussak *et al.*, 2000). However many of the processes remain conserved, especially those relating to depolarisation and the mouse heart therefore remains a useful model for the study of both AP generation and propagation in atrial and ventricular arrhythmogenesis (Papadatos *et al.*, 2002). Furthermore, both mice and humans display a similar relationship between action potential duration and refractory periods (Koller *et al.*, 1995; Fabritz *et al.*, 2003*a*). Additionally, both species have near identical transmural conduction velocities (Higuchi & Nakaya, 1984; Liu *et al.*, 2004) and there are similar differences in transmural heterogeneity in APD (Knollmann *et al.*, 2001*b*).

The mouse genome is amenable to genetic manipulation with relative ease and genetic mouse models of monogenic ion channel abnormalities have provided valuable insights into mechanisms of arrhythmogenesis. Murine models of BrS bearing mutations in the *SCN5A* gene recapitulate many of the features of the human form of the disease. Surface ECG recordings in these mice display the stereotypical ST elevation and QT dispersion (Martin *et al.*, 2010*a*). The electrophysiological aberrations and arrhythmic tendency are similarly accentuated by flecainide (Stokoe *et al.*, 2007) and ameliorated by quinidine (Stokoe *et al.*, 2007; Martin *et al.*, 2010*b*). Murine hearts carrying genetically altered RyR2 Ca^{2+} release channel and SR Ca^{2+} storage protein calsequestrin-2 have successfully modeled arrhythmogenic triggering

events. They recapitulate features associated with the chronic pro-arrhythmic condition of human catecholaminergic polymorphic ventricular tachycardia (CPVT) (Jiang *et al.*, 2005; Goddard *et al.*, 2008). Transgenic mice have also been used to successfully model forms of LQTS (Benhorin *et al.*, 2000).

Murine models of mitochondrial dysfunction, particularly those focused on the study of arrhythmias, have proven to be riddled with difficulties on several fronts. Firstly, efforts to introduce mutations into mitochondrial DNA (mtDNA) is fraught with logistical challenges. DNA transformation of mitochondria inside living cells appears unfeasible, as the introduced DNA must cross not one, but three membranes (the plasma membrane, plus two mitochondrial membranes), while preserving cell and organelle integrity and viability. Furthermore, mtDNA exists in high copy number in each cell, meaning that numerous transformation events are required to ensure introduced mtDNA reach meaningful levels. Secondly, the widespread and integral function of mitochondria mean that animals with deficient mitochondrial function are burdened with a multiplicity of pathologies. For example, Mito-mice carrying mutations in mtDNA develop progressive lactic acidosis and renal failure amongst a host of issues, and have an average lifespan of seven months (Inoue *et al.*, 2000; Nakada *et al.*, 2001). The nuclear encoded mitochondrial transcription factor A (TFAM) protein specifically binds mtDNA promoters and activates transcription (Larsson *et al.*, 1996). Tissue-specific *Tfam* knockouts faithfully reproduce phenotypes seen in humans with mtDNA disorders. Selective cardiac knockouts develop AV block, dilated cardiomyopathy and die at 2 - 4 weeks (Larsson *et al.*, 1998; Wang *et al.*, 1999). Indeed cardiomyopathy is a common feature of murine models of mitochondrial dysfunction, with utility in the study of heart failure but poses obstacles in arrhythmic investigations (Russell *et al.*, 2005).

1.8 Peroxisome proliferator-activated receptor γ coactivator-1 family

Overall mitochondrial mass and function within a given tissue are regulated by several transcriptional coactivators, however crucial amongst these are the peroxisome proliferator-activated receptor γ coactivator-1 (PGC-1) family. This family includes PGC-1α and PGC-1β, which are found with a reasonable degree of ubiquity but are most highly expressed in oxidative tissues including heart, brain, skeletal muscle and kidney (Sonoda *et al.*, 2007).

Peroxisome proliferator-activated receptors (PPARs) themselves were initially identified as a regulator of adipocyte differentiation and glucose metabolism in adipocytes, but are now known to be more widely expressed and are involved in the immune response, inflammation, cell growth and differentiation. PPARs therefore tactually target a broader range of transcription factors and demonstrate a role for the PGC-1 family of coactivators in a diverse range of processes.

Preliminary studies assessing roles of PGC-1 proteins demonstrated that either of these coactivators, PGC-1α or PGC-1β, are sufficient to activate gene regulatory programs that drive increased capacity for cellular energy production in mammalian cells. They achieve this through interacting with a host of nuclear receptor targets including PPARα (Vega *et al.*, 2000), PPARβ (Wang *et al.*, 2003), thyroid hormone receptor (Puigserver *et al.*, 1998), retinoid receptors (Puigserver *et al.*, 1998), glucocorticoid receptor (Knutti *et al.*, 2000), estrogen receptor (Puigserver *et al.*, 1998; Knutti *et al.*, 2000), farnesyl X receptor (Zhang *et al.*, 2004), pregnane X receptor (Bhalla *et al.*, 2004), hepatic nuclear factor-4 (HNF-4) (Rhee *et al.*, 2003), liver X receptor (Lin *et al.*, 2005), and the estrogen-related receptors (ERR) (Huss *et al.*, 2002). PGC-1α coactivates nuclear respiratory factor-1 (NRF-1) and -2 (NRF-2) (Wu *et al.*, 1999), which modulate expression of *Tfam*, a nuclear-encoded transcription factor essential for the replication, maintenance, and transcription of mitochondrial DNA (Larsson *et al.*, 1998; Garesse & Vallejo, 2001). NRF-1 and NRF-2 further regulate the expression of a range of other proteins required for mitochondrial function including nuclear genes encoding respiratory chain subunits (Virbasius *et al.*, 1993; Scarpulla, 2002). Additionally, several non-nuclear receptor PGC-1 partners have also been identified, including myocyte enhancer factor-2 (MEF-2) (Michael *et al.*, 2001), forkhead box O1 (FOXO1) (Puigserver *et al.*, 2003), sterol regulatory element-binding protein-1 (SREBP1) (Lin *et al.*, 2005), and Sry-related HMG box-9 (Sox9) (Kawakami *et al.*, 2005). PGC-1 proteins, through these interactions, exert multi-level regulation of cellular mitochondrial function and metabolism as a whole. For example PPARα is a key regulator of genes involved in mitochondrial fatty acid oxidation, while another PGC-1 target ERRα is an important regulator of mitochondrial energy transduction pathways including fatty acid oxidation and oxidative phosphorylation (Vega *et al.*, 2000). Furthermore several of the PGC-1 coactivation targets regulate pathways outside of the mitochondrion — such as HNF-4 and FOXO1 (gluconeogenesis), MEF-2 (glucose transport), SREBP1 (lipogenesis), and Sox9 (chondrogenesis).

Overexpression of PGC-1 proteins in various cell types has been shown to increase mitochondrial density and augment their oxidative capacity (Lehman *et al.*, 2000; Russell *et al.*, 2004). In cardiac cells, PGC-1α has been shown to interact with NRF- 1, ERRα and PPARα, leading to increased mitochondrial biogenesis (Vega *et al.*, 2000; Huss *et al.*, 2004). Ad-PGC-1-infected cardiomyocytes exhibit a marked induction in the expression of genes encoding mitochondrial fatty acid oxidation enzymes (Lehman *et al.*, 2000). Here, forced expression of PGC-1 in cardiomyocytes in culture also induced the expression of nuclear genes encoding mitochondrial proteins involved in other energy production pathways, including the tricarboxylic acid cycle, and nuclear and mitochondrial genes encoding components of the electron transport chain and oxidative phosphorylation complex. Transgenic mice with cardiac-specific overexpression of PGC-1 via the cardiac myosin heavy chain gene promoter develop a cardiomyopathy (Lehman *et al.*, 2000). Electron microsopic analysis of these mice demonstrated that the cardiac myocytes exhibited loss of sarcomeric structure due to uncontrolled mitochondrial proliferation. Taken together, these studies suggest that PGC-1 proteins promote FAO enzyme gene expression, and also activate the mitochondrial biogenesis programme in cardiomyocytes thus serving as a critical regulatory link between control of the mitochondrial FAO pathway and overall mitochondrial function.

Expression of PGC-1 proteins is increased by a number of upstream signals thus serving as a link between cellular energy stores and external stimuli such as cold exposure, fasting and exercise, ultimately coordinating mitochondrial activity to match cellular energy demands. Interestingly, PGC-1 levels are found to be reduced in obesity, insulin resistance, type II diabetes mellitus and ageing, correlating with the mitochondrial dysfunction that is seen in these conditions and implicating it in the their pathogenesis (Leone & Kelly, 2011; Dillon *et al.*, 2012).

Mice deficient in both PGC-1α and PGC-1β develop a low cardiac output state and conduction system disease, which contribute to their death before weaning (Lai *et al.*, 2008). Ablation of either the α or β member of the PGC-1 family in isolation produces a milder phenotype, particularly in the non-stressed state, possibly indicating a redundancy in function between the two forms. Several studies have examined the cardiac phenotype associated with genetic ablation of PGC-1α in animal models. Murine hearts lacking PGC-1α have normal contractile function at baseline but developed cardiac failure in response to increased afterload (Arany *et*

al., 2005). Information regarding *Pgc-1β* deficiency is more limited. PGC-1β deficient hearts demonstrate similarly preserved baseline features despite reduced mitochondrial content, but develop a blunted heart rate response compared to wild type (WT) hearts following adrenergic stimulation (Lelliott *et al.*, 2006). Furthermore the absence of *Pgc-1β* expression appears to increase the propensity to arrhythmia. Langendorff-perfused *Pgc-1β*$^{-/-}$ hearts demonstrate action potential duration alternans, recognised as a harbinger of arrhythmia, and significantly more frequent episodes of ventricular tachycardia in response to programmed electrical stimulation (Gurung *et al.*, 2011). Single cell studies from these hearts revealed alteration in the expression of a number of ion channels as well as evidence of spontaneous diastolic Ca^{2+} transients, previously associated with after-depolarisations that can trigger arrhythmias. Taken together, isolated absence of a single PGC-1 protein has little impact on the contractile function in the non-stressed state but produces an arrhythmic phenotype through alterations in the electrical landscape giving rise to a trigger and substrate for arrhythmia initiation and maintenance. The absence of overt cardiac dysfunction does make this an attractive model to investigate the role of mitochondrial impairment in arrhythmia without the confounding issue of heart failure.

1.9 Scope of this thesis

There is now greater appreciation for the metabolic changes that accompany, and possibly define, ageing as well as a number of conditions which seem to become more prevalent with advancing age. These conditions also exhibit an increased propensity to develop atrial arrhythmias, and there is speculation that this susceptibility to such rhythm disturbances are likely to be a consequence, in part at least, of these metabolic disturbances.

Current understanding of the upstream aberrations that manifest as AF or other age-related atrial arrhythmias such as AFL are however fragmentary, with much evidence imputed from studies of ventricular arrhythmias. Moreover little is known regarding the role of metabolic dysfunction in atrial arrhythmogenesis. Several studies have described impaired mitochondrial function in atria of individuals with a history of chronic AF. Mitochondrial dysfunction is also observed following experimentally induced AF in animal studies. These findings would imply such mitochondrial abnormalities develop as a consequence of AF. However, abnormal mitochondrial activity is seen in ageing and conditions such as obesity,

hypertension and type II diabetes mellitus in the absence of atrial arrhythmias, and therefore is likely to pre-exist in patients with these conditions who later develop AF. Such metabolic compromise may therefore actually contribute to the vulnerability to these arrhythmias. This is particularly relevant in AF where the underlying pathology seems to progress even while in sinus rhythm interspersed between paroxysms of AF. Indeed abnormal mitochondrial function is known to be arrhythmogenic in itself through a multitude of mechanisms. Much of the data however, has been gathered through in vitro studies or models of profound metabolic stress mimicking acute ischaemia. Information regarding the electrophysiological consequences of chronic mitochondrial dysfunction and the pathways involved is on the other hand limited. Murine models of mitochondrial dysfunction generally develop cardiomyopathy, and therefore further confounding the electrophysiological phenotypes observed. The murine *Pgc-1β* knockout model displays a mild cardiac phenotype with no overt contractile dysfunction. Importantly the *Pgc-1β*$^{-/-}$ hearts have abnormal Ca^{2+} handling, slowed conduction and a susceptibility to ventricular arrhythmias. Its atrial phenotype has as yet not been investigated.

The *Pgc-1β*$^{-/-}$ model will provide valuable mechanistic insights into the interplay between a metabolic lesion and cardiomyocyte excitation in murine atria. The thesis is intended to address the hypothesis that the metabolically defective *Pgc-1β*$^{-/-}$ murine cardiac system develops an atrial arrhythmic phenotype with age that arises from energetic deficiency and the abstraction of ROS production from the usual stringent controls, disrupting Ca^{2+} homeostasis through alterations in RyR2 function and thus instigating triggered activity. This in turn alters conduction of cardiac excitation through downstream reduction in I_{Na}, together providing a trigger and substrate for AF induction and maintenance.

Chapter 2 provides an overview of the methods that were employed to examine the arrhythmogenic tendency and the underlying electrophysiological mechanisms underpinning these at the whole animal, isolated heart and tissue levels. Each of the subsequent chapters describes a set of experiments, followed by a discussion of the results. The last chapter (Chapter 7) summarises all the results and discusses their limitations, and relevance to future work.

Assessment was first performed in the in vivo setting utilising surface ECG recordings under baseline conditions and then in response to adrenergic stress, given the known tendency for

AF to arise in circumstances of autonomic imbalance (Chapter 3). The intact animal studies preserve the extra-cardiac factors that influence cardiac activity and tendency to arrhythmia. As the sequelae of mitochondrial dysfunction progress with age, experiments were performed in young and aged *Pgc-1β*$^{-/-}$ animals and compared to age-matched wild type counterparts.

In chapters 4 and 5, a Langendorff perfusion system was utilised to analyse tissue and cellular electrophysiological parameters with sharp microelectrode measurements taken from the LA. The sharp electrode technique enables exquisite assessment of AP characteristics including precise indices of conduction and APD. Hearts were analysed for total arrhythmic episodes and associated electrophysiological properties in intrinsic rhythm, regular pacing and in response to programmed stimulation.

In chapter 6, the electrophysiological properties observed in the preceding experiments are correlated with a novel loose patch clamp technique that enabled assessment of ionic currents in the intact tissue, which is not possible with conventional whole-cell tight patch clamp technique. Additionally structural remodelling was assessed with histological sampling of atrial tissue.

2 Materials and methods

2.1 Experimental animals

All experiments were approved by the University of Cambridge Animal Welfare and Ethical Review Body (AWERB). The procedures performed complied with the UK Home Office regulations (Animals (Scientific Procedures) Act 1986) under a UK project licence (PPL number: 80/1974) for studies of cardiac arrhythmia and also conformed to the Guide for the Care and Use of Laboratory Animals, U.S. National Institutes of Health (NIH Publication No. 85-23, revised 1996) and NC3R guidelines.

All mice were inbred from a C57BL/6 strain to avoid possible strain-related confounds, and maintained by inter-crossing. *Pgc-1β*$^{-/-}$ mice were generated by genetic manipulation using a triple LoxP targeting vector (Lelliott *et al.*, 2006). The *Pgc-1β* locus was targeted with a ~8 kilobase 129/SvJ mouse genomic subclone targeting vector containing a floxed neomycin phosphotransferase selectable marker cassette inserted into intron 3 and a single LoxP site inserted into intron 5. Deletion of exons 4 and 5 was confirmed by southern blotting analysis, and germ line transmission of the modified *Pgc-1β* allele was confirmed by PCR. Heterozygous triple-LoxP–containing mice were then bred with ROSA26Cre mice to generate mice heterozygous for the *Pgc-1β* deletion. The latter were then intercrossed to generate mice homozygous for *Pgc-1β* deletion.

Breeding pairs of homozygote *Pgc-1β*$^{-/-}$ and wild type (WT) mice were set up and offspring were weaned and used when of the correct age. As the consequences of chronic mitochondrial dysfunction likely accumulate with age, mice were divided into four groups. Young WT and *Pgc-1β*$^{-/-}$ groups consisted of mice between the ages of 12-16 weeks. Previous studies in transgenic mice reported increased fibrotic and electrophysiological alterations at ages above 12 months (Jeevaratnam *et al.*, 2011). The latter two groups accordingly consisted of animals above this age to investigate the effects of age on electrophysiological parameters. Thus the aged WT and *Pgc-1β*$^{-/-}$ groups consisted of mice greater than 52 weeks.

Mice were housed in plastic cages maintained at 21 ± 1°C, and were subjected to 12 hour dark/light cycles with access to bedding and environmental stimuli. Sterile rodent chow (RM3 Maintenance Diet, SDS, Witham, Essex, UK) and water were available ad libitum.

2.2 In vivo electrocardiography

ECG recordings were obtained in intact mice, preserving all extra-cardiac influences upon cardiac excitation (Chapter 3). Recordings were taken under general anaesthesia to circumvent issues with movement artefact.

2.2.1 Electrocardiography recordings

Mice were anaesthetised with tribromoethanol (avertin: 2,2,2 trimethylethanol, Sigma-Aldrich, Poole UK) administered into the intra-peritoneal space with a 27G hypodermic needle. Avertin was selected as the anaesthetic of choice as it modifies the haemodynamic and electrophysiological properties to a lesser extent than other available compounds such as ketamine (Mitchell *et al.*, 1998). Mice were then weighed, placed supine on a warmed (37°C) platform, and their limbs secured with adhesive tape to minimise movement artefact and enable correct lead positioning. Three 2-mm diameter electrodes (MLA1204; ADInstruments, Colorado Springs, CO, USA) placed in the right forelimb, left forelimb and left hindlimb respectively enabled lead I and lead II ECG recordings. The electrodes were connected to a 4-channel NL844 pre-amplifier whose outputs were then led through 4-channel NL820 isolator and NL135 low-pass filter units (set at a 1.0-kHz cut-off and with a 50-Hz notch) within a NL900D chassis and power supply (Neurolog-Digitimer, Hertfordshire, UK). To reduce electrical noise, all recordings were carried out within a grounded Faraday cage. Signals were sampled at 5 kHz and analogue-to-digital conversion employed a CED 1401c interface (Cambridge Electronic Design, Cambridge, UK). This then conveyed the signal to a computer for display and recording using Spike II software (Cambridge Electronic Design).

ECG recordings commenced immediately following electrode attachment in anaesthetised animals. These were continued for 5 minutes to permit preparations to reach a steady state,

and for a further 5 minutes to obtain traces for quantitative analysis. Dobutamine hydrochloride (3 mg/kg; Sigma Aldrich, Poole UK) was then administered into the intraperitoneal space**.** ECG recording was then continued until a new steady state was reached. A further 5 min recording period provided traces for quantitative ECG analysis following pharmacological challenge.

2.2.2 Digital signal processing

All analysis employed custom-written software in the open-source R programming language (R Core Team, 2015). Data was imported into the R program. An infinite impulse response high pass Butterworth filter of order 2 was designed and the signal passed through to eliminate baseline drift. The signal was filtered in both forward and reverse directions to negate effects of any phase shift. A low-pass Savitzky-Golay algorithm was then applied. R peak fiducial points were identified with a peak-finding algorithm used to detect QRS complexes. An iterative process determined the signal envelope and an adaptive threshold was used to identify time points in the signal that were greater than threshold in the continuous ECG signal. QRS complex timing positions were determined; peaks on a more substantive upward or downward trend were disregarded in favour of the peak with the larger absolute value. If multiple peaks were detected within 2 ms, the peaks were analysed again and the larger maximum value taken as the correct peak, and the smaller peak discarded. In addition, all detections were visually verified. P waves were analyzed independently of QRS complexes by deleting the QRS complexes and subsequent isolation of the P wave parameters. This analysis thus made no assumption of QRS complexes being preceded by P waves. Analysis was performed on 300 sec periods of ECG data immediately prior to and following administration of dobutamine hydrochloride. The effect of dobutamine was judged from observed ECG parameter changes. Figure 2.1 depicts a typical murine ECG recording with parameters calculated based upon this archetypal signal. Intervals were corrected using the formula previously described (Mitchell *et al.*, 1998).

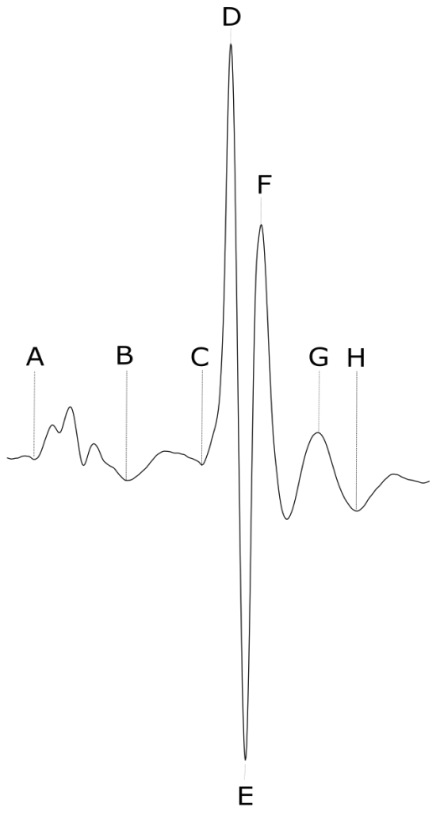

Figure 2.1 Typical murine electrocardiogram complex and relevant intervals

Typical ECG and definition of deflections used in quantitative analysis (a) start of P wave start; (b) P wave trough/end of P wave; (c) start of QRS complex; (d) R wave peak; (e) trough of S wave; (f) peak of R' deflection; (g) C wave peak; (h) trough or end of C wave. The corrected QT interval, QT_c is taken as the interval from c to h and corrected for RR intervals (Mitchell *et al.*, 1998).

2.3 Whole heart studies

2.3.1 Experimental solutions

All buffering media utilised in the study were based on Krebs-Henseleit (KH) solution, containing NaCl (119 mM), $NaHCO_3$ (25 mM), KCl (4 mM), $MgCl_2$ (1 mM), KH_2PO_4 (1.2 mM), $CaCl_2$ (1.8 mM), glucose (10 mM) and sodium pyruvate (1.8 mM), pH adjusted to 7.4 and bubbled with 95% O_2/5% CO_2 (British Oxygen Company, Manchester, UK). All chemical reagents were purchased from Sigma-Aldrich (Dorset, Poole, UK) except where otherwise indicated. Hearts were electromechanically uncoupled using blebbistatin (20 μM, Selleckchem, Houston, USA) to minimize motion artefact during the microelectrode studies,

permitting stable impalement of the cardiomyocyte.

2.3.2 Langendorff perfused preparation

In chapters 4 and 5, electrocardiograph and microelectrode studies were performed using a horizontal Langendorff perfusion system adapted for the murine heart incorporated into a Faraday cage, together with a light microscope (objective ×5, eyepiece ×5, W. Watson and Sons Limited, London, UK), custom built head stage and a warmed bath superfused with the buffering media. All equipment was electrically insulated. The stimulating and recording electrodes were positioned at appropriate positions on the right and left atrium respectively using two precision micromanipulators (Prior Scientific Instruments, Cambridge, UK).

Mice were anticoagulated with heparin sodium 200 IU (Sigma-Aldrich, Poole, UK) prior to sacrifice, administered into the intra-peritoneal space with a 27G hypodermic needle. Following an interval of 10 minutes, mice were killed by cervical dislocation (Schedule 1: UK Animals (Scientific Procedures) Act (1986)), a sternotomy and cardiectomy rapidly performed, and the excised heart placed in ice-cold bicarbonate-buffered KH solution. The proximal segment of the aorta was identified and cannulated with a modified 21G hypodermic needle, and secured in place with an aneurysm clip (Harvard Apparatus, Kent, UK) and a 5-0 braided silk suture. The cannulated heart was mounted on to the Langendorff apparatus and retrogradely perfused with KH solution at a constant flow rate of 2.05 ml min^{-1} by a peristaltic pump (MINIPULS3, Gilson, Luton, UK) passing first through 200 μm and 5 μm Millipore filters (Millipore, Watford, UK) and maintained at 37°C by a water jacket and circulator (model C-85A, Techne, Cambridge, UK). Upon perfusion, hearts were selected for experimentation if they demonstrated sustained intrinsic activity with a basic cycle length (BCL) <200 ms and 1:1 atrioventricular conduction for 10 minutes. Preparations meeting these criteria were subsequently perfused with 150 ml KH solution containing 20 μM blebbistatin and then normal KH solution throughout the remainder of the study.

2.3.3 Volume conducted electrocardiograph recordings

Whole heart volume conducted ECG recordings were taken concurrently with intracellular recordings to distinguish between isolated cellular and generalised atrial phenomena. Two

unipolar ECG leads were immersed into the warmed bath flanking the right and left atria respectively. Signals were amplified using a model NL104A amplifier (NeuroLog; Digitimer, Hertfordshire, UK), filtered at low and high cut-off frequencies of 5 and 500 Hz (model NL125/126 filter) and digitized using a model 1401 interface (Cambridge Electronic Design) for analysis with Spike II software (Cambridge Electronic Design).

2.3.4 Whole heart intracellular microelectrode recordings

Glass micropipettes were drawn from 1.2 mm outer diameter and 0.69 mm internal diameter borosilicate glass (Harvard Apparatus, Cambridge, UK) using a homebuilt microelectrode puller, and cut above the shoulders to an appropriate length. The microelectrodes were backfilled with 3 M KCl immediately before use, with tip resistances ranging between 15 – 25 MΩ. The filled microelectrode was mounted on to a right-angled microelectrode holder connected to a high-input impedance direct-current microelectrode amplifier system (University of Cambridge, Cambridge, UK). Intracellular voltage was measured relative to that of the Ag/AgCl reference electrode. AP recordings were used for analysis if obtained from an impalement associated with the abrupt appearance of a resting membrane potential (RMP) between -65 mV and -90 mV, stable and normal AP morphology and an amplitude >75 mV.

Hearts were placed in the anatomical position within the bath with the LA reflected back and fixed in position using three A1 insect pins. A bipolar platinum-coated stimulating electrode (NuMed, New York, USA) was positioned against the epicardial surface of the right atrium, pacing the heart using square-wave stimuli of 2 ms duration using a constant voltage stimulator (model DS2A-Mk.II, Digitimer, Welwyn Garden City, Herts., UK) controlled by Spike II software (Cambridge Electrical Design, Cambridge, UK) and delivering a voltage that was twice the diastolic excitation threshold plus 0.5 mV.

2.3.5 Pacing protocols

The experiments described in chapter 4 examined the hearts under conditions of regular pacing at a basic cycle length (BCL) of 125 ms (8 Hz). Hearts were then studied using a programmed electrical stimulation (PES) protocol comprising drive trains of eight regularly paced (S1) beats at a BCL of 125 ms, followed by an isolated premature extra stimulus (S2)

every ninth beat. The S2 stimulus was imposed at progressive shortening S1-S2 coupling intervals, initially being 89 ms and reducing by 1 ms every subsequent cycle to a final coupling interval of 5 ms. The protocol was terminated upon establishment of the atrial effective refractory period (ERP), defined as the first S1-S2 coupling interval at which the S2 stimulus failed to successfully elicit an AP, or sustained arrhythmia was observed.

The restitution analyses described in chapter 5 were performed utilising incremental pacing protocols that was initiated after achieving stable microelectrode impalement. These consisted of cycles of regular pacing each of 100 stimulations. They began with a basic cycle length (BCL) of 130 ms, that was then decremented by 5 ms for each subsequent cycle. These were repeated until the heart entered into 2:1 block or arrhythmia.

2.3.6 Quantification of AP parameters and arrhythmic incidence

The electrophysiological parameters were calculated from each AP individually and averaged across the protocol to give an overall mean for each heart. The AP amplitude was measured from the baseline to the peak voltage excursion and the AP duration was measured as 90% recovery to baseline (APD_{90}) (Figure 2.2). AP latencies were measured as the time elapsed between the pacing stimulus and peak of the AP. Maximum rates of depolarization $(dV/dt)_{max}$ were calculated from the differentiated intracellular AP waveform. The incidence of abnormal atrial rhythms were determined from the regular pacing and PES protocols, corroborating cellular phenomena to tissue-level activity. Isolated non-triggered APs were classified as ectopic beats, two successive non-triggered beats termed a couplet and atrial tachycardia (AT) was defined as an episode consisting of ≥3 consecutive non-triggered beats.

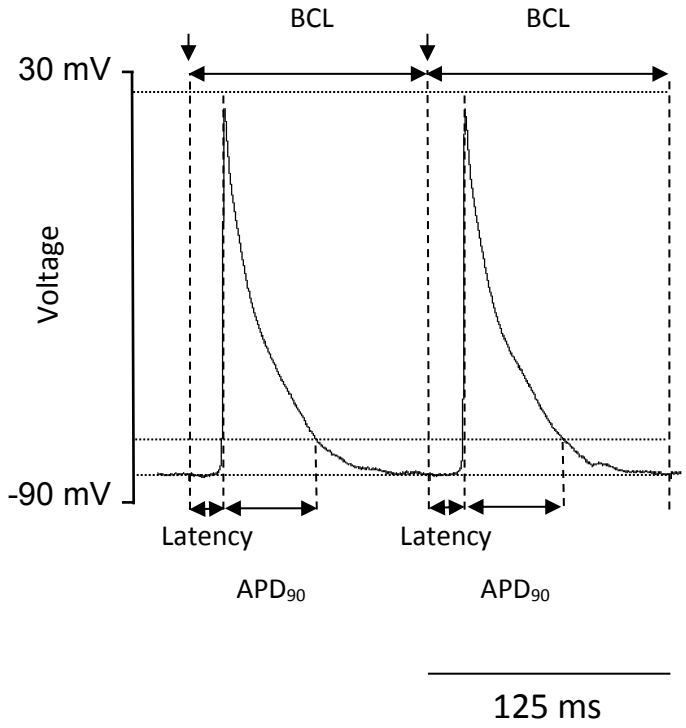

Figure 2.2 Typical atrial AP waveform relevant electrophysiological parameters

Basic measures of atrial action potential (AP) propagation, activation and recovery. AP amplitude was measured from the baseline to the peak voltage excursion. AP duration was measured as 90% recovery to baseline (APD_{90}), and AP latencies were measured as the time elapsed between the pacing stimulus and peak of the AP. Maximum rates of depolarization $(dV/dt)_{max}$ were calculated from the first differential of the intracellular AP waveform.

2.4 Loose patch clamp studies

2.4.1 Experimental preparation

In chapter 6, the various determinates of AP propagation were evaluated to investigate for remodeling phenomena downstream of mitochondrial impairment. This included a novel loose patch clamp protocol to assess for transmembrane currents in an intact atrial preparation. Immediately following sacrifice, the heart was excised and transferred into ice-cold Krebs–Henseleit (KH) solution: (mM) NaCl, 108; $NaHCO_3$, 25; KCl, 4.0; KH_2PO_4, 1.2; $MgCl_2$, 1.0; $CaCl_2$, 1.8; glucose, 10; and Na-pyruvate, 2.0; pH adjusted to 7.4 and bubbled with 95% O_2/5% CO_2 (British Oxygen Company, Manchester, UK). The aorta was cannulated with a trimmed and filed 21G hypodermic needle, and secured onto the cannula with an aneurysm

clip and 5-0 braided silk suture. The heart was perfused retrogradely in a Langendorff system under constant flow (2.1 ml/min) by a Watson-Marlow (Falmouth, UK) peristaltic pump with 75 ml of a modified KH solution containing 10 mM 2,3-butanedione monoxime (BDM) and 10 μM blebbistatin (Cayman Chemical Company, Ann Arbor, Michigan, USA) (to give a KH-BDM/blebbistatin solution) to electromechanically uncouple the heart. The heart was then immediately transferred into ice-cold KH-BDM/blebbistatin solution. The atria were dissected from the rest of the heart, mounted onto Sylgard (Dow Chemical Company, Staines, UK) and placed in a bath containing filtered KH buffer solution. The latter was thermostatically maintained at 27 °C through all the experimental procedures performed.

2.4.2 Loose patch clamp current recordings

Pipettes were pulled from borosilicate glass capillaries (GC150-10 Harvard Apparatus, Cambourne, Cambridge, UK) using a Flaming/Brown micropipette puller (model P-97, Sutter Instrument Co. Novato, CA, USA). Pipettes were mounted and fractured with a diamond knife at 250× magnification under a microscope with a calibrated eyepiece graticule. Applying a transverse force to the distal tip of the pipette gave a fracture perpendicular to the main micropipette axis. Selected pipettes were fire polished using an electrically heated nichrome filament under visual guidance at 400× magnification. The pipette tips were then bent to make a ~45^{o} angle with the pipette shaft. This permitted them to approach the membrane vertically when mounted on the recording amplifier headstage. Maximum internal pipette tip diameters were measured at 1000× magnification.

All pipettes had diameters 28-32 μm following polishing. Their distal ends were filled with KH buffer and mounted onto the pipette holder connected to the headstage. Ag/AgCl electrodes maintained electrical connections to the organ bath and pipette. The pipette was lowered onto the membrane surface. Gentle suction was applied through an air-filled line connected to the pipette holder using a syringe to induce seal formation around the membrane patch. Voltage-clamp steps were delivered under computer control relative to resting membrane potential. The loose patch clamp configuration results in larger leakage currents than conventional patch clamp owing to relatively low seal resistances. A custom-built amplifier compensated for most of the leakage current, series resistance errors and

displacement currents through the pipette capacitance (Stühmer *et al.*, 1983). Residual leakage and capacitative currents were then corrected for using reference records from subsequent P/4 control protocols applying steps of the opposite sign relative to the test steps, with amplitudes scaled down by a factor of 4 as fully described previously (Almers *et al.*, 1983*a*, 1983*b*). Once established all patches were subject to the complete set of pulse procedures bearing on either inward or outward current activation (Figure 2.3).

2.5 Quantification of cardiac fibrosis

The quantification of cardiac fibrosis was performed (Chapter 6) as previously described (Jeevaratnam *et al.*, 2011). Briefly, the excised heart was first flushed with KH solution and then perfused for five minutes with 4% buffered paraformaldehyde before being immersed in the paraformaldehyde overnight. Following the fixation process, longitudinal cardiac sections were cut and subjected to routine tissue processing and paraffin embedding. Serial sections of 7 μm thickness were then taken and stained with picrosirius red for fibrotic change. All sections were subsequently viewed, magnified and digitally acquired using the Nano Zoomer 2.0 Digital Pathology system (Hamamatsu, Hertfordshire, UK). A custom made 17 cm × 30 cm morphometric grid was superimposed on each magnified photomicrograph and each successive 1 cm × 1 cm, corresponding to 0.2 mm × 0.2 mm area of tissue, was scored first for the presence or absence of cardiac tissue, and in turn for presence of fibrosis. The degree of fibrosis was quantified as the proportion of squares occupied by cardiac tissue showing evidence of fibrotic change. The analysis was performed independently by two investigators blinded to the animal genotype and age, and an inter-class correlation coefficient analysis (ICC) was performed to assess the consistency of their results, which can be interpreted as follows: 0 – 0.2 indicates poor agreement; 0.3 – 0.4 indicates fair agreement; 0.5 – 0.6 indicates moderate agreement; 0.7 – 0.8 indicates strong agreement; and >0.8 indicates almost perfect agreement.

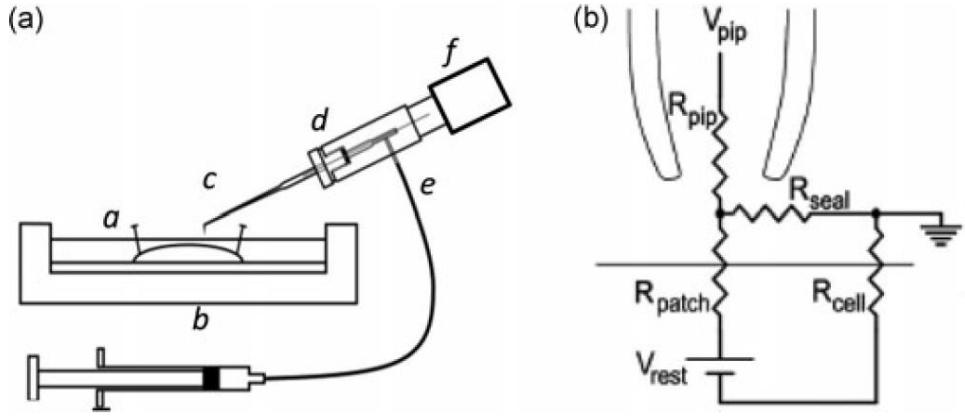

Figure 2.3 Loose patch clamp of murine atrial tissue

(a) Experimental loose patch configuration: (a) mounted muscle preparation under Krebs–Henseleit solution within (b) experimental chamber. (c) Loose patch pipette mounted at 45° to the preparation but bent to permit right-angled contact of pipette tip with the myocyte surface. Pipette held within (d) half-cell chamber in turn connected to (e) air line and suction syringe, and mounted on (f) headstage moved under micromanipulator and upright microscope guidance. (b) Equivalent circuit of loose patch clamp electrode on membrane. Pipette clamped at voltage Vpip. Compensation for the voltage error arising from currents flowing through the series combination of the pipette resistance (Rpip) and the seal resistance (Rseal) achieved using a bridge circuit in the custom-designed loose patch clamp amplifier. As the loose patch technique alters the extracellular potential within the patch relative to RMP, negative and positive voltage excursions in Vpip, respectively, produce hyperpolarising and depolarising voltage steps relative to RMP.RMP: resting membrane potential; Rpatch: patch membrane resistance; Rcell: overall cell membrane resistance

2.6 Statistical procedures

Data from the experiments were analysed using a custom written programme in the python programming language and all statistical analysis performed in the R programming language (R Core Team, 2015). Data are expressed as mean ± standard error of the mean (SEM), and in all cases a $p < 0.05$ was taken to be significant, with application of Bonferroni correction where appropriate. The statistical procedures pertaining to data analysis for each experiment are outlined in detail at the beginning of each respective chapter.

3 Age-related electrocardiographic changes in *Pgc-1β* deficient murine hearts

3.1 Introduction

As discussed in chapter 1, there is growing evidence linking increased arrhythmic risk to the energetic dysfunction that is seen in ageing as well as a range of common ageing-related chronic conditions. Indeed, the incidence of both atrial and ventricular arrhythmias rises with age (Deo & Albert, 2012; Zoni-Berisso *et al.*, 2014). Additionally, chronic conditions such as obesity, diabetes mellitus and heart failure constitute independent risk factors for such arrhythmias, independent of any co-existent coronary artery disease (Vianna *et al.*, 2006; Sato *et al.*, 2009; Kucharska-Newton *et al.*, 2010; Yeung *et al.*, 2012; Menezes *et al.*, 2013*b*).

However few studies have investigated the role of chronic mitochondrial dysfunction on atrial electrophysiological properties and arrhythmic tendency. The PGC-1 family of transcriptional coactivators include PGC-1α and PGC-1β, are highly expressed in oxidative tissues such as the heart, and form key regulators of mitochondrial mass, function, and cellular metabolism (Lin *et al.*, 2005; Finck & Kelly, 2006). Studies on *Pgc-1β* deficient hearts are limited. They nevertheless report preserved baseline cardiac function despite reduced mitochondrial content, but blunted heart rate responses following adrenergic stimulation (Lelliott *et al.*, 2006). Furthermore, Langendorff-perfused *Pgc-1β*$^{-/-}$ hearts demonstrated increased arrhythmic propensity reflected in increased frequencies of VT following programmed electrical stimulation (Gurung *et al.*, 2011). Detailed examination of the atrial electrophysiological profile in these hearts has not been conducted.

Murine models are now extensively utilised in the study of arrhythmogenesis and the surface ECG represents the only non-invasive tool for interrogating the electrophysiological properties in the intact system. Murine ECG with the subsequently developed analysis of its waveform (Goldbarg *et al.*, 1968) has an established usefulness for exploring electrophysiological changes in induced cardiac disease, particularly in laboratory settings (Belevych *et al.*, 2012). Murine and human ECGs show some differences reflecting higher sinus

rates, shorter action potential waveforms lacking plateau phases and distinct repolarisation characteristics (London, 2001; Danik *et al.*, 2002; Boukens *et al.*, 2014; Zhang *et al.*, 2014*a*). Nevertheless, murine results can translate to human ECG determinations of heart rate, its variability, and changes in timings of, the cardiac excitation sequence (Wehrens *et al.*, 2000). Thus, P waves, PR, QRS and QT intervals, reflect atrial and ventricular, depolarisation and repolarisation phases with their shortening or prolongation reflecting particular physiological changes potentially portending arrhythmic risk. Previous experimental studies reported altered murine ECG waveforms replicating those seen with human *SCN5A* mutations associated with the BrS (Jeevaratnam *et al.*, 2010; Martin *et al.*, 2010*a*), long QT syndrome type 3 (Wu *et al.*, 2012) and CPVT (Zhang *et al.*, 2011).

The experiments described in this chapter investigate changes in individual components of ECG waveforms reflecting particular electrophysiological components of excitation, and their association with *Pgc-1β* ablation, known to result in energetic dysfunction. The likely cumulative phenotypic effects of chronic mitochondrial lesions with advancing age, were studied in young and aged, WT and genetically modified animals both at baseline and following adrenergic stress, thus providing additional insights into possible interactions between genotype and ageing.

3.2 Specific methods

3.2.1 Experimental Animals

Mice were divided into four groups: groups 1 and 2 composed of mice aged between 12-16 weeks, and consisted respectively of littermate WT controls (n = 5) and *Pgc-1β*$^{-/-}$ mice (n = 9). Group 3 was composed of aged (greater than 52 weeks) littermate WT controls (n = 8). Group 4 consisted of *Pgc-1β*$^{-/-}$ mice of age similarly greater than 52 weeks (n = 6). Both male and female mice were used and groups were balanced for gender.

3.2.2 *Statistical analysis*

Statistical analysis used the R programming language. Data sets were first tested for normality with the Shapiro-Wilk test before statistical analysis using two way factorial multivariate analysis of variance, i.e. MANOVA with Pillai trace. The data sets analysed were the steady state heart rates, P wave durations, PR intervals, activation parameters of QR, QS and QR' durations, recovery parameters of RT_c, $R'T_c$ and ST_c durations, as well as the QT_c interval. Each of these were measured from ECG records of young and aged, WT and *Pgc-1β*$^{-/-}$ mice respectively, both before and following dobutamine challenge. The initial MANOVA tests examined each parameter for significant effects of age, genotype or interactive effects of age and genotype either prior to or following dobutamine challenge. Where MANOVA testing indicated existence of significant differences prior to dobutamine administration, further ANOVA analyses were conducted on pre-drug parameters testing for effects of genotype, age of interacting effects of the two. The presence of significant effects then prompted pairwise Tukey honest significant difference testing of differences between pairs of individual parameters. Similarly, where significant differences were indicated post-dobutamine, a similar procedure of significance testing was performed examining for significant effects post drug challenge. Peak heart rates were obtained following dobutamine challenge, and were analysed by a two way factorial ANOVA: there was no meaningful peak heart rate pre-dobutamine. These were then also followed by post hoc Tukey tests for differences between individual parameters if prompted by the significance levels. A $p < 0.05$ following Bonferroni correction where appropriate was considered to indicate a significant difference. Murine ECGs which demonstrated P wave dissociation in the analysis period were discarded for P wave dependent parameter analysis. All diagrams were produced with the R-grammar of graphics package.

3.3 Results

3.3.1 *Baseline characteristics*

There were no significant differences in weights between different groups, whether stratified by age or genotype. Aged *Pgc-1β*$^{-/-}$ mice had a mean weight of 35.49 ± 1.44 g compared to 35.57 ± 1.13 g for aged WT mice. Young *Pgc-1β*$^{-/-}$ and WT mice had mean weights of 31.30 ± 1.56 g and 35.31 ± 2.26 g respectively. Inspection of complete ECG records confirmed sinus rhythm

as the predominant rhythm (Figure 3.1 A). This initial analysis also assessed for the presence or absence of ST segment changes that might signal acute ischaemic change. These were never observed prior to dobutamine challenge. Two mice, both aged *Pgc-1β*$^{-/-}$, showed multiple ectopic beats (Figure 3.1 B) (Table 3.1). Following challenge, ST segment depression occurred in a small number of both WT and *Pgc-1β*$^{-/-}$ aged mice (Figure 3.1 D and 3.1 E).

Figure 3.1 ECG recordings from *Pgc-1β*$^{-/-}$ hearts

Typical ECG records from Pgc-1β$^{-/-}$ *hearts illustrating (A) normal sinus rhythm; (B) ectopic beat; (C) atrioventricular (AV) dissociation; records obtained from the same mouse. Arrows indicate timings of P-waves (D) pre-dobutamine and (E) following dobutamine challenge with ECG showing ST depression*

Table 3.1	Incidence of particular electrocardiographic features in the experimental groups				
		WT		*Pgc-1β*$^{-/-}$	
		Young	Aged	Young	Aged
A)	Ischaemic change				
	Ischaemic changes present	0	2	0	2
	Ischaemic changes absent	5	6	9	4
B)	Arrhythmic ECG patterns				
	Sinus Rhythm only	5	4	8	3
	Isorhythmic AV dissociation	0	4	1	3
	Ventricular ectopic beats	0	0	0	1

Electrocardiographic records obtained at baseline prior to pharmacological intervention in young WT (n = 5), aged WT (n = 8), young *Pgc-1β*$^{-/-}$ (n = 9) and aged *Pgc-1β*$^{-/-}$ (n = 6)

3.3.2 Pgc-1β$^{-/-}$ *hearts display impaired heart rate responses*

Chronotropic incompetence is an established clinical feature of cardiac failure (Brubaker & Kitzman, 2007, 2011) as well as constituting an indicator of other cardiac pathology (Girotra *et al.*, 2012). It has been variably defined, commonly identified as a failure to reach an arbitrary percentage of the predicted maximum heart rate following sympathetic challenge, ranging from 70 – 85 % (Lauer et al. 1999, Dresing et al. 2000, Elhendy et al. 1999) (Brubaker & Kitzman, 2011). A previous study had reported an impaired chronotropic response in isolated ex-vivo *Pgc-1β*$^{-/-}$ hearts challenged with dobutamine. These findings had not been statistically significant at a 10 ng/kg/min infusion rate and depended on single heart rate recordings at each predefined, time point (Lelliott *et al.*, 2006). The present experiments systematically analysed steady-state parameters over 5-min recording periods before and following dobutamine challenge in intact animals.

Figure 3.2 shows typical heart rate profiles at baseline and in response to dobutamine for each experimental group. As there is no algorithm predicting normal murine heart rates at different ages as there is with humans, the chronotropic response to dobutamine challenge was assessed using two different parameters: (1) peak heart rate attained after dobutamine administration and (2) mean heart rate observed post dobutamine administration. Figure 3.3 plots mean heart rates observed before dobutamine challenge against results obtained

following dobutamine challenge for each individual animal. *Pgc-1β*$^{-/-}$ animals displayed a tendency to slower basal heart rates under both conditions. A Pearson product-moment correlation coefficient assessing the co-variance between mean heart rates before and following dobutamine challenge demonstrated a positive association between variables, ($r=0.692$, $p < 0.0001$). Lower resting heart rates thus correlated with lower heart rates after dobutamine challenge.

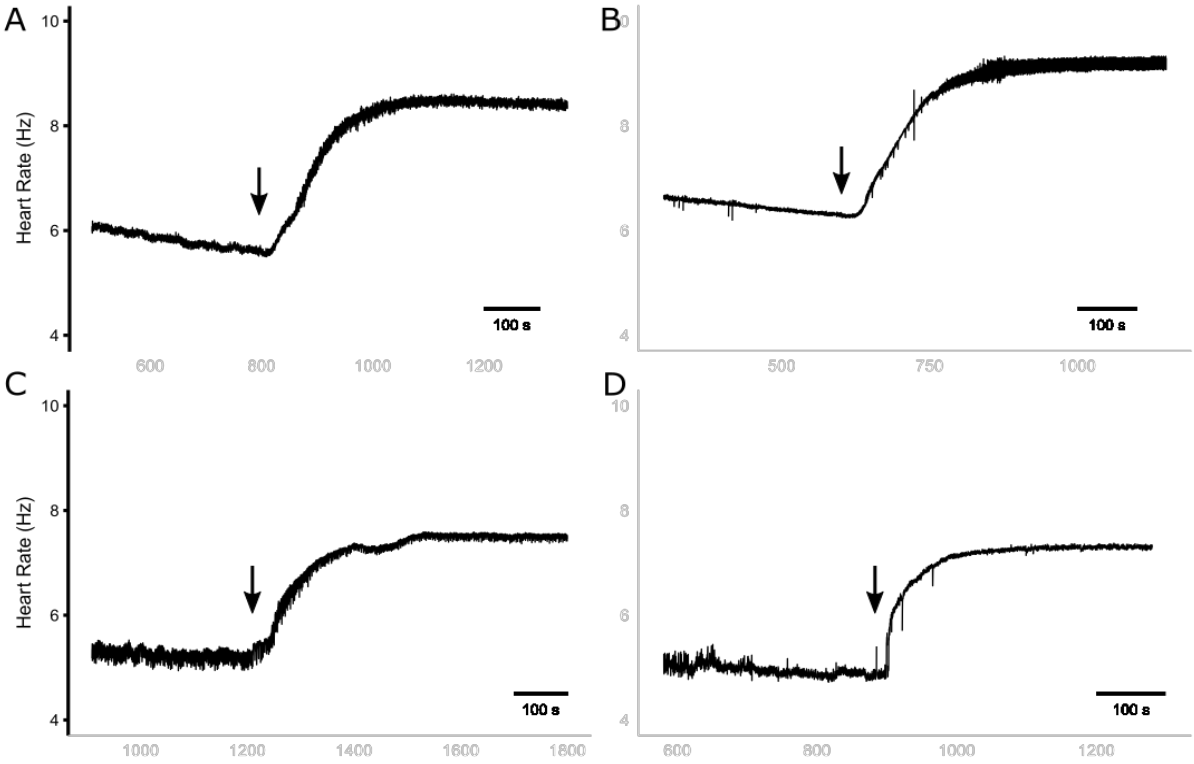

Figure 3.2 Heart rate response to dobutamine challenge

Traces plotting heart rate response curves before and following dobutamine challenge in (A) young WT, (B) aged WT; (C) young Pgc-1β$^{-/-}$ *and (D) aged Pgc-1β*$^{-/-}$ *mouse*

MANOVA analysis demonstrated significant effects of genotype ($p = 0.022$) and age ($p = 0.048$) on steady state heart rates (Table 3.2 A). Post hoc analysis demonstrated that neither these factors by themselves nor their interaction together influenced baseline steady state heart rates. In contrast, the *Pgc-1β*$^{-/-}$ mutation significantly reduced heart rates obtained following dobutamine challenge (*Pgc-1β*$^{-/-}$ 8.30 ± 0.28 Hz, n=15; WT: 9.11 ± 0.11 Hz, n = 13; $p = 0.021$)

(Figure 3.4). However, there were no demonstrable effects either of age or interactions between age and genotype. Maximum heart rates after dobutamine challenge were next analysed. ANOVA demonstrated significant effects of genotype ($p = 0.011$) but not of either age or interactive effects between genotype and age. Post-hoc Tukey tests demonstrated that *Pgc-1β*$^{-/-}$ mice had significantly lower peak heart rates than WT mice (mean peak heart rate 8.47 ± 0.28 vs 9.53 ± 0.21 Hz, $p = 0.0084$, n = 13 vs 15 respectively).

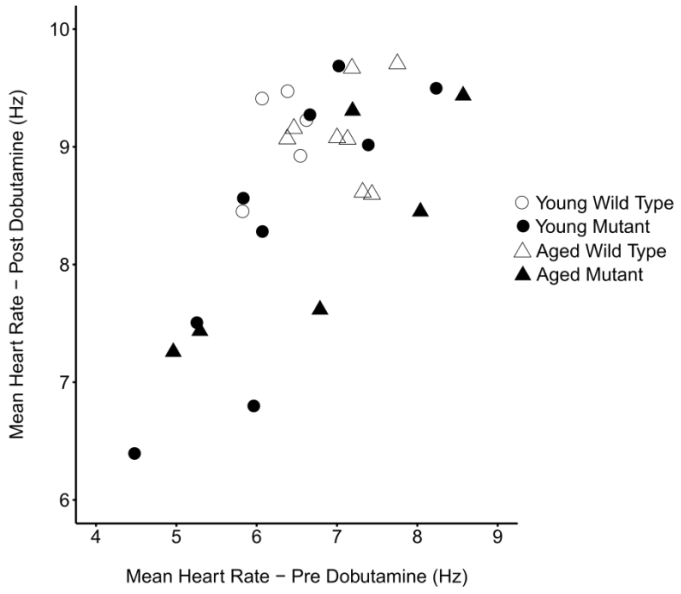

Figure 3.3 Mean heart rates pre- and post- adrenergic challenge

Correlations between heart rates observed pre- vs post-dobutamine challenge in Pgc-1β$^{-/-}$ *and WT hearts*

Reduced heart rate variability in humans is known to portend to adverse mortality risk. Heart rate variability was therefore analysed to assess cardiac autonomic influence on the systems in the present study. A Poincare plot was constructed for each experimental group (Figure 3.5 A and B) and the dispersion of points quantified by the standard deviation of the ΔRR interval. ANOVA demonstrated no significant differences in dispersion of the Poincare plots before or after dobutamine addition between the different experimental groups (Figure 3.5 C and D). These results attribute the present findings to an existence of sino-atrial node (SAN) as opposed to autonomic dysfunction in the *Pgc-1β*$^{-/-}$ mice.

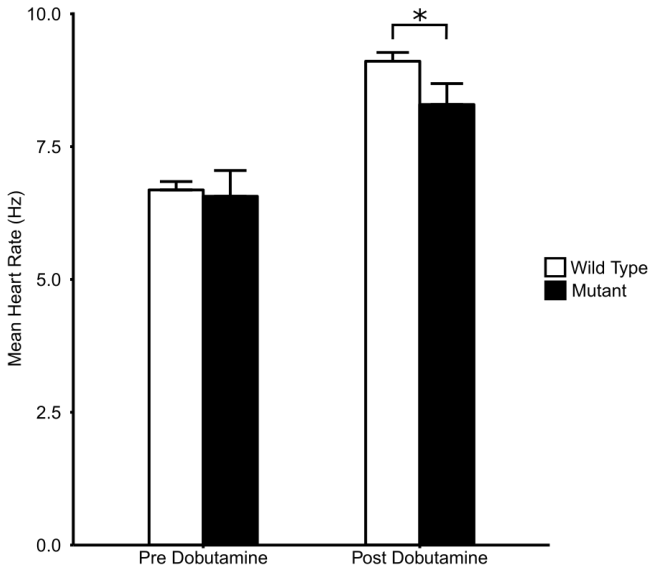

Figure 3.4 Chronotropic incompetence in *Pgc-1β*$^{-/-}$ hearts

Mean heart rates in the 5 minute analysis window before and after dobutamine administration in WT and Pgc-1β$^{-/-}$ *mice*

3.3.3 Aged-related SA node disease in WT and Pgc-1β$^{-/-}$ *murine hearts*

Although sinus rhythm was the prevailing rhythm in all groups, both WT and *Pgc-1β*$^{-/-}$ mice demonstrated intermittent episodes of isorhythmic AV dissociation (Massumi & Ali, 1970) during the recording period. These episodes were predominantly recorded in aged animals, affecting 3/6 aged WT mice and 4/8 aged *Pgc-1β*$^{-/-}$ mice, although it was observed in one mouse in the young *Pgc-1β*$^{-/-}$ cohort (Table 3.1). No episodes of such AV dissociation were seen in young WT animals. This rhythm was most commonly seen immediately following dobutamine challenge, where RR intervals were decreasing from their baseline, pre-treatment values. During these episodes, the RR intervals were shorter than their corresponding PP intervals, however the ventricular complexes remained identical to those during sinus rhythm, compatible with a supraventricular (most likely junctional) pacemaker focus driving the ventricular activity (Figure 3.1 C)

Table 3.2 *Electrocardiographic features related to sino-atrial, atrio-ventricular and atrial conduction*

		WT		*Pgc-1β*$^{-/-}$	
		Young	**Aged**	**Young**	**Aged**
A)	**Heart rate response**				
	Mean HR prior to dobutamine challenge (Hz)	6.29 ± 0.15	7.08 ± 0.16	6.32 ± 0.38	6.81 ± 0.59
	Mean HR post dobutamine challenge (Hz)	9.10 ± 0.19	9.12 ± 0.15	8.33 ± 0.40	8.25 ± 0.39
	Peak HR post dobutamine challenge (Hz)	9.32 ± 0.21	9.66 ± 0.32	8.51 ± 0.40	8.41 ± 0.39
B)	**Atrial conduction**				
	P wave duration prior to dobutamine challenge (ms)	26.08 ± 0.50	25.57 ± 1.06	26.06 ± 0.47	27.64 ± 0.67
	P wave duration post dobutamine challenge (ms)	25.43 ± 0.58	26.08 ± 0.79	26.21 ± 0.48	26.90 ± 0.86
(C)	**AV conduction**				
	Mean PR interval prior to dobutamine challenge (ms)	54.20 ± 2.57	63.26 ± 4.89	56.35 ± 5.56	66.62 ± 4.25
	Mean PR interval post dobutamine challenge (ms)	52.53 ± 2.22	53.61 ± 2.76	58.38 ± 5.41	76.95 ± 9.54
	Hearts showing decreased PR interval post dobutamine challenge	5 of 5	6 of 6	5 of 9	1 of 6
	Hearts showing increased PR interval post dobutamine challenge	0 of 5	0 of 6	4 of 9	5 of 6

Electrocardiographic features gave (A) heart rates responses in studies of young WT (n = 5), aged WT (n = 8), young *Pgc-1β*$^{-/-}$ (n = 9) and aged *Pgc-1β*$^{-/-}$ mice (n = 6), in which two of the aged WT showed AV dissociation within the ECG analysis window. Studies of atrial (B) and AV (C) conduction were therefore based on young WT (n = 5), aged WT (n = 6), young *Pgc-1β*$^{-/-}$ (n = 9) and aged *Pgc-1β*$^{-/-}$ mice (n = 6) respectively.

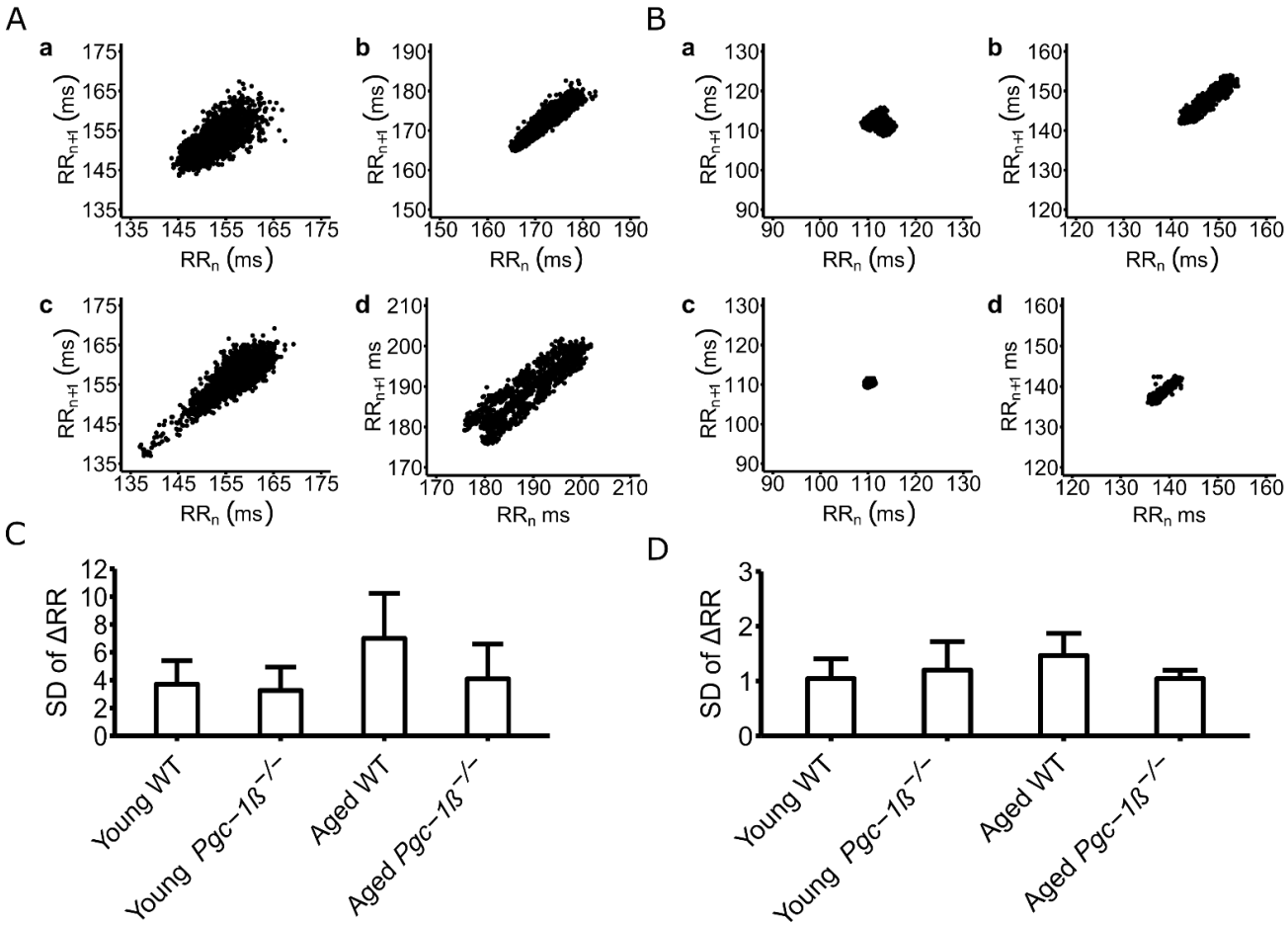

Figure 3.5 Heart rate variability in WT and *Pgc-1β*$^{-/-}$ mice

Poincare plots pre- (A) and post-dobutamine (B) in young (a,b) and aged (c,d), WT (a,c) and Pgc-1β$^{-/-}$ *hearts (b,d) and (C, D) the standard deviations (SDs) of their ΔRR intervals before (C) and following dobutamine challenge (D)*

3.3.4 *Pgc-1β$^{-/-}$ hearts display paradoxical atrioventricular node function*

MANOVA analysis excluded effects of age, genotype or interactions between them on P wave duration whether before or following dobutamine challenge (Table 3.2 B). PR intervals were next analysed to assess atrioventricular node (AVN) function. Two typical patterns of PR interval change were observed with dobutamine administration: either the expected positive dromotropic effects of dobutamine (a decrease in PR interval) or a negative dromotropic effect (i.e. an increase in PR interval) (Figure 3.6). These changes took place despite normal atrial conduction as reflected in similar P wave durations between groups (Table 3.2 B).

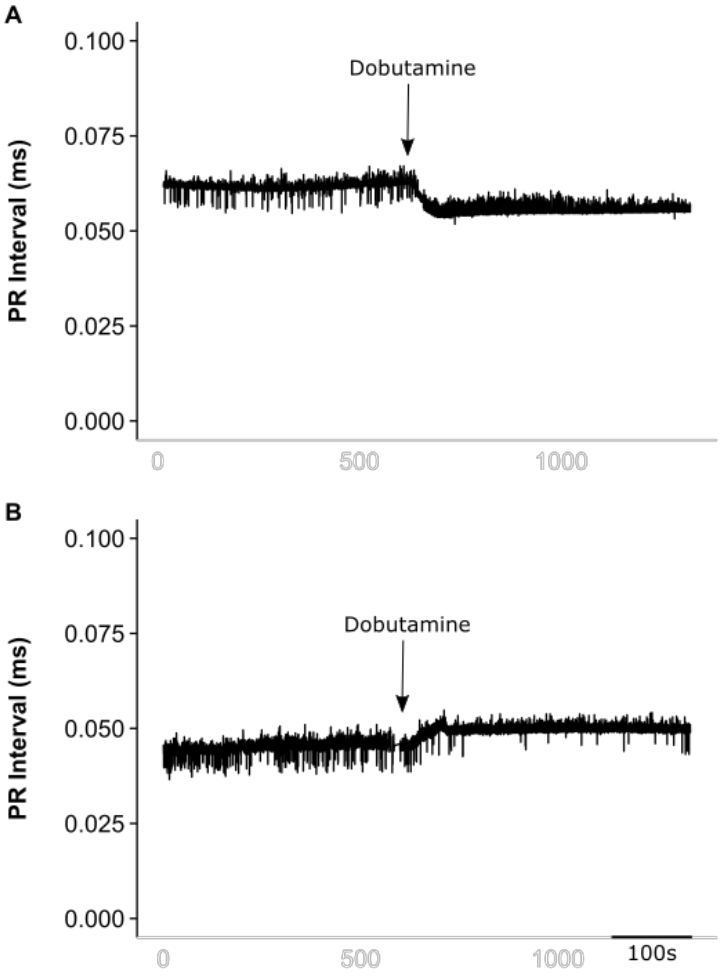

Figure 3.6 PR interval change in response to dobutamine

Adaptation of the PR interval pre- and post-dobutamine in WT (A) and Pgc-1β$^{-/-}$ (B) mice. The Pgc-1β$^{-/-}$ mice displayed a paradoxical negative dromotropic response suggesting altered AVN function.

MANOVA indicated that neither age nor genotype affected PR interval whether before or following dobutamine challenge (Table 3.2 C). Nevertheless, the alteration in PR interval following dobutamine challenge demonstrated differing responses from WT and *Pgc-1β*$^{-/-}$ mice. All young (5 of 5) and aged (6 of 6) WT mice showed decreased PR intervals following dobutamine challenge. In contrast, the PR interval decreased in 5 of 9 and increased in the remaining four young *Pgc-1β*$^{-/-}$ mice. In aged *Pgc-1β*$^{-/-}$ mice the result was even more marked with only one mouse showing the expected positive dromotropic effect with dobutamine administration and the 5 of 6 mice showing a paradoxical negative dromotropic effect in response to dobutamine. In addition to the SAN dysfunction seen with the *Pgc-1β* knockout there was compromised AVN conduction in a subset of mutant hearts, an effect exacerbated by increasing age.

The presence of AVN dysfunction in mutant mice which also demonstrated impaired heart rate responses prompted further examination as to whether paradoxical AV node dysfunction underlies or is associated with the blunted chronotropic response. Such a comparison demonstrated that *Pgc-1β*$^{-/-}$ animals with a normal AVN response showed a mean heart rate of 9.10 ± 0.22 Hz (n = 6) following dobutamine challenge. In contrast, *Pgc-1β*$^{-/-}$ animals with a paradoxical AVN response to dobutamine showed a heart rate of 7.77 ± 0.34 Hz (n = 9). A two-tailed student t test confirmed that the difference was significant (p = 0.0061). Thus these findings suggest that the *Pgc-1β*$^{-/-}$ mutation is associated only with significantly altered AV nodal function in a subset of mutant mice, and that the presence of AV nodal dysfunction itself may be a marker for impaired heart rate responses.

3.3.5 Aged Pgc-1β$^{-/-}$ *hearts display slowed ventricular activation*

Ventricular activation is a synchronised, sequential process that occurs in a defined time window. The onset of ventricular *activation* is easily detected as the beginning of the Q wave deflection (Figure 2.1). Ventricular *recovery* has been reported to begin at a time point between the S wave trough, and the beginning of the R' peak. We examined three independent ECG indicators, of QR, QS and QR' durations, to examine ventricular activation. All three ECG indices indicated interacting effects of age and genotype upon the timing of ventricular activation (Table 3.3).

Table 3.3 Electrocardiographic intervals representing ventricular activation

	WT		*Pgc-1β*$^{-/-}$	
	Young	**Aged**	**Young**	**Aged**
QR duration before dobutamine challenge (ms)	6.85 ± 0.67	5.89 ± 0.63	6.20 ± 0.48	8.35 ± 0.52
QR duration following dobutamine challenge (ms)	7.14 ± 0.75	6.12 ± 0.60	6.12 ± 0.48	8.56 ± 0.56
QS duration before dobutamine challenge (ms)	10.19 ± 0.47	9.43 ± 0.45	9.67 ± 0.45	11.78 ± 0.7
QS duration following dobutamine challenge (ms)	10.60 ± 0.62	9.76 ± 0.40	9.91 ± 0.43	12.07 ± 0.77
QR' Duration before dobutamine challenge (ms)	14.24 ± 0.60	14.22 ± 0.40	13.82 ± 0.34	16.20 ± 0.92
QR' Duration following dobutamine challenge (ms)	14.95 ± 0.41	14.39 ± 0.55	14.15 ± 0.38	16.72 ± 0.89

Electrocardiographic features gave (A) heart rates responses in studies of young WT (n = 5), aged WT (n = 8), young *Pgc-1β*$^{-/-}$ (n = 9) and aged *Pgc-1β*$^{-/-}$ mice (n = 6), in which two of the aged WT showed AV dissociation within the ECG analysis window. Studies of atrial (B) and AV (C) conduction were therefore based on young WT (n = 5), aged WT (n = 6), young *Pgc-1β*$^{-/-}$ (n = 9) and aged *Pgc-1β*$^{-/-}$ mice (n = 6) respectively.

MANOVA demonstrated that although neither genotype nor age exerted independent effects, they interacted to produce significant effects on ***QR duration*** ($p = 0.032$). Post hoc Tukey tests confirmed interacting effects of genotype and age both prior to ($p = 0.029$) and following dobutamine administration ($p = 0.016$). Prior to dobutamine administration, QR durations were significantly longer in aged *Pgc-1β*$^{-/-}$ than aged WT ($p = 0.030$). There was a trend towards longer QR durations in aged compared to young *Pgc-1β*$^{-/-}$ mice ($p = 0.059$). Following dobutamine administration, aged *Pgc-1β*$^{-/-}$ showed significantly longer QR durations than aged WT ($p = 0.035$) as well as young *Pgc-1β*$^{-/-}$ ($p = 0.030$). Similarly, neither genotype nor age exerted independent effects, but showed interacting effects on ***QS durations*** ($p = 0.040$). They did so both before ($p = 0.029$) and following dobutamine challenge ($p = 0.022$). Before dobutamine administration, post hoc Tukey tests demonstrated that aged *Pgc-1β*$^{-/-}$ mice showed significantly longer QS intervals than young *Pgc-1β*$^{-/-}$ mice ($p = 0.040$) and aged WT mice ($p = 0.024$). Following dobutamine administration, aged *Pgc-1β*$^{-/-}$ mice showed longer QS durations than both young *Pgc-1β*$^{-/-}$ mice ($p = 0.035$) and aged WT mice ($p = 0.026$). Finally, neither genotype nor age exerted independent effects, but exerted interacting effects on ***QR' durations*** ($p = 0.039$). These interactions were not significant prior to ($p = 0.086$), but were significant following ($p = 0.026$) dobutamine administration. Post hoc Tukey tests then demonstrated that aged *Pgc-1β*$^{-/-}$ mice showed significantly longer QR' durations than both aged WT ($p = 0.039$) and young *Pgc-1β*$^{-/-}$ mice ($p = 0.017$) after dobutamine administration.

3.3.6 Pgc-1β$^{-/-}$ hearts show shortened ventricular recovery times after adrenergic challenge

Age and genotype exerted contrasting effects on ventricular recovery times. Genotype affected all three measures of such recovery (RT_c, $R'T_c$ and ST_c durations; $p = 0.0098$, $p = 0.0014$ and $p = 0.0029$ respectively) (Table 3.4). In contrast, age did not significantly affect any of these recovery parameters, nor were there any interactive effects of age and genotype. Post hoc testing showed that (for all parameters) the difference lay in findings obtained post dobutamine challenge; there were no differences due to age, genotype or their interaction prior to dobutamine administration. Following dobutamine administration all three parameters showed a marked effect of genotype ($p = 0.015$, $p = 0.021$ and $p = 0.0067$ respectively) but no other effects. Post hoc Tukey tests showed that *Pgc-1β*$^{-/-}$ showed

significantly shorter RT_c, $R'T_c$ and ST_c intervals than WT mice ($p = 0.0053$, $p = 0.018$ and $p = 0.0080$ respectively). Thus, all three recovery parameters were highly concordant confirming that the *Pgc-1β* ablation significantly shortened ventricular recovery parameters (Table 3.5).

3.3.7 Emergence of a short-QT phenotype in Pgc-1β$^{-/-}$ animals

The ***QT_c interval*** has traditionally been used as a marker for repolarisation abnormalities in that the electrocardiographic phenotype is usually caused by a defect in ventricular recovery. However, it is more accurate to describe the QT_c interval as a parameter that describes the combined durations of both activation and recovery i.e. the duration of ventricular excitation. The onset of ventricular activation is represented by the Q wave deflection; the C wave trough was taken to represent the end of ventricular recovery and hence used for calculation of the QT interval in the present study (Figure 2.1). Genotype, but neither age ($p= 0.083$) nor interactions between age and genotype ($p = 0.075$), significantly affected QT_c interval ($p = 0.0071$) (Table 3.6). Post hoc ANOVA indicated no differences between groups at baseline. Following dobutamine challenge, genotype ($p = 0.032$), but not age affected QT_c interval. Post hoc Tukey HSD tests revealed that, following dobutamine administration, young *Pgc-1β$^{-/-}$* had shorter QT_c intervals than both young WT ($p = 0.026$) and aged WT mice ($p = 0.041$). There was also a trend towards young *Pgc-1β$^{-/-}$* mice having shorter QT_c intervals than aged *Pgc-1β$^{-/-}$* mice ($p = 0.094$). Thus, *Pgc-1β$^{-/-}$* mice had shorter QT_c intervals than their WT counterparts with most of the effect arising from shortening of the QT_c intervals in young *Pgc-1β $^{-/-}$* mice.

Table 3.4 Electrocardiographic intervals representing ventricular recovery

	WT		*Pgc-1β*$^{-/-}$	
	Young	**Aged**	**Young**	**Aged**
RT_c duration before dobutamine challenge (ms)	29.00 ± 0.54	30.60 ± 0.87	28.51 ± 1.05	28.89 ± 0.87
RT_c duration following dobutamine challenge (ms)	33.43 ± 0.77	33.75 ± 0.44	31.41 ± 0.86	31.79 ± 0.41
$R'T_c$ duration before dobutamine challenge (ms)	23.15 ± 0.45	23.64 ± 0.71	22.55 ± 0.91	22.55 ± 0.56
$R'T_c$ duration following dobutamine challenge (ms)	25.97 ± 0.43	25.88 ± 0.55	24.16 ±0.66	24.40 ± 0.29
ST_c duration before dobutamine challenge (ms)	26.35 ± 0.38	27.65 ± 0.77	25.79 ± 0.92	26.06 ± 0.55
ST_c duration following dobutamine challenge (ms)	30.13 ± 0.68	30.31 ± 0.50	28.00 ± 0.71	28.40 ± 0.30

Electrocardiographic measurements made in RT_c, $R'T_c$ and ST_c durations before and following dobutamine challenge in young WT (n = 5), aged WT (n = 8), young *Pgc-1β*$^{-/-}$ (n = 9) and aged *Pgc-1β*$^{-/-}$ (n = 6) mice. One young and one aged *Pgc-1β*$^{-/-}$ mouse were excluded as these showed paradoxical dromotropic effects that lead to prolonged PR intervals and P waves that interfered with determinations of the end of the C wave to give the following n values: young WT (n = 5), aged WT (n = 8), young *Pgc-1β*$^{-/-}$ (n = 8) and aged *Pgc-1β*$^{-/-}$ (n = 5),

Table 3.5 Electrocardiographic recovery intervals: WT and *Pgc1β*$^{-/-}$ compared

	WT	*Pgc-1β*$^{-/-}$
RT_c duration before dobutamine challenge (ms)	29.99 ± 0.60	28.65 ± 0.70
RT_c duration following dobutamine challenge (ms)	33.63 ± 0.38	31.53 ± 0.57
$R'T_c$ duration before dobutamine challenge (ms)	23.45 ± 0.46	22.55 ± 0.58
$R'T_c$ duration following dobutamine challenge (ms)	25.91 ± 0.37	24.24 ± 0.44
ST_c duration before dobutamine challenge (ms)	27.15 ± 0.51	25.89 ± 0.59
ST_c duration following dobutamine challenge (ms)	30.24 ± 0.39	28.13 ± 0.48

Electrographic measurements made in RTc, R'Tc and STc durations before and following dobutamine challenge in young WT (n = 5), aged WT (n = 8), young *Pgc-1β*$^{-/-}$ (n = 9) and aged *Pgc-1β*$^{-/-}$ mouse (n = 6). One young and one aged *Pgc-1β*$^{-/-}$ mouse were excluded as these showed paradoxical dromotropic effects that lead to prolonged PR intervals and P waves that interfered with determinations of the end of the C wave to give the following n values: young WT (n = 5), aged WT (n = 8), young *Pgc-1β*$^{-/-}$ (n = 8) and aged *Pgc-1β*$^{-/-}$ (n = 5). This gave total n values of WT and *Pgc-1β*$^{-/-}$ of 13 in both cases.

Table 3.6 Mean electrocardiographic QT_c durations

	WT		*Pgc-1β*$^{-/-}$	
	Young	**Aged**	**Young**	**Aged**
Mean QT_c before dobutamine challenge (ms)	34.43 ± 0.20	35.60 ± 0.79	33.37 ± 1.12	35.78 ± 1.18
Mean QT_c following dobutamine challenge (ms)	40.23± 0.45	39.64 ± 0.52	37.01 ±0.87	39.77 ± 0.81

Electrographic measurements made in QTc durations before and following dobutamine challenge in young WT (n = 5), aged WT (n = 8), young *Pgc-1β*$^{-/-}$ (n = 9) and aged *Pgc-1β*$^{-/-}$ (n = 6) mice. One young and one aged *Pgc-1β*$^{-/-}$ mouse were excluded as these showed paradoxical dromotropic effects that lead to prolonged PR intervals and P waves that interfered with determinations of the end of the C wave to give the following n values: young WT (n = 5), aged WT (n = 8), young *Pgc-1β*$^{-/-}$ (n = 8) and aged *Pgc-1β*$^{-/-}$ (n = 5). This gave total n values of WT and *Pgc-1β*$^{-/-}$ of 13 in both cases.

3.4 Discussion

The ECG is a primary clinical investigational tool yielding much prescient and strategic electrophysiological information. Its recent experimental application has similarly demonstrated valuable insights into electrophysiological abnormalities in murine hearts modeling clinical arrhythmic conditions. Mitochondrial dysfunction is increasingly recognised as an important factor in the aetiology of atrial and ventricular arrhythmias. The ECG alterations associated with mitochondrial dysfunctions were therefore investigated in murine hearts lacking the transcriptional coactivator *Pgc-1β*, which has been associated with altered ion channel function and ventricular arrhythmias in a Langendorff-perfused heart preparation (Gurung et al., 2011).

ECG analysis demonstrated a range of age-dependent abnormalities associated with the *Pgc-1β*$^{-/-}$ genotype, hitherto associated with abnormal mitochondrial and therefore energetic function. The latter has been implicated in ventricular arrhythmia through the consequent alterations in ion channel function, action potential heterogeneity, and cell excitability (Brown & O'Rourke, 2010; Asghar *et al.*, 2012; Isik *et al.*, 2012). Metabolic disturbances are known to have wide ranging consequences on the electrical properties of the cardiac system, including destabilisation of the inner mitochondrial membrane potentials, causing up to a 10-fold increases in reactive oxygen species production (Grivennikova *et al.*, 2010). This is known to affect maximum sodium current (I_{Na}) (Liu *et al.*, 2010), potassium current (I_K) (Wang *et al.*, 2004), sarcolemmal K_{ATP} channels, Na^+ and L-type Ca^{2+} channel inactivation kinetics, late Na^+ current (I_{NaL}) and ryanodine receptor (RyR2) function. These alterations in turn affect surface membrane excitability and intracellular Ca^{2+} homeostasis (Terentyev *et al.*, 2008; Brown & O'Rourke, 2010; Bovo *et al.*, 2012). Mitochondria are also the main cardiac cellular source of ATP (O'Rourke, 2007). ATP/ADP depletion increases sarcolemmal ATP-sensitive K^+ channel (sarcK_{ATP}) open probabilities (Akar & O'Rourke, 2011) with consequences for action potential duration (APD), effective refractory period (ERP) (Fosset *et al.*, 1988; Faivre & Findlay, 1990) and forming heterogenous current sinks driving cell membrane potential towards the K^+ Nernst potential potentially causing current-load mismatch. The wide range of resulting, potentially pro-arrhythmic, effects might then include alterations in cell-cell coupling (Smyth *et al.*, 2010), AP conduction (Liu *et al.*, 2010) and repolarisation (Wang *et al.*, 2004). There may

also be an appearance of alternans and Ca^{2+} mediated triggering phenomena (Terentyev *et al.*, 2008).

A number of the observed ECG alterations paralleled findings in a variety of arrhythmic cardiac exemplars, providing some insights to possible underlying mechanisms. ECG analysis of anaesthetised Nav1.5 haplo-insufficient *Scn5a*$^{+/-}$ mice modeling BrS, recapitulated conduction deficits associated with the corresponding human condition (Jeevaratnam *et al.*, 2010), and presaged changes observed with more detailed electrophysiological analysis (Tessier *et al.*, 1999; Lei *et al.*, 2005; Martin *et al.*, 2010*b*). The *Scn5a*$^{+/-}$ hearts developed age-related dysfunction in SA node function and features of altered repolarisation. Altered Nav1.5 profiles and conduction slowing are also seen secondary to Ca^{2+} handling abnormalities in *RyR2-P2328S* hearts (Zhang *et al.*, 2011; King *et al.*, 2013*b*; Ning *et al.*, 2016*b*). *Scn5a*$^{+/\Delta KPQ}$ mice modeling long QT3 syndrome showed evidence for depressed intra-atrial, AV, and intra-ventricular conduction, in addition to prolonged QT and QT_c intervals (Wu *et al.*, 2012). Thus the spectrum of ECG abnormalities reported in the present study potentially implicate several alterations at the cellular level, consistent with the central role of mitochondria in cardiomyocyte function and the range of ion channel changes previous reported in *Pgc-1β*$^{-/-}$ hearts (Gurung *et al.*, 2011).

The present experiments in intact anaesthetised *Pgc-1β*$^{-/-}$ mice characterised the intervals separating specific ECG waveform components more closely than did previous studies. Quantitative statistical analysis of these steady-state parameters then employed two-way factorial MANOVA testing for interacting and non-interacting effects of age and genotype before and after dobutamine challenge. The presence of significant differences then prompted further, two way factorial ANOVA to ascertain whether the difference occurred before or following dobutamine application. Finally, appropriate Tukey HSD tests assessed for particular differences between individual parameters. Peak heart rates following dobutamine challenge were analysed by themselves by a two way factorial ANOVA followed by post hoc Tukey tests. The present study therefore yielded electrophysiological features associated with *Pgc-1β* ablation in the in vivo system with intact autonomic innervation and normal cardiac mechanical function, building upon earlier reports from cellular studies (Gurung *et al.*, 2011) and ex-vivo hearts (Lelliott *et al.*, 2006). In the latter studies, the pharmacological manoeuvres involving dobutamine challenge would largely be expected to arise through β1-adrenergic

receptors activity. The in vivo evaluation of the effects of dobutamine, as utilised in this study, would include β2-adrenergic receptor mediated changes including peripheral vasodilatation. Thus differences between genotypes reported here may reflect to some degree extra-cardiac differences, which in the clinical setting are also known to influence arrhythmic risk.

The predominant ECG pattern in both young and aged, WT and *Pgc-1β*$^{-/-}$ mice was one of sinus rhythm. Any ischaemic ECG changes observed were associated with age but were not specific to *Pgc-1β*$^{-/-}$ or WT genotypes, suggesting that there was no underlying difference in vascular function between the two groups. The electrophysiological phenotype of the *Pgc-1β*$^{-/-}$ mice was therefore due to primary cardiomyocyte abnormalities. This impression was reinforced by the range and nature of the electrocardiographic abnormalities.

Blunted chronotropic responses were demonstrated in an intact *Pgc-1β*$^{-/-}$ mammalian system. Previous reports had demonstrated compromised heart rate responses in ex-vivo Langendorff perfused *Pgc-1β*$^{-/-}$ hearts following dobutamine challenge (Lelliott *et al*., 2006). The current results similarly suggest that *Pgc-1β*$^{-/-}$ hearts in intact animals attain significantly lower mean and peak heart rates than their WT counterparts after dobutamine administration. Ageing did not affect this chronotropic response, implicating the mutation and not any background deterioration of maximal heart rate with age. Modulation of heart rate ultimately depends upon interactions between the autonomic system, and its myocyte response. It is apparent that autonomic modulation cannot compensate for this phenomenon in intact systems. These results together suggest that the impaired heart rate response of *Pgc-1β*$^{-/-}$ hearts does not reflect generalised autonomic dysfunction but rather alterations in the intrinsic myocardial response to dobutamine.

Aged mice, independent of genotype, also displayed runs of isorhythmic AV dissociation when challenged with dobutamine. During these episodes regular ventricular responses were seen, with complexes retaining their normal, narrow waveform despite the absence of a fixed PR interval, and even when P wave complexes were buried within the ventricular signal. These findings suggest that the murine SAN is vulnerable to degenerative changes with age, with appearances of supraventricular, most likely junctional, pacemaker foci intermittently dictating the ventricular rate.

Pgc-1β$^{-/-}$ ablation also appeared to cause a more generalised nodal defect affecting the ***AVN*** in addition to the SAN defect described above. A significant proportion (9/15) of mutant mice demonstrated abnormal negatively dromotropic responses to dobutamine challenge, and all but one of the aged mutants displayed this paradoxical effect. This suggests progressive deterioration in AVN function in *Pgc-1β*$^{-/-}$ hearts with age. Furthermore, mice in which this abnormal AVN function was observed appeared to have more pronounced blunting of the chronotropic response to dobutamine, implicating dysfunction at the level of the AVN to the chronotropic deficit noted in the present study as well as in previous reports.

Pathological bradycardic rhythms secondary to cardiac conduction system disease are known to occur with ageing, and often necessitate permanent pacemaker implantation (Bradshaw *et al.*, 2014). Progressive fibrotic change is a recognised feature of cardiac ageing in both animal (Eghbali *et al.*, 1989; Orlandi *et al.*, 2004; Lin *et al.*, 2008; Jeevaratnam *et al.*, 2012, 2016) and human studies (Gazoti Debessa *et al.*, 2001), and the age-related deterioration in function of the cardiac conduction system has classically been attributed to this, compromising both SAN (Thery *et al.*, 1977; Evans & Shaw, 1977) and AVN (Fujino *et al.*, 1983) activity. Interestingly, TGF-β activity, which has been implicated in age-related myocardial fibrosis (Brooks & Conrad, 2000; Davies *et al.*, 2014) is increased with oxidative stress (Barcellos-Hoff & Dix, 1996; Sullivan *et al.*, 2008), possibly linking mitochondrial impairment to such node dysfunction. Furthermore, augmented mitochondrial anti-oxidant capacity has previously been shown to protect against features of cardiac ageing including fibrotic change (Dai *et al.*, 2009). More recent studies also suggest a role for abnormal gap junction function in both SAN and AVN disease (Jones *et al.*, 2004; Nisbet *et al.*, 2016). Indeed fibrotic change could potentially disrupt gap junction function directly and therefore increase tissue resistance (Xie *et al.*, 2009), or increase fibroblast-cardiomyocyte coupling and consequently increase effective membrane capacitance (Camelliti *et al.*, 2004; Chilton *et al.*, 2007). Moreover, the mitochondrial dysfunction in *Pgc-1β*$^{-/-}$ hearts could also potentially directly impair gap junctions through elevating intracellular [Ca^{2+}] (De Mello, 1983) or altered connexin phosphorylation states secondary to oxidative stress (Sovari *et al.*, 2013). Finally, a range of ionic currents are involved in SAN and AVN activity (Marionneau *et al.*, 2005), and therefore potentially modulated by mitochondrial dysfunction. Of these, altered RyR2 channel function appears particularly important (Bhuiyan *et al.*, 2007). Isolated cardiomyocytes from *Pgc-1β*$^{-/-}$ hearts have previously

been reported to display altered diastolic Ca^{2+} transients in keeping with abnormal *Ryr2* function (Gurung *et al.*, 2011).

The ECG deflections relating to ***ventricular activation and recovery*** confirmed previous reports that murine ECGs lack well-defined ST segments (Danik *et al.*, 2002; Zhang *et al.*, 2014). The murine ECG shows a deflection, the R' wave, immediately following the S wave not seen in the human ECG. This is followed by a further but variably reported deflection which has not been systematically identified or formally correlated with particular action potential components. This variability may be attributed to the greater rostro-caudal anatomical alignment of the mouse heart in the thoracic cavity and variations in limb positioning during experimental recording between reports, with consequent variations in the effective positioning of the centre of the Einthoven triangle relative to the heart. Thus, although we also identified C waves, small changes in lead positioning could lead to its apparent disappearance in one or both ECG leads. This may account for the controversy concerning its inconsistent appearance (Danik *et al.*, 2002).

The onset of ventricular recovery in the murine ECG has been considered to occur from time points ranging from the S wave nadir to the R' peak. A number of authors have suggested that the late component of the R' wave or the R' wave in totality is in fact part of ventricular repolarisation (Goldbarg *et al.*, 1968; Boukens *et al.*, 2014; Zhang *et al.*, 2014*b*). Others suggested that inclusion of the R' wave may lead to systematic overestimation of ventricular activation, while its exclusion in genetically modified mouse models, such as that of the Brugada syndrome, which displays slowed conduction, may lead to underestimation of ventricular activation times (Boukens *et al.*, 2014).

These reports prompted exploration of a set of related recovery parameters that utilised both the S wave nadir and peak of the R' wave as cut-off separating ventricular activation and recovery phases. Each parameter is likely to capture activation and recovery in different areas of myocardium, reflecting the non-simultaneous nature of electrical activity in the myocardium. This increased the robustness of our analysis and permitted us to assess the possibility of early repolarisation in our genetic model. The statistical analysis of the different parameters of recovery and activation were highly concordant.

Pgc-1β$^{-/-}$ hearts showed prolongation of all the measures of the ventricular activation phase with age whether before or following adrenergic stress. Age alone or mutation alone did not account for the changes observed. These findings parallel previous reports of reduced conduction velocity in other arrhythmic genetic models. These had accompanied fibrotic change resulting in altered tissue impedance, or Na^+ current density following Nav1.5 haploinsufficiency in *Scn5a*$^{+/-}$ (Jeevaratnam *et al.*, 2011, 2012, 2016), and Nav1.5 downregulation in *RyR2-P2328S* hearts (King *et al.*, 2013*b*; Zhang *et al.*, 2014*b*; Ning *et al.*, 2016). These findings are also compatible with reports that mitochondrial abnormalities could alter I_K and therefore result in current-load mismatch (O'Rourke, 2007; Akar & O'Rourke, 2011; Bates *et al.*, 2012; Kabunga *et al.*, 2015).

Pgc-1β$^{-/-}$ hearts also showed shorter recovery parameters than WT after dobutamine administration. There was no effect of age or compounding interaction with genotype. Previous studies in murine models variously attributed ventricular arrhythmic syndromes to abnormalities in depolarisation or in repolarisation characteristics as in the Brugada and long QT syndromes respectively (Martin *et al.*, 2012*a*). Such shortened repolarisation intervals have been implicated in arrhythmic risk. In human short QT, the J point to T peak interval is used as a diagnostic criterion (Gollob *et al.*, 2011), and is thought to represent the interval between the end of the ventricular complex to the peak of the repolarisation wave. Short QT syndrome has been traced to HERG and other K^+ channel mutations and more recently, Ca^{2+} channel function (Brugada *et al.*, 2004; Priori *et al.*, 2005; Antzelevitch *et al.*, 2007). The present findings are consistent with reported alterations in K^+ conductance properties in the *Pgc-1β*$^{-/-}$ system that would also modify current-load matching (Gurung *et al.*, 2011). These changes appeared to result in shortened QT_c intervals for mutant mice with adrenergic stress. Although the mechanisms underlying these changes remain unclear, increased expression of *Kcna5* was reported in the latter study and may contribute to the increased K^+ conductance observed. Additionally, the opening and K^+ conductance of the sarcK_{ATP} is linked to rising cellular ADP levels, therefore correlating its activity to cellular metabolic status. Its activity is known to reduce the action potential duration and is thought to contribute to increased arrhythmic risk (Billman, 2008). Oxidative stress is also known to enhance sarcK_{ATP} activity, however the cellular mechanism are yet to be established but may occur through depletion of cellular ATP. Nevertheless, the effects of ROS upon sarcK_{ATP} activity could be attenuated through inhibition

of protein kinase C, protein kinase G and calcium-calmodulin kinase II but not protein kinase A, providing some insights into the pathways involved (Yan *et al.*, 2009).

Finally, these findings prompted the measurement of QT_c intervals reflecting the total activation times of the ventricular myocardium. *Pgc-1β*$^{-/-}$ mice showed shorter QT_c intervals than their WT counterparts. The majority of this effect seemed to be due to young mutant mice, though this was not significant. This is in contrast to the shortened *repolarisation* parameters in both young and aged *Pgc-1β*$^{-/-}$. This likely reflects the additional, prolonged, *depolarisation* parameters in aged *Pgc-1β*$^{-/-}$ mice, offsetting to some degree the shortening in the repolarisation parameters.

In summary, ECG analysis demonstrates a range of electrocardiographic abnormalities associated with the *Pgc-1β*$^{-/-}$ genotype and those features particularly vulnerable to advanced age. Thus, *Pgc-1β*$^{-/-}$ mice show reduced sino-atrial response to dobutamine, paradoxical atrioventricular nodal function increasing in prevalence with age, slowed ventricular activation with ageing and shortened recovery parameters after dobutamine challenge.

4 Age-dependent atrial arrhythmic phenotype in *Pgc-1β* deficient hearts

4.1 Introduction

Arrhythmogenesis is a complex physiological phenomenon of dysregulated cardiac electrical activity with both short and long term consequences. The complex embryological origins and anatomical structure of the atria make it particularly vulnerable to arrhythmic syndromes. Atrial fibrillation (AF) is of particular clinical importance, affecting 1 – 3% of individuals in Western countries (Friberg & Bergfeldt, 2013). The processes underpinning its induction and maintenance remain incompletely explained, but involve complex interactions between altered cardiac electrical properties and functional changes in the atria which occur over the short and long term. It has been suggested that AF is a self-perpetuating process, triggered initially by focal ectopic activity arising in the pulmonary veins that drive cumulative, electrical and structural remodeling processes, themselves generating an arrhythmic substrate (Haïssaguerre *et al.*, 1998).

These changes are exacerbated by several interacting upstream factors, with ageing and metabolic disease central to a number of these. There is a pronounced increase in the prevalence of AF with age, from ~4% of individuals aged 60-70 years to nearly 20% of individuals ≥80 years (Zoni-Berisso *et al.*, 2014). Similarly, metabolic factors may explain ~60% of current upward trends in incidences of AF (Miyasaka *et al.*, 2006). Metabolic disease and obesity have been implicated as risk factors, themselves age-dependent, for *ventricular* arrhythmias (Adabag *et al.*, 2015). Similarly, the risk of *AF* increases with physical inactivity (Mozaffarian *et al.*, 2008), obesity (Tedrow *et al.*, 2010), diabetes mellitus (Nichols *et al.*, 2009) and metabolic syndrome (Watanabe *et al.*, 2008). Amelioration of metabolic disease improves both risk profiles and responses to therapy (Tedrow *et al.*, 2010). Further, it has been shown that manipulation of key components of cellular energy production pathways suppress arrhythmia in known arrhythmogenic models (Liu *et al.*, 2009).

Mitochondrial function may be integral to relationships between ageing, metabolism and

arrhythmia. Mitochondria provide >95% of the ATP required for Ca^{2+} homeostasis and maintenance of trans-membrane ionic gradients in addition to cardiac muscle contraction (Barth & Tomaselli, 2009). A number of targeted mitochondrial DNA mutations accumulate both with age and show increased incidences in AF (Lai *et al.*, 2003). Furthermore, abnormal mitochondrial structure and function have been reported in animal models for AF (Ausma *et al.*, 1997*b*) and in human studies (Tsuboi *et al.*, 2001; Lin *et al.*, 2003; Bukowska *et al.*, 2008). Mitochondrial dysfunction also results in generation of reactive oxygen species (ROS) which has been implicated in the pathogenesis of human atrial fibrillation (Korantzopoulos *et al.*, 2007).

However, few experiments have explored the effects of *chronic* age-dependent energetic deficiency arising from ageing and mitochondrial dysfunction on generation of *atrial* arrhythmias or determined their underlying electrophysiological abnormalities. The experiments described in this chapter evaluated the influence of ageing and mitochondrial dysfunction, through homozygous deficiency in *Pgc-1β*, upon atrial arrhythmic tendency and the associated electrophysiological alterations. Simultaneous ECG and intracellular microelectrode readings were recorded from Langendorff perfused WT and *Pgc-1β*$^{-/-}$ hearts. The presence of altered electrophysiological properties were evaluated through the imposition of extrasystolic S2 stimuli at differing S1S2 intervals following trains of regular S1 pacing as well as steady-state pacing at progressively decreased basic cycle lengths. Young and aged WT and genetically modified hearts were therefore studied at both the whole heart and cellular level, assessing arrhythmic tendency and correlating this with electrophysiological parameters and structural changes.

4.2 Specific methods

4.2.1 Experimental Animals

As in chapter 3, mice were divided into four groups consisting of young WT (n = 26) and young *Pgc-1β*$^{-/-}$ mice (n = 34) aged between 12-16 weeks. The other groups included aged (greater than 52 weeks) littermate WT controls (n = 27) and aged *Pgc-1β*$^{-/-}$ mice of age similarly greater than 52 weeks (n = 25).

4.2.2 *Statistical analysis*

Data from AP recordings were analysed using a custom written programme in the python programming language and all statistical analysis performed in the R programming language (R Core Team, 2015). Discrete incidences of abnormal rhythms were separated according to their type and the pacing protocol, either regular pacing or PES, in which they were observed. As often multiple episodes of AT were seen during a single protocol, the propensity to arrhythmia was expressed as protocols with one or more episode of AT expressed relative to the total number studied, and compared using the Fisher Exact Test. Parameters describing electrophysiological properties measured during regular pacing were compared using a two-way analysis of variance (ANOVA) testing for significant effects of genotype, ageing, and an interaction between the two. Where the *F*-ratio yielded a significant result, post-hoc Tukey honesty significant testing was performed. Similar electrophysiological measurements from PES protocols were compared in two separate ways. Firstly, differences spanning the duration of the protocol were compared using ANOVA analysis of area under the curve (AUC) values for each group. To further evaluate the temporal nature of any differences between groups, mean protocol start and protocol end values for each experimental group were compared in the same manner as data from the regular pacing protocol. Where the data from PES protocols was normalised, the corresponding data from regular pacing was used as reference values. Data are expressed as mean ± standard error of the mean (SEM), and in all cases a $p < 0.05$ was taken to be significant, with application of Bonferroni correction where appropriate.

4.3 Results

4.3.1 *Pgc-1β$^{-/-}$ hearts develop an age-related arrhythmic phenotype*

Volume conducted ECGs and intracellular AP recordings were first obtained from Langendorff perfused hearts during regular pacing at a BCL of 125 ms (8 Hz) mimicking murine resting heart rates, thus enabling quantification of occurrence of spontaneous arrhythmia and electrophysiological characterisation under conditions of baseline activity. Figure 4.1(a(i)) demonstrates a typical ECG recording from a young WT heart during regular 8 Hz pacing and Figure 4.1(a(ii)) is the simultaneous intracellular AP from a left atrial (LA) cardiomyocyte. The intracellular recordings confirmed normally polarised resting membrane potentials (RMPs) statistically indistinguishable between groups (young WT: -76.62 ± 1.37 mV,

n = 26; aged WT: -76.72 ± 1.47 mV, n = 27, young *Pgc-1β*$^{-/-}$: 75.82 ± 0.68 mV, n = 34; aged *Pgc-1β*$^{-/-}$: -77.43 ± 1.49 mV, n = 25). Similarly, AP amplitudes confirmed positive AP overshoots through all experimental groups, consistent with intracellular recordings from viable atrial cardiomyocytes in situ, though amplitudes were marginally lower in aged *Pgc-1β*$^{-/-}$ hearts (young WT: 96.76 ± 1.14 mV, n = 26; aged WT: 96.92 ± 1.55 mV, n = 27, young *Pgc-1β*$^{-/-}$: 93.19 ± 1.12 mV, n = 34; aged *Pgc-1β*$^{-/-}$: 91.21 ± 1.63 mV, n = 25, $p < 0.05$). No spontaneous arrhythmias were observed from hearts in any experimental group during the regular pacing protocols.

Hearts were then subjected to a programmed electrical stimulation (PES) protocol consisting of repeated cycles of nine beats, of which the first eight (S1) beats were separated by a regular interval of 125 ms and the ninth was a premature extra stimulus (S2) at an initial S1-S2 coupling interval of 89 ms that was decremented by 1 ms with each successive cycle. This permitted evaluation of the arrhythmic tendency of hearts in response to provocation with an imposed premature S2 beat, the alterations in electrophysiological parameters with varying coupling intervals, and differences in atrial effective refractory periods (ERPs) between groups. Figure 4.1(b) show typical (i) ECG and (ii) AP recordings during PES pacing from a young WT heart with a refractory as opposed to an arrhythmic outcome. Several abnormal rhythms were observed during PES pacing as exemplified in Figure 4.2. These were triggered by the S2 premature stimulus and included isolated ectopic beats (Figure 4.2(a)), paired beats termed a couplet (Figure 4.2(b)) and episodes of atrial tachycardia (AT) defined as three or more consecutive non-stimulated beats (Figure 4.2(c)).

Table 4.1 summarises the number of episodes of the different abnormal rhythms observed during PES, stratified by experimental group. Incidences of atrial tachycardia (AT) were significantly greater in aged *Pgc-1β*$^{-/-}$ hearts compared to any other group with respect to the overall proportion affected ($p < 0.05$, Fisher Exact Test) and the number of arrhythmic events

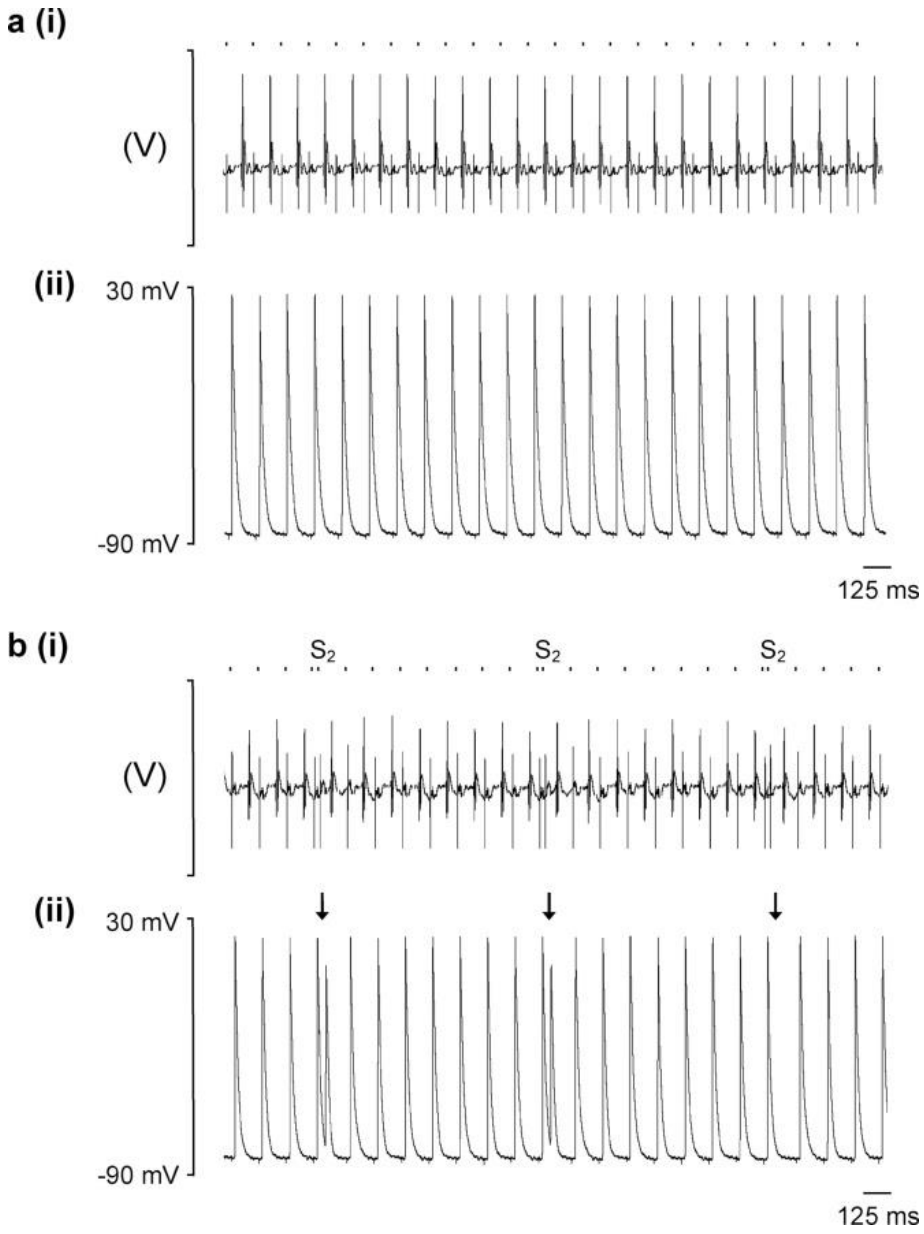

Figure 4.1 Simultaneous volume conducted ECG and left atrial cellular AP recordings

Typical recordings from Langendorff-perfused WT hearts during regular pacing and programmed electrical stimulation. Electrocardiograph (ECG) (i) and left atrial intracellular action potential (AP) recordings (ii) during (a) regular 8 Hz pacing and (b) a protocol imposing programmed electrical stimulation with a refractory outcome. The timings of stimulus delivery are given dashed bar above the AP recordings, and corresponding stimulation artefacts can be seen on the ECG and AP traces, preceding the respective complexes. In panel (B), arrows indicate the imposition of S2 extrastimuli. The first two S2 stimuli trigger APs, whereas the third S2 stimulus fails to elicit a response, thus representing a refractory outcome.

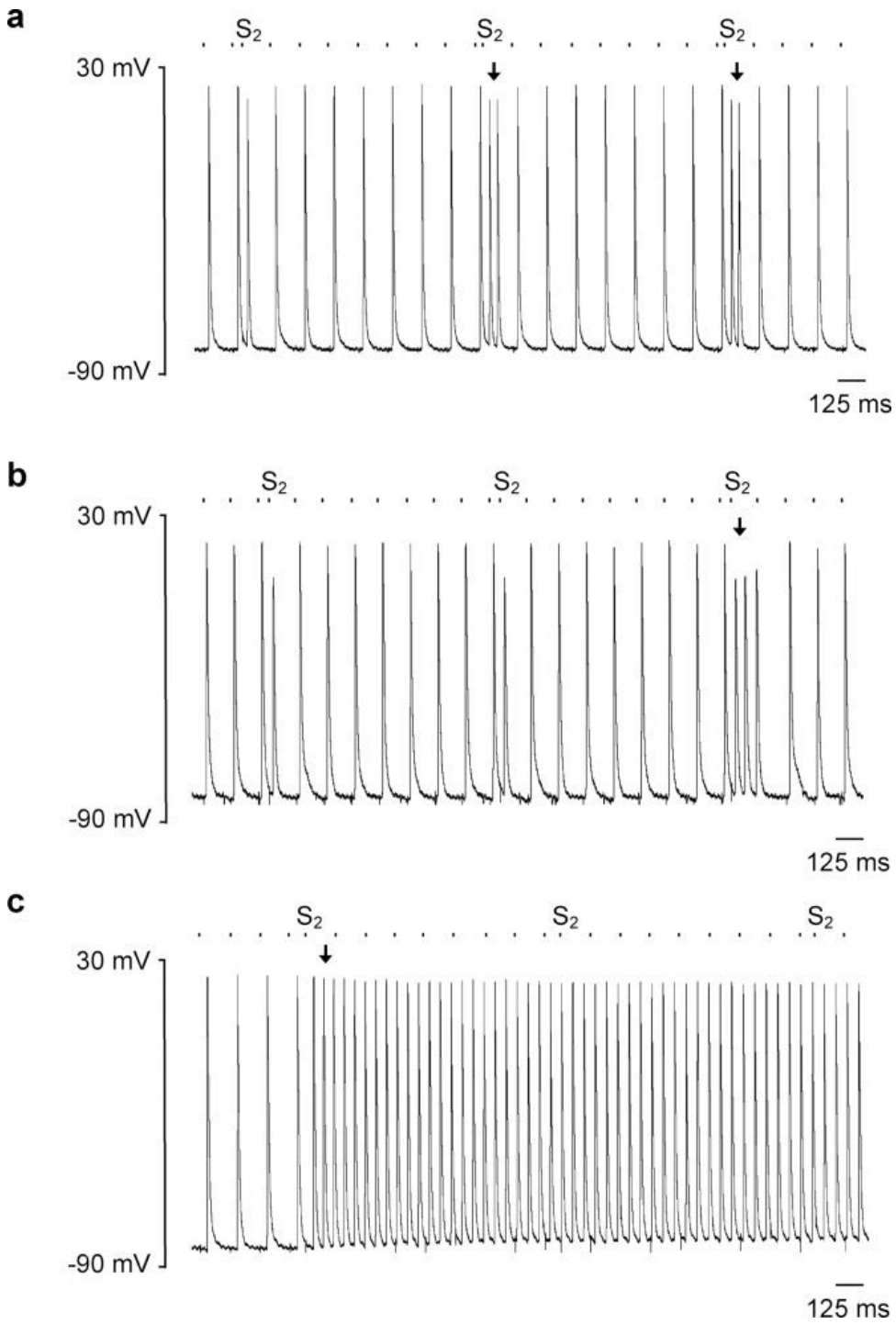

Figure 4.2 Abnormal atrial in response to premature extra-stimuli

Examples of abnormal rhythms elicited by S2 premature stimuli during PES pacing, including (a) isolated ectopic beats, (b) paired beats forming couplets and (c) episodes of atrial tachycardia (AT) defined as three or more consecutive non-stimulated beats. The timings of stimulus delivery are given dashed bar above the AP recordings and arrows indicate the onset of the abnormal rhythm.

per individual heart, suggesting an arrhythmic phenotype associated with mitochondrial dysfunction that progresses with age. AT was more frequently observed in the young *Pgc-1β*$^{-/-}$ group compared to either of the WT groups, with no difference in incidence observed between the young and aged WT groups. Although a similar proportion of young and aged WT hearts were arrhythmic, arrhythmic event rates were higher in the latter further reinforcing an effect of age upon arrhythmic risk. Thus ANOVA analysis of mean AT events per heart demonstrated a significant effect of genotype ($F = 7.13$, $p < 0.01$) with *Pgc-1β*$^{-/-}$ hearts having higher event rates and age ($F = 7.26$, $p < 0.01$), but no interactive effect ($F = 2.37$, $p > 0.05$). Post hoc Tukey tests demonstrated significant differences in rates of AT between aged *Pgc-1β*$^{-/-}$ hearts and young WT hearts ($p < 0.01$), aged WT hearts ($p < 0.05$) and young *Pgc-1β*$^{-/-}$ hearts ($p < 0.05$).

This increased propensity to AT is further highlighted on analysis of the critical coupling intervals, given by the S1-S2 coupling interval at which arrhythmia was triggered as shown in Figure 4.3. Episodes of AT in WT hearts (Figure 4.3(a) and (b)) were triggered predominantly at latter parts of the PES protocol corresponding to shorter S1-S2 coupling intervals. In contrast *Pgc-1β*$^{-/-}$ hearts developed arrhythmias at earlier stages of the protocol and over a wider range of coupling intervals (Figure 4.3(c) and (d)), with aged *Pgc-1β*$^{-/-}$ hearts particularly appearing vulnerable throughout the duration of the protocol. The mean critical coupling interval was longer in *Pgc-1β*$^{-/-}$ hearts ($F = 8.35$, $p < 0.01$) and aged hearts ($F = 3.93$, $p < 0.05$), though no interactive effect was observed ($F = 0.004$, $p = 0.95$). Post hoc analysis demonstrated significant differences between aged *Pgc-1β*$^{-/-}$ and young WT hearts ($p < 0.05$) and a trend to significance between aged *Pgc-1β*$^{-/-}$ and aged WT hearts ($p < 0.10$).

Table 4.1 Summary of arrhythmic events during programmed electrical stimulation

Experimental Group	No. that developed AT (n / total)	Ectopic Beats Mean (± SEM)	Couplets Mean (± SEM)	AT Mean (± SEM)	Critical Coupling Interval Mean (± SEM)
Young Wild Type	5 / 27	1.48 ± 0.50	0.41 ± 0.26	0.26 ** ± 0.11	28.71 # ± 3.46
Aged Wild Type	4 / 27	0.79 ± 0.53	1.17 ± 0.62	0.48 † ± 0.36	32.71 ± 4.21
Young *Pgc-1β*$^{-/-}$	11 / 34	1.22 ± 0.47	0.42 ± 0.21	0.86 ‡ ± 0.35	35.70 ± 1.35
Aged *Pgc-1β*$^{-/-}$	12 / 25*	1.64 ± 0.66	1.28 ± 0.55	2.64 **, †, ‡ ± 0.70	39.39 # ± 1.12

Each action potential parameter detailed on the top row was compared between young and aged, WT and hearts as detailed in the left column. Symbols denote significant difference based on post hoc analysis, performed if the *F* value from two-way ANOVA was significant. Single, double and triple symbols denote $p < 0.05$, $p < 0.01$ and $p < 0.001$ respectively

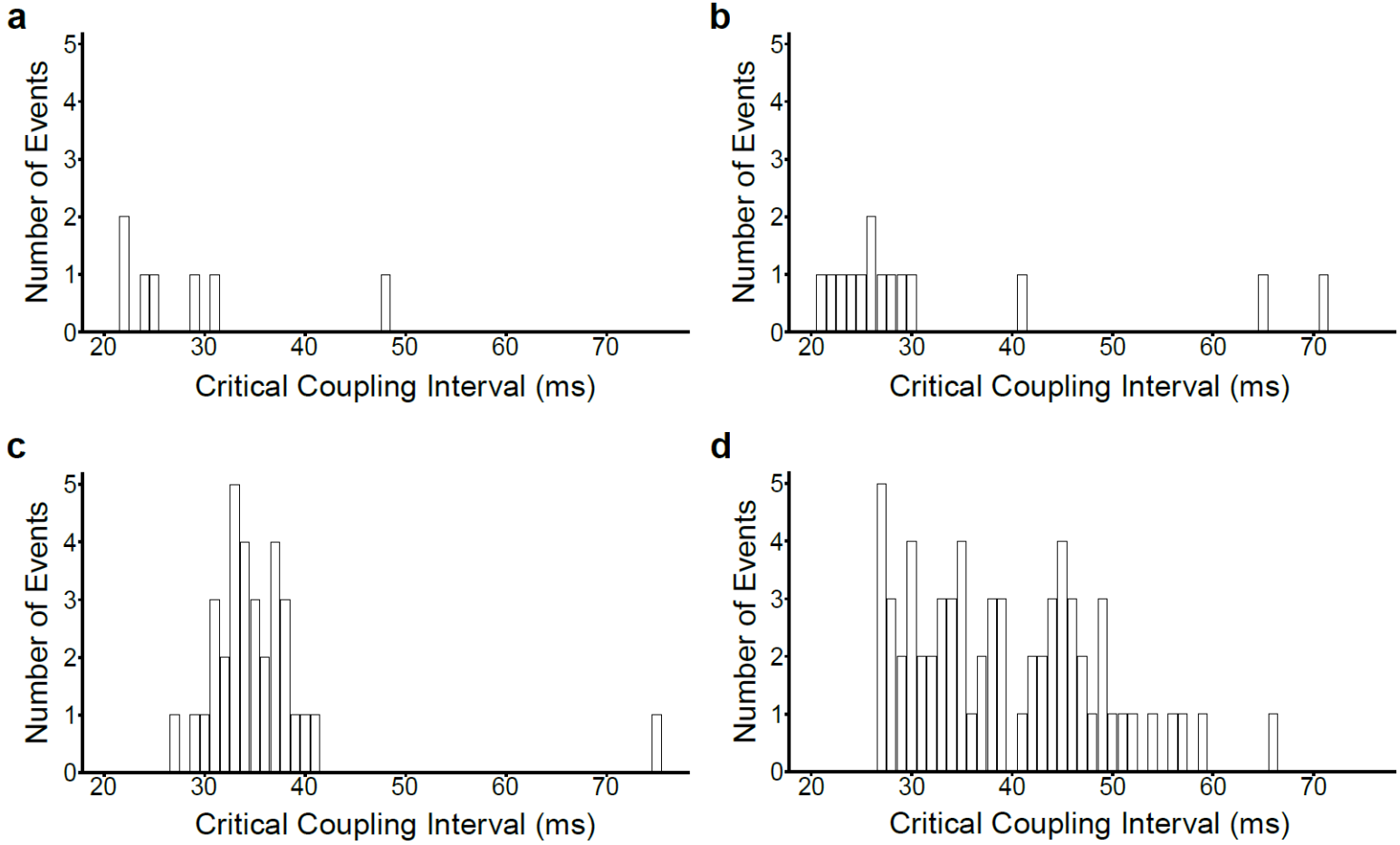

Figure 4.3 **Critical coupling interval at which episodes of arrhythmia were induced**

Stratification of the occurrence of AT episodes by critical coupling intervals in young ((a), (c)) and old ((b), (d)), WT ((a), (b)) and Pgc-1β$^{-/-}$ hearts ((c), (d)). Pgc-1β$^{-/-}$ hearts display vulnerability to arrhythmia earlier, and through wider range of S1-S2 coupling intervals.

4.3.2 Action potential parameters during regular pacing

These differing arrhythmic profiles were next compared with electrophysiological parameters corresponding to AP initiation, propagation and recovery during regular pacing at 8 Hz. AP initiation was measured first through maximum rates of AP depolarisation $(dV/dt)_{max}$, derived from left atrial intracellular microelectrode recordings. $(dV/dt)_{max}$ measurements serve to quantify the depolarisation of the cardiomyocyte membrane capacitance by regenerative inward Na^+ current. Reductions in $(dV/dt)_{max}$ are known to correlate with compromised conduction velocity of an AP wavefront, potentially providing a substrate permissive to AP re-entry and arrhythmia. *Pgc-1β*$^{-/-}$ hearts showed significantly lower values of $(dV/dt)_{max}$ compared to WT ($F = 18.41$, $p < 0.001$) but there was no effect of age ($F = 0.17$, $p > 0.05$) or interaction between age and genotype ($F = 0.001$, $p > 0.05$). On post hoc Tukey testing, each *Pgc-1β*$^{-/-}$ group, whether young or aged, showed significantly lower $(dV/dt)_{max}$ values than either of the WT groups (Table 4.2).

AP conduction through respective cardiac chambers is determined by properties of the inward Na^+ current, reflected by the cellular $(dV/dt)_{max}$ values, but also the total membrane capacitance and resistance (King *et al.*, 2013*a*). AP propagation was therefore further assessed through comparisons of AP latency times, measured as the time intervening between stimulus delivery at the right atrial pacing site and the peak AP voltage measured at the left atrial recording site. In all experiments, the stimulating electrode was consistently positioned at the posterior aspect of the RA and recordings were made from the central region of the LA, minimising variability in distances between the respective electrodes. ANOVA of AP latency times demonstrated significant effects of genotype ($F = 9.91$, $p < 0.01$), age ($F = 5.32$, $p < 0.05$) and an interaction of the two ($F = 12.47$, $p < 0.001$). As detailed in Table 4.2, these differences were driven by young WT hearts, which had significantly shorter AP latency times than aged WT hearts ($p < 0.001$), young *Pgc-1β*$^{-/-}$ hearts ($p < 0.001$), and aged *Pgc-1β*$^{-/-}$ hearts ($p < 0.01$), There was no significant difference between the aged WT hearts and either of the *Pgc-1* $^{-/-}$ groups.

Pro-arrhythmic tissue substrate has also been associated with altered repolarisation associated with action potential shortening or prolongation (Sabir *et al.*, 2007*c*, 2007*b*; Killeen *et al.*, 2007). Electrophysiological parameters describing repolarisation are given in Table 4.2. No differences in APD at 90% repolarisation (APD_{90}) were found during regular 8 Hz pacing

either through effects of genotype ($F = 1.07$, $p > 0.05$), age ($F = 0.001$, $p > 0.05$) or an interaction of the two ($F = 0.20$, $p > 0.05$). Repolarisation properties were further assessed through measurement of the ERP obtained from the PES protocol, defined as the longest S1-S2 coupling interval at which the S2 stimulus failed to trigger an AP. The ERP generally correlates with the APD, and in keeping with this no differences between groups were observed when compared according to genotype ($F = 3.36$, $p > 0.05$) or age ($F = 0.04$, $p > 0.05$).

4.3.3 Action potential parameters following premature extrasystolic stimuli

The trigger-substrate model of arrhythmogenesis comprises initiation of the abnormal rhythm through an arrhythmogenic trigger, such as an extrasystole, occurring within a pro-arrhythmic substrate capable of sustaining the arrhythmia (Antzelevich et al 1999, Kalin et al 2010). The PES protocol consisted of pulse trains of S1 beats 125 ms apart, punctuated every ninth beat by a premature S2 stimulus, mimicking such triggering extrasystoles. The external application of these premature beats thus controlled for incidence of ectopic stimuli between groups and so assessed for the presence of such an arrhythmogenic substrate.

Figure 4.4 a(i) plots mean $(dV/dt)_{max}$ values for APs triggered by S2 stimuli across the range of coupling intervals explored during the PES protocol. All experimental groups displayed the expected progressively reduced $(dV/dt)_{max}$ values with shortening of the S1-S2 coupling interval. In common with findings obtained during regular pacing, an analysis of the areas beneath the data curve (AUC) demonstrated that the overall rates of depolarisation were significantly higher in WT than *Pgc-1β*$^{-/-}$ hearts ($F = 6.41$, $p < 0.05$) (Table 4.3); there were no effects of age ($F = 0.84$, $p > 0.05$) or interacting effects of genotype and age ($F = 0.27$, $p > 0.05$). The difference between WT and *Pgc-1β*$^{-/-}$ hearts was most pronounced at the beginning of the protocol (Figure 4.4 a(ii)) (ANOVA - genotype: $F = 13.19$, $p < 0.001$; age: $F = 0.15$, $p > 0.05$; interaction: $F = 0.002$, $p > 0.05$) and was of a similar magnitude as had been observed during 8 Hz pacing. On post hoc analysis, each WT group showed significantly higher $(dV/dt)_{max}$ values compared against either of the *Pgc-1β*$^{-/-}$ groups. In contrast, no difference in $(dV/dt)_{max}$ values was observed at the shortest coupling intervals at the end of the protocol, whether tested for effects of genotype ($F = 0.09$, $p > 0.05$), age ($F = 0.18$, $p > 0.05$) or interaction ($F = 0.31$, $p > 0.05$).

Table 4.2 Action potential properties in WT and *Pgc-1β*$^{-/-}$ hearts during regular 8 Hz pacing

Experimental Group	$(dV/dt)_{max}$ (V s^{-1})	AP Latency (ms)	APD_{90} Duration (ms)	Effective Refractory Period (ms)	Wavelength
Young Wild Type	171.06 *, †	17.69 ***, †††, ‡‡	24.87	26.62	4.21 *, †
	± 6.60	± 0.23	± 1.18	± 1.27	± 0.25
Aged Wild Type	171.73 ‡‡, #	23.93 ***	25.51	27.33	4.34 ‡‡, ##
	± 5.15	± 1.24	± 1.59	± 1.77	± 0.29
Young *Pgc-1β*$^{-/-}$	141.28 *, ‡‡	24.61†††	23.97	29.82	3.28 *, ‡‡
	± 7.19	± 0.65	± 0.93	± 0.54	± 0.16
Aged *Pgc-1β*$^{-/-}$	142.39 †, #	23.48 ‡‡	23.28	28.33	3.15 †, ##
	± 8.08	± 1.66	± 2.16	± 1.33	± 0.25

All values are given as mean (± SEM)

Each action potential parameter detailed on the top row was compared between young and aged, WT and *Pgc-1β*$^{-/-}$ hearts as detailed in the left column.

Symbols denote significant difference based on post hoc analysis, performed if the *F* value from two-way ANOVA was significant. Single, double and triple symbols denote $p < 0.05$, $p < 0.01$ and $p < 0.001$ respectively.

Similar plots for AP latencies are given in Figure 4.4 (b(i)) and 4.4 (b(ii)). In keeping with findings during regular 8 Hz pacing and the observed differences in $(dV/dt)_{max}$ values, AP latency times were significantly prolonged in *Pgc-1β*$^{-/-}$ hearts when surveyed through the entirety of the protocol on AUC analyses ($F = 12.98$, $p < 0.001$), but there were no independent effects of age ($F = 1.11$, $p > 0.05$) or compound effect of age and genotype ($F = 1.36$, $p > 0.05$). Young WT hearts had significantly shorter AP latency times compared to young *Pgc-1β*$^{-/-}$ hearts ($p < 0.01$) and aged *Pgc-1β*$^{-/-}$ hearts ($p < 0.05$) on post hoc testing. ANOVA analysis of AP latencies at the longest S1-S2 intervals demonstrated significant effects of genotype ($F = 19.23$, $p < 0.001$), age ($F = 4.79$, $p < 0.05$) and interacting effects of genotype and age ($F = 6.12$, $p < 0.05$). Here the AP latency times for young WT hearts were significantly shorter than all other groups including aged WT ($p < 0.01$), young *Pgc-1β*$^{-/-}$ ($p < 0.001$) and aged *Pgc-1β*$^{-/-}$ hearts ($p < 0.001$). AP latencies progressively lengthened in all groups as the S1-S2 interval shortened but to varying degrees. Thus, at the shortest S1-S2 intervals, a significant difference between WT and *Pgc-1β*$^{-/-}$ hearts persisted ($F = 10.15$, $p < 0.001$), however significant effects of age ($F = 1.19$, $p > 0.05$) or interaction ($F = 2.79$, $p > 0.05$) were no longer evident. AP latency times remained significantly shorter in young WT hearts when compared with young *Pgc-1β*$^{-/-}$ ($p < 0.01$) and *Pgc-1β*$^{-/-}$ aged hearts ($p < 0.05$), however the lengthening of AP latency in aged WT was less pronounced than that of the *Pgc-1β*$^{-/-}$ hearts and thus the difference with the young WT hearts was no longer significant.

The adaptation of AP duration, given by APD_{90} times, through progressively shortening S1-S2 coupling intervals is shown in Figure 4.4 (c(i)). Overall APD_{90} times did not differ between experimental groups (ANOVA - genotype: $F = 2.95$, $p > 0.05$; age: $F = 1.71$, $p > 0.05$; interaction: $F = 0.002$, $p > 0.05$), reflecting the findings during regular 8 Hz pacing. Accordingly, APD_{90} times at the beginning of the protocol, corresponding to the longest S1-S2 intervals, also did not differ between groups (ANOVA - genotype: $F = 1.63$, $p > 0.05$; age: $F = 0.02$, $p > 0.05$; interaction: $F = 1.30$, $p > 0.05$). APD_{90} times in all groups displayed the expected shortening as the S1-S2 interval decreased, however a small but significant difference in APD_{90} between WT and *Pgc-1β*$^{-/-}$ hearts was seen at the shortest coupling intervals ($F = 6.60$, $p < 0.05$), where *Pgc-1β*$^{-/-}$ hearts had shorter APD_{90}. No differences were noted based upon age ($F = 0.02$, $p > 0.05$), or interacting effects of genotype and age ($F = 1.52$, $p > 0.05$). There were no significant differences between groups on post hoc Tukey testing.

Reductions in the AP wavelength have been suggested to correlate with increased arrhythmic risk, indicating the presence of substrate favourable to AP re-entry. It has previously been calculated from terms relating to AP conduction and AP duration, and similar analyses were conducted in the present study. *Pgc-1β*$^{-/-}$ hearts had significantly shorter wavelength values at resting hearts as measured during 8 Hz pacing ($F = 20.62$, $p < 0.001$), however there were no effects of ageing ($F = 0.01$, $p > 0.05$) or interacting effects of the two variables ($F = 0.32$, $p > 0.05$) (Table 4.2). AP wavelengths profiles for beats triggered by S2 extrastimuli during PES pacing are shown in Figure 4.4(d). Wavelengths were shorter throughout the protocol in *Pgc-1β*$^{-/-}$ hearts ($F = 9.19$, $p < 0.01$), with effect of either age ($F = 0.03$, $p > 0.05$) or interaction of genotype and age ($F = 0.01$, $p > 0.05$) having no significant effect. The differences between WT and *Pgc-1β*$^{-/-}$ hearts noted during regular 8 Hz pacing was similarly evident at the longest S1-S2 intervals ($F = 18.93$, $p < 0.01$) with no other significances noted (ageing: $F = 0.01$, $p > 0.05$; genotype - age interaction: $F = 1.20$, $p > 0.05$) (Fig. 5(d(ii))). Post hoc Tukey revealed significant differences between young WT and aged *Pgc-1β*$^{-/-}$ hearts ($p < 0.05$), aged WT and young *Pgc-1β*$^{-/-}$ hearts ($p < 0.01$), and aged WT and aged *Pgc-1β*$^{-/-}$ hearts ($p < 0.01$). Wavelength values reduced in all groups as the S1-S2 coupling interval shortened, correlating with the increased vulnerability to arrhythmias seen in all hearts. However, AP wavelengths for young *Pgc-1β*$^{-/-}$ hearts more closely converged to those of both WT groups, whereas wavelengths remained shorter in aged *Pgc-1β*$^{-/-}$ hearts. Thus though *Pgc-1β*$^{-/-}$ hearts continued to display significantly shorter wavelengths at the shortest S1-S2 intervals (ANOVA – genotype: $F = 5.00$, $p < 0.05$; age: $F = 0.51$, $p > 0.05$, interaction: $F = 2.40$, $p > 0.05$) no significant differences were noted between any groups on post hoc testing.

4.3.4 Relative changes in action potential parameters following premature extrasystolic stimuli

The energetic dysfunction associated with mitochondrial impairment would be expected to particularly compromise cardiac activity in the stressed state. Indeed *Pgc-1α* deficient hearts show normal contractile function at baseline but develop pronounced cardiac failure in response to aortic banding. *Pgc-1β*$^{-/-}$ hearts are known to develop chronotropic incompetence

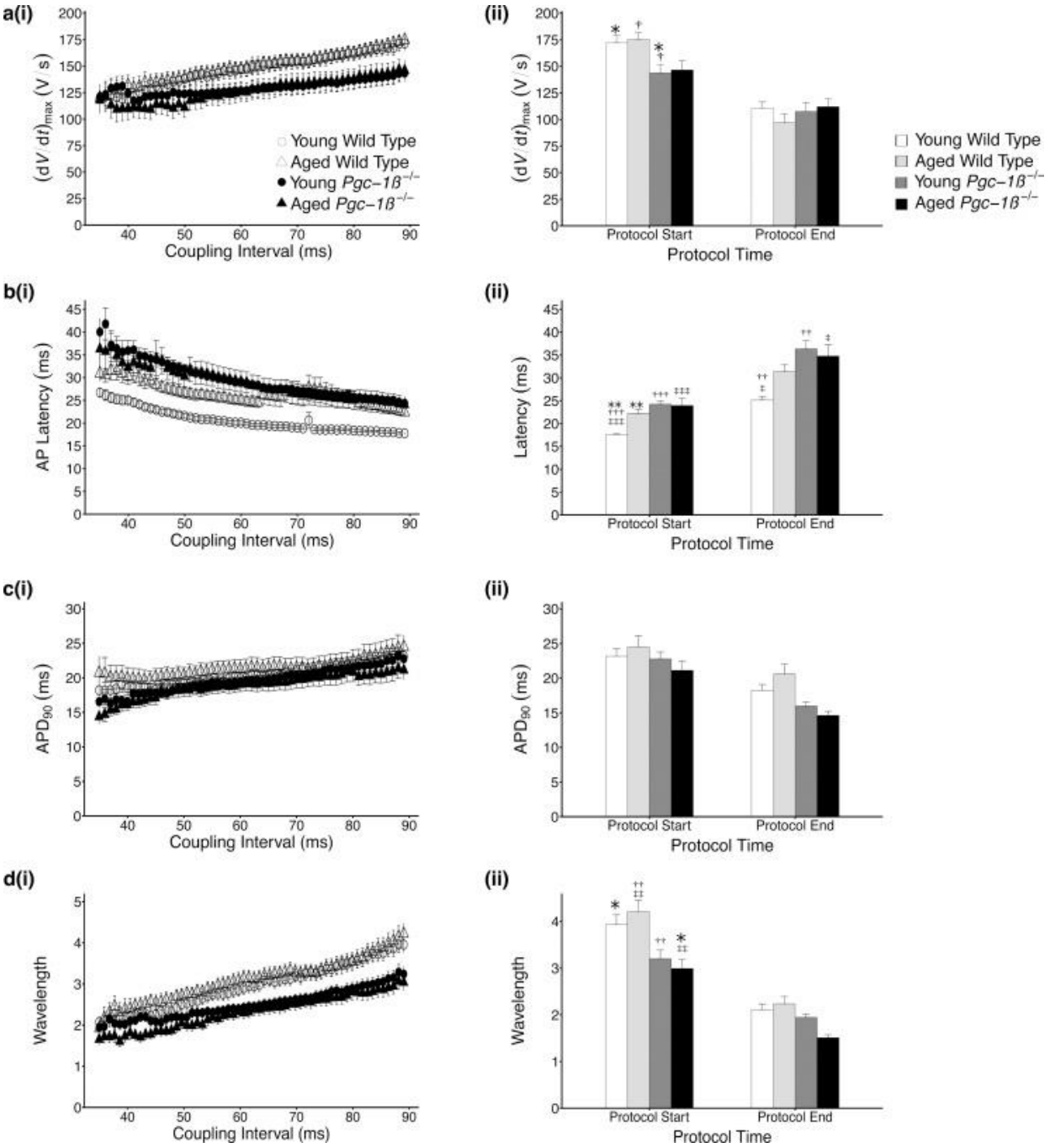

Figure 4.4 AP parameters for S2 extras-stimuli

Plots of mean ± SEM (a) $(dV/dt)_{max}$, (b) AP latency and (c) time to 90% AP recovery (APD_{90}) for APs obtained in response to S2 stimuli (i) through the range of coupling intervals explored, reducing from 89 ms to 30 ms. Panel (ii) for each provides a comparison of these values at the beginning and termination of the pacing protocol, corresponding to a refractory outcome or the onset of sustained arrhythmia. The symbols denote significant differences between each pair, obtained from post hoc Tukey testing, which was conducted if the ANOVA indicated a significant outcome. Single, double and triple symbols denote $p < 0.05$, $p < 0.01$ and $p < 0.001$ respectively.

Table 4.3 Area under the curve analysis for S2 triggered APs during programmed electrical stimulation

Experimental Group	$(dV/dt)_{max}$ ($V \times 10^{-3}$)	AP Latency (ms^2)	APD_{90} (ms^2)	Wavelength (ms)
Young Wild Type	6.68 ± 0.32	1.06 ††, ‡ ± 0.04	1.06 ± 0.05	0.085 ± 0.005
Aged Wild Type	6.11 ± 0.35	1.21 ± 0.05	0.93 ± 0.06	0.082 ± 0.007
Young *Pgc-1β*$^{-/-}$	5.44 ± 0.37	1.39 †† ± 0.08	0.95 ± 0.05	0.066 ± 0.005
Aged *Pgc-1β*$^{-/-}$	5.30 ± 0.64	1.38 ‡ ± 0.01	0.82 ± 0.06	0.065 ± 0.005

All values are given as mean (± SEM)

Symbols denote significant difference based on post hoc analysis, performed if the *F* value from two-way ANOVA was significant. Single, double and triple symbols denote $p < 0.05$, $p < 0.01$ and $p < 0.001$ respectively

in response to adrenergic challenge despite normal resting heart rates. To further characterise the cardiac phenotype in response to increasing metabolic demand in the form of shortening pacing intervals, electrophysiological parameters during PES pacing were normalised internally to their corresponding values measured during regular 8 Hz pacing. The normalised profiles for the relevant parameters are show in Figure 4.5(a – c). Normalised $(dV/dt)_{max}$ (Fig. 7a) and normalised APD_{90} (Fig. 7c) displayed similar reductions with shortening S1-S2 intervals, and there were no significant differences in AUC values for either parameter (Table 4.4). Despite differing absolute AP latency times, normalised AP latency profiles for young and aged WT hearts were similar (Figure 4.5(b)). In contrast *Pgc-1β*$^{-/-}$ hearts displayed greater increments in normalised latency, with aged *Pgc-1β*$^{-/-}$ hearts appearing most compromised. ANOVA analysis of AUC values for normalised AP latency showed no independent effect of genotype ($F = 0.49$, $p > 0.05$) or age ($F = 0.05$, $p > 0.05$), but a significant interacting effect of the two ($F = 4.31$, $p < 0.05$) with aged *Pgc-1β*$^{-/-}$ hearts having the highest AUC values. No significant differences were seen on individual comparisons with post hoc Tukey testing.

4.3.5 Contrasting impacts of $(dV/dt)_{max}$ upon AP latency in WT and Pgc-1β$^{-/-}$ hearts

Findings from the regular 8 Hz and PES pacing protocols suggested an arrhythmic substrate in *Pgc-1β*$^{-/-}$ hearts through compromised conduction parameters, with few alterations in repolarisation characteristics. Here, *Pgc-1β*$^{-/-}$ hearts displayed deficits in $(dV/dt)_{max}$ that were independent of age, and a corresponding altered conduction through the myocardium, reflected by prolonged AP latency times. However, the latter differed from $(dV/dt)_{max}$, in appearing to be influenced by age to some degree. This prompted further exploration of the relationship between these conduction parameters. Mean AP latency times from extrasystolic S2 beats recorded during the PES protocols are plotted against their corresponding mean $(dV/dt)_{max}$ values for each experimental group in Figure 4.6. Reductions in $(dV/dt)_{max}$ with shortening S1-S2 coupling intervals is associated with increasing AP latency times for all groups, suggesting that much of the increase in AP latency observed with progressively shortening coupling intervals is attributable to concurrent reductions in $(dV/dt)_{max}$. However distinct associations between these parameters were seen in WT and *Pgc-1β*$^{-/-}$ hearts. As shown in Figure 4.6 (a), prolongation of AP latency independent of $(dV/dt)_{max}$ occurs in WT hearts

with age, such that for any given $(dV/dt)_{max}$ value, the AP latency time is longer in aged WT hearts compared to young WT hearts. In contrast, young and aged *Pgc-1β*$^{-/-}$ hearts display a more homogeneous association between $(dV/dt)_{max}$ and AP latency, with values in line with those of aged WT hearts. Thus young *Pgc-1β*$^{-/-}$ hearts develop electrophysiological features resembling those of normal ageing, which may explain their increased propensity to arrhythmia.

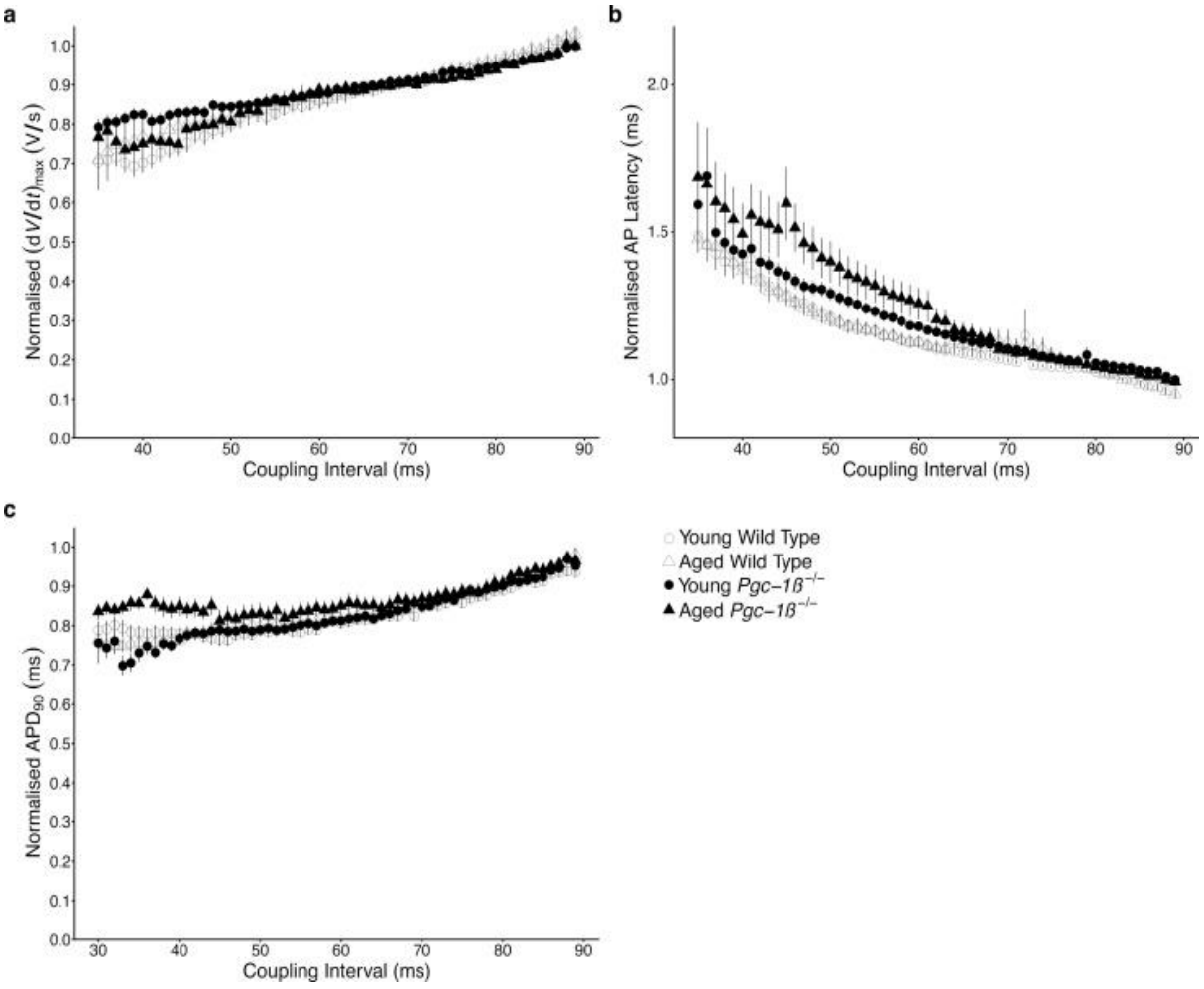

Figure 4.5 Normalised S2 beat AP parameters

Plots of mean ± SEM (a) $(dV/dt)_{max}$, (b) AP latency and (c) time to 90% AP recovery (APD_{90}) in APs obtained in response to S2 stimuli, normalized to their corresponding values obtained during regular 8 Hz pacing through progressively shortening S1-S2 coupling intervals.

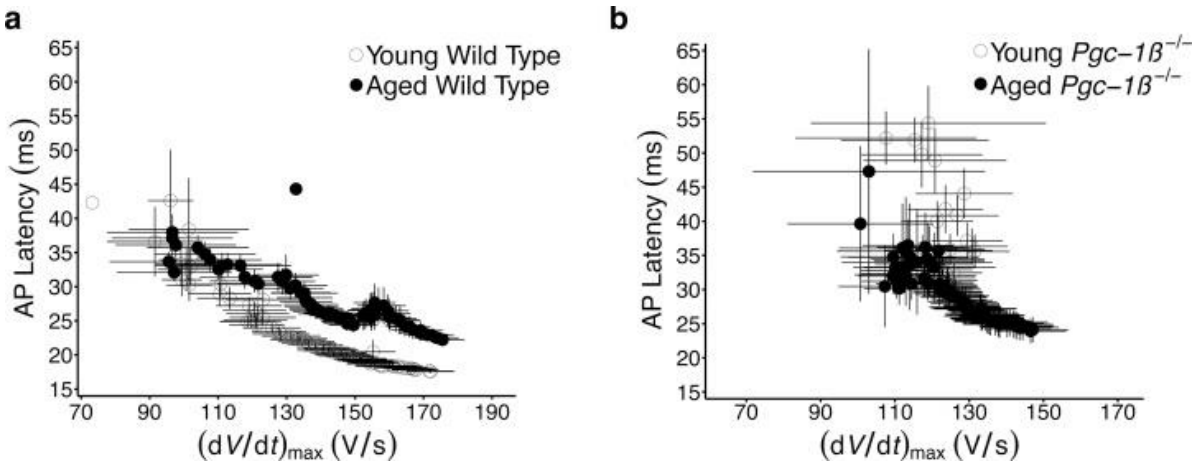

Figure 4.6 Relationship between $(dV/dt)_{max}$ and AP latency

Dependences of AP latency times upon $(dV/dt)_{max}$ through the programmed electrical stimulation protocol compared in (a) young and old WT and (b) young and aged Pgc-1β$^{-/-}$ hearts.

4.3.6 Compromised conduction triggering arrhythmia in all hearts

The bearing of the observed electrophysiological parameters upon the initiation of arrhythmic events was next explored. The mean values of the relevant electrophysiological parameters from the first S2 AP that triggered an episode of AT in a given heart are given in Table 4.5. *Pgc-1β$^{-/-}$* hearts showed significantly higher values of $(dV/dt)_{max}$ for triggering S2 APs compared to WT ($F = 4.55$, $p < 0.05$), but there were no effects of age ($F = 0.00$, $p > 0.05$) or interacting effects of age and genotype ($F = 0.28$, $p > 0.05$). No significant differences were found upon individual comparisons during post hoc analysis. Interestingly, ANOVA analysis of AP latencies for the same S2 trigger APs revealed no differences with respect to genotype ($F = 0.001$, $p > 0.05$), age ($F = 0.15$, $p > 0.05$) or interaction of the two ($F = 3.46$, $p > 0.05$). No significant differences were seen in APD_{90} between trigger S2 APs of the different experimental groups (ANOVA - genotype: $F = 1.02$, $p > 0.05$; age: $F = 0.37$, $p > 0.05$; interaction: $F = 0.39$, $p > 0.05$). Similarly AP wavelengths for trigger S2 AP were also indistinguishable between groups (ANOVA - genotype: $F = 1.96$, $p > 0.05$; age: $F = 0.07$, $p > 0.05$; interaction: $F = 1.04$, $p > 0.05$). Thus AT was initiated in WT and *Pgc-1β$^{-/-}$* hearts through premature beats that were indistinguishable in terms of measures of conduction across the tissue. The differing profiles of conduction between the groups, and the earlier development of compromise in *Pgc-1β$^{-/-}$* hearts may explain their increase vulnerability to arrhythmia.

Table 4.4 Area under the curve analysis for S2 triggered APs during programmed electrical stimulation, normalised to corresponding values from regular pacing

Experimental Group	$(dV/dt)_{max}$ (ms)	AP Latency (ms)	APD_{90} (ms)
Young Wild Type	0.045 ± 0.001	0.039 ± 0.02	0.025 ± 0.001
Aged Wild Type	0.041 ± 0.002	0.035 ± 0.002	0.023 ± 0.002
Young *Pgc-1β*$^{-/-}$	0.042 ± 0.002	0.037 ± 0.002	0.023 ± 0.001
Aged *Pgc-1β*$^{-/-}$	0.041 ± 0.003	0.043 ± 0.003	0.023 ± 0.002

All values are given as mean (± SEM)

Symbols denote significant difference based on post hoc analysis, performed if the *F* value from two-way ANOVA was significant. Single, double and triple symbols denote $p < 0.05$, $p < 0.01$ and $p < 0.001$ respectively

Table 4.5 AP parameters for S2 triggered APs that initiated the first episode of atrial tachycardia during programmed electrical stimulation

Experimental Group	$(dV/dt)_{max}$ (V s^{-1})	AP Latency (ms)	APD_{90} (ms)
Young Wild Type	100.10 ± 5.68	27.42 ± 1.52	15.96 ± 0.50
Aged Wild Type	112.53 ± 10.63	33.90 ± 3.39	17.60 ± 3.59
Young *Pgc-1β*$^{-/-}$	142.03 ± 11.77	32.86 ± 1.77	15.17 ± 0.61
Aged *Pgc-1β*$^{-/-}$	137.46 ± 14.65	28.57 ± 2.56	15.43 ± 0.85

All values are given as mean (± SEM)

Symbols denote significant difference based on post hoc analysis, performed if the *F* value from two-way ANOVA was significant. Single, double and triple symbols denote $p < 0.05$, $p < 0.01$ and $p < 0.001$ respectively

4.4 Discussion

Atrial fibrillation is characterised by an irregular, often rapid atrial rhythm that may be asymptomatic in the short term, but nevertheless carry substantial risks of long term morbidity and mortality. Ageing represents the major risk factor for AF itself: AF affects <0.1 % in those under the age of 50, 4% in individuals aged 60-69 and up to 20% in those aged above 85 (Go *et al.*, 2001*b*; Krijthe *et al.*, 2013; Zoni-Berisso *et al.*, 2014). A decline in mitochondrial function is correspondingly observed in ageing, and has been postulated to account for age-related decrements in organ function with associated susceptibility to disease (Biala *et al.*, 2015; Lane *et al.*, 2015), including predisposition to AF (Tsuboi *et al.*, 2001; Ad *et al.*, 2005; Montaigne *et al.*, 2013). The present experiments therefore investigated the electrophysiological alterations associated with ageing and mitochondrial dysfunction in murine atria with homozygous deficiency of the transcriptional co-activator *Pgc-1β*. The results suggest an age-related increase in arrhythmic incidence that was exacerbated by mitochondrial dysfunction. This propensity to arrhythmia developed predominantly through deficits in parameters pertaining to AP conduction at the cellular and tissue level.

The heart is a highly oxidative organ and served by a rich network of mitochondria, which account for up to 30% of myocardial volume and produce approximately 95% of its cellular ATP (Schaper *et al.*, 1985). Understandably mitochondrial dysfunction is associated with altered cardiac electrical properties, giving rise to AP heterogeneities that provide a substrate for arrhythmia, and has been the subject of much attention in the context of ventricular arrhythmogenesis (Brown & O'Rourke, 2010*b*; Yang *et al.*, 2014). Mitochondrial abnormalities have also been reported in studies of AF but their role in its pathogenesis have been relatively unexplored. Evidence of altered mitochondrial structure was found in dog (Morillo *et al.*, 1995) and goat (Ausma *et al.*, 1997*b*) models of AF. Here, AF was induced by rapid atrial pacing with the noted mitochondrial defects appearing as a possible consequence of the pacing protocol and/or AF itself. Similarly, evidence of mitochondrial abnormalities have been reported in tissue samples obtained during cardiac surgery from AF patients (Tsuboi *et al.*, 2001; Lin *et al.*, 2003; Slagsvold *et al.*, 2014; Emelyanova *et al.*, 2016). In these studies the selected cohorts had established AF and it remains difficult to distinguish whether the observed mitochondrial lesions were caused by or resulted from AF, or indeed were a confound of ageing or other age-related conditions associated with metabolic compromise.

However baseline mitochondrial deficits were found to predict development of post-operative AF following cardiac surgery in patients with no prior history of AF (Ad *et al.*, 2005; Montaigne *et al.*, 2013), suggesting a more direct role in its pathogenesis. Furthermore, Marks and colleagues recently reported diastolic Ca^{2+} leak, through progressive oxidisation of ryanodine receptors, was associated with age-dependent development of AF in a murine model (Xie *et al.*, 2015). Reductions in mitochondrial ROS production attenuated these diastolic Ca^{2+} transients and prevented AF.

Electrophysiological alterations secondary to chronic mitochondrial impairment have not been well characterised to date. The PGC-1 family of transcriptional coactivators, which includes PGC-1α and PGC-1β, serve as key modulators of cellular metabolic activity, particularly in oxidative tissues such as the heart and brain (Riehle & Abel, 2012). Overexpression of specific individual members of the PGC-1 family in various cell types results in increased mitochondrial density and augments their overall oxidative capacity (Lehman *et al.*, 2000; Russell *et al.*, 2004). Conversely, cardiomyocytes deficient in *Pgc-1α* demonstrate impaired maximal capacity for mitochondrial ATP synthesis (Vega *et al.*, 2000; Huss *et al.*, 2004) . Mice deficient in both *Pgc-1α* and *Pgc-1β* develop a low cardiac output state and conduction system disease, contributing to their death before weaning (Lai *et al.*, 2008). The cardiac phenotype of mice lacking individual members of the Pgc-1 family is less severe. *Pgc-1β* deficiency is not associated with cardiac dysfunction at baseline (Lelliott *et al.*, 2006), but increased susceptibility to ventricular arrhythmias (Gurung *et al.*, 2011). This model was therefore utilised to investigate electrophysiological alterations secondary to mitochondrial dysfunction in murine atria. The modified Langendorff preparation utilised here, permitted simultaneous volume conducted ECG and intracellular microelectrode recordings during regular pacing and programmed electrical stimulation applying premature extra stimuli, enabling assessment of AP activation and recovery properties.

Hearts were first paced at a frequency of 8 Hz, reflecting murine resting heart rates and therefore providing steady state electrophysiological characterisation. No arrhythmias were observed in any group during regular pacing. This is consistent with previous reports that *Pgc-1β* ablation is not associated with a pronounced cardiac phenotype under conditions of baseline activity. In contrast arrhythmias were seen in all experimental groups during programmed electrical stimulation. Incidences of arrhythmia increased with age in both WT

and *Pgc-1β*$^{-/-}$ hearts, in keeping with the cumulative risk of both atrial and ventricular arrhythmias with age seen in the clinical setting (Deo & Albert, 2012; Zoni-Berisso *et al.*, 2014). Young WT hearts displayed the fewest episodes of AT of all groups, and the incidence was higher in aged WT hearts. The mitochondrial theory of ageing posits progressive deterioration in mitochondrial function, through accumulation of mutations in mitochondrial DNA and impaired autophagy, underpinning the ageing process and may contribute to this increased vulnerability to arrhythmia. Accordingly young and aged *Pgc-1β*$^{-/-}$ hearts, possessing a pronounced mitochondrial defect, had even higher incidences of AT. Here aged *Pgc-1β*$^{-/-}$ hearts displayed the greatest propensity to arrhythmia of all groups, in terms of proportion of hearts that were arrhythmic and the overall number of episodes of arrhythmia.

The electrophysiological alterations underlying the greater propensity to arrhythmia in *Pgc-1β*$^{-/-}$ hearts were examined with intracellular AP recordings from the left atrium, which suggested these occurred primarily through abnormalities in AP conduction. At the cellular level, young and aged *Pgc-1β*$^{-/-}$ hearts had significantly reduced $(dV/dt)_{max}$ values compared to WT hearts during regular pacing. There was no difference in $(dV/dt)_{max}$ based upon age in either group. A similar pattern was also observed in AP triggered by S2 stimuli during the PES protocol. As would be expected, $(dV/dt)_{max}$ values progressively reduced with shortening of the coupling interval in all groups. At the longest coupling intervals $(dV/dt)_{max}$ values differed between WT and *Pgc-1β*$^{-/-}$ hearts to similar extents as during 8 Hz pacing, whereas they converged to become indistinguishable at the shortest coupling intervals. Thus *Pgc-1β*$^{-/-}$ hearts demonstrated compromise at modest levels of stress represented by the longer coupling intervals, and correlated with their increased susceptibility to arrhythmia through greater parts of the protocol.

Reduced atrial conduction velocities have been reported as an early feature in patients with AF (Zheng *et al.*, 2016) and potentially play a significant role in providing a substrate for its maintenance in the long term (Park *et al.*, 2009; Miyamoto *et al.*, 2009). Values of $(dV/dt)_{max}$ are known to correlate with peak Na^+ currents (I_{Na}) (Hondeghem & Katzung, 1977) and conduction velocity in skeletal and cardiac cells (Usher-Smith *et al.*, 2006; Fraser *et al.*, 2011). Time-dependent reductions in I_{Na} and consequent reductions in atrial conduction velocity have previously been implicated in the pathogenesis in a canine model of AF (Gaspo *et al.*, 1997*a*). Furthermore SCN5A gene variants, which encodes the cardiac sodium channel

responsible for the inward Na^+ current, are associated with increased risk of developing AF (Olson *et al.*, 2005; Darbar *et al.*, 2008). Interestingly, mitochondrial dysfunction can alter I_{Na} through a number of potential mechanisms. Firstly reductions in I_{Na} in cardiomyocytes were observed in response to metabolic stress (Liu *et al.*, 2009) and could be recovered with application of the mitochondrial ROS scavenger mitoTEMPO (Liu *et al.*, 2010). Secondly, fluctuations in cytosolic [Ca^{2+}] could also potential modify sodium channel properties through binding in its C-terminal region, either directly at an EF hand motif (Wingo *et al.*, 2004) and indirectly through an IQ domain sensitive to calmodulin/calmodulin kinase II (Mori *et al.*, 2000)(Mori et al 2000). Elevated intracellular [Ca^{2+}] caused reductions in I_{Na} density and $(dV/dt)_{max}$ in cardiomyocytes in vitro (Casini *et al.*, 2009), and in whole hearts following diastolic Ca^{2+} leaks, through application of caffeine (Zhang *et al.*, 2009*b*), known to increase diastolic Ca^{2+} release, or mutations associated with diastolic Ca^{2+} release (King *et al.*, 2013*c*; Li *et al.*, 2014; Glukhov *et al.*, 2015). Abnormal diastolic Ca^{2+} transients have been recorded in cardiomyocytes in *Pgc-1β*$^{-/-}$ hearts (Gurung *et al.*, 2011).

The conduction of an AP wavefront through tissue is influenced by the membrane capacitance and its resistance, in addition to $(dV/dt)_{max}$ (Jeevaratnam *et al.*, 2011; King *et al.*, 2013*a*). Conduction was therefore further assessed through evaluation of AP latency times. These were significantly prolonged in *Pgc-1β*$^{-/-}$ hearts compared to WT during regular pacing, with young WT hearts having significantly shorter AP latency durations than any other experimental group including aged WT hearts. During PES pacing, AP latency times increased with shortening of the S1-S2 coupling interval in all groups, but with differing magnitudes. Conduction slowing was most pronounced in *Pgc-1β*$^{-/-}$ hearts, particularly aged *Pgc-1β*$^{-/-}$ hearts, at the shorter coupling intervals correlating with their greater vulnerability to arrhythmia during the PES protocols. The differing comparisons of $(dV/dt)_{max}$ and AP latency between groups were further explored by evaluating the dependency of AP latency upon $(dV/dt)_{max}$ within groups. In all cases AP latency lengthened with reductions in $(dV/dt)_{max}$, in keeping with the known relationship between $(dV/dt)_{max}$, I_{Na} and conduction velocity (Hunter *et al.*, 1975). However young and aged WT hearts displayed distinct relationships between AP latency and $(dV/dt)_{max}$, with age-related delays in latency observed at any given $(dV/dt)_{max}$ value. In contrast this correlation was indistinguishable between young and aged *Pgc-1β*$^{-/-}$ hearts, where both resembled the conduction slowing seen with ageing in WT hearts.

Myocardial fibrosis is associated with increased tissue capacitance and resistance, contributing to conduction slowing independent of the influence of $(dV/dt)_{max}$ and may explain the conduction properties described in the present study. Fibrotic change is thought to be a key element of the remodelling seen in AF (Frustaci *et al.*, 1997; Kostin *et al.*, 2002). Progressive fibrosis is a common feature of cardiac ageing in animal (Eghbali *et al.*, 1989; Orlandi *et al.*, 2004; Lin *et al.*, 2008; Jeevaratnam *et al.*, 2012) and human (Gazoti Debessa *et al.*, 2001) studies.

A pro-arrhythmic substrate can also develop through altered repolarisation properties including reductions in the APD or shortening of the atrial ERP. Reductions in APD have been documented in AF and were also seen in the present study, consistent with the previously reported effect of mitochondrial dysfunction upon AP repolarisation properties (Brown & O'Rourke, 2010). However these were witnessed in aged *Pgc-1β*$^{-/-}$ hearts and most pronounced at shorter S1-S2 coupling intervals in the PES protocol and would favour re-entry and arrhythmogenesis. These parameters pertaining to AP recovery can be combined with those of AP activation to give the AP wavelength, defined as the distance travelled by the depolarising wave over one refractory period (Allessie *et al.*, 1977). Shortening of the AP wavelength favours re-entry whereas its lengthening is thought to be protective (Davidenko *et al.*, 1995; Zaitsev *et al.*, 2000; Weiss *et al.*, 2005; Pandit & Jalife, 2013; Spector, 2013). AP wavelength was shorter in *Pgc-1β*$^{-/-}$ hearts than WT heart, both at circumstances mimicking resting heart rates and PES pacing. With reductions in the S1-S2 coupling interval, the shorter AP wavelengths in aged *Pgc-1β*$^{-/-}$hearts persisted, whereas those for young *Pgc-1β*$^{-/-}$ hearts and WT hearts overlapped, correlating with the differing arrhythmic susceptibilities observed in the present study.

Finally, the influence of these electrophysiological parameters upon arrhythmia induction was examined in the first S2 AP that provoked an episode of AT in each heart. Interestingly $(dV/dt)_{max}$ values were higher for S2 beats triggering AT in *Pgc-1β*$^{-/-}$ hearts than WT hearts, however no difference was seen in AP latency times. Similarly, no difference in APD_{90} or AP wavelength were seen in S2 beats triggering arrhythmias in WT and *Pgc-1β*$^{-/-}$ hearts. This suggested critical electrophysiological thresholds common to all groups, below which the susceptibility to arrhythmias is increased. The differing parameters measured in the current experiments indicate these circumstances arise earlier through ageing and mitochondrial

dysfunction, thus widening the range of S1-S2 intervals at which the *Pgc-1β*$^{-/-}$ hearts were at risk of arrhythmia compared to WT hearts. Accordingly, the critical coupling intervals were longer in *Pgc-1β*$^{-/-}$ hearts compared to WT hearts, and in particular in aged *Pgc-1β*$^{-/-}$ hearts.

Together, the present experiments further previous work reporting enhanced susceptibility to ventricular arrhythmias secondary to a chronic mitochondrial deficit, demonstrating an atrial arrhythmic phenotype secondary to *Pgc-1β*$^{-/-}$ ablation. The arrhythmic substrate develops through maladaptive alterations in AP conduction and propagation through electrical changes at the cellular level and allude to possible structural changes at the tissue level.

5 Atrial restitution properties in incrementally paced murine *Pgc1β*$^{-/-}$ hearts

5.1 Introduction

Electrophysiological research has increasingly been concerned with unpicking the mechanisms that lead to atrial arrhythmogeneisis, with a number of key themes emerging as important factors in this regard. The impact of ageing on arrhythmogenesis is recognised to be profound. The prevalence of AF increases with age, from around 4% of individuals aged 60-70 years being affected, to nearly 20% of people aged 80 years and above (Zoni-Berisso *et al.*, 2014). The epidemiology of AF points to important cumulative effects of ageing on tissue, cellular and biochemical changes. Age related increase in fibrosis of cardiac tissue is a known cause of human cardiac conduction disease (Lenegre 1964; Lev, 1964). Atrial fibrosis and remodeling has been implicated as one of the driving forces behind the increased propensity for AF in human studies (Frustaci *et al.*, 1997; Kostin *et al.*, 2002). This parallels insights gained from murine studies which similarly showed increased fibrosis with increasing age (Hayashi *et al.*, 2002; Jeevaratnam *et al.*, 2012). In addition, changes in intracellular calcium handling occur with age leading to potentially pro arrhythmic changes (Froehlich *et al.*, 1978; Lakatta & Sollott, 2002). The abnormal calcium handling in a number of arrhythmic models has been linked to age-dependent process (Hatch *et al.*, 2011; Yang *et al.*, 2015).

An array of competing theories have taken hold to explain such arrhythmias. The fractionation of the propagating action potential wavefront into multiple smaller wavefronts which are more likely to follow local tissue heterogeneities (both structural and functional) and thus lead to self-perpetuating chaotic excitation pathways has been the dominant paradigm. Closely related to this is the APD restitution theory, which predicts the occurrence of a particular oscillatory electrophysiological phenomenon known as alternans. This theorises a critical pacing frequency (given by DI_{crit}) at which alternans becomes unstable through a feedback loop. Alternans in APD is thought to contribute to arrhythmic substrate by allowing regional heterogeneities in adjacent areas of myocardium.

Restitution analysis has been a mainstay of arrhythmic theory for ventricular tachycardia and fibrillation. Mathematical modelling has shown that in models displaying APD restitution slopes greater than unity, spiral waves are unstable and spontaneously degenerate into multiple wavelets (Garfinkel *et al.*, 2000; Qu *et al.*, 2000). Experimental studies have demonstrated that steep restitution slopes contribute to oscillations in APD and the maintenance of ventricular arrhythmias (Riccio *et al.*, 1999). However the role of APD restitution in atrial arrhythmias has been subject to relatively little investigation. Previous work has suggested steeper APD restitution slopes in patients with atrial fibrillation than controls however the role of alternans was not examined (Kim *et al.*, 2002). Further in a vagally mediated canine model of AF, the arrhythmia was associated with a suppression of APD alternans (Lu *et al.*, 2011).

The experiments in this chapter complement previous reports in murine hearts carrying genetic abnormalities in specific ion channels modelling ventricular arrhythmic conditions (Huang, 2017). The arrhythmic substrate in these different exemplars was variously identified with altered AP initiation and conduction (Martin *et al.*, 2011*b*; Ning *et al.*, 2016), AP recovery (Sabir *et al.*, 2007*b*) and arrhythmic triggers (Thomas *et al.*, 2007; Goddard *et al.*, 2008). The present experiments similarly investigated for the presence of arrhythmic phenotypes provoked by the imposition of extrasystolic S2 stimuli at differing S1S2 intervals following trains of regular S1 pacing as well as steady-state pacing at progressively decreased basic cycle lengths. The findings were then matched to results from simultaneous determinations of AP activation and recovery, as well as temporal instabilities in the form of AP alternans (Matthews *et al.*, 2010), APD-diastolic interval (DI) restitution relationships (Kim *et al.*, 2002; Matthews *et al.*, 2012), and spatiotemporal indicators of AP wavelength. The results presented represent the first report of such measurements in murine atria.

5.2 Specific methods

5.2.1 Experimental Animals

Four experimental groups were studied: young WT (n=20), young *Pgc-1β*$^{-/-}$ (n=23), aged WT (n = 22) and aged *Pgc-1β*$^{-/-}$ (n = 22). All young mice were aged between 12-16 weeks and aged mice greater than 52 weeks.

5.2.2 *Pacing protocols*

Hearts were stimulated at an amplitude of twice diastolic threshold voltage plus 0.5 mV. Hearts underwent two separate pacing protocols during each experiment. First, a standardised S1S2 protocol was used to determine the atrial effective refractory period (AERP) from the ECG recordings. This delivered successive trains of eight, S1, stimuli separated by an interval of 125 ms, followed by a solitary extra-systolic stimulus (S2) initially delivered 89 ms after the preceding S1 stimulus. This pattern of stimulation was repeated with the S1S2 interval decremented by 1 ms for each successive cycle until failure of stimulus capture. Incremental pacing protocols then began after achieving stable microelectrode impalement. These consisted of cycles of regular pacing each of 100 stimulations. They began with a basic cycle length (BCL) of 130 ms that was then decremented by 5 ms for each subsequent cycle. These were repeated until the heart entered into 2:1 block or sustained arrhythmia.

5.2.3 *Statistical analysis*

Data captured by the Spike2 software package (Cambridge Electronic Design) was analysed using a custom written program using the python programming language. Alternans was defined as an occurrence of alternating beat to beat changes in the value of a parameter such that the direction of the change oscillates for at least twelve successive action potentials. Statistical analysis was carried out using the R programming language (R Core Team, 2015) and plots with the grammar of graphics package. All data is expressed as mean ± standard error of mean (SEM) and a p value of less than 0.05 taken to be significant. Different experimental groups were compared with a two-factor analysis of variance (ANOVA). F values that were significant for interactive effects prompted post-hoc testing with Tukey honest significant difference testing. If single comparisons were made, a two-tailed student's t-test was used to compare significance. Categorical variables were compared using Fisher's exact test. Kaplan Meier estimates were compared with the log rank test.

5.3 Results

5.3.1 Aged Pgc-1β$^{-/-}$ hearts develop a pro-arrhythmic phenotype

Electrocardiographic (ECG) recordings were first made through the S1S2 protocol. Extrasystolic (S2) stimuli were interposed at successively shorter intervals following trains of 8 regular (S1) stimuli applied at a 125 ms basic cycle length (BCL). This explored for the presence, and the frequency, of arrhythmic phenotypes in the intact ex-vivo Langendorff-perfused hearts. Figure 1 shows typical ECG recordings from aged *Pgc1β*$^{-/-}$ hearts at a slow time base during a S1S2 stimulation protocol. These include episodes of premature atrial complexes following successive S2 stimuli and a short run of atrial tachycardia captured during a typical stimulus train at the end of an S1S2 protocol (Figure 5.1A). On an expanded time base, these could be characterized by spontaneous atrial P waves (dotted arrow) in contrast to the paced P waves (continuous downward pointing arrows) following imposed pacing spikes (Figure 5.1B, arrowed) between successive ventricular complexes (upward pointing arrows). Some protocols also elicited runs of atrial tachycardia (Figure 5.1C). The S1S2 interval at the onset of failure of stimulus capture made it possible to determine the atrial effective refractory periods (ERP) corresponding to the specific (8 Hz) pacing rate. A comparison of atrial ERPs obtained from the S1S2 protocol in young WT (24.8 ± 1.3 ms), aged WT (28.8 ± 1.3 ms), young *Pgc-1β*$^{-/-}$ (29.3 ± 0.8 ms) and aged *Pgc-1β*$^{-/-}$ hearts (30.1 ± 1.9 ms), demonstrated no significant differences between groups, and provided indications of the extent to which BCLs could be decreased in the succeeding incremental pacing experiments.

Simultaneous whole heart ECG recordings and intracellular action potential (AP) measurements from single cardiomyocytes were then performed after achieving stable microelectrode impalements, with consistent stimulating and recording electrode positions. The intracellular AP recordings provided accurate measurements of AP characteristics related to AP initiation, activation, and recovery. These included maximum AP upstroke rates $(dV/dt)_{max}$, AP latencies corresponding to the interval separating the pacing spike and the AP peak, AP durations at 90% recovery (APD_{90}), and resting membrane potentials (RMP). The measurements of $(dV/dt)_{max}$ and RMPs would not have been available with the monophasic-action potential electrode methods used on previous occasions (Sabir *et al.*, 2007*a*, 2008*b*). The incremental pacing protocols applied cycles of 100 regular pacing stimuli at successively

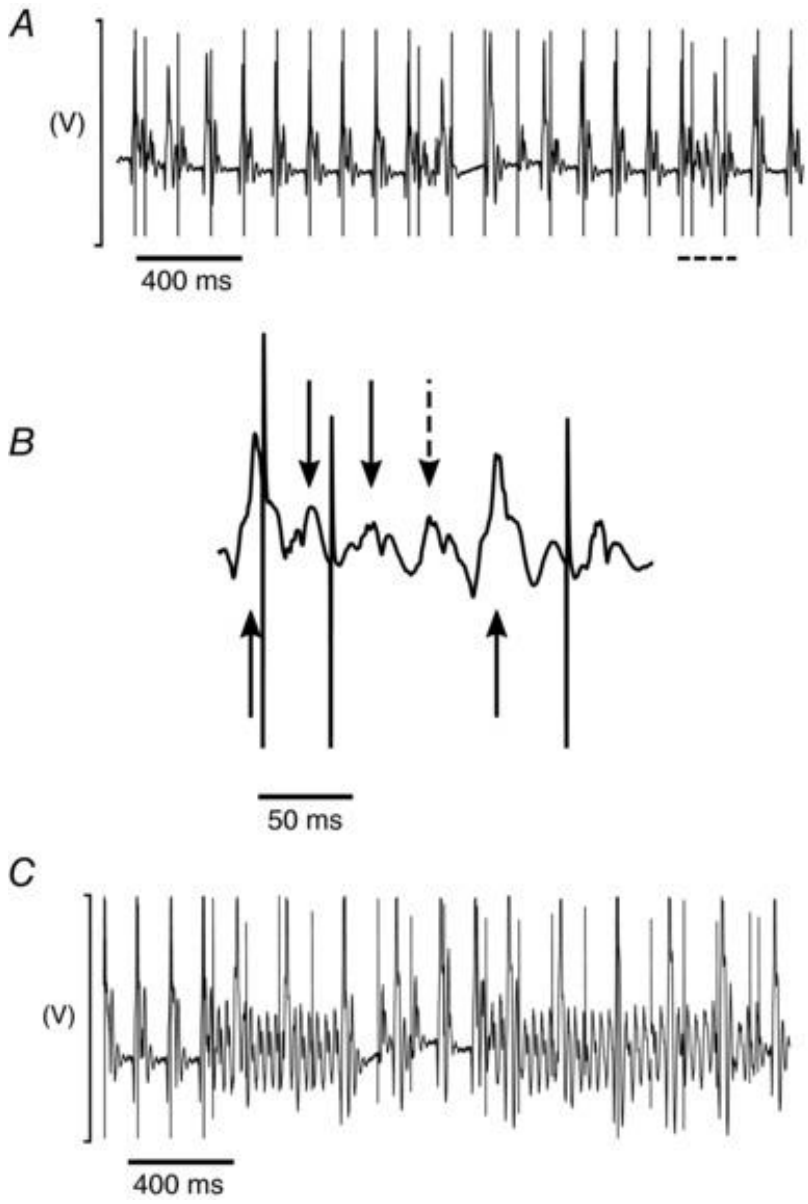

Figure 5.1 Volume conducted ECG recordings

Typical ECG recordings from S1-S2 protocols demonstrating premature atrial complexes (A), dashed section visualized in (B) with an expanded timebase. Solid downward pointing arrows denote atrial complexes as a result of stimulation, the dashed arrow indicates a premature atria complex with no preceding stimulation spike. Solid upward pointing arrows denote ventricular complexes. Panel (C) illustrates atrial tachycardia in response to an S2 stimulus.

decremented BCLs. Figure 5.2 illustrates results of the subsequent incremental pacing procedure comparing ECG (i) and intracellular traces (ii) under conditions of regular activity (A), and occurrences of premature atrial complexes (Figure 5.2B), atrial fibrillation (Figure 5.2C) and APD_{90} alternans (Figure 5.2D) in an aged *Pgc1β*$^{-/-}$ heart. Individual hearts subjected to incremental pacing could therefore display phenotypes that differed from the results of extrasystolic (S2) stimuli.

The cycles of incremental pacing continued with decreasing BCLs until the onset of either 2:1 capture or arrhythmia was reached. Kaplan Meier curves plotting the probability of 1:1 capture of the groups as a function of BCL (Figure 5.3) demonstrated a progressive reduction in the number of hearts continuing to show 1:1 capture at BCLs shorter than ~70 ms. This would reflect their refractory properties at the steady state pacing frequencies close to this cutoff. The statistical analysis to follow will therefore analyse data for parameters at BCLs no shorter than around 50 ms. A log rank test confirmed that the survival curves were in fact significantly different ($p = 0.0028$). Young WT hearts showed fall-offs at shorter BCLs than in the remaining groups and thus could be paced at higher frequencies than the other hearts, including aged WT hearts.

Table 5.1 summarizes the incidences of arrhythmic phenomena, whether in the form of atrial tachycardia or ectopic atrial deflections, through both pulse protocols. These together suggested a more marked pro-arrhythmic phenotype in aged *Pgc-1β*$^{-/-}$ hearts than in the remaining groups. With the S1S2 pulse protocol, the incidence of ectopic deflections were similar between groups, but those of atrial tachycardia were greater in aged *Pgc-1β*$^{-/-}$ hearts than in young WT, aged WT or young *Pgc-1β*$^{-/-}$ hearts, which all showed similar incidences of atrial tachycardia ($p = 0.043$). Hearts displaying arrhythmias with extra systolic (S2) provocation often failed to show arrhythmias on incremental pacing, and a relatively small number (3) of hearts showed arrhythmia amongst the experimental groups. The incremental pacing protocol thus resulted in few incidences of atrial tachycardia. Nevertheless, incidences of ectopic deflections were then greater in aged *Pgc-1β*$^{-/-}$ hearts than in young WT, aged WT and young *Pgc-1β*$^{-/-}$ hearts ($p = 0.041$).

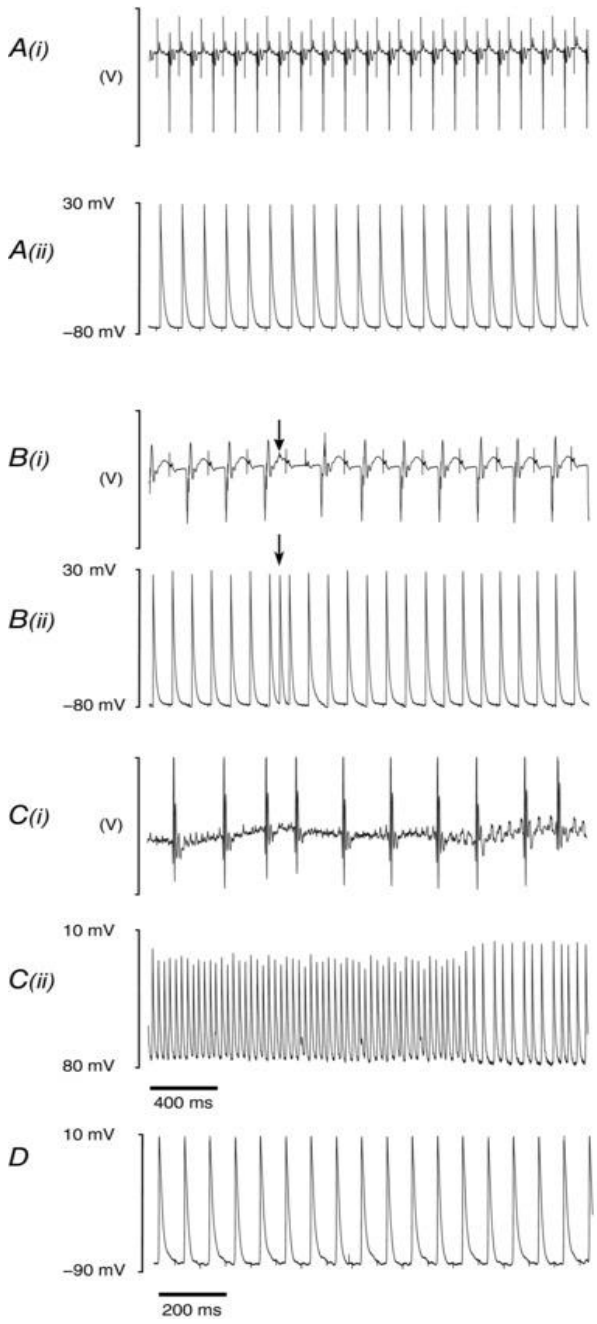

Figure 5.2 ECG and AP recording during incremental pacing

Typical recordings from incremental pacing protocols illustrating steady state (A) ECG recordings (i) from a WT heart as well as the corresponding intracellular AP recordings (ii). Ectopic activity (arrow) from an aged Pgc-1β$^{-/-}$ heart is shown in panel (B), with the corresponding ECG (i) and intracellular AP recordings (ii). Evidence of AF (C) in the ECG (i) recording of an aged Pgc-1β$^{-/-}$ heart with concurrent intracellular AP recording (ii). Panel (D) illustrates APD alternans in an AP recording from a young WT heart.

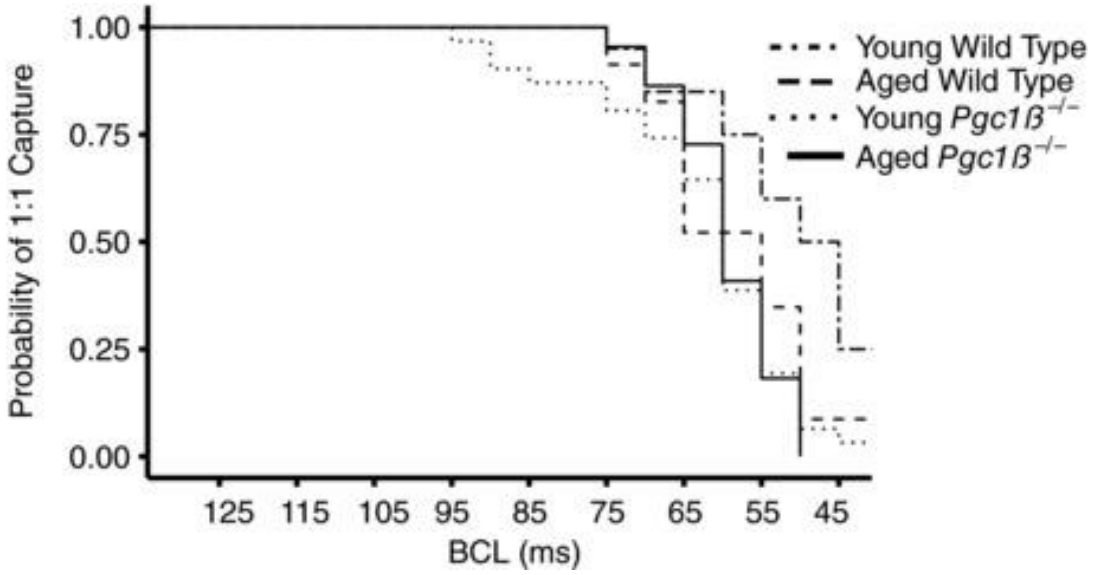

Figure 5.3 Kaplan Meier plot of stimulus capture during incremental pacing

Kaplan Meier plot of probability of 1:1 capture as BCL is varied for each experimental group.

Table 5.1 Incidences of atrial arrhythmic events during programmed electrical stimulation and incremental pacing in young and aged, WT and *Pgc-1β*$^{-/-}$ hearts.

Experimental Group	S1S2 protocol		Incremental pacing	
	Atrial tachycardia	Ectopic events	Atrial tachycardia	Ectopic events
Young WT	3/20	8/20	0/20	2/20
Aged WT	4/23	8/23	1/23	4/23
Young *Pgc-1β*$^{-/-}$	5/23	13/23	1/23	4/23
Aged *Pgc-1β*$^{-/-}$	11/22 *	8/22	1/22	10/22 *

Data represented as arrhythmic over total number studied.* denotes $p < 0.05$ on Fisher exact testing.

5.3.2 *Altered atrial AP characteristics in young and aged Pgc-1β$^{-/-}$ hearts*

Figure 5.4 summarises the activation and recovery characteristics of APs obtained through the incremental pacing procedures. It illustrates the corresponding alterations in maximum rates of AP depolarization, $(dV/dt)_{max}$ (Figure 5.4A), AP latencies (Figure 5.4B), APD_{90} (Figure 5.4C), resting membrane potentials RMP (Figure 5.4D) and diastolic intervals, DI_{90}, (Figure 5.4E) with alterations in BCL in young and aged, *Pgc-1β*$^{-/-}$ and WT, hearts. These parameters varied approximately linearly with BCL, and their overall magnitudes could be compared by the areas beneath their curves (see Table 5.2 for values). The *Pgc-1β*$^{-/-}$ hearts displayed decreased $(dV/dt)_{max}$ ($p = 0.000020$) and lower APD_{90} values ($p = 0.00018$) compared to WT hearts; there were no variations in RMP between groups. Genotype and age exerted significant interacting effects on DI_{90} and AP latency values ($p = 0.0081$, $p = 0.043$ respectively). Post hoc tests did not reveal further statistically significant differences.

5.3.3 *Reduced temporal heterogeneities in atrial AP characteristics in aged Pgc-1β$^{-/-}$ hearts*

Instabilities in characteristics of successive APs, often taking the form of episodes of alternans, presage major ventricular arrhythmias in clinical situations. They have been described under experimental conditions as alternating variations in temporal properties of AP excitation and/or recovery that occur with varying heart rates in analyses of pro-arrhythmic tendencies associated with ventricular arrhythmogenesis (Sabir *et al.*, 2007*a*, 2008*b*). We sought to analyse whether such phenomena are important in atrial arrhythmogenesis. Figure 5.5 summarises the incidences of such alternans in the activation parameters $(dV/dt)_{max}$ (Figure 5.5A) and AP latency (Figure 5.5B) and the recovery parameters APD_{90} (Figure 5.5C) and RMP (Figure 5.5D) in young and aged WT and *Pgc-1β*$^{-/-}$ hearts through the incremental pacing protocol. Overall incidences of alternans were assessed by summing the individual incidence of alternans at each BCL. The different groups showed similar distributions in the occurrence of alternans at different BCLs. However, statistical comparisons of the overall incidences of alternans throughout the entire range of BCLs indicated that *Pgc-1β*$^{-/-}$ hearts have *reduced* incidences and durations of alternans episodes.

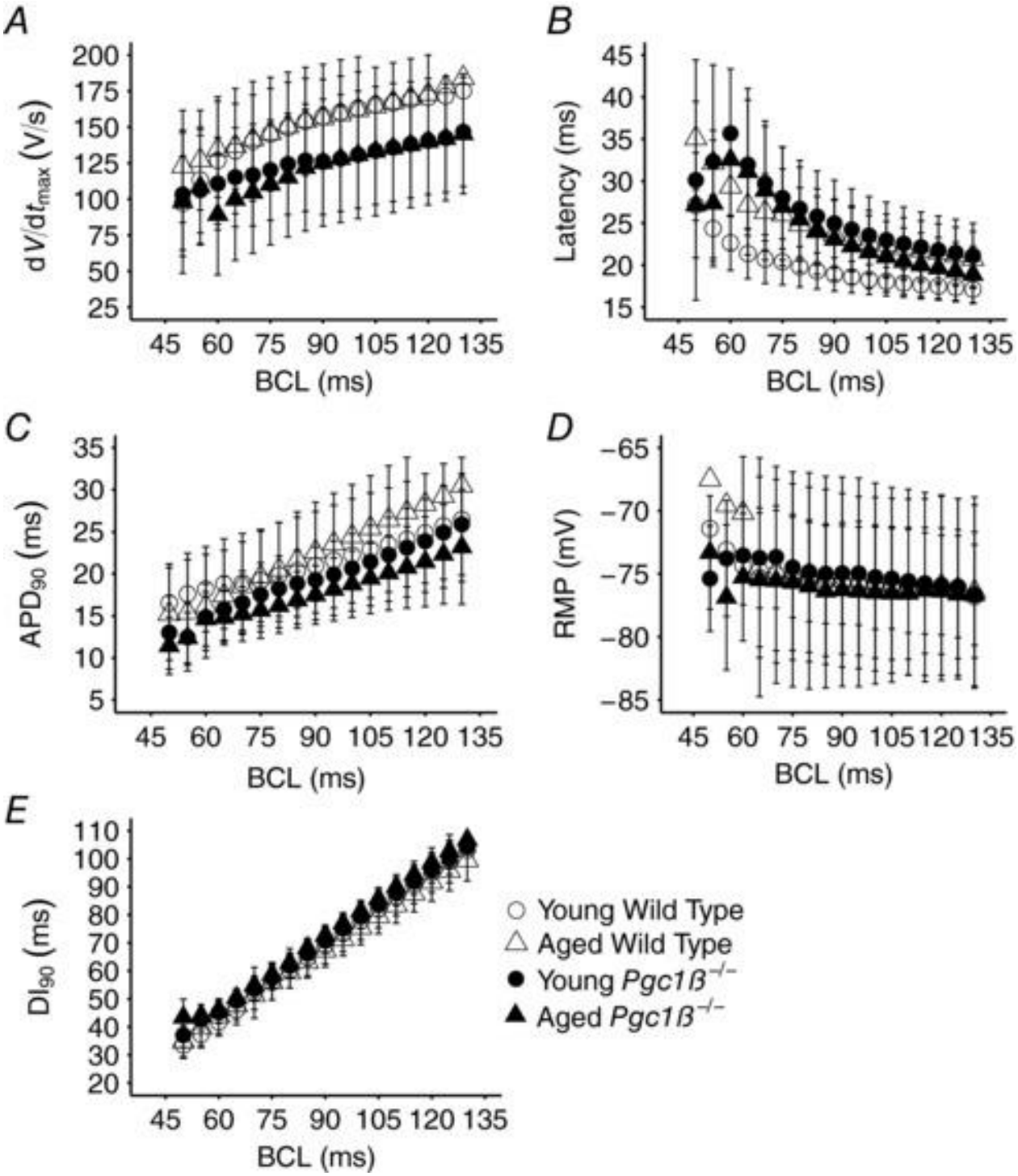

Figure 5.4 Action potential parameters during incremental pacing

Dependence of maximum rate of AP depolarization, $(dV/dt)_{max}$ (A), AP latency (B), APD_{90} (C), RMP (D) and DI (E) on BCL in young and aged, WT and Pgc-1β$^{-/-}$ hearts.

Table 5.2 Areas under the curves (AUC) of AP parameter with respect to BCL

Parameter	WT	Young WT	Aged WT	*Pgc-1β*$^{-/-}$	Young *Pgc-1β*$^{-/-}$	Aged *Pgc-1β*$^{-/-}$	Young	Aged
$(dV/dt)_{max}$ (mV)	11765.1 ± 397.27****	12049.22 ± 631.58	11518.04 ± 507.71	8979.36 ± 449.38****	8945.29 ± 602.9	9027.37 ± 687.57	10162.52 ± 487.79	10300.38 ± 459.79
APD_{90} (ms^2)	1702.79 ± 76.83†††	1703.66 ± 120.15	1702.03 ± 101.14	1364.53 ± 46.13†††	1396.49 ± 65.47	1319.49 ± 62.44	1516.95 ± 64.53	1515.01 ± 65.99
DI_{90} (ms^2)	5292.48 ± 93.69ǁǁ	5486.3 ± 133.32	5123.95 ± 123.32	5300.77 ± 91.07ǁǁ	5160.93 ± 133.86	5497.81 ± 101.23	5288.52 ± 98.43ǁǁ	5306.73 ± 84.09ǁǁ
AP Latency	1721.39 ± 57.76‡	1638.49 ± 71.15	1793.47 ± 87.15	1831.90 ± 51.02‡	1890.34 ± 78.40	1753.00 ± 53.72	1779.43 ± 55.85‡	1774.65 ± 52.39‡
RMP (mV)	-5374.7 ± 96.19	-5492.91 ± 159.87	-5271.93 ± 113.12	5226.35 ± 111.51	-5075.36 ± 166.85	-5439.1 ± 120.22	-5239.11 ± 121.62	-5353.66 ± 82.47

Each symbol represents statistical results from ANOVA; **** and ††† denote $p < 0.0001$ and < 0.001 respectively for independent effects of genotype; ǁǁ and ‡ denote $P<0.01$ and <0.05 for interacting effects of genotype and age respectively.

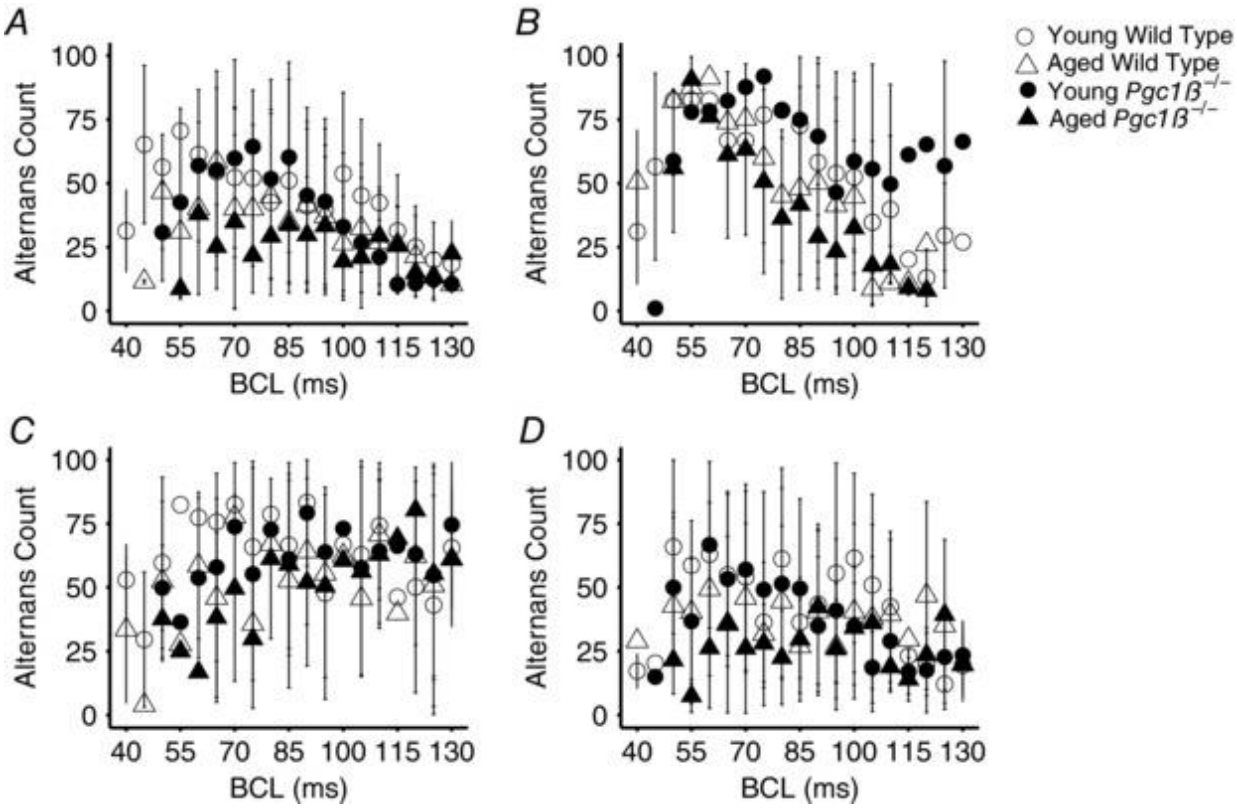

Figure 5.5 Incidence of alternans in AP variables during incremental pacing

Incidence of alternans out of 100 beats at each BCL in the activation variables of maximal rate of AP depolarization, dV/dt_{max} (A) and AP latency (B), and the recovery variables of APD_{90} (C) and RMP (D) in young WT (open circles), young Pgc1β $^{-/-}$ (filled circles), old WT (open triangles) and Pgc1β $^{-/-}$ hearts (filled triangles). Number of replicates: young WT, n = 20; young Pgc1β $^{-/-}$, n = 23; aged WT, n = 22; and aged Pgc1β $^{-/-}$, n = 22.

There were no significant effects of genotype on ***incidence*** of alternans in $(dV/dt)_{max}$, APD_{90}, AP latency or RMP. Ageing independently *reduced* the incidence of alternans in aged compared to young hearts ($(dV/dt)_{max}$: 24 ± 3 beats vs 39 ± 3 beats ; p = 0.0013; APD_{90}: 37 ± 3 beats vs. 50 ± 3 beats; p = 0.0051; AP latency: 53 ± 3 beats vs. 68 ± 3 beats; p = 0.00045; RMP: 30± 2 beats vs. 40 ± 2 beats; p = 0.0011). Age and genotype exerted interacting effects on the incidence of AP latency alternans (p = 0.032). Post hoc testing demonstrated *less* AP latency alternans in aged than young *Pgc-1β*$^{-/-}$ hearts (47 ± 5 beats vs. 71 ± 3 beats, p = 0.00041) and in aged *Pgc-1β* $^{-/-}$ than young WT hearts (47 ± 5 beats 64 ± 5 beats, p = 0.036).

Similarly, the ***magnitude*** of $(dV/dt)_{max}$, APD_{90} and RMP (though not AP latency) alternans, reflected in the areas under the respective curves, was *smaller* in aged than young hearts (p =

0.037, p = 0.038, p = 0.052 and p = 0.066 respectively) (Figure 5.6). There were no effects of genotype or interacting effects of genotype and age together on the overall magnitudes of oscillation. The ***total number of episodes*** of APD_{90}, AP latency or RMP alternans were indistinguishable between groups, whilst *Pgc-1β*$^{-/-}$ hearts showed *fewer* episodes of $(dV/dt)_{max}$ alternans than WT hearts (8.54 ± 0.75 vs 13.37 ±1.47 episodes of alternans; p = 0.0021) and aged hearts *fewer* episodes of $(dV/dt)_{max}$ alternans than young hearts (9.24 ± 1.13 vs 12 ± 1.14 episodes of alternans; p = 0.030).

Maximum durations of individual episodes of $(dV/dt)_{max}$, AP latency, APD_{90} or RMP alternans were all *shorter* in aged than young hearts ($(dV/dt)_{max}$: 44 ± 10 beats vs 139 ± 27 beats, p = 0.0015; AP latency: 140 ± 19 beats vs 352 ± 28, p = 2.7×10^{-8}; APD_{90}: 247 ± 49 beats vs 390 ± 60 beats, p = 0.049; RMP: 64 ± 10 beats vs. 136 ± 20 beats, p = 0.0011). Although they were affected by interacting effects of age and genotype (p = 0.036), post hoc testing demonstrated that these maximum durations were *shorter* in both aged *Pgc-1β*$^{-/-}$ and aged WT hearts than young *Pgc-1β*$^{-/-}$ hearts (98 ± 17 beats vs 379 ± 35 beats, p < 0.00001 and 180 ±32 beats vs. 379 ± 35 beats, p = 0.00029 respectively). Furthermore, aged *Pgc-1β*$^{-/-}$ hearts also showed *shorter* maximum durations of AP latency alternans than young WT hearts (98 ± 17 beats vs. 311 ± 47 beats, p = 0.00061).

Finally, ***alternans simultaneously involving different AP characteristics*** could involve alternating high/low AP latencies or reduced/increased $(dV/dt)_{max}$ coinciding with or, in the more pro-arrhythmic pattern, occurring out of phase with higher/lower APD_{90} values. However, *reduced* frequencies of simultaneous $(dV/dt)_{max}$ and APD_{90} alternans occurred in aged compared to young hearts (14.91 ± 2.42% vs. 27.74 ± 3.03%; p = 0.00043) and *Pgc-1β*$^{-/-}$ compared to WT hearts (17.77 ± 2.57% vs. 26.59 ± 3.23%, p = 0.024). *Reduced* and *similar* proportions of out of phase alternans occurred in *Pgc-1β*$^{-/-}$ hearts compared to WT hearts (7.83 ± 1.39% vx 19.30 ± 4.63%; p = 0.010), and aged compared to young hearts respectively (p = 0.070). Similarly, *reduced* frequencies of simultaneous APD_{90} and AP latency alternans occurred in aged compared to young hearts (25.67 ± 2.48% vs. 45.53 ± 2.43%; p = 0.082×10^{-5}) which showed fewer beats of the more pro-arrhythmic alternans pattern (132 ± 23 beats vs. 334 ± 40 beats; p = 0.00017).

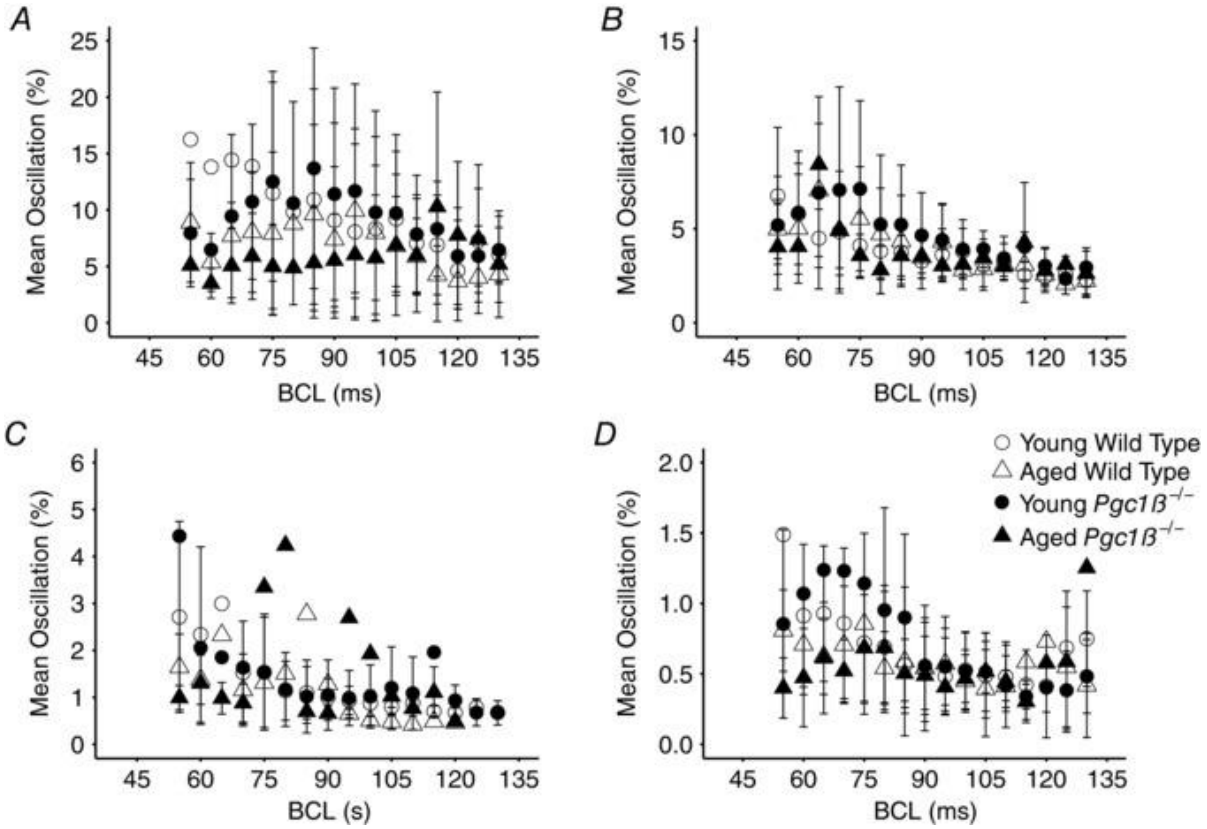

Figure 5.6 Magnitude of alternans in AP variables during incremental pacing

Magnitude of alternans as a percentage of the previous beat at each BCL for $(dV/dt)_{max}$ (A), AP latency (B), APD_{90} (C) and RMP (D)

5.3.4 Spatiotemporal representations of AP excitation in Pgc-1β$^{-/-}$ and WT hearts

Previous reports in murine hearts have correlated AP recovery properties at different BCLs with the presence of instabilities in the form of alternans. Restitution curves displaying dependences of APD_{90} upon BCL or upon diastolic intervals (DI_{90}) from 90% action potential recovery (Sabir *et al.*, 2008*c*, 2008*b*) were analysed. They had shown that the onsets of pro-arrhythmic instabilities were associated with increasing limiting slopes in plots of APD_{90} against DI_{90} with shortening DI_{90} (Matthews *et al.*, 2012). It was further demonstrated that a unity gradient in such plots was associated with waxing patterns of alternans in AP properties presaging the onset of arrhythmia. Figure 5.7 demonstrates consistently shorter APD_{90} in *Pgc1β*$^{-/-}$ hearts, particularly aged *Pgc1β*$^{-/-}$ hearts, compared to either young or aged WT hearts across the full range of DI_{90}. It is also apparent that the limiting slopes in Figure 5.7A are similar for all groups, or slightly reduced in *Pgc1β*$^{-/-}$ hearts compared to WT hearts. Statistical

analysis of the respective restitution curves implicated neither genotype (two-way ANOVA: $p = 0.12$) nor age ($p = 0.15$) in independently influencing these limiting slopes. These factors did interact ($p = 0.0001$), but this gave reduced slopes in aged *Pgc1β*$^{-/-}$ atria (Tukey's tests: aged *Pgc1β* $^{-/-}$ *versus* aged WT, $p = 0.001$; aged WT *versus* young WT, $p = 0.001$), consistent with the observed paradoxically decreased incidences and durations of alternans in aged and *Pgc1β* $^{-/-}$ hearts and contrasting with their increased arrhythmogenic properties.

The electrophysiological abnormalities underlying the arrhythmic phenotypes observed in aged *Pgc1β*$^{-/-}$ hearts could be demonstrated using previously described spatial representations of action potential activation. The wavelength (λ) of the action potential travelling wave, derived from the product of conduction velocity (given by the inverse of AP latency) and APD (given by APD_{90}) was used in these analyses (Matthews *et al.*, 2013). We derived restitution plots from the dependence of wavelength upon either BCL (Figure 5.7B) or upon the resting wavelength (λ_0), which itself is derived from the DI_{90} and AP latency values (Figure 5.7C) (Matthews *et al.*, 2013*b*; Ning *et al.*, 2016). These were then compared in young and aged WT and *Pgc1β* $^{-/-}$ atria through the different BCLs examined. Areas under plots of λ against BCL (Figure 5.7*B*) then demonstrated that the *Pgc1β* $^{-/-}$ as opposed to the WT genotype, but not age, independently (two-way ANOVA: $p = 0.6 \times 10^{-4}$ and 0.14, respectively) reduced λ. Additional, interacting effects ($p = 0.048$) through the range of explored BCLs, were reflected in the shorter λ values in both young (Tukey's test: $p = 0.0001$) and aged *Pgc1β* $^{-/-}$ (Tukey's test: $p = 0.0008$) compared with young WT atria. Likewise, λ values from the experimental groups all declined and converged with declining λ_0 and with shortening BCL, as previously reported (Matthews et al., 2013; Ning et al., 2016) (Figure 5.7*C*). Nevertheless, λ values in aged *Pgc1β* $^{-/-}$ hearts consistently fell below those in remaining groups ($n = 14$ points, sign test, $p < 0.01$). Accordingly, areas beneath the curves reflected significantly greater λ at the longer (85-130 ms; two-way ANOVA: $p = 0.042$) but not the shorter (<85 ms) BCLs, resulting from interacting effects of age and *Pgc1β* $^{-/-}$ genotype (Matthews et al., 2013; Ning et al., 2016).

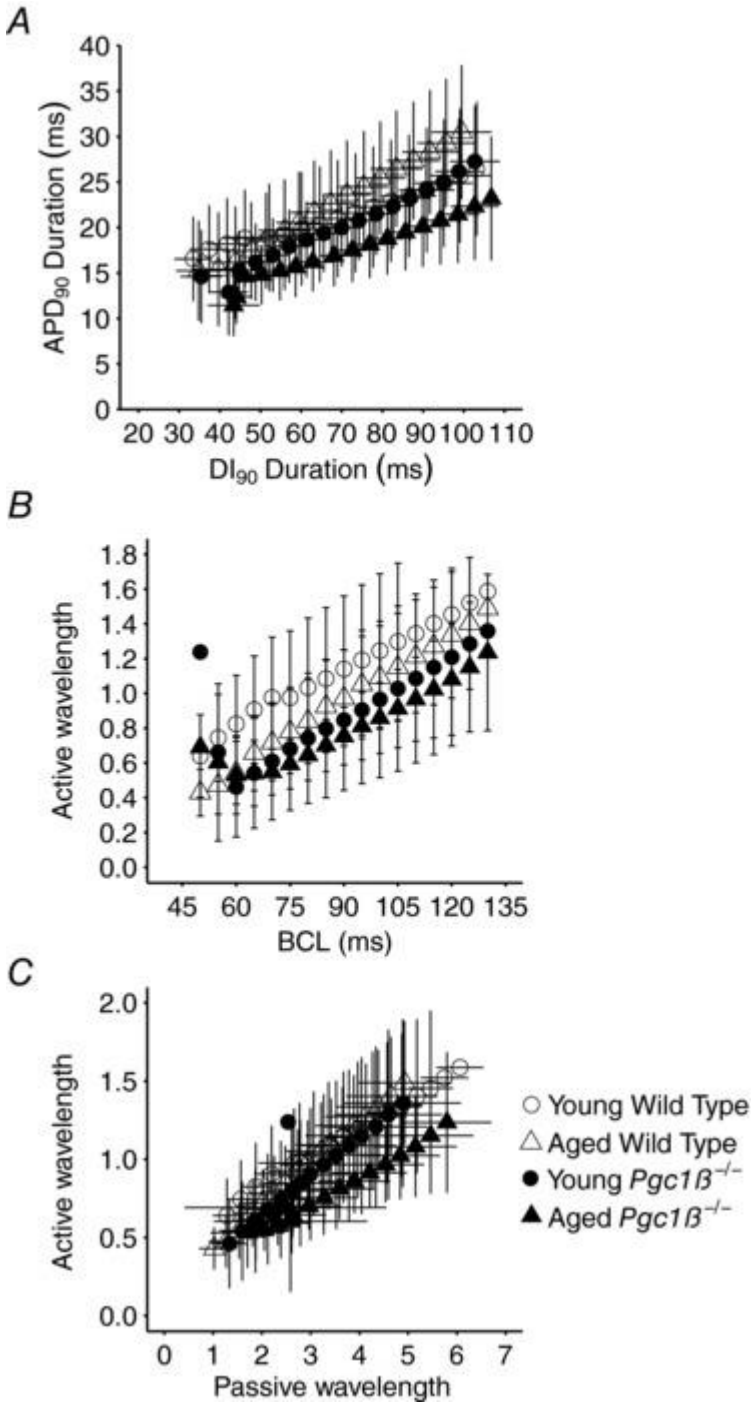

Figure 5.7 Restitution curves using APD and AP wavelength

Restitution plots of APD_{90} against DI_{90} (A) and of active AP wavelength (B) and passive wavelengths (C) observed at different BCLs through the incremental pacing procedure in young and old WT and Pgc-1β$^{-/-}$ hearts.

5.4 Discussion

Both age and energetic dysfunction are known risk factors for atrial fibrillation (Go *et al.*, 2001*a*; Menezes *et al.*, 2013*a*). The experimental basis for this effect was studied in young and aged peroxisome proliferator activated receptor-γ coactivator-1 (Pgc-1) deficient hearts used

in previous *biochemical* studies of mitochondrial dysfunction. *Pgc-1* upregulates mitochondrial function and cellular energy homeostasis (Lin *et al.*, 2005; Finck & Kelly, 2006), acting on genes participating in fatty acid oxidation and the electron transport chain (Arany *et al.*, 2005). Previous studies reported that in common with changes in ageing WT hearts (Froehlich *et al.*, 1978; Lakatta & Sollott, 2002; Hatch *et al.*, 2011; Yang *et al.*, 2015), isolated *Pgc-1β*$^{-/-}$ cardiomyocytes show compromised energetics, altered ionic current balances and abnormal Ca^{2+} homeostasis (Gurung *et al.*, 2011). The latter are associated with delayed after-depolarisation events potentially initiating pro-arrhythmic triggering activity. Intact perfused murine *Pgc-1β*$^{-/-}$ hearts show both compromised heart rate responses to adrenergic stimulation (Lelliott *et al.*, 2006), and pro-arrhythmic ventricular phenotypes (Gurung *et al.*, 2011).

Age and metabolic disorders may therefore exert interacting effects upon arrhythmic risk. The experiments in this chapter investigated the electrophysiological consequences of the cellular changes that accompany ageing and energetic disruption. This is the first study to use cellular electrophysiological recordings in intact hearts to determine steady state restitution properties of atrial tissue. These measurements were made in cardiomyocytes in situ in normally functioning intact Langendorff-perfused hearts as opposed to individual cells following cell isolation which are exposed to remarkably unphysiological conditions.

The experimental approach permitted simultaneous study of atrial arrhythmic properties of the whole heart and electrophysiological properties of single atrial cells. Aged *Pgc-1β*$^{-/-}$ hearts demonstrated a significantly greater incidence of arrhythmogenic phenotypes compared to all the remaining groups. The stimulation procedures that applied extrasystolic S2 stimuli resulted in a higher incidence of atrial tachycardias, while those applying incremental increases in steady heart rates resulted in a higher incidence of ectopic atrial events. The latter suggests atrial cardiomyocytes have a greater capacity for rapid pacing without producing pro-arrhythmic phenomena.

The association of the arrhythmic phenotype with alterations in the corresponding AP characteristics was then examined. Of the measured AP parameters, resting membrane potentials remained uniform throughout all experimental groups, consistent with clinical findings in atrial fibrillation (Bosch *et al.*, 1999). The statistically most noticeable alterations involved compromised AP activation which has been implicated in arrhythmic substrate on previous occasions (Huang *et al.*, 2012; King *et al.*, 2013*a*; Huang, 2017). Thus, *Pgc-1β*$^{-/-}$ atria

displayed decreased $(dV/dt)_{max}$ compared to WT atria, in an absence of statistical effects of age or interactions between age and genotype. $(dV/dt)_{max}$ correlates with peak Na^+ current, which in turn markedly influences AP conduction velocity to extents dependent upon conductivity between cells (Hunter *et al.*, 1975; Hondeghem & Katzung, 1977; Usher-Smith *et al.*, 2006; Fraser *et al.*, 2011). Although young and aged *Pgc-1β*$^{-/-}$ atria did not demonstrate significant differences in $(dV/dt)_{max}$, AP latency measurements reflecting conduction velocity were influenced by interactions between age and genotype. They therefore account for the more marked pro-arrhythmic phenotype in the aged than the young *Pgc-1β*$^{-/-}$ atria.

A hypothesis relating reduced $(dV/dt)_{max}$ and increased AP latency to decreased peak Na^+ current (Hondeghem & Katzung, 1977; Usher-Smith *et al.*, 2006; Fraser *et al.*, 2011) in the presence of age-dependent mitochondrial dysfunction in *Pgc-1β*$^{-/-}$ hearts is compatible with altered Na^+ channel function in related situations. Disruptions in normal mitochondrial activity are thought to be pro-arrhythmic through reduced provision of ATP and/or aberrant production of reactive oxygen species (ROS) (Manning *et al.*, 1984; Fosset *et al.*, 1988; Faivre & Findlay, 1990). Mitochondrial dysfunction resulting in excess ROS generation or perturbed cytosolic NAD^+/NADH, has been reported to alter Na^+ channel function in metabolically stressed cardiomyocytes (Liu *et al.*, 2009), which were rescued by the mitochondrial ROS scavenger mitoTEMPO (Liu *et al.*, 2010). In addition, abnormal diastolic Ca^{2+} transients have been reported in *Pgc-1β*$^{-/-}$ cardiomyocytes (Gurung *et al.*, 2011). The elevated cytosolic $[Ca^{2+}]$ could potentially modify sodium channel properties through Ca^{2+} binding to its C-terminal region, either directly at an EF hand motif (Wingo *et al.*, 2004) and indirectly through an IQ domain sensitive to calmodulin/calmodulin kinase II (Mori *et al.*, 2000). Acute elevations of intracellular $[Ca^{2+}]$ are known to reduce Na^+ current density and $(dV/dt)_{max}$ in cardiomyocytes in vitro (Casini *et al.*, 2009). The effect is also seen in whole hearts exposed to caffeine which is known to increase diastolic Ca^{2+} release (Zhang *et al.*, 2009*b*), or hearts carrying the RyR2-P2328S/P2328S mutations associated with diastolic Ca^{2+} release (King *et al.*, 2013*c*; Zhang *et al.*, 2013; Li *et al.*, 2014; Ning *et al.*, 2016). These situations lead to pro-arrhythmic effects not dissimilar to those reported with primary sodium channel Nav1.5 channel deficiencies reported on earlier occasions (Martin *et al.*, 2012*a*).

The electrophysiological alterations of atrial cardiomyocytes presented in this study led to investigations for arrhythmic substrate at the tissue level. However, alternans in AP

characteristics, a temporal manifestation of such substrate, did not appear to contribute to arrhythmic instability in the atria of aged *Pgc-1β*$^{-/-}$ hearts. Alternans did occur in atrial AP trains in the course of incremental steady state pacing. However, genotype did not influence the incidence of atrial alternans, and aged hearts showed *decreased* incidences of atrial alternans compared to young hearts. *Pgc-1β*$^{-/-}$ and aged hearts showed *fewer* alternans episodes than WT and young atria respectively. Restitution curves of APD_{90} against diastolic interval (DI_{90}) (Nolasco & Dahlen, 1968; Sabir *et al.*, 2008*b*; Matthews *et al.*, 2010, 2012) demonstrated *similar* or even slightly *reduced* limiting slopes, hitherto corresponding to an onset of unstable alternans in both young, and particularly aged *Pgc1β*$^{-/-}$ compared to either young or aged WT hearts. These findings parallel previous reports in the vagally induced model of canine AF that showed paradoxically less alternans than in the non-arrhythmic control state (Lu *et al.*, 2011) and a flatter restitution slope. This greater capacity for atrial cardiomyocytes for rapid pacing without producing pro-arrhythmic alternans phenomena was compatible with the observed shorter APDs in *Pgc1β*$^{-/-}$ atrial cardiomyocytes reflecting more rapid AP recoveries, despite the more prolonged activation processes.

Nevertheless, spatiotemporal properties derived from AP conduction, as opposed to restitution, were compatible with the greater pro-arrhythmic phenotype in aged *Pgc-1β*$^{-/-}$ hearts. AP wavelengths (λ) were derived from conduction velocity (reflected by 1/(AP latency)) and APD terms (given by APD_{90}) (Matthews *et al.*, 2013). These could be plotted against either BCL or resting wavelength, λ_0, made up of DI_{90} and AP latency terms (Matthews et al., 2013 a; Ning et al., 2016). *Pgc-1β*$^{-/-}$, particularly aged, *Pgc-1β*$^{-/-}$ atria gave consistently shorter λ at all BCLs and λ_0 in direct parallel with pro-arrhythmic phenotype, in agreement with the association between short AP wavelengths and AF inducibility and maintenance (Hwang *et al.*, 2015) particularly in AF patients (Padeletti *et al.*, 1995). They thus constitute a potential mechanism for the atrial arrhythmic changes associated with age and energetic compromise reported here.

6 Age-dependent remodelling in *Pgc-1β*$^{-/-}$ hearts

6.1 Introduction

The electrocardiographic studies in chapter 3 demonstrated age-dependent slowing of myocardial action potential conduction in *Pgc-1β*$^{-/-}$ hearts. The intracellular recording studies thereafter in chapters 4 and 5 corroborated these findings and highlighted age-dependent *atrial* arrhythmic phenotypes associated with the AP conduction abnormalities in intact Langendorff perfused *Pgc-1β*$^{-/-}$ hearts, agreeing with previous reports on their pro-arrhythmic *ventricular* phenotypes (Gurung *et al.*, 2011). The slowed conduction in *Pgc-1β*$^{-/-}$ atria was attributable to reduced maximum action potential upstroke rates, $(dV/dt)_{max}$, relative to those in WT. $(dV/dt)_{max}$ has been correlated with both peak Na^+ currents (I_{Na}), responsible for the rising, activation phase of the propagating AP and its conduction velocity in both skeletal and cardiac muscle cells (Usher-Smith *et al.*, 2006; Fraser *et al.*, 2011). Such young and aged, WT and *Pgc-1β*$^{-/-}$ atria contrastingly showed indistinguishable resting potentials, as maintained by outward K^+ currents.

These associations suggest hypotheses attributing pro-arrhythmic changes in *Pgc-1β*$^{-/-}$ atria to compromised Na^+ channel ($Na_V1.5$) function reducing voltage-dependent Na^+ currents. Previous evidence at the cellular as opposed to tissue levels had suggested that in addition to compromised ATP provision, disrupted cardiomyocyte mitochondrial activity increases reactive oxygen species (ROS) production (Fosset *et al.*, 1988; Faivre & Findlay, 1990) and perturbs cytosolic NAD^+/NADH, both implicated in I_{Na} reductions (Liu *et al.*, 2009), which can be rescued by the mitochondrial ROS scavenger mitoTEMPO (Liu *et al.*, 2010). In addition, recent studies reported altered Ca^{2+} homeostasis manifest as abnormal diastolic Ca^{2+} transients in *Pgc-1β*$^{-/-}$ cardiomyocytes (Gurung *et al.*, 2011). In addition to driving pro-arrhythmic triggering delayed after-depolarisations, such cytosolic $[Ca^{2+}]$ elevations could potentially modify $Na_V1.5$ properties through either direct or indirect Ca^{2+} actions at its C-terminal region (Mori *et al.*, 2000; Wingo *et al.*, 2004) or calmodulin kinase II-phosphorylatable sites in its DI-

II linker (Mori *et al.*, 2000; Wagner *et al.*, 2011; Grandi & Herren, 2014). Slowed AP conduction with reduced $(dV/dt)_{max}$ similarly associated with reduced I_{Na} have been reported in other pro-arrhythmic murine, *RyR2*-P2328S/P2328S, cardiomyocyte models similarly showing abnormal Ca^{2+} handling (Zhang *et al.*, 2013). This was attributed to both reduced expression (Ning *et al.*, 2016*b*) and acute effects of altered $[Ca^{2+}]_i$ upon. Nav1.5 function (King *et al.*, 2013*c*, 2013*b*).

The following experiments explored whether the observed pro-arrhythmic atrial phenotype in *Pgc-1β*$^{-/-}$ hearts is similarly accompanied by altered I_{Na}. The loose patch technique employed for voltage-clamping in intact, young and aged, WT and *Pgc-1β*$^{-/-}$, atrial cardiomyocytes apposes an electrode containing extracellular solution against intact cardiomyocyte surface membrane without accessing intracellular space. It therefore measures ion currents under conditions of unperturbed extracellular $[Na^+]$ and intracellular Ca^{2+} homeostasis (Almers *et al.*, 1983*b*; Stühmer *et al.*, 1983; King *et al.*, 2013*b*). This contrasts with the cardiomyocyte isolation and intracellular Ca^{2+} chelation required with conventional whole-cell patch clamp techniques (Lei *et al.*, 2005; Gurung *et al.*, 2011; Martin *et al.*, 2012*b*). Recent studies involving reversible manipulations of extracellular $[Na^+]$ had identified early inward currents in response to step depolarisations measured under loose patch with Na^+ currents responsible for AP conduction and the maximum upstroke rate, $(dV/dt)_{max}$, of the cardiac action potential (King *et al.*, 2013*b*). The present experiments assessed activation, inactivation, and recovery from inactivation of depolarising inward currents attributable to Nav1.5, comparing these with corresponding activation and rectification properties of repolarising outward K^+ currents.

Whereas $(dV/dt)_{max}$ primarily reflects discharge of the cardiomyocyte membrane capacitance by sodium current, AP conduction velocity is further influenced by increases or decreases in tissue resistance and capacitance (Jeevaratnam *et al.*, 2011; King *et al.*, 2013*a*). Previous reports had associated such conduction changes with progressive myocardial fibrosis with age in various animal (Eghbali *et al.*, 1989; Orlandi *et al.*, 2004; Lin *et al.*, 2008; Jeevaratnam *et al.*, 2012, 2016) and human studies (Gazoti Debessa *et al.*, 2001). Histological assessment from animal atrial tissue and from human samples indicate progressive fibrosis associated with AF (Wijffels et al., 1995; Morillo et al., 1995; Frustaci et al., 1997). WT and *Pgc-1β*$^{-/-}$ atria were therefore also evaluated for evidence of additional influence of fibrosis on the differences in AP propagation noted in the earlier experiments.

6.2 Specific methods

6.2.1 Loose patch clamp procedure

Loose patch clamping was performed as described in chapter 2. A total of 25 patches from male and 21 patches from female WT mice were studied, and likewise 24 patches from male and 17 patches from female *Pgc-1β*$^{-/-}$ hearts, but found no significant differences (P>0.05) between maximum Na^+ currents in preparations from male and female hearts. We accordingly grouped such data together when examining effects of the remaining factors of age and genotype.

Once established all patches were subject to the complete set of pulse procedures bearing on either inward or outward current activation, which could be accomplished within 30 s making effects arising from prolonged changes in the patch such as bleb formation unlikely (Milton & Caldwell, 1990). Patch consistency was monitored through repeat calibrations of leakage current, series resistance and pipette capacitance (Stühmer *et al.*, 1983). The loose patch clamp controls the voltage at the extracellular surface of the membrane within the seal in an intact cardiomyocyte. Accordingly, positive and negative voltage steps applied through the pipette respectively hyperpolarise and depolarise the membrane potential relative to the cardiomyocyte resting membrane potential (RMP). Voltage steps are therefore described in terms of the alterations they produce relative to the RMP, following the convention in earlier studies that introduced this technique (Almers et al., 1983a, 1983b).

6.2.2 Statistical analysis

Construction of current–voltage curves used values of current densities ($pA/\mu m^2$) obtained by normalizing the observed currents (nA) to the cross sectional area (πa^2) of the pipette tip radius a. Values in inactivation curves plotted observed maximum currents normalized to the maximum currents obtained at the most polarised holding potentials. Curve-fitting procedures of both plots against membrane potential used the curve fitting algorithm in the open source R programming language. Statistical analysis of results applied two-way analysis of variance (ANOVA) to the experimental groups of young and aged, WT and *Pgc-1β*$^{-/-}$ preparations to test for significant differences arising from independent or interacting effects

of age and/or genotype on fitted parameters. The presence of such differences was then explored by pairwise tests for differences using Tukey's honestly significant difference testing.

6.3 Results

Patches obtained following seal formation were subject to pulse protocols that could completely characterise the properties of either voltage dependent inward or outward currents, each within 30 s. This made the likelihood of effects due to rundown minimal. In any case, measured currents remained consistent, when protocols were repeated over longer time intervals (~15-20 min) in a number of control experiments. Finally, any given pulse protocol was always completed without altering the patch seal. This made differences between results attributable to changes in the patch over prolonged intervals such as bleb formation unlikely (Milton & Caldwell, 1990). As adopted in previous reports utilizing this technique, membrane potentials are expressed as voltage excursions relative to the RMP in the protocols illustrated in Figures 6.1-5 (Almers *et al.*, 1983*a*, 1983*b*). Thus the loose patch configuration differs from that involved in intracellular microelectrode or conventional cell-attached tight patch recording in leaving the intracellular space unperturbed. Instead, it applies a patch electrode on, forming a seal with, the external face of an intact surface membrane of the cell, initially at its resting membrane potential (RMP). It then applies voltage steps on the *extracellular* surface of the resulting membrane patch within the seal. Accordingly *positive* and *negative* voltage steps applied through the pipette respectively *hyperpolarise* and *depolarise* the membrane potential from its RMP.

6.3.1 Currents reflecting atrial inward Na+ current activation

Figure 6.1 illustrates results obtained from the isolated atrial preparations. These explored activation properties of inward Na^+ currents in young (panels A, C; E, G) and aged (B, D, F, H) wild-type (WT; A, B, E, F) and *Pgc-1β*$^{-/-}$ atria (C, D, G, H). Results are shown both at slow (A-D) and rapid (E-H) timebases demonstrating full decays in and regions of the trace displaying the detailed kinetics of the currents respectively. The pulse protocols that investigated the voltage dependence of Na^+ current activation (panel I) first held the cells at

their RMP for 5 ms from the beginning of the recording period to establish an initial steady resting baseline. This was followed by a 5-ms duration prepulse to a hyperpolarised voltage, V_0 = (RMP – 40 mV), that was expected to fall within a voltage range in which both Na^+ channel activation and inactivation would be minimal. This thus both removed any residual Na^+ current inactivation and standardised the initial activation state of the Na^+ channels within the patch. This was followed by imposition of the depolarising test steps which became successively larger through the 13 successive recorded sweeps. They were made to voltages successively incremented between V_1 = RMP to (RMP + 120) mV in +10 mV increments. The voltage steps extended to the end of the record length which was of total duration 80 ms. The currents were corrected for residual leakage by a P/4 protocol to give the family of records reflecting the voltage dependence of Na^+ channel activation in which inward currents are represented as downward, negative deflections.

Traces typically began with a consistent small upward deflection in response to the -40 mV prepulse (A-D). The subsequent voltage steps to level V_1 yielded a family of inward currents characteristic of Na^+ currents, initially increasing with time to a peak value that increased with more positive V_1. This was followed by a decay reflecting channel inactivation whose extent and kinetics was similarly determined by the voltage V_1 (E-H). However, although young and aged atria showed similar current magnitudes, *Pgc-1β*$^{-/-}$ atria showed consistently reduced Na^+ current amplitudes compared to WT.

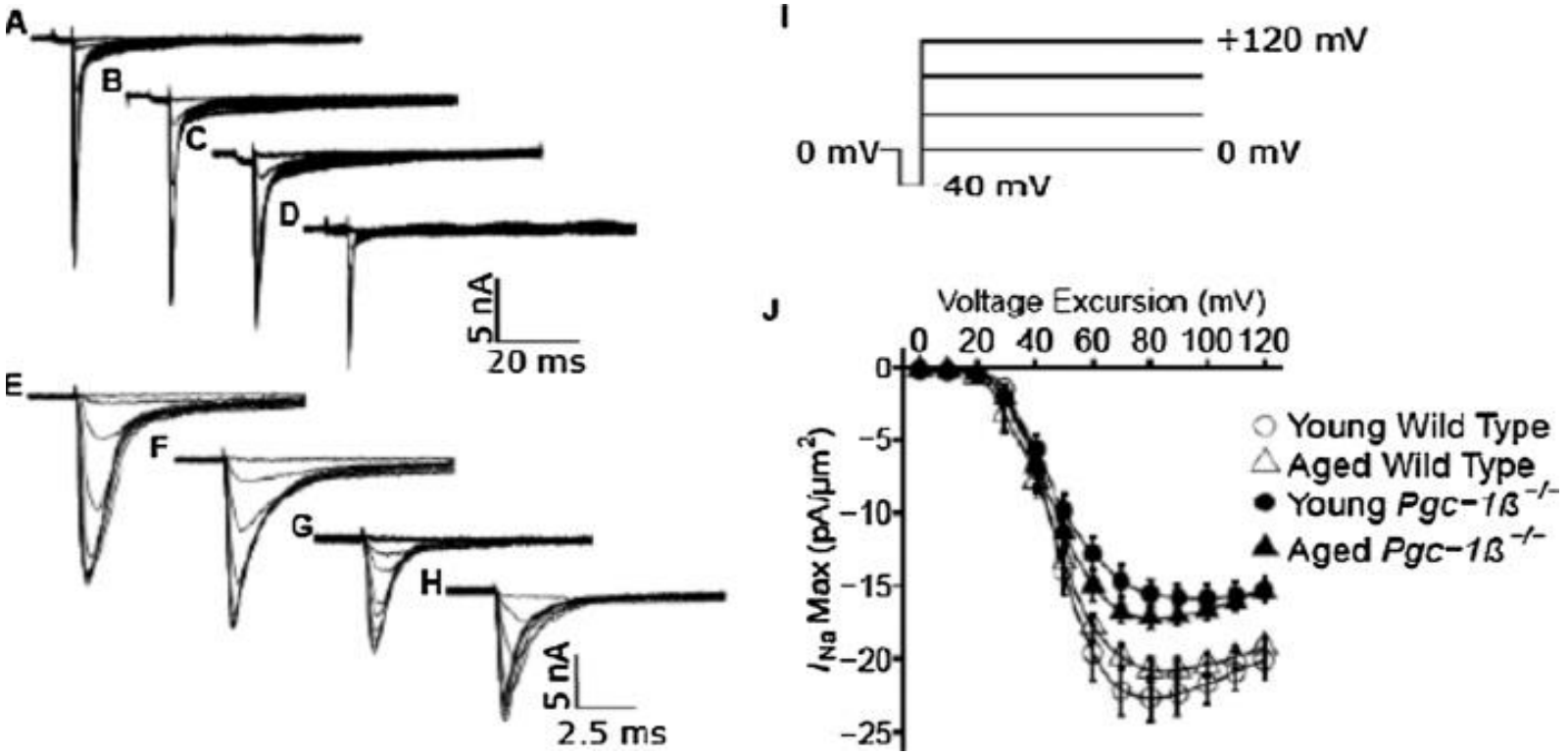

Figure 6.1 Activation properties shown by voltage-dependent inward Na+ currents

Typical records in young (A, C, E, G) and aged (B, D, F, H) wild-type (WT; A, B, E, F) and Pgc-1β-/- atria (C, D, G, H), at slow (A-D) and fast (E-G) time bases in response to (I) activation pulse protocols beginning from the resting membrane potential (RMP). A prepulse (duration 5 ms) was made 5 ms into the recording period to (RMP - 40 mV). This was followed by successively larger depolarising test voltage steps increased in +10 mV increments up to (RMP + 120 mV). (J) Peak currents, $I_{NaMax,}$ plotted against voltage excursion for young (circles) and aged (triangles), wild-type (clear symbols) and Pgc-1β$^{-/-}$ atria (filled symbols).

143

6.3.2 *Currents reflecting atrial Na+ current inactivation*

In contrast, Figure 6.2 shows records from protocols exploring atrial Na^+ current inactivation properties in young (panels A, C; E, G) and aged (B, D, F, H), wild-type (WT; A, B, E, F) and *Pgc-1β*$^{-/-}$ atria (C, D, G, H). As previously, cells were first held at the RMP for 5 ms to establish an initial steady resting baseline. This was followed by application of a 5-ms duration prepulse to V_0 = (RMP - 40) mV. This thus removed any residual Na^+ current inactivation and standardised the initial activation state of Na^+ channels within the patch, prior to the voltage steps that followed. This was followed by depolarising steps to conditioning voltages that were varied with the 13 successive sweeps between V_1 = RMP to (RMP + 120 mV) in +10 mV increments. This conditioning step would elicit a voltage-dependent Na^+ current activation as similarly achieved in the previous protocols that had been used to study Na^+ channel activation properties. However, maintaining the imposed depolarisation then produced a Na^+ current decline reflecting a Na^+ channel inactivation whose extent would be dependent upon the prepulse voltage excursion V_1. Following a 5 ms interval following imposition of the conditioning step, a test step was applied to a fixed voltage V_2 = (RMP + 100 mV) and this extended to the end of the record length (panel I). This yielded a second set of current responses (Figure 6.2A-H) that gave peak Na^+ currents corresponding to a constant level of channel activation, that were however modified by the prior channel *inactivation* brought about by the conditioning voltage excursion to V_1. This accordingly gave families of Na^+ currents that *decreased* in amplitude with the previous inactivation brought about by the increasing V_1. Thus, only channels spared inactivation by the prepulse to V_1 would contribute currents in response to the step to the fixed voltage V_2. Again, young and aged atria showed similar current magnitudes, but *Pgc-1β-/-* atria showed consistently reduced Na^+ current amplitudes compared to WT.

6.3.3 *Voltage dependences of atrial Na^+ current activation*

Figures 6.1J and 6.2J respectively illustrate voltage-dependences of atrial Na^+ current activation and inactivation for young (circles) and aged (triangles), WT (open symbols) and *Pgc-1β*$^{-/-}$ atria, plotting peak Na^+ current (means ± standard error of the mean (SEM)) against voltage excursion to V_1. The quantifications of current-voltage and inactivation curves expressed the observed currents (nA) as current densities (pA/μm^2) using the formula:

$$Current\ density\ = \frac{1000\ x\ current}{(\pi\ x\ pipette\ radius^2)}$$

In activation plots, peak inward Na^+ current increased with the amplitudes of the depolarising steps exceeding +10 mV in size to a maximum value at a voltage excursion around +80 mV. They then decreased with further depolarisation as expected with approach of V_1 towards the Na^+ current reversal potential. Peak Na^+ currents, $I = I_{NaMax}$, reflecting activation properties were empirically related to the activating voltage $V = V_1$ by a Boltzmann function: $I = I_{max}/\{1 + \exp(V - V^*/k)\}$ where I_{max} is maximum current, V^* is voltage at half-maximal current, and k is the steepness factor (Chadda *et al.*, 2017).

Young and aged *Pgc-1β*$^{-/-}$ then showed similar maximum values of peak atrial inward currents (-16.97 ± 0.88 (n = 20) and -18.07 ± 0.89 (n = 21) pA/μm^2 respectively) (Figure 6.1J). These were reduced compared to values in both young (-23.93 ± 1.52 (n = 24) pA/μm^2) and aged WT (-21.53 ± 0.84 (n = 22) pA/μm^2). Two-way ANOVA demonstrated differences attributable to independent effects of genotype ($F = 22.28$; $p = 0.95 \times 10^{-5}$), but not age ($F = 0.46$; $p = 0.50$), or interacting effects of age and genotype ($F = 2.48$; $p = 0.12$). Post hoc Tukey tests demonstrated significant differences between young WT and young *Pgc-1β*$^{-/-}$ ($p = 0.00016$), young WT and aged *Pgc-1β*$^{-/-}$ ($p = 0.0016$) and aged WT and young *Pgc-1β*$^{-/-}$ atria ($p = 0.027$).

In contrast, V^* values were similar amongst young (49.22 ± 1.92 (n = 24) mV) and aged WT (46.04 ± 1.65 (n = 22) mV), and young (48.94 ± 2.92 (n = 20) mV) and aged *Pgc-1β*$^{-/-}$ atria (46.31 ± 1.95 (n = 21) mV). Thus two-way ANOVA demonstrated no independent effects of either genotype ($F = 0.003$; $p = 0.959$) or age ($F = 1.90$; $p = 0.172$), nor interacting effects of age and genotype ($F = 0.016$; $p = 0.898$). Values of k were also similar amongst young (6.21 ± 0.41 (n = 24) mV) and aged WT (7.18 ± 0.45 (n = 22) mV), and young (7.49 ± 0.42 (n = 20) mV) and aged *Pgc-1β*$^{-/-}$ (6.85 ± 0.44 (n = 21) mV). The two-way ANOVA demonstrated no independent effects of either genotype ($F = 1.33$; $p = 0.25$) or age ($F = 0.24$; $p = 0.63$), nor interacting effects of age and genotype ($F = 3.51$; $p = 0.065$).

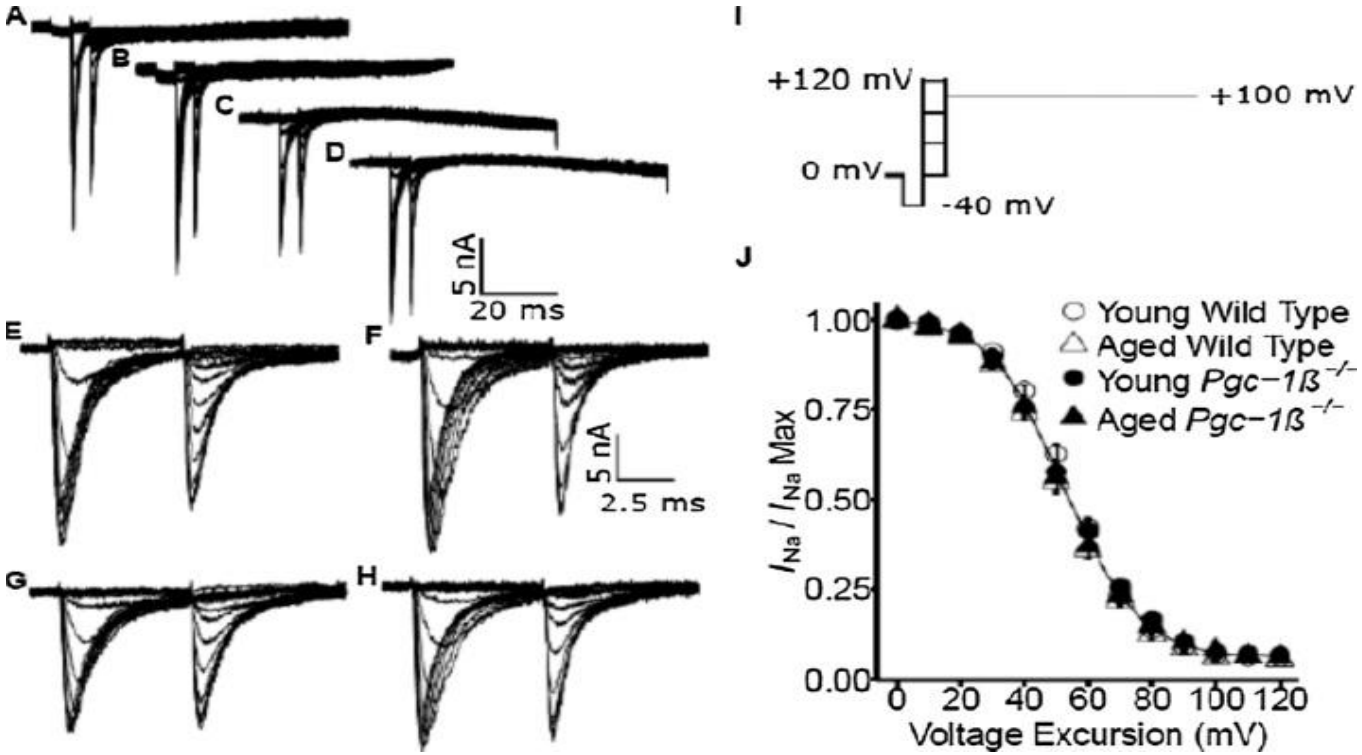

Figure 6.2 Investigation of inactivation properties shown by voltage-dependent inward Na^+ currents.

Typical records in young (A, C, E, G) and aged (B, D, F, H) wild-type (WT; A, B, E, F) and Pgc-1β$^{-/-}$ atria (C, D, G, H), at slow (A-D) and fast (E-G) time bases in response to inactivation pulse protocols applied from the resting membrane potential (RMP). (I) In the pulse protocol, a prepulse (duration 5 ms) was made 5 ms into the recording period to (RMP - 40 mV). This was followed by successively larger depolarising conditioning voltage steps increased in +10 mV increments up to (RMP + 120 mV) of 5 ms duration. Finally the voltage was stepped to a constant test level of (RMP + 100 mV), and the resulting Na^+ currents quantified to investigate the inactivation brought about by the preceding conditioning step. (J) Peak currents I_{NaMax} plotted against voltage excursion for the conditioning voltage step in young (circles) and aged (triangles), wild-type (clear symbols) and Pgc-1β$^{-/-}$ atria (filled symbols).

6.3.4 *Voltage dependences of atrial Na+ current inactivation*

In the inactivation plots, peak inward currents observed in response to depolarising steps to a constant voltage decreased with more positive prepulse voltages V_1, reflecting inactivation increasing with increasing degrees of prior depolarization (Figure 6.2J). The peak currents reflecting inactivation properties, normalised to their maximum value observed with fully polarised prepulse voltages, were similarly empirically related to the inactivating voltage $V = V_1$ by a Boltzmann function: $I = I_{max}$ {1 - [1/{1 + exp(V - V*/k)]}. These gave similar values for V* amongst young (54.75 ± 0.98 (n = 24) mV) and aged WT (51.44 ± 1.14 (n = 22) mV), and young (52.98 ± 1.24 (n = 20) mV) and aged *Pgc-1β-/-* atria (51.94 ± 1.71 (n = 21) mV). Two way ANOVA demonstrated no independent effects of either genotype (F= 0.32; p = 0.57) or age (F=3.09; p = 0.082), nor interacting effects of age and genotype (F = 0.79; p = 0.38). Similar k values occurred amongst young (10.62 ± 0.35 (n = 24) mV) and aged WT (11.15 ± 0.35 (n = 22) mV), and young (11.61 ± 0.25 (n = 20) mV) and aged *Pgc-1β-/-* atria (10.65 ± 0.60 (n = 21) mV). Two-way ANOVA demonstrated no independent effects of either genotype (F= 0.35; p = 0.55) or age (F=0.18; p = 0.67), nor interacting effects of age and genotype (F = 3.33; p = 0.072).

Together these findings demonstrated effects of genotype but not age upon maximum peak Na^+ currents I_{max}, but not voltages at half maximal current V* or steepness factors, k, of Boltzmann functions describing either their activation or inactivation properties.

6.3.5 *Time courses of atrial Na+ channel recovery from inactivation*

Figure 6.3(A-D) show typical currents obtained from young (A, C) and aged (B, C), WT (A, B) and *Pgc-1β-/-* atria (C, D) reflecting time courses of Na^+ current recovery from inactivation following restoration of the baseline voltage after an initial conditioning depolarising step to a fixed voltage. The pulse protocols (Figure 6.3F) held the membrane voltages at the RMP for 1 ms from the beginning of the recording period, then imposed a hyperpolarising prepulse to voltage V_0 = (RMP - 40 mV) for 4 ms to establish consistent baseline levels of Na^+ current inactivation as in the previous protocols. A 5 ms-duration P1 conditioning step between V_0 and V_1 = (RMP + 80 mV) then elicited a Na^+ current activation followed by its inactivation decay. Subsequent depolarising 5 ms-duration P2 steps to voltage V_3 = (RMP + 80 mV) were imposed after different time intervals, ΔT that were successively increased between 2 and 75 ms, in 2 ms increments for the first 5 sweeps and in 5 ms increments for the remainder of the

16 successive sweeps making up the protocol. The P2 steps elicited a Na^+ current activation whose peak amplitude reflected the Na^+ current recovery from inactivation with time, when normalized to corresponding values in the P1 step. Fits of time constants, τ, to the exponential function $I = I_{max}(1 - \exp(-\Delta T/\tau))$ describing this recovery (Figure 6.3G) gave similar values of τ in young (3.44 ± 0.39 (n = 24) ms) and aged WT (3.70 ± 0.30 (n = 22) ms), and young (3.88 ± 0.31 (n = 20) ms) and aged *Pgc-1β*$^{-/-}$ (3.64 ± 0.30 (n = 21) ms) that did not reflect any independent effects of either genotype (F = 0.334; p = 0.565) or age (F = 0.007; p = 0.932), or of interacting effects of age and genotype (F = 0.561; p = 0.456) with two-way ANOVA.

6.3.6 Voltage dependences of atrial outward K+ current activation

These findings contrast with the similar voltage dependences and rectification properties of voltage-dependent total outward, K^+, current amongst the experimental groups studied. The present experiments thus investigated such outward currents in murine atrial preparations using the loose-patch technique for the first time. Figure 6.4 displays typical currents obtained from pulse procedures comparing voltage dependences of overall K^+ current activation in young (Figure 6.4A, C, E, G) and aged (Figure 6.4B, D, F, H), WT (Figure 6.4A, B, E, F) and *Pgc-1β*$^{-/-}$ (Figure 6.4B, D, F, H) atria at slow (A-D) sweep speeds encompassing the entire record as well as rapid timebases encompassing the current tail reflecting K^+ channel activation at the end of the preceding depolarising step (E-H).

The pulse procedure (Panel I) involved an initial imposition of a voltage step from the RMP to (RMP – 20 mV) between 1-10 ms from the beginning of the recording period to establish an initial steady resting state of channels within the patch. This was followed by a 10 ms duration test step made to a series of test voltages between (RMP – 60 mV) to (RMP + 170 mV) to explore the voltage dependence of K^+ channel activation. The latter was incremented in 10 mV steps through the 24 sweeps that were investigated. These activation steps resulted in an initial inward Na^+ channel activation, followed by its inactivation. However, this was succeeded in some traces by the gradual development of a small outward current reflecting activation of a rectified voltage dependent K^+ current whose extent was dependent upon the voltage of the test step. This was then followed by a hyperpolarising step of duration 10 ms to a fixed post

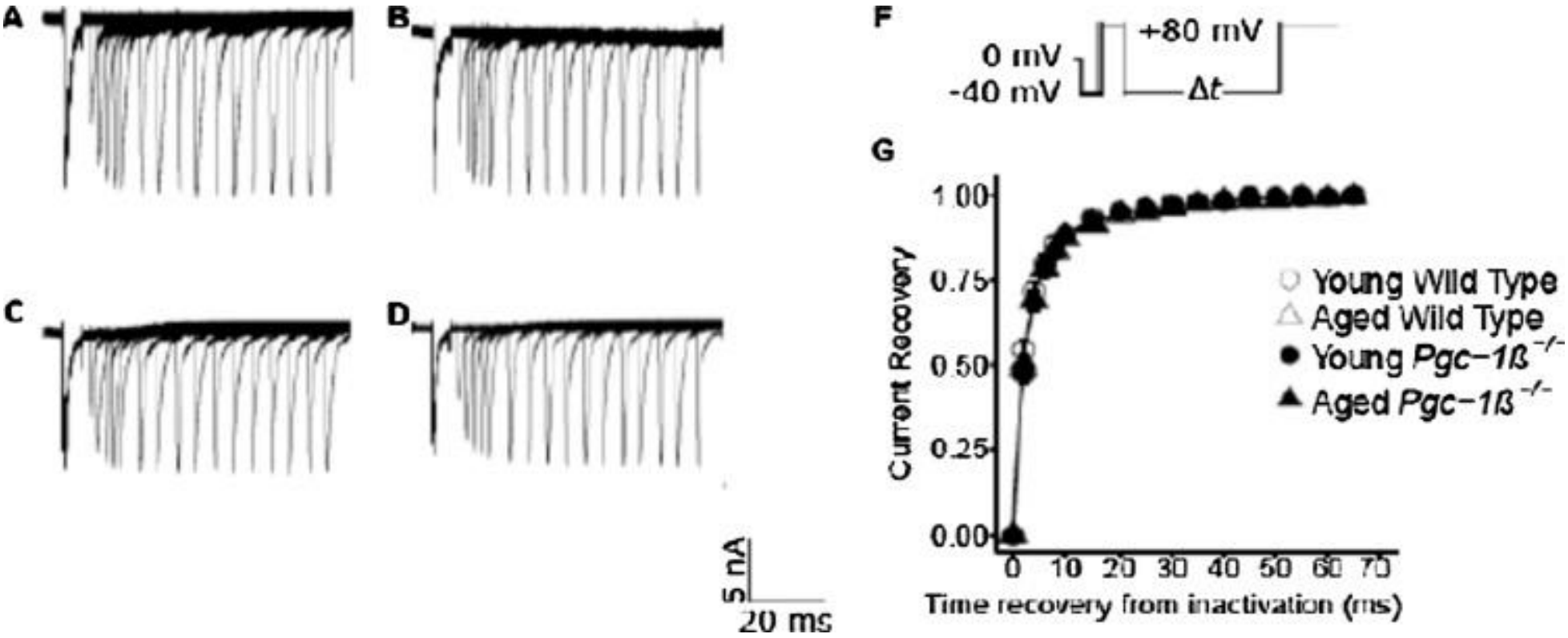

Figure 6.3 Currents illustrating Na^+ channel recovery from inactivation

Records in young (A, C) and aged (B, D) wild-type (WT; A, B) and Pgc-1β$^{-/-}$ atria (C, D). The pulse protocols (F) first held membrane voltages at RMP for 1 ms from the beginning of the recording period, then imposed a hyperpolarising prepulse to (RMP - 40) mV prior to the 5 ms duration P1 conditioning step to (RMP + 80 mV). The subsequent 5 ms duration test steps to (RMP + 80 mV) were imposed after different time intervals, ΔT, The latter were successively increased between 2 and 75 ms, in 2 ms increments for the first 5 sweeps and in 5 ms increments for the remainder of the 16 successive sweeps making up the protocol. (G) Plots of the recovery of peak I_{Na} against time intervening between termination of the conditioning and imposition of the test pulse.

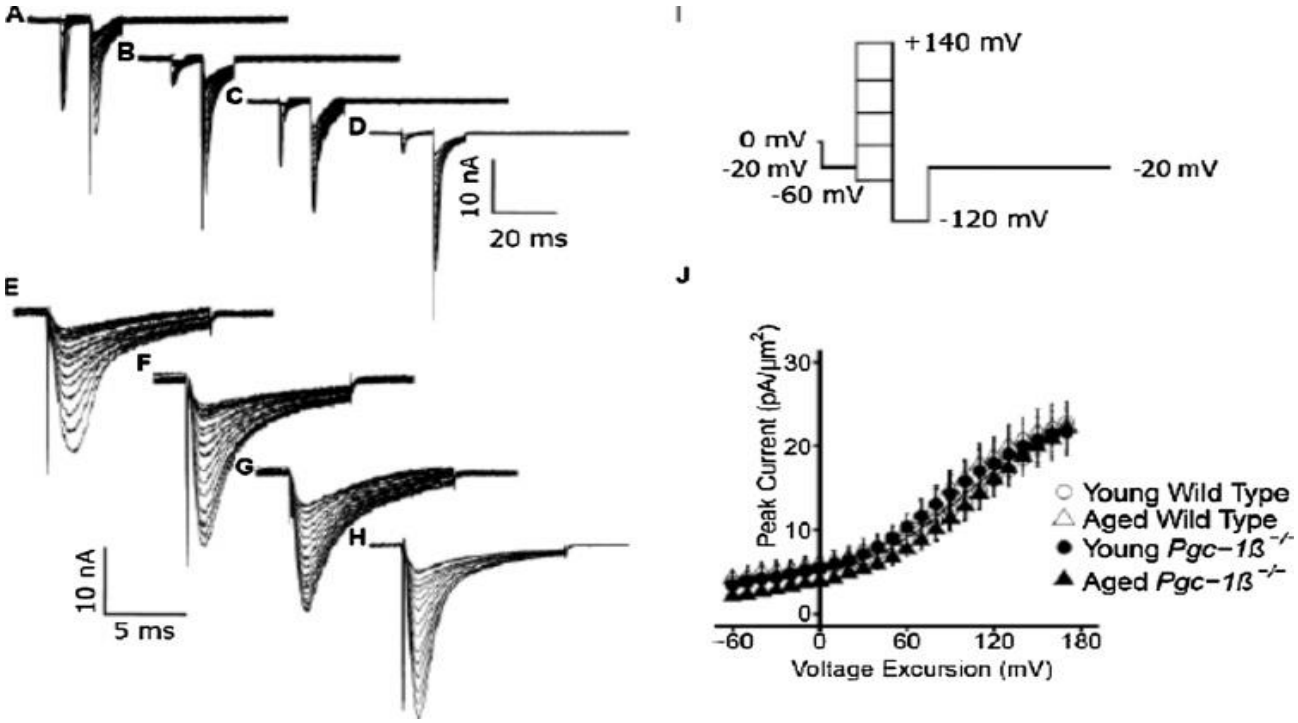

Figure 6.4 K⁺ current activation properties reflected in tail currents.

Records from young (A, C, E, G) and aged (B, D, F, H) wild-type (WT; A, B, E, F) and Pgc-1β-/- atria (C, D, G, H), at slow (A-D) and fast (E-G) time bases. Pulse procedures (I) first applied a voltage step between 1-10 ms following the beginning of the recording period from RMP to (RMP – 20 mV). The following 10 ms duration test steps were made to voltages between (RMP – 60 mV) to (RMP + 170 mV) incremented in 10 mV steps through the 24 sweeps investigated. The final 10 ms duration hyperpolarising step to (RMP – 120 mV) that preceded final restoration of the membrane potential to (RMP - 20 mV) gave tail currents reflecting (J) the preceding K^+ current activation, plotted against voltage excursion in the young (circles) and aged (triangles) WT (open symbols) and Pgc-1$\beta^{-/-}$ atria (filled symbols).

pulse voltage of (RMP – 120 mV) that would thereby apply a fixed driving voltage upon any K^+ current flow through channels opened by the preceding test step. In the resulting family of K^+ tail currents, their maximum magnitudes would therefore be determined by the instantaneous conductance reflecting the preceding K^+ current activation. The pulse protocol ended with final restoration of the membrane potential to (RMP - 20 mV).

Figure 6.4J plots typical activation current-voltage curves for the young (circles) and aged (triangles) WT (open symbols) and *Pgc-1β*$^{-/-}$ (filled symbols) atrial preparations investigated. They demonstrated close to superimposable plots enclosing areas with the abscissa in which there were neither independent (F = 0.39; P =0.54 and F = 0.079; P =0.79 respectively) nor interacting (F = 1.75; P =0.20) effects of either genotype or age.

6.3.7 Rectification properties of outward K+ currents in loose patched atrial preparations

The corresponding K^+ current rectification properties were investigated by a pulse procedure similarly imposing an initial voltage step between 1-10 ms into the recording period from RMP to (RMP – 20 mV). However, the succeeding 10 ms duration test step was then made to a fixed voltage of (RMP + 140 mV) to achieve a specific level of K^+ current activation. This was followed by a further voltage step to a range of voltages between (RMP-120 mV) to (RMP + 50 mV) in order to derive the instantaneous current-voltage relationship reflecting the rectification properties of the activated channel (Figure 6.5I). Figure 6.5(A-H) shows typical tail currents suggesting little or no difference in instantaneous current amplitudes between experimental groups.

Figure 6.5J plots typical instantaneous current-voltage curves for young (circles) and aged (triangles) WT (open symbols) and *Pgc-1β*$^{-/-}$ atria (filled symbols) demonstrating close to superimposable plots enclosing areas with the abscissa in which there were neither independent (F = 0.043; P = 0.84 and F = 0.97; P = 0.33 respectively) nor interacting (F = 0.005; P = 0.95) effects of either genotype or age.

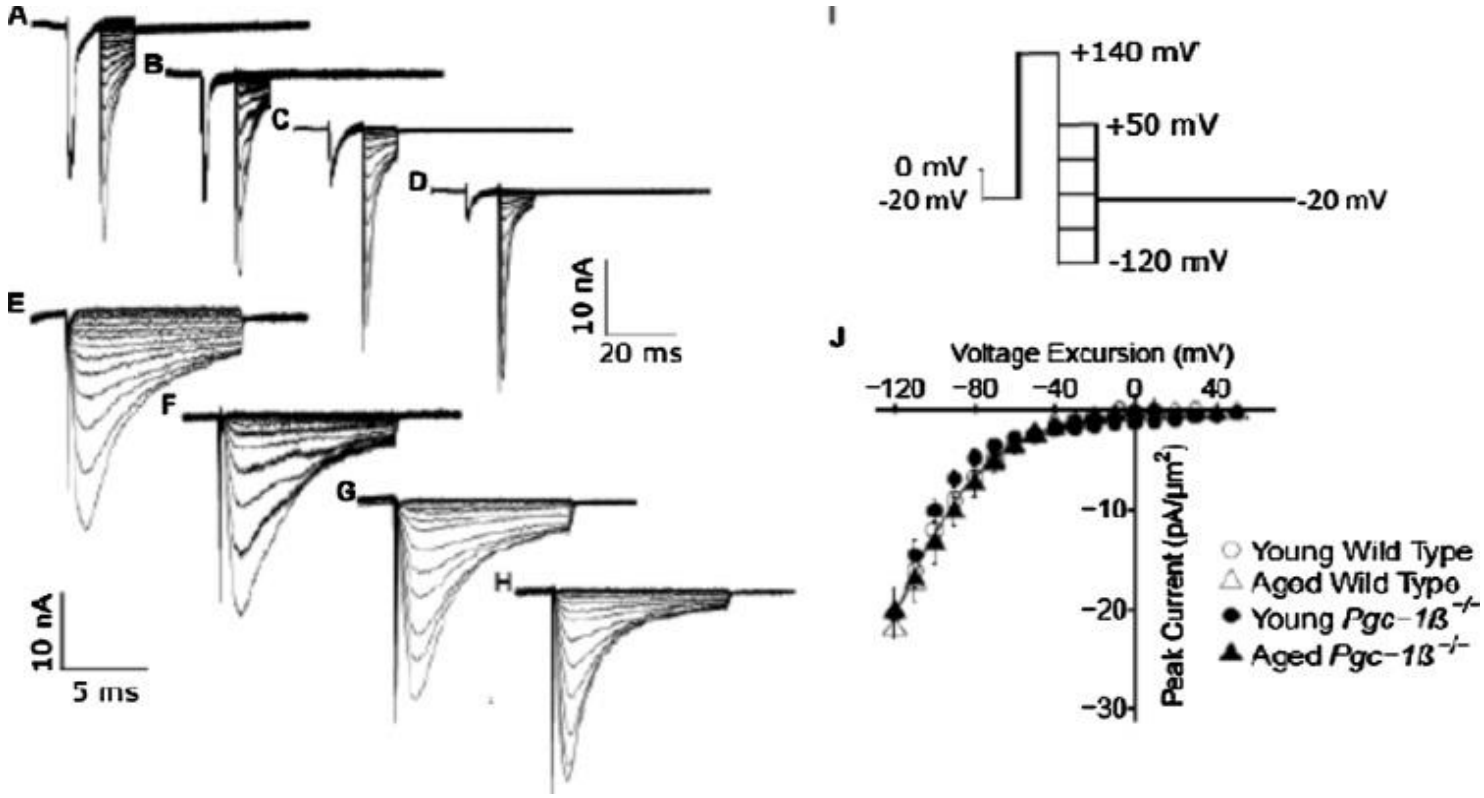

Figure 6.5 K^+ current rectification properties reflected in tail currents

Typical records from young (A, C, E, G) and aged (B, D, F, H) wild-type (WT; A, B, E, F) and Pgc-1β$^{-/-}$ atria (C, D, G, H), at slow (A-D) and fast (E-G) time bases. The pulse procedure (I) first applied a voltage step between 1-10 ms after commencement of the recording period from RMP to (RMP – 20 mV). A following 10 ms duration test step was then made to a fixed voltage of (RMP + 140 mV). The following step to a varying voltages between (RMP - 120 mV) to (RMP + 50 mV) provided tail currents which could be plotted to obtain (J) instantaneous current-voltage relationships reflecting rectification properties of the activated channel in the young (circles) and aged (triangles) WT (open symbols) and Pgc-1β$^{-/-}$ atria (filled symbols). The protocol ended by restoration of the membrane potential to (RMP – 20 mV).

6.3.8 Increased fibrotic change with Pgc-1β ablation

The influence of ageing and genotype upon the relationship between rates of depolarisation and latency prompted histological assessment for fibrotic change. Fibrosis is known to impede AP conduction through the myocardium through decoupling of myocytes, resulting in disrupted gap junction functioning and consequent increases in resistivity. In addition, fibroblast fusion with myocytes increases membrane capacitance. Histological assessment was conducted blindly by two investigators independently and in the ICC, a measure if consistency between their findings, was 0.88 suggesting a high degree of consistency in the results.

Figure 6.6(a) represent typical histological sections from young and aged WT and *Pgc-1β*$^{-/-}$ hearts, the quantification of fibrotic change is shown in figure 6.6(b). Genotype ($F = 33.02$, $p < 0.001$) and age ($F = 4.75$, $p < 0.05$) independently increases levels of fibrosis in the atria, but there was no evidence of interaction between the two. These findings complement the changes in latency noted in the earlier electrophysiological studies. The fibrotic change witnessed in WT aged hearts compared to WT young hearts explains the increased latency seen in this group. Young *Pgc-1β*$^{-/-}$ hearts show similar levels of fibrosis to aged WT hearts further supporting the suggestion of premature ageing in this group.

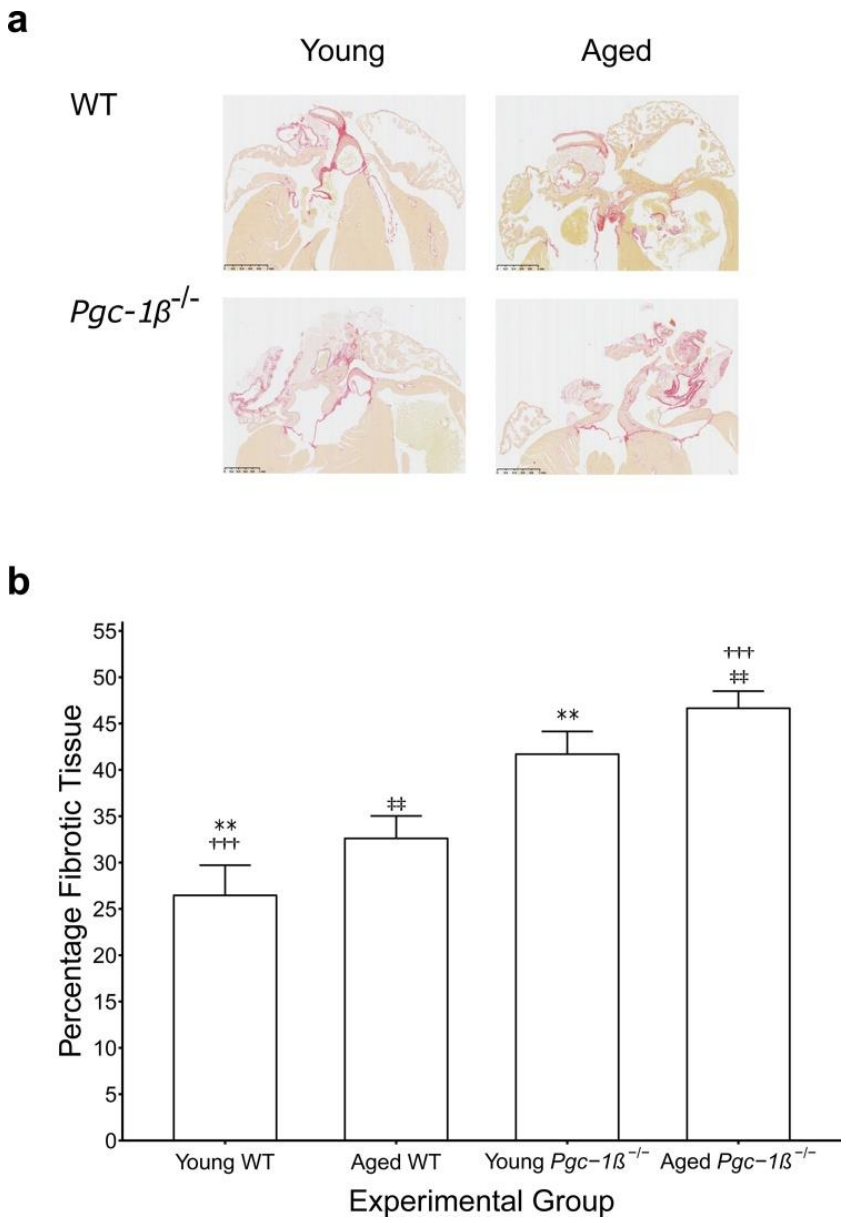

Figure 6.6 Structural remodelling in *Pgc-1β*$^{-/-}$ hearts

(a) Representative images of histological samples used for morphological assessment of fibrotic change. (b) The degree of fibrotic change was assessed as the proportion of morphometric squares covering tissue that demonstrated evidence of fibrosis as detected by picrosirius red staining. The numbers of hearts examined: young WT (n = 6), aged WT (n = 6), young Pgc-1β$^{-/-}$ (n = 6), aged Pgc-1β$^{-/-}$ (n = 6). Symbols denoted pairs of points showing significant differences from post hoc Tukey testing, where Single, double and triple symbols denote $p < 0.05$, $p < 0.01$ and $p < 0.001$ respectively.

6.4 Discussion

Increasing evidence implicates metabolic, particularly mitochondrial, dysfunction, a recognised feature of both ageing (Sun *et al.*, 2016) and age-related metabolic disorders (Patti & Corvera, 2010; Bournat & Brown, 2010; Dikalov & Ungvari, 2013), in the pathogenesis of atrial fibrillation (Menezes *et al.*, 2013*b*), in both animal models (Morillo *et al.*, 1995; Ausma *et al.*, 1997*b*) and clinical situations (Lin *et al.*, 2003; Ad *et al.*, 2005; Bukowska *et al.*, 2008). The present studies examined accompanying alterations in electrophysiological function at the cellular and tissue level were prompted by results in chapters 3 - 5 describing electrophysiological pro-arrhythmic atrial phenotypes at the tissue level in murine *Pgc-1β*$^{-/-}$ hearts consequently deficient in this key mitochondrial regulator involved in the tricarboxylic acid cycle, fatty acid β–oxidation and oxidative phosphorylation (Arany *et al.*, 2005; Lin *et al.*, 2005; Finck & Kelly, 2006). The pro-arrhythmic phenotypes progressed with age to extents accentuated by the *Pgc-1β*$^{-/-}$ as opposed to the WT genotype. These were accompanied by slowed AP conduction and compromised maximum action potential (AP) depolarization rates, $(dV/dt)_{max}$ despite normal effective refractory periods and baseline action potential durations. These features together could potentially furnish arrhythmic substrate. Reduced atrial conduction velocities have previously been reported in early clinical AF (Zheng *et al.*, 2016) and to contribute to substrate for its long term maintenance (Park *et al.*, 2009; Miyamoto *et al.*, 2009).

At the tissue level, AP conduction depends upon local circuit currents generated by the rate of action potential depolarization $(dV/dt)_{max}$ whose spread are in turn modified by membrane capacitance and cytosolic resistance, but for which previous studies correlated $(dV/dt)_{max}$ with peak Na^+ currents (I_{Na}) (Jeevaratnam *et al.*, 2011; King *et al.*, 2013*a*). The recent studies accordingly suggested a hypothesis implicating the *Pgc-1β*$^{-/-}$ as opposed to WT genotype, independently of age, in Na^+ current reductions, but implicating both genotype and age in fibrotic changes that would additionally compromise local circuit currents propagating the resulting action potential activity. The consequent reductions in conduction velocity would then result in atrial pro-arrhythmic effects, as previously suggested for some canine AF models (Gaspo *et al.*, 1997*a*). *SCN5A* gene variants leading to reduced cardiac Na^+ channel

function have similarly been implicated in increased AF risks both in clinical situations (Olson *et al.*, 2005; Darbar *et al.*, 2008) and experimental studies in genetically modified *Scn5a*+/- murine hearts (Sabir *et al.*, 2008*a*; Kalin *et al.*, 2010; Martin *et al.*, 2011*a*, 2011*b*; Huang, 2017*b*).

The present experiments applied a loose patch clamp method, which detects transmembrane current flowing into an extracellular electrode apposed to the membrane surface of cardiomyocytes within intact atrial tissue preparations (King *et al.*, 2013*b*; Salvage *et al.*, 2015; Ning *et al.*, 2016). It thus avoids cytosolic disruptions that would follow the cell isolation and intracellular Ca^{2+} chelation required by conventional whole-cell patch-clamp recordings (Lei *et al.*, 2005; Martin *et al.*, 2012*b*). It also allowed employment of in vivo rather than reduced extracellular [Na^+] levels thereby sparing Na^+-Ca^{2+} exchange processes. Ion currents were thus studied in atrial preparations under conditions similar to those employed in the earlier chapters, and their associated changes in conduction velocity and $(dV/dt)_{max}$. Finally, previous reports had identified early inward currents obtained with this technique with Na^+ currents mediating action potential (AP) conduction and upstroke (King *et al.*, 2013*b*). The loose patch clamp technique has thus not been employed to study other inward, such as Ca^{2+}, currents in detail. However, this may reflect the nature of the skeletal muscle and murine atrial preparations studied to date. These are associated with small Ca^{2+} relative to Na^+ inward current contributions following activation by depolarising steps (Huang, 2017*b*).

The loose patch clamp experiments demonstrated a voltage dependent activation of inward currents consisting of increases to a peak current followed by an inactivation decay giving a time course and a dependence upon the amplitude of progressively larger depolarising steps characteristic of Na^+ currents in all the, young and aged, WT and *Pgc-1β*$^{-/-}$ atria studied. However, the presence of a *Pgc-1β*$^{-/-}$ genotype specifically resulted in a reduction in the peak Na^+ current, without either independent or interacting influences of age. The remaining Na^+ current characteristics in the form of either voltage at half maximum current, V^*, or the steepness, k, of the Na^+ current activation characteristics derived from the current-voltage curves were unaffected by either age or genotype. Imposition of steps to a fixed depolarised voltage level from a range of prepulse voltages similarly elicited currents rising to a peak followed by decay. The peaks now declined in amplitude with depolarising prepulse levels,

reflecting the resulting voltage-dependent inactivation they would produce. However, inactivation curves constructed from plotting such peak currents against prepulse level yielded similar inactivation functions, as reflected in the similar V^* or k values derived from voltage dependences of inactivation obtained in all four experimental groups. Finally, the specific differences in maximum Na^+ current took place against indistinguishable outward repolarising, K^+, current characteristics between groups. These first investigated voltage dependences of K^+ current activation in response to pulse procedures employing a range of test steps, followed by hyperpolarising steps to a fixed voltage in order to assess the current tails reflecting the preceding activation. Conversely K^+ current rectification properties were investigated imposing fixed voltage step to produce a constant level of activation. Accordingly, the succeeding steps to varying voltages then permitted open channel rectification properties to be explored. Both experiments yielded similar atrial currents from all four experimental groups, which accordingly yielded closely concordant activation and instantaneous current-voltage curves.

Together these findings thus demonstrate a possible mechanism for the genotypically-related variations in arrhythmic phenotype, with their accompanying reductions in AP conduction velocity and peak AP upstroke rates $(dV/dt)_{max}$ in *Pgc-1β*$^{-/-}$ atria. They attribute these to reductions in maximum Na^+ currents against a constant background of outward K^+ current characteristics. They fulfil predictions at the level of intact atria, from previous studies at the cellular level reporting that metabolic stress potentially alters Na^+ currents. This could take place through effects on Na^+ channel activity of increased production of reactive oxygen species (ROS) or compromised NAD^+/NADH ratios, effects potentially rescued by the mitochondrial ROS scavenger mitoTEMPO and NAD^+ restoration respectively (Liu *et al.*, 2010; Gomes *et al.*, 2013). *Pgc-1β*$^{-/-}$ cardiomyocytes also showed evidence for abnormal Ca^{2+} homeostasis (Gurung *et al.*, 2011), in common with murine *RyR2*-P2328S atrial myocytes (Goddard *et al.*, 2008), which similarly showed parallel AP conduction velocity and Na^+ current reductions (King *et al.*, 2013*b*). These were attributed to both *chronically* downregulated $Na_v1.5$ expression (King *et al.*, 2013*b*; Ning *et al.*, 2016) as well as acute (King *et al.*, 2013*c*, 2013*b*; Zhang *et al.*, 2013) and potentially reversible loss of $Na_v1.5$ function (Knollmann *et al.*, 2001*a*; Salvage *et al.*, 2015, 2017). The recent findings associating *Pgc-1β-/-* with increased rather than

decreased *SCN5A* expression would be consistent with the latter mechanism involving direct effects of altered cytosolic [Ca^{2+}] upon Nav1.5 function (Tan *et al.*, 2002; Aiba *et al.*, 2010; Ashpole *et al.*, 2012). Such interactions could involve Ca^{2+}-binding at the Na+ channel C-terminal region, either directly at an EF hand motif (Wingo *et al.*, 2004) or indirectly through an IQ domain sensitive to calmodulin/calmodulin kinase II (Mori *et al.*, 2000). There are also multiple phosphorylatable sites in the Na^+ channel DI-II linker region including serines 516 and 571, and threonine 594 targeted by calmodulin kinase II (CaMKII) (Mori *et al.*, 2000; Wagner *et al.*, 2011; Grandi & Herren, 2014). Certainly previous studies have reported that elevations or sequestration of intracellular [Ca^{2+}] respectively reduced or restored Na^+ currents and $(dV/dt)_{max}$ in WT cardiomyocytes in vitro (Casini *et al.*, 2009).

Myocardial fibrosis is associated with increased tissue capacitance and resistance, contributing to conduction slowing independent of the influence of $(dV/dt)_{max}$ and may explain the conduction properties described in the present study. Fibrotic change is thought to be a key element of the remodelling seen in AF (Frustaci *et al.*, 1997; Kostin *et al.*, 2002). Progressive fibrosis is a common feature of cardiac ageing in animal (Eghbali *et al.*, 1989; Orlandi *et al.*, 2004; Lin *et al.*, 2008; Jeevaratnam *et al.*, 2012) and human (Gazoti Debessa *et al.*, 2001) studies. Age-dependent fibrosis was similarly recorded in these experiments, in both WT and *Pgc-1β*$^{-/-}$ hearts, and mitochondrial dysfunction through *Pgc-1β* ablation was associated with a further additive effect on the degree of fibrosis. Aged *Pgc-1β*$^{-/-}$ hearts therefore displayed the greatest degree of fibrosis whereas young WT hearts had the least and AP latency times reported in chapter 4 correlated with the observed degrees of fibrosis in the respective groups.

The fibrosis mediated reductions in cardiac conduction reported here could potentially occur through increased coupling of fibroblasts to cardiomyocytes through Cx43 and/or Cx45, thereby increasing membrane capacitance (Camelliti *et al.*, 2004; van Veen *et al.*, 2005; Chilton *et al.*, 2007). More direct disruption of gap junctions has also been reported consequently increasing tissue resistance, further slowing conduction (Xie *et al.*, 2009). Interestingly, mice lacking the mitochondrial sirtuin SIRT3 display augmented mitochondrial ROS production and enhanced cardiac fibrosis (Hafner *et al.*, 2010). Upregulated antioxidant capacity through

a mitochondrial specific overexpression of catalase protected against features of cardiac ageing including myocardial fibrosis, highlighting mechanisms of fibrosis secondary to abnormal mitochondrial activity and putative rescue strategies (Dai *et al.*, 2009). Furthermore, transforming growth factor-β1 (TGF-β_1) is thought to have a significant role in age-related myocardial fibrosis (Brooks & Conrad, 2000; Rosenkranz *et al.*, 2002). Mice over expressing TGF-β_1 develop pronounced atrial fibrosis, have reduced atrial conduction velocities and greater inducibility to atrial tachyarrhythmias including AF (Verheule *et al.*, 2014). Serum levels of TGF-β_1 are increased in individuals with AF compared to control (Lin *et al.*, 2015). TGF-β_1 activity is also enhanced by oxidative stress (Barcellos-Hoff & Dix, 1996; Sullivan *et al.*, 2008).

Together, suggest that the arrhythmic substrate in *Pgc-1β*$^{-/-}$ hearts develops through maladaptive alterations in AP conduction with ionic changes at the cellular level and structural changes at the tissue level. While these results do not conclusively attribute the similar changes seen associated with human age-related atrial arrhythmias, however support a causative role for mitochondrial dysfunction in the adverse remodeling events that define their pathogenesis.

7 Summary & General Discussion

7.1 Background

Atrial fibrillation (AF) affects 1 – 3% of the population in the developed world (Majeed *et al.*, 2001; DeWilde *et al.*, 2006; Friberg & Bergfeldt, 2013) and is associated with significant morbidity and mortality, including a five-fold increase in the risk of stroke (Wolf *et al.*, 1978) and a significant increase in the risk of all-cause mortality (Benjamin *et al.*, 1998; Friberg *et al.*, 2007; Chamberlain *et al.*, 2015). Its prevalence appears to great extent to be a function of age, affecting 0.1 % under the age of 55 and in excess of 10 % above the age of 85 (Go *et al.*, 2001*b*). Recent studies forecast a substantial increase in the incidence and prevalence of AF in the coming decades, with potentially 9 million cases in the US (Miyasaka *et al.*, 2006) and 18 million in Europe by 2060 (Krijthe *et al.*, 2013), underpinning its recognition as a global epidemic.

Despite much progress in our understanding of its pathophysiology, mechanisms underlying the initiation and perpetuation of AF remain incompletely explained. It is however clear that AF is a dynamic process, which at its inception is characterised by fleeting episodes of the abnormal rhythm triggered by focal ectopic activity in the pulmonary vein sleeves (Haïssaguerre *et al.*, 1998). With time, these episodes become more protracted and eventually permanent through progressive electrical and structural remodelling, ultimately producing a tissue substrate conducive to arrhythmia maintenance. Treatment in these latter stages is far less efficacious, highlighting the need to develop therapies targeted to the upstream processes. There is also growing appreciation for a role of metabolic, and in particular mitochondrial, dysfunction in the pathogenesis of AF. Mitochondrial dysfunction is a recognised feature of a number of the constituents of metabolic syndrome including obesity (Bournat & Brown, 2010), insulin resistance (Patti & Corvera, 2010) and hypertension (Dikalov & Ungvari, 2013), as well as ageing (Sun *et al.*, 2016), all of which are recognised risk factors for AF (Menezes et al., 2013). Abnormal mitochondrial structure and function have been reported in animal

models of AF (Morillo *et al.*, 1995; Ausma *et al.*, 1997*b*). Moreover, analysis of cardiomyocytes from human patients with AF demonstrate greater degrees of DNA damage (Tsuboi *et al.*, 2001; Lin *et al.*, 2003), structural abnormalities (Bukowska *et al.*, 2008) and evidence of impaired function (Lin *et al.*, 2003; Ad *et al.*, 2005). Whether the observed mitochondrial abnormalities are a cause or consequence of AF, or the mechanisms through which these changes occur remains unclear.

Disruptions in normal mitochondrial activity are known to be pro-arrhythmic, through restricted provisions of ATP and/or aberrant production of ROS, and therefore a potential upstream mediator of arrhythmogenesis (Manning *et al.*, 1984; Fosset *et al.*, 1988; Faivre & Findlay, 1990). Much of this work has however been in the context of acute, profound mitochondrial impairment during ischaemia-reperfusion and focussed on mechanisms of ventricular arrhythmias. Interestingly, Chen & colleagues recently demonstrated increased ectopic activity, burst firing and shortening of the APD in pulmonary veins and left atria of rabbit hearts subjected to ischaemia-reperfusion (Lin *et al.*, 2012). Sustained arrhythmias are generally thought to occur through maladaptive changes in the electrophysiological properties of a tissue, promoting the formation of re-entrant circuits. Such would arise through slowed conduction of the depolarising wavefront and/or shortening of the effective refractory period (ERP). Indeed, time-dependent alterations in both atrial conduction (Gaspo *et al.*, 1997*b*; Zheng *et al.*, 2016) and repolarisation (Daoud *et al.*, 1996; Gaspo *et al.*, 1997*a*; Bosch *et al.*, 1999) properties have been noted in human AF. Reductions in the inward sodium currents (I_{Na}), a major determinant of conduction velocity (King *et al.*, 2013*a*), have been reported secondary to excess mitochondrial ROS production (Liu *et al.*, 2010). Gap junction activity is also known to be similarly sensitive to mitochondrial function (Sovari *et al.*, 2013; Li *et al.*, 2016) and may also contribute to conduction slowing in this context. Mitochondrial impairment and cardiac oxidative stress in general are also recognised to reduce the action potential duration and ERP (Lesnefsky *et al.*, 1991; Chen *et al.*, 2007; Kurokawa *et al.*, 2011), both of which favour re-entry and arrhythmia.

The electrophysiological sequelae of chronic mitochondrial dysfunction have however been challenging to study, confounded by the early and often terminal development of contractile

dysfunction but now appears feasible in murine models lacking members of the peroxisome proliferator activated receptor-γ coactivator-1 (PGC-1) family of transcriptional coactivators. The PGC-1 family include PGC-1α and PGC-1β, which though found with a reasonable degree of ubiquity, are preferentially expressed in tissues with high oxidative capacity such as the heart, brain and skeletal muscle (Riehle & Abel, 2012) and act as key regulators of mitochondrial mass and function (Lin *et al.*, 2005; Finck & Kelly, 2006). In cardiac cells, the PGC-1 coactivators interact with NRF-1, ERR-α and PPAR-α, leading to increased mitochondrial biogenesis (Vega *et al.*, 2000; Huss *et al.*, 2004). They also act to upregulate expression of nuclear and/or mitochondrial encoded mitochondrial proteins involved in the tricarboxylic acid cycle, fatty acid β–oxidation and components of oxidative phosphorylation complex (Arany *et al.*, 2005). PGC-1 protein expression itself is increased by upstream signals such as those arising from cold exposure and aerobic exercise, thereby serving as a link between cellular energy stores and external stimuli ultimately coordinating mitochondrial activity with cellular energy demands (Sonoda *et al.*, 2007). Interestingly, their expression levels are found to be reduced in obesity, insulin resistance, type II diabetes mellitus and ageing, correlating with the mitochondrial dysfunction that is seen in these conditions and implicating it in the their pathogenesis (Mootha *et al.*, 2003; Leone & Kelly, 2011; Dillon *et al.*, 2012).

Murine hearts lacking either *Pgc-1α* or *Pgc-1β* do not develop cardiac failure in the non-stressed state. Homozygous deficiency of Pgc-1α is associated with a mild cardiac phenotype at baseline with no overt contractile dysfunction, but does result in cardiac failure following transverse aortic banding (Arany *et al.*, 2005). Similarly, genetic ablation of *Pgc-1β* does not appear to be detrimental to cardiac function at baseline, but these hearts do display a blunted rate response following adrenergic challenge alluding to possible electrophysiological alterations in this setting (Lelliott *et al.*, 2006). Indeed, Langendorff-perfused murine hearts lacking *Pgc-1β* displayed features consistent with increased vulnerability to ventricular arrhythmia. These hearts demonstrate greater episodes of action potential alternans, known to presage arrhythmia, and more frequent episodes of ventricular tachycardia during programmed electrical stimulation (Gurung et al., 2011). Isolated cardiomyocytes from these hearts showed altered patterns of ion channel expression, spontaneous diastolic Ca^{2+}

transients, and pro-arrhythmic after-depolarisation events. The electrophysiological alterations and any associated change in arrhythmic propensity in the atria of these hearts have hitherto not been investigated.

A potential role for mitochondrial dysfunction in atrial arrhythmogenesis was investigated in the present work, utilising a murine model with homozygous deficiency of Pgc-1β. As the downstream effects of chronic mitochondrial deficits appear to accumulate with age, atrial electrophysiological parameters were evaluated in young and old *Pgc-1β*$^{-/-}$ animals and compared with age-matched WT mice. The experimental strategy employed a systematic approach beginning with baseline assessments in the in vivo setting, preserving all extra-cardiac and neurological inputs that may influence electrical activity of the heart, succeeded by ex vivo isolated heart preparations and finally tissue level studies.

7.2 Electrocardiographic features of adverse remodelling

The initial experiments sought to assess surface ECG markers of altered electrophysiological properties and arrhythmic tendency (chapter 3). Young (12-16 weeks) and aged (>52 weeks), WT and *Pgc-1β*$^{-/-}$ mice were anaesthetised and used for ECG recordings. Time intervals separating successive ECG deflections were analysed for differences between groups before and after β1-adrenergic (intraperitoneal dobutamine 3 mg/kg) challenge. Heart rates before dobutamine challenge were indistinguishable between groups. P wave duration, taken as a surrogate for overall atrial conduction, also did not significantly differ between WT and *Pgc-1β*$^{-/-}$ mice of any age. Slowed conduction increases the probability of re-entry and is thought to play a role in providing a substrate for re-entry and thus sustaining AF. In patients with a history of chronic AF, prolongation of the P wave duration was evident following successful DC cardioversion from AF to sinus rhythm (Kumagai *et al.*, 1991). However this prolongation was only observed during premature atrial beats but not during normal sinus beats. Additionally, in a separate study similarly assessing surface ECG parameters of atrial conduction, P wave duration did not differ significantly from those of control patients however there was greater heterogeneity in conduction properties across the atria in those

with AF (Holmqvist *et al.*, 2011). Thus the absence of a difference in P wave parameters between WT and *Pgc-1β*$^{-/-}$ mice during sinus rhythm is consistent with findings from human AF studies and does not discount an underlying atrial arrhythmic substrate.

Small or regional differences in atrial electrophysiological properties may be difficult to discern from surface ECGs and more readily observed in ventricular tissues owing to the large muscle mass and longer period of excitation. Analysis of indices of ventricular excitation and recovery revealed electrocardiographic features consistent with the existence of a pro-arrhythmic substrate in *Pgc-1β*$^{-/-}$ mice. Firstly, ventricular activation was prolonged in these mice consistent with slowed conduction. Additionally, *Pgc-1β*$^{-/-}$ mice had shorter ventricular repolarisation intervals, likely attributable to altered K^+ conductance properties, ultimately resulting in a shortened QT_c interval, which is known to be associated with increased arrhythmic risk.

The *Pgc-1β*$^{-/-}$ genotype was also associated with compromised nodal function in response to adrenergic challenge, manifest as an impaired heart rate response suggesting a defect at the level of the sino-atrial node, and a negative dromotropic response suggesting an atrioventricular conduction defect. Incidence of the latter was most pronounced in aged *Pgc-1β*$^{-/-}$ mice, suggesting progressive deterioration in AVN function in *Pgc-1β*$^{-/-}$ hearts with age. SAN dysfunction is largely a disease of ageing, the incidence of which increases exponentially with advancing age (Kusumoto *et al.*, 2002) and has classically been attributed to fibrosis and structural remodelling of the atria (LEV, 1964; Davies & Pomerance, 1972). Recent evidence has challenged this perception with mounting evidence suggesting age-related alterations in ionic currents may be responsible (Alings & Bouman, 1993; Jones *et al.*, 2007; Yanni *et al.*, 2010; Tellez *et al.*, 2011). Interestingly, fibrosis and ion channel remodelling may not be mutually exclusive mechanisms. Mice heterozygous for *SCN5A* display age-related fibrosis in the region of the SAN (Hao *et al.*, 2011) as well as more globally within the myocardium both in the atria and the ventricles (van Veen *et al.*, 2005). Electrical and structural remodelling may therefore synergistically contribute to the conduction system disease observed and portend towards remodelling processes that also influence susceptibility to atrial tachy-arrhythmias.

7.3 Conduction slowing and arrhythmic tendency in *Pgc-1β*$^{-/-}$ hearts

In chapter 4 the impact of ageing and mitochondrial insufficiency upon atrial arrhythmogenesis was investigated in a Langendorff-perfused preparation during regular pacing and in response to PES. Hearts were paced from the right atrium and the rhythm recorded using volume conductor ECGs giving information of the electrical activity at the organ level and sharp microelectrode recordings in the LA providing high fidelity representation of AP parameters at the cellular level. The *Pgc-1β*$^{-/-}$ genotype was associated with an arrhythmic atrial phenotype that progressed with age.

The simultaneous whole heart and cellular recordings enabled discrimination of local triggered activity from that of generalised atrial excitation. No triggered activity was observed in any experimental group and nor was there any evidence of spontaneous arrhythmias during intrinsic rhythms. Ectopic activity, predominantly arising from the PVs is thought to define the early stages of AF (Haïssaguerre *et al.*, 1998) and the absence of such phenomena in the *Pgc-1β*$^{-/-}$ model may reflect alternate mechanisms for genesis. Differences in the PV anatomy, especially pertaining to the architecture of the muscular sleeves, between murine and human hearts must be borne in mind. Additionally, the ex vivo preparation may have disrupted the integrity of the PV connections into the LA. Moreover, the lack of observed triggered activity in those left atrial cells impaled with sharp electrodes does not exclude triggered activity in other cells.

Whereas, imposition of premature extrasystoles during PES resulted in similar numbers of isolated ectopic beats and salvos (couplets) in WT and *Pgc-1β*$^{-/-}$ hearts, both young and aged, significantly greater number of arrhythmic episodes were observed in *Pgc-1β*$^{-/-}$ hearts, and this was most marked in aged *Pgc-1β*$^{-/-}$ hearts. These findings were compatible with mitochondrial impairment contributing to the generation of an atrial substrate supporting sustained arrhythmia, which progressed with age. Young and aged *Pgc-1β*$^{-/-}$ hearts showed evidence of slowed AP conduction at the cellular level, through deficits in maximum rates of AP depolarization $(dV/dt)_{max}$, and at the tissue level through prolonged AP latencies. APD_{90} and

atrial ERPs were indistinguishable between groups at baseline; however APD_{90} was significantly shorter in *Pgc-1β*$^{-/-}$ hearts at shorter stimulation intervals during PES. Electrical properties of individual APs triggering arrhythmia were nevertheless similar between WT and *Pgc-1β*$^{-/-}$ hearts.

These findings associate ageing and its accompanying mitochondrial deficits with the generation of a pro-arrhythmic atrial substrate, through slowed AP conduction and altered repolarisation characteristics. The absence of significant attenuation in APD and atrial ERPs at baseline in *Pgc-1β*$^{-/-}$ hearts, is at odds with the alterations seen in human atria following chronic AF. Shortening of the APD and ERP have been noted in various animal models of AF and human studies (Morillo *et al.*, 1995; Daoud *et al.*, 1996; Elvan *et al.*, 1996; Goette *et al.*, 1996). The divergence between the findings in this work and that of previous AF studies may represent mechanisms distinct from mitochondrial dysfunction generating the altered repolarisation properties in AF. It would seem from those earlier studies that the changes in repolarisation play a greater role in the initiation of AF whereas conduction slowing may be more relevant to the maintenance of AF in its chronic form and, in concert with the findings of the current work, mitochondrial impairment is linked to the latter (Morillo *et al.*, 1995; Wijffels *et al.*, 1995; Stiles *et al.*, 2009). The absence of differences in APD may also be a reflection of species-dependent differences in AP properties. In rodents, high I_{to} densities dominate all phases of repolarization and account for the significantly abbreviated APs, and absence of a clear plateau phase (Gussak *et al.*, 2000). These differences in ionic currents responsible for repolarisation and overall AP characteristics may underlie some of the variation in findings from those reported in alternate animal models.

7.4 APD restitution and propensity to atrial arrhythmias

To further explore the electrophysiological mechanisms responsible for the arrhythmic propensity associated with mitochondrial impairment, atrial restitution properties were assessed in *Pgc-1β*$^{-/-}$ hearts (chapter 5). APD restitution describes the phenomenon that APD shortens physiologically to preserve a sufficient DI in order to maintain blood flow during

rapid heart rates. The APD restitution hypothesis purports that when the slope of the APD restitution curve, in which APD is plotted against the preceding DI, exceeds unity AP alternans and wavebreak may ensue, leading to initiation and maintenance of fibrillation. It is thought that such temporal or dynamic heterogeneity is important pathophysiology of ventricular fibrillation, with previous studies reporting this to be an important feature of malignant ventricular arrhythmias resulting from LQTS and BrS (Moss & Kass, 2005; Sabir *et al.*, 2008*b*; Matthews *et al.*, 2010). However its relevance to AF has been far less well studied though a similar role in human AF has been postulated (Kim *et al.*, 2002; Narayan *et al.*, 2008; Krummen *et al.*, 2012).

In the current experiments the incidence of alternans or steepness of the restitution curves did not correlate with arrhythmic tendency. On the contrary, episodes of alternans in a variety of electrophysiological parameters was generally reduced in aged hearts, either WT or *Pgc-1β*$^{-/-}$, compared to young hearts. Ageing was also associated with flattening of the APD restitution curve, with this being most pronounced in the aged *Pgc-1β*$^{-/-}$ hearts – the most arrhythmic. In contrast, arrhythmogenecity correlated best with AP wavelength parameters as reported in the previous chapter where hearts were evaluated during regular pacing and S1S2 protocols.

Ro and colleagues constructed restitution curves for patients with chronic and paroxysmal AF, and compared these to controls individuals (Kim *et al.*, 2002). They reported paroxysmal AF was related to steeply sloped APD restitution kinetics, where chronic AF was associated with the greatest degree of spatiotemporal heterogeneity in electrophysiological parameters. APD alternans has also been shown to herald the degeneration of typical AFL to AF (Narayan *et al.*, 2002). However not all previous studies have reported such a positive correlation between the restitution profile and atrial arrhythmia. In a canine model, AF was difficult to induce despite the presence of steep APD restitution gradients in the majority of hearts (Burashnikov & Antzelevitch, 2005). Upon application of acetylcholine AF was far more easily induced, despite flattening of the restitution curves. Here the inducibility and persistence of AF appeared to reflect altered intracellular Ca^{2+} dynamics. In a more recent human study of atrial restitution in AF, steep APD restitution curves were reported in the LA adjacent to the PVs and correlated with inducibility of AF in response to rapid pacing in patients with

paroxysmal AF (Narayan *et al.*, 2008). However, restitution gradients were less steep in patients with a history of persistent AF and had no bearing on AF inducibility. In the latter group, the mechanism for AF induction appeared more related to marked conduction slowing. APD restitution may therefore promote wavebreak and reentry in the early stages of AF but have less of a role in established AF where significant electrical and structural remodelling has occurred, forming a heterogeneous atrial substrate with slowed conduction and altered anisotropy, favouring reentry. The authors suggested that in circumstances of marked increase in the latency of atrial activation, the electrical properties do not follow the classical features of restitution. Such would be consistent with the findings of the current work where significant alteration in in the underlying atrial substrate was evident. Indeed dynamic slowing of ventricular conduction promotes fibrillation in ventricles in the presence of rather flat restitution curves (Banville & Gray, 2002). In canine atria, conduction slowing from cellular uncoupling increased AF vulnerability independent APD dynamics or changes in restitution properties (Ohara *et al.*, 2002).

7.5 Electrical and structural remodelling in *Pgc-1β*$^{-/-}$ hearts

The experiments in chapters 3 – 5 demonstrated increased propensity to atrial arrhythmias in *Pgc-1β*$^{-/-}$ hearts that was principally a consequence of slowed conduction, evidenced by significant reductions in $(dV/dt)_{max}$, and corresponding increases in AP latency. The experiments in chapter 6 therefore sought to explore the mechanisms underlying conduction slowing associated with mitochondrial dysfunction. Previous experimental studies have suggested a range of mechanisms through which changes in AP propagation leading to increased arrhythmic tendency can take place. They have been attributed to alterations in Na^+ channel, gap junction function, and/or the consequences of fibrotic change (Mendez *et al.*, 1970; Spach *et al.*, 1982; Firouzi *et al.*, 2004; Remme *et al.*, 2006). These could potentially alter the major determinants of conduction velocity: transmembrane current, cell-to-cell coupling and cell capacitance.

A novel loose patch clamp techniques was utilised to measure transmembrane currents in

intact young and aged, WT and *Pgc-1β*$^{-/-}$, atrial cardiomyocyte preparations preserving their in vivo extracellular and intracellular conditions. Depolarising steps activated typical voltage-dependent activating and inactivating inward (Na^+) currents whose amplitude increased or decreased with the amplitudes of the activating, or preceding inactivating, steps. Maximum values of peak Na^+ current were independently influenced by genotype but not age or interacting effects of genotype and age. Both young and aged *Pgc-1β*$^{-/-}$ atria had significantly lower I_{Na} than that of WT preparations, correlating to the differences in $(dV/dt)_{max}$ values obtained from sharp electrode measurements. Neither genotype, nor age, whether independently or interactively, influenced voltages at half-maximal current, or steepness factors, for current activation and inactivation, or time constants for recovery from inactivation following repolarisation. In contrast, delayed outward (K^+) currents showed similar activation and rectification properties through all experimental groups, mirroring the observed absence of differences in repolarization properties between experimental groups.

These findings directly demonstrate and implicate reduced Na^+ as a mechanism for slowed conduction causing atrial arrhythmogenicity in *Pgc-1β*$^{-/-}$ hearts. Previous studies had failed to identify any changes in I_{Na} or its channel expression in AF (Bosch *et al.*, 1999; Brundel *et al.*, 2001*b*) however more recent patch clamp studies in atrial myocytes suggest such reductions in Nav function (Sossalla *et al.*, 2010). Mitochondrial dysfunction therefore represents means of adverse electrical remodelling predisposing to reentry and arrhythmogenesis.

Chronic AF is also associated with structural remodelling with progressive fibrosis. Mitochondrial impairment has been suggested to promote such fibrotic through fibroblast activation and production of transforming growth factor-β (TGF-β) (Friedrichs *et al.*, 2012). This was assessed in *Pgc-1β*$^{-/-}$ atria through morphometric analysis using picrosirius red staining. While WT and *Pgc-1β*$^{-/-}$ hearts demonstrated age-dependent fibrotic change, *Pgc-1β* deficiency was associated with accelerated fibrosis: young *Pgc-1β*$^{-/-}$ hearts displayed similar levels of fibrosis as aged WT, and aged *Pgc-1β*$^{-/-}$ hearts displayed the greatest fibrotic change. Disruption of normal myocardium with insulating connective tissue gives rise to conduction delay through non-uniform dispersion of current. The resulting current to load mismatches are seen in fibrotic myocardium (Spach *et al.*, 1988; de Bakker *et al.*, 1993) and have been shown

to impede AP propagation (Mendez *et al.*, 1970; Spach *et al.*, 1982). In canine models of fibrosis deposition of insulating extra-cellular matrix results in decoupling of myocytes leading to the interruption of both longitudinal and transverse cardiomyocyte-bundle continuity, producing zigzag conduction patterns (Spach & Boineau, 1997; Burstein *et al.*, 2009). Thus in addition to electrical remodelling, mitochondrial impairment promotes structural remodelling akin to that witnessed in human AF and recognised to participate in the production of a substrate favouring AF persistence.

7.6 Limitations

Animal models of clinical conditions have proven invaluable in investigations of pathogenic mechanisms of human disease and the development of putative therapies. Findings nonetheless cannot be directly translated to clinical conditions owing to species specific differences in physiology, and in turn pathophysiology, and inevitable limitations in experimental techniques.

As outlined in chapter 1, murine models have been instrumental in informing our understanding of arrhythmogenesis. However the murine cardiac AP varies from its human counterpart in number of way. The murine basal heart rate far exceeds that of humans reflecting difference in body size, and can accommodate a manifold increase in this upon exertion. This is reflected at the cellular level in a far more brisk action potential, lacking the pronounced plateau phase seen in larger mammals. In rodents, high I_{to} densities dominate all phases of repolarization and account for the significantly abbreviated APs, and absence of a clear plateau phase (Gussak *et al.*, 2000). However many of the processes remain conserved,, especially those relating to depolarisation and the mouse heart therefore remains a useful model for the study of both AP generation and propagation in atrial and ventricular arrhythmogenesis (Papadatos *et al.*, 2002). The absence of significant repolarisation differences between the WT and *Pgc-1β*$^{-/-}$ hearts is at variance to that seen in human studies of AF. The mechanisms underpinning this may be distinct from a metabolic imbalance, explaining the observations in this thesis. Alternatively, it may reflect specific difference in AP characteristics.

The murine model is particularly amenable to the study of genetic abnormalities however such an approach has caveats. It is possible that the targeted introduction of a mutation may lead to inadvertent alterations in the expression of other genes. The *Pgc-1β* knockout is known to alter the expression of a host of nuclear and mitochondrial-encoded genes involved in metabolism (Lelliott *et al.*, 2006). A more extensive study of the overall genetic profile has to date not been performed and it is possible that such unintended effects, if present, may alter the arrhythmic tendency of the animal. Species specific differences in the phenotypic impact of certain genetic abnormalities is also recognised. For example mutations in the *RyR2* are associated in humans with sudden cardiac death at a young age. The same mutation in a murine model a far less malignant and requires far more provocation to induce arrhythmia.

As mentioned in the relevant discussion sections, the long term cardiac electrophysiological evaluation of murine *Pgc-1β* knockout mice has not been performed and based upon the current findings, would be of use. Thus knowledge of its tendency to spontaneous arrhythmia is lacking. In reality, this does not detract from the current findings but may better inform us the long term consequences of chronic mitochondrial impairment. The murine surface ECG complex is clearly different to that of humans and the relative contributions of activation and repolarisation to the various waveform deflections remains unclear. The electrocardiographic evaluation of activation and repolarisation in this thesis was however extensively exhaustive to mitigate for the various possible permutations.

Arrhythmogenesis is understandably complex and influenced by factors outside of the heart. The isolated heart studies performed remove the heart from such extra-cardiac factors and is therefore a limitation. However, the preparations were identical for WT and *Pgc-1β*$^{-/-}$ hearts thus controlling for this. Moreover, in controlling for these factors, the cardiac consequences of mitochondrial dysfunction was obtained, clear of the confounds of such non-cardiac factors. The recently available means of organ or even chamber specific genetic alterations raises the possibility for more focussed studies in the future. The AP latency measurements utilised in the current work was taken as the time from stimulus delivery to the AP peak deflection. There may have been a degree of inter-heart variability in positioning of the stimulating and recording electrodes. However, electrode position was controlled by two precision micromanipulators and electrode position was consistent between hearts.

Additionally, a large number of recordings were taken to provide a more accurate overall representation of conduction and latency.

With these caveats borne in mind, the work presented in this thesis provides important insights into the role of mitochondrial impairment in atrial arrhythmias.

7.7 Future studies

The findings of this thesis form the foundation for several lines of further study. Mitochondrial impairment through homozygous deficiency of the transcriptional co-activator *Pgc-1β*$^{-/-}$ is associated with the development of an atrial substrate conducive to arrhythmia, predominantly through progressive electrical and structural remodelling causing slowed conduction. While no evidence of triggered activity that would initiate arrhythmia was observed, experimental limitations mean these cannot be conclusively discounted. Firstly, the experimental groups included aged animals to account for progressive abnormalities that are thought to develop with normal ageing and account for the age-related incidence of atrial arrhythmias (Go et al., 2001). Mice >52 weeks were used for ageing studies and demonstrated such age-related changes in arrhythmic parameters. However the average life expectancy of mice is over twice this and it is possible that further pro-arrhythmic phenomena including triggering events would develop over longer-term evaluation, as seen in humans. Secondly, the in vivo recordings were over a relatively brief period and conceivably insufficient to capture such events. Additionally, the ex vivo preparations may have disrupted the vascular connections required for such events to be conducted into the atrial body. More comprehensive evaluation would require long term in vivo evaluation of cardiac excitation through implantable telemeters. This would provide means to potentially capture isolated/regional triggered events and also spontaneous arrhythmic activity. The findings of this thesis provide the necessary justification for such a protracted and resource intensive undertaking.

The conduction slowing observed in *Pgc-1β*$^{-/-}$ hearts was, in part, secondary to reductions in I_{Na}. Multiple pathways can potentially modulate Na^+ channel function and therefore I_{Na},

including PKA mediated phosphorylation of Nav1.5 at serine 525 and 528 (Murphy *et al.*, 1996), G protein dependent pathways (Matsuda *et al.*, 1992), or phosphorylation at serine 1505 by protein kinase C (Qu *et al.*, 1996). Interestingly intracellular Ca^{2+} may itself exert direct regulatory effects on Na^+ channel function. Indeed the C-terminal of Na^+ channel constructs have been shown to contain two Ca^{2+} sensitive regions - a calmodulin binding, IQ, domain and a Ca^{2+} binding, EF-hand, motif (Wingo *et al.*, 2004; Chagot *et al.*, 2009). Elevated $[Ca^{2+}]_i$ both in cardiomyocytes in vitro (Casini *et al.*, 2009) and at the whole heart level following diastolic Ca^{2+} leaks result in reductions in I_{Na} density and $(dV/dt)_{max}$ (Zhang et al., 2009). Additionally mutations in RyR2 or proteins that interact with it give rise to diastolic Ca^{2+} release and are associated with reductions in I_{Na} (King *et al.*, 2013*b*; Li *et al.*, 2014; Glukhov *et al.*, 2015).

The *Pgc-1β*$^{-/-}$ dependent reductions in I_{Na} observed here may therefore potentially represent downstream effects of dysregulated Ca^{2+} handling. Beyond their role in ATP generation for ion homeostasis, cardiomyocyte mitochondria are spatially located in close proximity to the SR and are intimately involved in Ca^{2+} handling (García-Pérez *et al.*, 2008). Additionally isolated ventricular myocytes from *Pgc-1β*$^{-/-}$ hearts show spontaneous diastolic Ca^{2+} transients. Thus confocal microscopy of atrial cardiomyocytes and optical mapping studies of whole isolated atrial preparations would provide insights into possible Ca^{2+} handling abnormalities contributing to the arrhythmic substrate in *Pgc-1β*$^{-/-}$ atria.

Evidence of diastolic Ca^{2+} leak in these studies would also raise possibility of rescue manoeuvres. Recent studies have suggested that flecainide exerts anti-arrhythmic effects in human CPVT (Watanabe *et al.*, 2009; van der Werf *et al.*, 2011). Flecainide reduced ventricular bigeminy and VT, ECG features associated with human CPVT, in murine CSQ2$^{-/-}$ hearts. This anti-arrhythmic mechanism of flecainide in CPVT is thought to be distinct from its known inhibition of Na^+ channel activity, and arises through reduced RyR2-mediated diastolic Ca^{2+} release and consequent triggering events (Watanabe *et al.*, 2009; Hilliard *et al.*, 2010; Hwang *et al.*, 2011). Interestingly Ning et al (2016) reported paradoxical increases in I_{Na} in response to flecainide treatment in a murine model of CPVT (Ning et al., 2016). Here the reductions in diastolic Ca^{2+} transients prevent Ca^{2+} induced alterations in Nav activity thereby restoring I_{Na},

thus favourably maintaining AP wavelength and reducing the likelihood of reentry. Consistent with this, activation of cardiomyocyte RyR2 channels by exchange protein directly activated by cAMP (Epac) was recently shown to result in reductions in I_{Na} in murine atrial and ventricular tissue (Valli *et al.*, 2018). In this study, RyR2 inhibition with dantrolene restored the Epac mediated reductions in I_{Na} to baseline levels . Thus inhibition of abnormal diastolic Ca^{2+} transients of *Pgc-1β*$^{-/-}$ hearts may restore some of the features of electrical remodeling observed and potentially reduce incidence of arrhythmia in this group. This could be attempted with dantrolene as reported in the Epac study, and further with flecainide, which if successful, would represent a novel anti-AF mode of action for flecainide.

Several lines of study implicate oxidative stress in the pathogenesis of AF and mitochondria are a significant source of ROS in cardiac cells. It is likely that dysregulated production of ROS secondary to mitochondrial insufficiency play a role in the cardiac sequelae of *Pgc-1β* insufficiency. High-resolution respirometry would therefore be useful in comparisons of mitochondrial oxygen consumption. A number of studies have investigated the utility of anti-oxidant therapy in the prevention of AF, particularly in the post-operative setting (Baker *et al.*, 2009; Rodrigo *et al.*, 2013; Shi *et al.*, 2018). Pre-treating patients undergoing cardiac surgery with ascorbate attenuated features of adverse atrial electrical remodelling and reduced the incidence of AF post-operatively (Carnes *et al.*, 2001). However not all studies have replicated such promising results with similar interventions (Hemilä & Suonsyrjä, 2017). ROS are generally highly reactive molecules, and their intracellular location highly specialised. Anti-oxidants may therefore not be adequate in neutralizing ROS molecules before they exert their effect, or sufficiently reach the relevant sub-cellular compartment. The mitochondrial-targeted anti-oxidant MitoTempo was effective in reducing adverse remodeling, arrhythmic episodes and sudden death in a murine model of ventricular arrhythmias (Sovari *et al.*, 2013). Use of anti-oxidants, particularly the novel mitochondrial-targeted agents, initially in the ex-vivo and subsequently the in vivo system, may aid in evaluating the relative contribution of oxidative stress in the features observed and potential for mitigating the deleterious consequences.

It is clear from the experimental results reported in this thesis, *Pgc-1β* deficiency is associated

with wide ranging alterations in atrial electrophysiological properties. The cardiac AP is determined by the properties of a host of ionic channels and transporters, all of which are possible downstream effectors. Genetic analysis would represent an efficient means of characterising the electrophysiological alterations responsible and identifying potential targets for intervention. These experiments would therefore provide more comprehensive assessment of the atrial electrophysiological phenotype and the underlying mechanisms responsible for this.

7.8 Conclusion

Mitochondrial dysfunction is evident in age-related atrial arrhythmias such as atrial fibrillation, atrial flutter and atrial tachycardias. It is also a feature of conditions that are known to predispose to these arrhythmias. The work in this thesis implicates mitochondrial dysfunction in the pathogenesis of these atrial rhythm disturbances rather than being a bystander phenomenon. The *Pgc-1β*$^{-/-}$ murine model of chronic mitochondrial impairment results in an atrial arrhythmic phenotype that progresses with age. The principle determinates of this phenotype was slowed AP conduction through progressive electrical and structural remodelling. *Pgc-1β*$^{-/-}$ hearts have reduced I_{Na} with corresponding decrements in $(dV/dt)_{max}$. They also display accelerated fibrotic change, together manifesting as increased AP latency, thus producing an atrial substrate promoting reentry. As such, mitochondrial impairment may represent an upstream effector of arrhythmogenecity and further clarification of pathways involved may highlight novel targets for therapeutic interventions.

8 References

Ad N, Schneider A, Khaliulin I, Borman JB & Schwalb H (2005). Impaired mitochondrial response to simulated ischemic injury as a predictor of the development of atrial fibrillation after cardiac surgery: in vitro study in human myocardium. *J Thorac Cardiovasc Surg* **129,** 41–45.

Adabag S, Huxley RR, Lopez FL, Chen LY, Sotoodehnia N, Siscovick D, Deo R, Konety S, Alonso A & Folsom AR (2015). Obesity related risk of sudden cardiac death in the atherosclerosis risk in communities study. *Heart*; DOI: 10.1136/heartjnl-2014-306238.

Aiba T, Hesketh GG, Liu T, Carlisle R, Villa-Abrille MC, O'Rourke B, Akar FG & Tomaselli GF (2010). Na+ channel regulation by Ca(2+)/calmodulin and Ca(2+)/calmodulin-dependent protein kinase II in guinea-pig ventricular myocytes. *Cardiovasc Res* **85,** 454–463.

Aimé-Sempé C, Folliguet T, Rücker-Martin C, Krajewska M, Krajewska S, Heimburger M, Aubier M, Mercadier JJ, Reed JC & Hatem SN (1999). Myocardial cell death in fibrillating and dilated human right atria. *J Am Coll Cardiol* **34,** 1577–1586.

Akar FG & O'Rourke B (2011). Mitochondria are sources of metabolic sink and arrhythmias. *Pharmacol Ther* **131,** 287–294.

Aksnes TA, Schmieder RE, Kjeldsen SE, Ghani S, Hua TA & Julius S (2008). Impact of new-onset diabetes mellitus on development of atrial fibrillation and heart failure in high-risk hypertension (from the VALUE Trial). *Am J Cardiol* **101,** 634–638.

Alings AM & Bouman LN (1993). Electrophysiology of the ageing rabbit and cat sinoatrial node--a comparative study. *Eur Heart J* **14,** 1278–1288.

Allessie MA, Bonke FI & Schopman FJ (1973). Circus movement in rabbit atrial muscle as a mechanism of trachycardia. *Circ Res* **33,** 54–62.

Allessie MA, Bonke FI & Schopman FJ (1976). Circus movement in rabbit atrial muscle as a mechanism of tachycardia. II. The role of nonuniform recovery of excitability in the occurrence of unidirectional block, as studied with multiple microelectrodes. *Circ Res* **39,** 168–177.

Allessie MA, Bonke FI & Schopman FJ (1977). Circus movement in rabbit atrial muscle as a mechanism of tachycardia. III. The "leading circle" concept: a new model of circus movement in cardiac tissue without the involvement of an anatomical obstacle. *Circ Res* **41,** 9–18.

Allessie MA, Konings K, Kirchhof CJHJ & Wijffels M (1996). *Electrophysiologic mechanisms of perpetuation of atrial fibrillation*. Available at: https://ac.els-cdn.com/S000291499789114X/1-s2.0-S000291499789114X-main.pdf?_tid=b3220527-43a5-4d85-86a3-f860e2ae4cb0&acdnat=1536668832_735c55c70dc80040ce742ef8c61dd4e1 [Accessed September 11, 2018].

Almers W, Stanfield PR & Stühmer W (1983*a*). Slow changes in currents through sodium channels in

frog muscle membrane. *J Physiol* **339,** 253–271.

Almers W, Stanfield PR & Stühmer W (1983*b*). Lateral distribution of sodium and potassium channels in frog skeletal muscle: measurements with a patch-clamp technique. *J Physiol* **336,** 261–284.

Amos GJ, Wettwer E, Metzger F, Li Q, Himmel HM & Ravens U (1996). Differences between outward currents of human atrial and subepicardial ventricular myocytes. *J Physiol* **491 (Pt 1),** 31–50.

Antzelevitch C et al. (2007). Loss-of-function mutations in the cardiac calcium channel underlie a new clinical entity characterized by ST-segment elevation, short QT intervals, and sudden cardiac death. *Circulation* **115,** 442–449.

Antzelevitch C & Oliva A (2006). Amplification of spatial dispersion of repolarization underlies sudden cardiac death associated with catecholaminergic polymorphic VT, long QT, short QT and Brugada syndromes. *J Intern Med* **259,** 48–58.

Arany Z, He H, Lin J, Hoyer K, Handschin C, Toka O, Ahmad F, Matsui T, Chin S, Wu P-H, Rybkin II, Shelton JM, Manieri M, Cinti S, Schoen FJ, Bassel-Duby R, Rosenzweig A, Ingwall JS & Spiegelman BM (2005). Transcriptional coactivator PGC-1 alpha controls the energy state and contractile function of cardiac muscle. *Cell Metab* **1,** 259–271.

Armoundas AA, Osaka M, Mela T, Rosenbaum DS, Ruskin JN, Garan H & Cohen RJ (1998). T-wave alternans and dispersion of the QT interval as risk stratification markers in patients susceptible to sustained ventricular arrhythmias. *Am J Cardiol* **82,** 1127–1129, A9.

Arora R, Verheule S, Scott L, Navarrete A, Katari V, Wilson E, Vaz D & Olgin JE (2003). Arrhythmogenic Substrate of the Pulmonary Veins Assessed by High-Resolution Optical Mapping. *Circulation* **107,** 1816–1821.

Asghar O, Alam U, Hayat SA, Aghamohammadzadeh R, Heagerty AM & Malik RA (2012). Diabetes, obesity and atrial fibrillation: Epidemiology, mechanisms and interventions. *Curr Cardiol Rev* **8,** 253–264.

Ashpole NM, Herren AW, Ginsburg KS, Brogan JD, Johnson DE, Cummins TR, Bers DM & Hudmon A (2012). Ca2+/calmodulin-dependent protein kinase II (CaMKII) regulates cardiac sodium channel Nav1.5 gating by multiple phosphorylation sites. *J Biol Chem* **287,** 19856–19869.

Attuel P, Childers R, Cauchemez B, Poveda J, Mugica J & Coumel P (1982). Failure in the rate adaptation of the atrial refractory period: its relationship to vulnerability. *Int J Cardiol* **2,** 179–197.

Ausma J, van der Velden HMW, Lenders M-H, van Ankeren EP, Jongsma HJ, Ramaekers FCS, Borgers M & Allessie MA (2003). Reverse structural and gap-junctional remodeling after prolonged atrial fibrillation in the goat. *Circulation* **107,** 2051–2058.

Ausma J, Wijffels M, van Eys G, Koide M, Ramaekers F, Allessie M & Borgers M (1997*a*). Dedifferentiation of atrial cardiomyocytes as a result of chronic atrial fibrillation. *Am J Pathol* **151,** 985–997.

Ausma J, Wijffels M, Thoné F, Wouters L, Allessie M & Borgers M (1997*b*). Structural changes of atrial myocardium due to sustained atrial fibrillation in the goat. *Circulation* **96,** 3157–3163.

Baker WL, Anglade MW, Baker EL, White CM, Kluger J & Coleman CI (2009). Use of N-acetylcysteine to reduce post-cardiothoracic surgery complications: a meta-analysis. *Eur J Cardio-Thoracic Surg* **35,** 521–527.

de Bakker JM, van Capelle FJ, Janse MJ, Tasseron S, Vermeulen JT, de Jonge N & Lahpor JR (1993). Slow conduction in the infarcted human heart. "Zigzag" course of activation. *Circulation* **88,** 915–926.

Balana B, Dobrev D, Wettwer E, Christ T, Knaut M & Ravens U (2003). Decreased ATP-sensitive K(+) current density during chronic human atrial fibrillation. *J Mol Cell Cardiol* **35,** 1399–1405.

Banville I & Gray RA (2002). Effect of action potential duration and conduction velocity restitution and their spatial dispersion on alternans and the stability of arrhythmias. *J Cardiovasc Electrophysiol* **13,** 1141–1149.

Bapat A, Anderson CD, Ellinor PT & Lubitz SA (2018). Genomic basis of atrial fibrillation. *Heart* **104,** 201–206.

Barcellos-Hoff MH & Dix TA (1996). Redox-mediated activation of latent transforming growth factor-beta 1. *Mol Endocrinol* **10,** 1077–1083.

Barth AS & Tomaselli GF (2009). Cardiac metabolism and arrhythmias. *Circ Arrhythm Electrophysiol* **2,** 327–335.

Barth E, Stämmler G, Speiser B & Schaper J (1992). Ultrastructural quantitation of mitochondria and myofilaments in cardiac muscle from 10 different animal species including man. *J Mol Cell Cardiol* **24,** 669–681.

Bartos DC, Grandi E & Ripplinger CM (2015). Ion Channels in the Heart. In *Comprehensive Physiology*, pp. 1423–1464. John Wiley & Sons, Inc., Hoboken, NJ, USA. Available at: http://www.ncbi.nlm.nih.gov/pubmed/26140724 [Accessed September 29, 2018].

Bates MGD, Bourke JP, Giordano C, D'Amati G, Turnbull DM & Taylor RW (2012). Cardiac involvement in mitochondrial DNA disease: Clinical spectrum, diagnosis, and management. *Eur Heart J* **33,** 3023–3033.

Belevych AE, Terentyev D, Terentyeva R, Ho HT, Gyorke I, Bonilla IM, Carnes C a., Billman GE & Györke S (2012). Shortened Ca(2+) signaling refractoriness underlies cellular arrhythmogenesis in a postinfarction model of sudden cardiac death. *Circ Res* **110,** 569–577.

Benhorin J, Taub R, Goldmit M, Kerem B, Kass RS, Windman I & Medina A (2000). Effects of flecainide in patients with new SCN5A mutation: mutation-specific therapy for long-QT syndrome? *Circulation* **101,** 1698–1706.

Benjamin EJ, Wolf PA, D'Agostino RB, Silbershatz H, Kannel WB & Levy D (1998). Impact of atrial fibrillation on the risk of death: the Framingham Heart Study. *Circulation* **98,** 946–952.

Bernstein J (1902). Untersuchungen zur Thermodynamik der bioelektrischen Ströme. *Pflüger Arch für die Gesammte Physiol des Menschen und der Thiere* **92,** 521–562.

Bers DM (2002). Cardiac excitation-contraction coupling. *Nature* **415,** 198–205.

Bhalla S, Ozalp C, Fang S, Xiang L & Kemper JK (2004). Ligand-activated pregnane X receptor interferes with HNF-4 signaling by targeting a common coactivator PGC-1alpha. Functional implications in hepatic cholesterol and glucose metabolism. *J Biol Chem* **279,** 45139–45147.

Bhardwaj R (2012). Atrial fibrillation in a tertiary care institute – A prospective study. *Indian Heart J* **64,** 476–478.

Bhuiyan ZA, van den Berg MP, van Tintelen JP, Bink-Boelkens MTEE, Wiesfeld ACPP, Alders M, Postma A V., van Langen I, Mannens MMAMAM & Wilde AAMM (2007). Expanding spectrum of human RYR2-related disease: new electrocardiographic, structural, and genetic features. *Circulation* **116,** 1569–1576.

Biala AK, Dhingra R & Kirshenbaum LA (2015). Mitochondrial dynamics: Orchestrating the journey to advanced age. *J Mol Cell Cardiol* **83,** 37–43.

Di Biase L, Schweikert RA, Saliba WI, Horton R, Hongo R, Beheiry S, Borkhardt DJ & Natale A (2010). Left Atrial Appendage Tip: An Unusual Site of Successful Ablation After Failed Endocardial and Epicardial Mapping and Ablation. *J Cardiovasc Electrophysiol* **21,** 203–206.

Billman GE (2008). The cardiac sarcolemmal ATP-sensitive potassium channel as a novel target for anti-arrhythmic therapy. *Pharmacol Ther* **120,** 54–70.

Bootman MD, Higazi DR, Coombes S & Roderick HL (2006). Calcium signalling during excitation-contraction coupling in mammalian atrial myocytes. *J Cell Sci* **119,** 3915–3925.

Bosch RF, Zeng X, Grammer JB, Popovic K, Mewis C & Kuhlka V (1999). Ionic mechanisms of electrical remodeling in human atrial fibrillation. *Cardiovasc Res* **44,** 121–131.

Boukens BJ, Rivaud MR, Rentschler S & Coronel R (2014). Misinterpretation of the mouse ECG: "musing the waves of Mus musculus." *J Physiol* **21,** 4613–4626.

Bournat JC & Brown CW (2010). Mitochondrial dysfunction in obesity. *Curr Opin Endocrinol Diabetes Obes* **17,** 446–452.

Bovo E, Lipsius SL & Zima A V (2012). Reactive oxygen species contribute to the development of arrhythmogenic Ca^{2+} waves during β-adrenergic receptor stimulation in rabbit cardiomyocytes. *J Physiol* **590,** 3291–3304.

Bradshaw PJ, Stobie P, Knuiman MW, Briffa TG & Hobbs MST (2014). Trends in the incidence and prevalence of cardiac pacemaker insertions in an ageing population. *Open Hear* **1,** e000177.

Brooks AG, Stiles MK, Laborderie J, Lau DH, Kuklik P, Shipp NJ, Hsu L-F & Sanders P (2010). Outcomes of long-standing persistent atrial fibrillation ablation: A systematic review. *Hear Rhythm* **7,** 835–846.

Brooks WW & Conrad CH (2000). Myocardial Fibrosis in Transforming Growth Factor β1Heterozygous Mice. *J Mol Cell Cardiol* **32,** 187–195.

Brown DA & O'Rourke B (2010*b*). Cardiac mitochondria and arrhythmias. *Cardiovasc Res* **88,** 241–249.

Brubaker PH & Kitzman DW (2007). Prevalence and management of chronotropic incompetence in

heart failure. *Curr Cardiol Rep* **9,** 229–235.

Brubaker PH & Kitzman DW (2011). Chronotropic incompetence: Causes, consequences, and management. *Circulation* **123,** 1010–1020.

Brugada R, Hong K, Dumaine R, Cordeiro J, Gaita F, Borggrefe M, Menendez TM, Brugada J, Pollevick GD, Wolpert C, Burashnikov E, Matsuo K, Wu YS, Guerchicoff A, Bianchi F, Giustetto C, Schimpf R, Brugada P & Antzelevitch C (2004). Sudden Death Associated with Short-QT Syndrome Linked to Mutations in HERG. *Circulation* **109,** 30–35.

Brundel BJ, Van Gelder IC, Henning RH, Tieleman RG, Tuinenburg AE, Wietses M, Grandjean JG, Van Gilst WH & Crijns HJ (2001*a*). Ion channel remodeling is related to intraoperative atrial effective refractory periods in patients with paroxysmal and persistent atrial fibrillation. *Circulation* **103,** 684–690.

Brundel BJ, van Gelder IC, Henning RH, Tuinenburg AE, Deelman LE, Tieleman RG, Grandjean JG, van Gilst WH & Crijns HJ (1999). Gene expression of proteins influencing the calcium homeostasis in patients with persistent and paroxysmal atrial fibrillation. *Cardiovasc Res* **42,** 443–454.

Brundel BJ, Van Gelder IC, Henning RH, Tuinenburg AE, Wietses M, Grandjean JG, Wilde AA, Van Gilst WH & Crijns HJ (2001*b*). Alterations in potassium channel gene expression in atria of patients with persistent and paroxysmal atrial fibrillation: differential regulation of protein and mRNA levels for K+ channels. *J Am Coll Cardiol* **37,** 926–932.

Bukowska A, Schild L, Keilhoff G, Hirte D, Neumann M, Gardemann A, Neumann KH, Röhl F-W, Huth C, Goette A & Lendeckel U (2008). Mitochondrial dysfunction and redox signaling in atrial tachyarrhythmia. *Exp Biol Med (Maywood)* **233,** 558–574.

Burashnikov A & Antzelevitch C (2005). Role of repolarization restitution in the development of coarse and fine atrial fibrillation in the isolated canine right atria. *J Cardiovasc Electrophysiol* **16,** 639–645.

Burashnikov A & Antzelevitch C (2006). Late-Phase 3 EAD. A Unique Mechanism Contributing to Initiation of Atrial Fibrillation. *Pacing Clin Electrophysiol* **29,** 290–295.

Burstein B, Comtois P, Michael G, Nishida K, Villeneuve L, Yeh Y-H & Nattel S (2009). Changes in connexin expression and the atrial fibrillation substrate in congestive heart failure. *Circ Res* **105,** 1213–1222.

Caballero R, de la Fuente MG, Gómez R, Barana A, Amorós I, Dolz-Gaitón P, Osuna L, Almendral J, Atienza F, Fernández-Avilés F, Pita A, Rodríguez-Roda J, Pinto A, Tamargo J & Delpón E (2010). In humans, chronic atrial fibrillation decreases the transient outward current and ultrarapid component of the delayed rectifier current differentially on each atria and increases the slow component of the delayed rectifier current in both. *J Am Coll Cardiol* **55,** 2346–2354.

Cabrera JA, Ho SY, Climent V, Fuertes B, Murillo M & Sánchez-Quintana D (2009). Morphological evidence of muscular connections between contiguous pulmonary venous orifices: relevance of the interpulmonary isthmus for catheter ablation in atrial fibrillation. *Hear Rhythm* **6,** 1192–1198.

Camelliti P, Devlin GP, Matthews KG, Kohl P & Green CR (2004). Spatially and temporally distinct

expression of fibroblast connexins after sheep ventricular infarction. *Cardiovasc Res* **62,** 415–425.

Carnes CA, Chung MK, Nakayama T, Nakayama H, Baliga RS, Piao S, Kanderian A, Pavia S, Hamlin RL, McCarthy PM, Bauer JA & Van Wagoner DR (2001). Ascorbate attenuates atrial pacing-induced peroxynitrite formation and electrical remodeling and decreases the incidence of postoperative atrial fibrillation. *Circ Res* **89,** E32-8.

Carnes CA, Janssen PML, Ruehr ML, Nakayama H, Nakayama T, Haase H, Bauer JA, Chung MK, Fearon IM, Gillinov AM, Hamlin RL & Van Wagoner DR (2007). Atrial glutathione content, calcium current, and contractility. *J Biol Chem* **282,** 28063–28073.

Casini S, Verkerk AO, van Borren MMGJ, van Ginneken ACG, Veldkamp MW, de Bakker JMT & Tan HL (2009). Intracellular calcium modulation of voltage-gated sodium channels in ventricular myocytes. *Cardiovasc Res* **81,** 72–81.

Chadda K, Jeevaratnam K, Lei M & Huang CL-H (2017). Sodium channel biophysics, late sodium current and genetic arrhythmic syndromes. *Pflugers Arch* **469,** 629–641.

Chagot B, Potet F, Balser JR & Chazin WJ (2009). Solution NMR Structure of the C-terminal EF-hand Domain of Human Cardiac Sodium Channel Na v 1.5. *J Biol Chem* **284,** 6436–6445.

Chamberlain AM, Gersh BJ, Alonso A, Chen LY, Berardi C, Manemann SM, Killian JM, Weston SA & Roger VL (2015). Decade-long Trends in Atrial Fibrillation Incidence and Survival: A Community Study. *Am J Med* **128,** 260–267.e1.

Chamberlain AM, Redfield MM, Alonso A, Weston SA & Roger VL (2011). Atrial Fibrillation and Mortality in Heart Failure: A Community Study. *Circ Hear Fail* **4,** 740–746.

Chauhan VS, Downar E, Nanthakumar K, Parker JD, Ross HJ, Chan W & Picton P (2006). Increased ventricular repolarization heterogeneity in patients with ventricular arrhythmia vulnerability and cardiomyopathy: a human in vivo study. *Am J Physiol Circ Physiol* **290,** H79–H86.

Chelu MG, Sarma S, Sood S, Wang S, van Oort RJ, Skapura DG, Li N, Santonastasi M, Müller FU, Schmitz W, Schotten U, Anderson ME, Valderrábano M, Dobrev D & Wehrens XHT (2009). Calmodulin kinase II-mediated sarcoplasmic reticulum Ca2+ leak promotes atrial fibrillation in mice. *J Clin Invest* **119,** 1940–1951.

Chen F, De Diego C, Xie L-H, Yang J-H, Klitzner TS & Weiss JN (2007). Effects of metabolic inhibition on conduction, Ca transients, and arrhythmia vulnerability in embryonic mouse hearts. *AJP Hear Circ Physiol* **293,** H2472–H2478.

Chen YJC, Chen SA, Chen YJC, Yeh HI, Chan P, Chang MS & Lin CI (2001). Effects of rapid atrial pacing on the arrhythmogenic activity of single cardiomyocytes from pulmonary veins: implication in initiation of atrial fibrillation. *Circulation* **104,** 2849–2854.

Chiang C-E, Naditch-Brule L, Murin J, Goethals M, Inoue H, O'Neill J, Silva-Cardoso J, Zharinov O, Gamra H, Alam S, Ponikowski P, Lewalter T, Rosenqvist M & Steg PG (2012). Distribution and Risk Profile of Paroxysmal, Persistent, and Permanent Atrial Fibrillation in Routine Clinical Practice: Insight From the Real-Life Global Survey Evaluating Patients With Atrial Fibrillation International Registry. *Circ Arrhythmia Electrophysiol* **5,** 632–639.

Chilton L, Giles WR & Smith GL (2007). Evidence of intercellular coupling between co-cultured adult rabbit ventricular myocytes and myofibroblasts. *J Physiol* **583,** 225–236.

Chinchilla A, Daimi H, Lozano-Velasco E, Dominguez JN, Caballero R, Delpon E, Tamargo J, Cinca J, Hove-Madsen L, Aranega AE & Franco D (2011). PITX2 Insufficiency Leads to Atrial Electrical and Structural Remodeling Linked to Arrhythmogenesis. *Circ Cardiovasc Genet* **4,** 269–279.

Chou C-C, Nihei M, Zhou S, Tan A, Kawase A, Macias ES, Fishbein MC, Lin S-F & Chen P-S (2005). Intracellular Calcium Dynamics and Anisotropic Reentry in Isolated Canine Pulmonary Veins and Left Atrium. *Circulation* **111,** 2889–2897.

Christ T, Wettwer E, Voigt N, Hála O, Radicke S, Matschke K, Várro A, Dobrev D & Ravens U (2008). Pathology-specific effects of the IKur/Ito/IK,ACh blocker AVE0118 on ion channels in human chronic atrial fibrillation. *Br J Pharmacol* **154,** 1619–1630.

Chudin E, Goldhaber J, Garfinkel A, Weiss J & Kogan B (1999). Intracellular Ca(2+) dynamics and the stability of ventricular tachycardia. *Biophys J* **77,** 2930–2941.

Chugh SS, Havmoeller R, Narayanan K, Singh D, Rienstra M, Benjamin EJ, Gillum RF, Kim YH, McAnulty JH, Zheng ZJ, Forouzanfar MH, Naghavi M, Mensah GA, Ezzati M & Murray CJL (2014). Worldwide epidemiology of atrial fibrillation: A global burden of disease 2010 study. *Circulation*; DOI: 10.1161/CIRCULATIONAHA.113.005119.

Colilla S, Crow A, Petkun W, Singer DE, Simon T & Liu X (2013). Estimates of current and future incidence and prevalence of atrial fibrillation in the U.S. adult population. *Am J Cardiol* **112,** 1142–1147.

Comtois P, Kneller J & Nattel S (2005). Of circles and spirals: Bridging the gap between the leading circle and spiral wave concepts of cardiac reentry. *Europace* **7,** S10–S20.

Cushny AE (1899). ON THE INTERPRETATION OF PULSE-TRACINGS. *J Exp Med* **4,** 327–347.

Dai D-F, Santana LF, Vermulst M, Tomazela DM, Emond MJ, MacCoss MJ, Gollahon K, Martin GM, Loeb LA, Ladiges WC & Rabinovitch PS (2009). Overexpression of Catalase Targeted to Mitochondria Attenuates Murine Cardiac Aging. *Circulation* **119,** 2789–2797.

Danik S, Cabo C, Chiello C, Kang S, Wit AL & Coromilas J (2002). Correlation of repolarization of ventricular monophasic action potential with ECG in the murine heart. *Am J Physiol Heart Circ Physiol* **283,** H372-81.

Daoud EG, Bogun F, Goyal R, Harvey M, Man KC, Strickberger SA & Morady F (1996). Effect of atrial fibrillation on atrial refractoriness in humans. *Circulation* **94,** 1600–1606.

Darbar D, Kannankeril PJ, Donahue BS, Kucera G, Stubblefield T, Haines JL, George AL & Roden DM (2008). Cardiac Sodium Channel (SCN5A) Variants Associated with Atrial Fibrillation. *Circulation* **117,** 1927–1935.

Davidenko JM, Kent PF, Chialvo DR, Michaels DC & Jalife J (1990). Sustained vortex-like waves in normal isolated ventricular muscle. *Proc Natl Acad Sci U S A* **87,** 8785–8789.

Davidenko JM, Salomonsz R, Pertsov AM, Baxter WT & Jalife J (1995). Effects of pacing on stationary

reentrant activity. Theoretical and experimental study. *Circ Res* **77,** 1166–1179.

Davies L, Jin J, Shen W, Tsui H, Shi Y, Wang Y, Zhang Y, Hao G, Wu J, Chen S, Fraser JA, Dong N, Christoffels V, Ravens U, Huang CLH, Zhang H, Cartwright EJ, Wang X & Lei M (2014). Mkk4 is a negative regulator of the transforming growth factor beta 1 signaling associated with atrial remodeling and arrhythmogenesis with age. *J Am Heart Assoc*; DOI: 10.1161/JAHA.113.000340.

Davies MJ & Pomerance A (1972). Pathology of atrial fibrillation in man. *Br Heart J* **34,** 520–525.

Demolombe S, Lande G, Charpentier F, van Roon M, van den Hoff, MJ Toumaniantz G, Baro I, Guihard G, Le Berre N, Corbier A, de Bakker J, Opthof T, Wilde A, Moorman A & Escande D (2001). Transgenic mice overexpressing human KvLQT1 dominant-negative isoform. Part I: phenotypic characterisation. *Cardiovasc Res* **50,** 314–327.

Denruijter H, Berecki G, Opthof T, Verkerk A, Zock P & Coronel R (2007). Pro- and antiarrhythmic properties of a diet rich in fish oil. *Cardiovasc Res* **73,** 316–325.

Deo R & Albert CM (2012). Epidemiology and genetics of sudden cardiac death. *Circulation* **125,** 620–637.

DeWilde S, Carey IM, Emmas C, Richards N & Cook DG (2006). Trends in the prevalence of diagnosed atrial fibrillation, its treatment with anticoagulation and predictors of such treatment in UK primary care. *Heart* **92,** 1064–1070.

Dewland TA, Olgin JE, Vittinghoff E & Marcus GM (2013). Incident Atrial Fibrillation Among Asians, Hispanics, Blacks, and Whites. *Circulation* **128,** 2470–2477.

Dikalov SI & Ungvari Z (2013). Role of mitochondrial oxidative stress in hypertension. *Am J Physiol Heart Circ Physiol* **305,** H1417-27.

Dillon LM, Rebelo AP & Moraes CT (2012). The role of PGC-1 coactivators in aging skeletal muscle and heart. *IUBMB Life* **64,** 231–241.

Draper MH & Weidmann S (1951). Cardiac resting and action potentials recorded with an intracellular electrode. *J Physiol* **115,** 74–94.

Driesen RB, Verheyen FK, Schaart G, de Mazière A, Viebahn C, Prinzen FW, Lenders M-H, Debie W, Totzeck A, Borgers M & Ramaekers FCS (2009). Cardiotin localization in mitochondria of cardiomyocytes in vivo and in vitro and its down-regulation during dedifferentiation. *Cardiovasc Pathol* **18,** 19–27.

Dublin S, Glazer NL, Smith NL, Psaty BM, Lumley T, Wiggins KL, Page RL & Heckbert SR (2010). Diabetes mellitus, glycemic control, and risk of atrial fibrillation. *J Gen Intern Med* **25,** 853–858.

Dudley SC, Hoch NE, McCann LA, Honeycutt C, Diamandopoulos L, Fukai T, Harrison DG, Dikalov SI & Langberg J (2005). Atrial fibrillation increases production of superoxide by the left atrium and left atrial appendage: role of the NADPH and xanthine oxidases. *Circulation* **112,** 1266–1273.

Eager KR & Dulhunty AF (1998). Activation of the cardiac ryanodine receptor by sulfhydryl oxidation is modified by Mg2+ and ATP. *J Membr Biol* **163,** 9–18.

Eghbali M, Eghbali M, Robinson TF, Seifter S & Blumenfeld OO (1989). Collagen accumulation in heart ventricles as a function of growth and aging. *Cardiovasc Res* **23,** 723–729.

Ellis K, Wazni O, Marrouche N, Martin D, Gillinov M, McCarthy P, Saad EB, Bhargava M, Schweikert R, Saliba W, Bash D, Rossillo A, Erciyes D, Tchou P & Natale A (2007). Incidence of atrial fibrillation post-cavotricuspid isthmus ablation in patients with typical atrial flutter: left-atrial size as an independent predictor of atrial fibrillation recurrence. *J Cardiovasc Electrophysiol* **18,** 799–802.

Elvan A, Wylie K & Zipes DP (1996). Pacing-induced chronic atrial fibrillation impairs sinus node function in dogs. Electrophysiological remodeling. *Circulation* **94,** 2953–2960.

Emelyanova L, Ashary Z, Cosic M, Negmadjanov U, Ross G, Rizvi F, Olet S, Kress D, Sra J, Tajik AJ, Holmuhamedov EL, Shi Y & Jahangir A (2016). Selective downregulation of mitochondrial electron transport chain activity and increased oxidative stress in human atrial fibrillation. *Am J Physiol - Hear Circ Physiol* **311,** H54–H63.

Erickson JR, Joiner MA, Guan X, Kutschke W, Yang J, Oddis C V, Bartlett RK, Lowe JS, O'Donnell SE, Aykin-Burns N, Zimmerman MC, Zimmerman K, Ham A-JL, Weiss RM, Spitz DR, Shea MA, Colbran RJ, Mohler PJ & Anderson ME (2008). A dynamic pathway for calcium-independent activation of CaMKII by methionine oxidation. *Cell* **133,** 462–474.

Euler DE (1999). Cardiac alternans: mechanisms and pathophysiological significance. *Cardiovasc Res* **42,** 583–590.

Evans R & Shaw DB (1977). Pathological studies in sinoatrial disorder (sick sinus syndrome). *Br Heart J* **39,** 778–786.

Fabritz L, Kirchhof P, Franz MR, Eckardt L, Mönnig G, Milberg P, Breithardt G & Haverkamp W (2003*a*). Prolonged action potential durations, increased dispersion of repolarization, and polymorphic ventricular tachycardia in a mouse model of proarrhythmia. *Basic Res Cardiol* **98,** 25–32.

Fabritz L, Kirchhof P, Franz MR, Nuyens D, Rossenbacker T, Ottenhof A, Haverkamp W, Breithardt G, Carmeliet E & Carmeliet P (2003*b*). Effect of pacing and mexiletine on dispersion of repolarisation and arrhythmias in DeltaKPQ SCN5A (long QT3) mice. *Cardiovasc Res* **57,** 1085–1093.

Faivre JF & Findlay I (1990). Action potential duration and activation of ATP-sensitive potassium current in isolated guinea-pig ventricular myocytes. *Biochim Biophys Acta* **1029,** 167–172.

Fareh S, Villemaire C & Nattel S (1998). Importance of refractoriness heterogeneity in the enhanced vulnerability to atrial fibrillation induction caused by tachycardia-induced atrial electrical remodeling. *Circulation* **98,** 2202–2209.

Fermini B, Wang Z, Duan D & Nattel S (1992). Differences in rate dependence of transient outward current in rabbit and human atrium. *Am J Physiol* **263,** H1747-54.

Finck BN & Kelly DP (2006). PGC-1 coactivators: inducible regulators of energy metabolism in health and disease. *J Clin Invest* **116,** 615–622.

Firouzi M, Ramanna H, Kok B, Jongsma HJ, Koeleman BPC, Doevendans PA, Groenewegen WA & Hauer RNW (2004). Association of Human Connexin40 Gene Polymorphisms With Atrial Vulnerability as a Risk Factor for Idiopathic Atrial Fibrillation. *Circ Res* **95,** e29-33.

Fischbach PS, White A, Barrett TD & Lucchesi BR (2004). Risk of ventricular proarrhythmia with selective opening of the myocardial sarcolemmal versus mitochondrial ATP-gated potassium channel. *J Pharmacol Exp Ther* **309,** 554–559.

Flegel KM (1995). From delirium cordis to atrial fibrillation: historical development of a disease concept. *Ann Intern Med* **122,** 867–873.

Fosset M, De Weille JR, Green RD, Schmid-Antomarchi H & Lazdunski M (1988). Antidiabetic sulfonylureas control action potential properties in heart cells via high affinity receptors that are linked to ATP-dependent K+ channels. *J Biol Chem* **263,** 7933–7936.

Fraser JA, Huang CL-H & Pedersen TH (2011). Relationships between resting conductances, excitability, and t-system ionic homeostasis in skeletal muscle. *J Gen Physiol* **138,** 95–116.

Friberg L & Bergfeldt L (2013). Atrial fibrillation prevalence revisited. *J Intern Med* **274,** 461–468.

Friberg L, Hammar N, Pettersson H & Rosenqvist M (2007). Increased mortality in paroxysmal atrial fibrillation: report from the Stockholm Cohort-Study of Atrial Fibrillation (SCAF). *Eur Heart J* **28,** 2346–2353.

Friedrichs K, Baldus S & Klinke A (2012). Fibrosis in Atrial Fibrillation - Role of Reactive Species and MPO. *Front Physiol* **3,** 214.

Froehlich JP, Lakatta EG, Beard E, Spurgeon HA, Weisfeldt ML & Gerstenblith G (1978). Studies of sarcoplasmic reticulum function and contraction duration in young adult and aged rat myocardium. *J Mol Cell Cardiol* **10,** 427–438.

Frustaci A, Chimenti C, Bellocci F, Morgante E, Russo MA & Maseri A (1997). Histological substrate of atrial biopsies in patients with lone atrial fibrillation. *Circulation* **96,** 1180–1184.

Fujino M, Okada R & Arakawa K (1983). The relationship of aging to histological changes in the conduction system of the normal human heart. *Jpn Heart J* **24,** 13–20.

Fye WB (2006). Tracing Atrial Fibrillation — 100 Years. *N Engl J Med* **355,** 1412–1414.

Fynn SP, Todd DM, Hobbs WJC, Armstrong KL, Fitzpatrick AP & Garratt CJ (2002). Clinical evaluation of a policy of early repeated internal cardioversion for recurrence of atrial fibrillation. *J Cardiovasc Electrophysiol* **13,** 135–141.

Ganesan AN, Shipp NJ, Brooks AG, Kuklik P, Lau DH, Lim HS, Sullivan T, Roberts-Thomson KC & Sanders P (2013). Long-term Outcomes of Catheter Ablation of Atrial Fibrillation: A Systematic Review and Meta-analysis. *J Am Heart Assoc* **2,** e004549–e004549.

García-Pérez C, Hajnóczky G & Csordás G (2008). Physical Coupling Supports the Local Ca^{2+} Transfer between Sarcoplasmic Reticulum Subdomains and the Mitochondria in Heart Muscle. *J Biol Chem* **283,** 32771–32780.

Garesse R & Vallejo CG (2001). Animal mitochondrial biogenesis and function: a regulatory cross-talk between two genomes. *Gene* **263,** 1–16.

Garfinkel A, Kim YH, Voroshilovsky O, Qu Z, Kil JR, Lee MH, Karagueuzian HS, Weiss JN & Chen PS (2000). Preventing ventricular fibrillation by flattening cardiac restitution. *Proc Natl Acad Sci U S A* **97,** 6061–6066.

Garratt CJ, Duytschaever M, Killian M, Dorland R, Mast F & Allessie MA (1999). Repetitive electrical remodeling by paroxysms of atrial fibrillation in the goat: no cumulative effect on inducibility or stability of atrial fibrillation. *J Cardiovasc Electrophysiol* **10,** 1101–1108.

Garrey WE (1914). The nature of fibrllary .contraction of he heart —it's relation to tissue mass and form. *Am J Physiol Content* **33,** 397–414.

Gaspo R, Bosch RF, Bou-Abboud E & Nattel S (1997*a*). Tachycardia-induced changes in Na+ current in a chronic dog model of atrial fibrillation. *Circ Res* **81,** 1045–1052.

Gaspo R, Bosch RF, Talajic M & Nattel S (1997*b*). Functional mechanisms underlying tachycardia-induced sustained atrial fibrillation in a chronic dog model. *Circulation* **96,** 4027–4035.

Gazoti Debessa CR, Mesiano Maifrino LB & Rodrigues de Souza R (2001). Age related changes of the collagen network of the human heart. *Mech Ageing Dev* **122,** 1049–1058.

Gherghiceanu M, Hinescu ME, Andrei F, Mandache E, Macarie CE, Faussone-Pellegrini M-S & Popescu LM (2008). Interstitial Cajal-like cells (ICLC) in myocardial sleeves of human pulmonary veins. *J Cell Mol Med* **12,** 1777–1781.

Girotra S, Kitzman DW, Kop WJ, Stein PK, Gottdiener JS & Mukamal KJ (2012). Heart rate response to a timed walk and cardiovascular outcomes in older adults: the cardiovascular health study. *Cardiology* **122,** 69–75.

Glukhov A V., Kalyanasundaram A, Lou Q, Hage LT, Hansen BJ, Belevych AE, Mohler PJ, Knollmann BC, Periasamy M, Györke S & Fedorov V V. (2015). Calsequestrin 2 deletion causes sinoatrial node dysfunction and atrial arrhythmias associated with altered sarcoplasmic reticulum calcium cycling and degenerative fibrosis within the mouse atrial pacemaker complex1. *Eur Heart J* **36,** 686–697.

Go AS, Hylek EM, Phillips KA, Chang Y, Henault LE, Selby J V. & Singer DE (2001*a*). Prevalence of Diagnosed Atrial Fibrillation in Adults. *JAMA* **285,** 2370.

Go AS, Hylek EM, Phillips KA, Chang Y, Henault LE, Selby J V & Singer DE (2001*b*). Prevalence of diagnosed atrial fibrillation in adults: national implications for rhythm management and stroke prevention: the AnTicoagulation and Risk Factors in Atrial Fibrillation (ATRIA) Study. *JAMA* **285,** 2370–2375.

Goddard CA, Ghais NS, Zhang Y, Williams AJ, Colledge WH, Grace AA & Huang CL-H (2008). Physiological consequences of the *P2328S* mutation in the ryanodine receptor (*RyR2*) gene in genetically modified murine hearts. *Acta Physiol* **194,** 123–140.

Goette A, Honeycutt C & Langberg JJ (1996). Electrical remodeling in atrial fibrillation. Time course and mechanisms. *Circulation* **94,** 2968–2974.

Gold MR, Bloomfield DM, Anderson KP, El-Sherif NE, Wilber DJ, Groh WJ, Estes NA, Kaufman ES, Greenberg ML & Rosenbaum DS (2000). A comparison of T-wave alternans, signal averaged electrocardiography and programmed ventricular stimulation for arrhythmia risk stratification. *J Am Coll Cardiol* **36,** 2247–2253.

Goldbarg AN, Hellerstein HK, Bruell JH & Daroczy AF (1968). Electrocardiogram of the normal mouse, Mus Musculus: General considerations and genetic aspects. *Cardiovasc Res* **2,** 93–99.

Gollob MH, Redpath CJ & Roberts JD (2011). The short QT syndrome: Proposed diagnostic criteria. *J Am Coll Cardiol* **57,** 802–812.

Gomes AP, Price NL, Ling AJY, Moslehi JJ, Montgomery MK, Rajman L, White JP, Teodoro JS, Wrann CD, Hubbard BP, Mercken EM, Palmeira CM, De Cabo R, Rolo AP, Turner N, Bell EL & Sinclair DA (2013). Declining NAD+ induces a pseudohypoxic state disrupting nuclear-mitochondrial communication during aging. *Cell* **155,** 1624–1638.

Grandi E & Herren AW (2014). CaMKII-dependent regulation of cardiac Na(+) homeostasis. *Front Pharmacol* **5,** 41.

Grivennikova VG, Kareyeva A V & Vinogradov AD (2010). What are the sources of hydrogen peroxide production by heart mitochondria? *Biochim Biophys Acta* **1797,** 939–944.

Guijian L, Jinchuan Y, Rongzeng D, Jun Q, Jun W & Wenqing Z (2013). Impact of body mass index on atrial fibrillation recurrence: a meta-analysis of observational studies. *Pacing Clin Electrophysiol* **36,** 748–756.

Gurung IS, Medina-Gomez G, Kis A, Baker M, Velagapudi V, Neogi SG, Campbell M, Rodriguez-Cuenca S, Lelliott C, McFarlane I, Oresic M, Grace AA, Vidal-Puig A & Huang CL-H (2011). Deletion of the metabolic transcriptional coactivator PGC1beta induces cardiac arrhythmia. *Cardiovasc Res* **92,** 29–38.

Gussak I, Chaitman BR, Kopecky SL & Nerbonne JM (2000). Rapid ventricular repolarization in rodents: electrocardiographic manifestations, molecular mechanisms, and clinical insights. *J Electrocardiol* **33,** 159–170.

Hafner A V, Dai J, Gomes AP, Xiao C-Y, Palmeira CM, Rosenzweig A & Sinclair DA (2010). Regulation of the mPTP by SIRT3-mediated deacetylation of CypD at lysine 166 suppresses age-related cardiac hypertrophy. *Aging (Albany NY)* **2,** 914–923.

Haïssaguerre M, Jaïs P, Shah DC, Takahashi A, Hocini M, Quiniou G, Garrigue S, Le Mouroux A, Le Métayer P & Clémenty J (1998). Spontaneous Initiation of Atrial Fibrillation by Ectopic Beats Originating in the Pulmonary Veins. *N Engl J Med*; DOI: 10.1056/NEJM199809033391003.

Halligan SC, Gersh BJ, Brown RD, Rosales AG, Munger TM, Shen W-K, Hammill SC & Friedman PA (2004). The natural history of lone atrial flutter. *Ann Intern Med* **140,** 265–268.

Hao X, Zhang Y, Zhang X, Nirmalan M, Davies L, Konstantinou D, Yin F, Dobrzynski H, Wang X, Grace A, Zhang H, Boyett M, Huang CL-H & Lei M (2011). TGF-β1-mediated fibrosis and ion channel remodeling are key mechanisms in producing the sinus node dysfunction associated with SCN5A deficiency and aging. *Circ Arrhythm Electrophysiol* **4,** 397–406.

Hassink RJ, Aretz HT, Ruskin J & Keane D (2003). Morphology of atrial myocardium in human pulmonary veins: a postmortem analysis in patients with and without atrial fibrillation. *J Am Coll Cardiol* **42,** 1108–1114.

Hatch F, Lancaster MK & Jones SA (2011). Aging is a primary risk factor for cardiac arrhythmias: disruption of intracellular Ca $^{2+}$ regulation as a key suspect. *Expert Rev Cardiovasc Ther* **9,** 1059–1067.

Hayashi H, Wang C, Miyauchi Y, Omichi C, Pak H-N, Zhou S, OHARA T, MANDEL WJ, LIN S-F, FISHBEIN MC, CHEN P-S & KARAGUEUZIAN HS (2002). Aging-Related Increase to Inducible Atrial Fibrillation in the Rat Model. *J Cardiovasc Electrophysiol* **13,** 801–808.

Hemilä H & Suonsyrjä T (2017). Vitamin C for preventing atrial fibrillation in high risk patients: a systematic review and meta-analysis. *BMC Cardiovasc Disord* **17,** 49.

Hersi A, Abdul-Moneim M, Almous'ad A, Al-Samadi F, AlFagih A & Sweidan R (2015). Saudi Atrial Fibrillation Survey: national, observational, cross-sectional survey evaluating atrial fibrillation management and the cardiovascular risk profile of patients with atrial fibrillation. *Angiology* **66,** 244–248.

Higuchi T & Nakaya Y (1984). T wave polarity related to the repolarization process of epicardial and endocardial ventricular surfaces. *Am Heart J* **108,** 290–295.

Hilliard FA, Steele DS, Laver D, Yang Z, Le Marchand SJ, Chopra N, Piston DW, Huke S & Knollmann BC (2010). Flecainide inhibits arrhythmogenic Ca2+ waves by open state block of ryanodine receptor Ca2+ release channels and reduction of Ca2+ spark mass. *J Mol Cell Cardiol* **48,** 293–301.

Ho SY, Cabrera JA, Tran VH, Farré J, Anderson RH & Sánchez-Quintana D (2001). Architecture of the pulmonary veins: relevance to radiofrequency ablation. *Heart* **86,** 265–270.

Hobbs WJ, Fynn S, Todd DM, Wolfson P, Galloway M & Garratt CJ (2000). Reversal of atrial electrical remodeling after cardioversion of persistent atrial fibrillation in humans. *Circulation* **101,** 1145–1151.

Hocini M, Ho SY, Kawara T, Linnenbank AC, Potse M, Shah D, Jaïs P, Janse MJ, Haïssaguerre M & De Bakker JMT (2002). Electrical conduction in canine pulmonary veins: electrophysiological and anatomic correlation. *Circulation* **105,** 2442–2448.

Hodgkin AL & Nastuk WL (1949). Membrane potentials in single fibres of the frog's sartorius muscle. *J Physiol* **108,** Proc., 42.

Hoffman BF & Rosen MR (1981). Cellular mechanisms for cardiac arrhythmias. *Circ Res* **49,** 1–15.

Holmqvist F, Olesen MS, Tveit A, Enger S, Tapanainen J, Jurkko R, Havmöller R, Haunsø S, Carlson J, Svendsen JH & Platonov PG (2011). Abnormal atrial activation in young patients with lone atrial fibrillation. *Europace* **13,** 188–192.

Hondeghem LM & Katzung BG (1977). Time- and voltage-dependent interactions of antiarrhythmic drugs with cardiac sodium channels. *Biochim Biophys Acta* **472,** 373–398.

Hoppe UC, Johns DC, Marbán E & O'Rourke B (1999). Manipulation of cellular excitability by cell fusion: effects of rapid introduction of transient outward K+ current on the guinea pig action potential. *Circ Res* **84,** 964–972.

Hove-Madsen L, Llach A, Bayes-Genís A, Roura S, Rodriguez Font E, Arís A & Cinca J (2004). Atrial fibrillation is associated with increased spontaneous calcium release from the sarcoplasmic reticulum in human atrial myocytes. *Circulation* **110,** 1358–1363.

Hsieh M-H, Tai C-T, Chiang C-E, Tsai C-F, Yu W-C, Chen Y-J, Ding Y-A & Chen S-A (2002). Recurrent atrial flutter and atrial fibrillation after catheter ablation of the cavotricuspid isthmus: a very long-term follow-up of 333 patients. *J Interv Card Electrophysiol* **7,** 225–231.

Huang C (2017). Murine electrophysiological models of cardiac arrhythmogenesis. *Physiol Rev* **97,** 283–409.

Huang CL-H, Lei L, Matthews GDK, Zhang Y & Lei M (2012). Pathophysiological mechanisms of sino-atrial dysfunction and ventricular conduction disease associated with SCN5A deficiency: insights from mouse models. *Front Physiol* **3,** 234.

Hunter PJ, McNaughton PA & Noble D (1975). Analytical models of propagation in excitable cells. *Prog Biophys Mol Biol* **30,** 99–144.

Huss JM, Kopp RP & Kelly DP (2002). Peroxisome proliferator-activated receptor coactivator-1alpha (PGC-1alpha) coactivates the cardiac-enriched nuclear receptors estrogen-related receptor-alpha and -gamma. Identification of novel leucine-rich interaction motif within PGC-1alpha. *J Biol Chem* **277,** 40265–40274.

Huss JM, Torra IP, Staels B, Giguère V & Kelly DP (2004). Estrogen-related receptor alpha directs peroxisome proliferator-activated receptor alpha signaling in the transcriptional control of energy metabolism in cardiac and skeletal muscle. *Mol Cell Biol* **24,** 9079–9091.

Husser D, Adams V, Piorkowski C, Hindricks G & Bollmann A (2010). Chromosome 4q25 Variants and Atrial Fibrillation Recurrence After Catheter Ablation. *J Am Coll Cardiol* **55,** 747–753.

Hwang HS, Hasdemir C, Laver D, Mehra D, Turhan K, Faggioni M, Yin H & Knollmann BC (2011). Inhibition of cardiac Ca2+ release channels (RyR2) determines efficacy of class I antiarrhythmic drugs in catecholaminergic polymorphic ventricular tachycardia. *Circ Arrhythm Electrophysiol* **4,** 128–135.

Hwang M, Park J, Lee Y-S, Park JH, Choi SH, Shim EB & Pak H-N (2015). Fibrillation number based on wavelength and critical mass in patients who underwent radiofrequency catheter ablation for atrial fibrillation. *IEEE Trans Biomed Eng* **62,** 673–679.

Inoue K, Nakada K, Ogura A, Isobe K, Goto Y, Nonaka I & Hayashi J-I (2000). Generation of mice with mitochondrial dysfunction by introducing mouse mtDNA carrying a deletion into zygotes. *Nat Genet* **26,** 176–181.

Isik T, Tanboga IH, Kurt M, Kaya A, Ekinci M, Ayhan E, Uluganyan M, Ergelen M, Guvenc TS, Altay S & Uyarel H (2012). Relation of the metabolic syndrome with proarrhythmogenic electrocardiographic parameters in patients without overt diabetes. *Acta Cardiol* **67,** 195–201.

Iwasaki Y -k., Nishida K, Kato T & Nattel S (2011). Atrial Fibrillation Pathophysiology: Implications for Management. *Circulation* **124,** 2264–2274.

Jabre P, Roger VL, Murad MH, Chamberlain AM, Prokop L, Adnet F & Jouven X (2011). Mortality Associated With Atrial Fibrillation in Patients With Myocardial Infarction. *Circulation* **123,** 1587–1593.

Jaïs P, Hocini M, Macle L, Choi K-J, Deisenhofer I, Weerasooriya R, Shah DC, Garrigue S, Raybaud F, Scavee C, Le Metayer P, Clémenty J & Haïssaguerre M (2002). Distinctive electrophysiological properties of pulmonary veins in patients with atrial fibrillation. *Circulation* **106,** 2479–2485.

Jalife J, Berenfeld O, Skanes A & Mandapati R (1998). Mechanisms of atrial fibrillation: mother rotors or multiple daughter wavelets, or both? *J Cardiovasc Electrophysiol* **9,** S2-12.

January CT, Riddle JM & Salata JJ (1988). A model for early afterdepolarizations: induction with the Ca2+ channel agonist Bay K 8644. *Circ Res* **62,** 563–571.

Jeevaratnam K, Chadda KR, Huang CL-H & Camm AJ (2018). Cardiac Potassium Channels: Physiological Insights for Targeted Therapy. *J Cardiovasc Pharmacol Ther* **23,** 119–129.

Jeevaratnam K, Guzadhur L, Goh YM, Grace AA & Huang CL-H (2016). Sodium channel haploinsufficiency and structural change in ventricular arrhythmogenesis. *Acta Physiol* **216,** 186–202.

Jeevaratnam K, Poh Tee S, Zhang Y, Rewbury R, Guzadhur L, Duehmke R, Grace AA, Lei M & Huang CL-H (2011). Delayed conduction and its implications in murine Scn5a(+/-) hearts: independent and interacting effects of genotype, age, and sex. *Pflugers Arch* **461,** 29–44.

Jeevaratnam K, Rewbury R, Zhang Y, Guzadhur L, Grace AA, Lei M & Huang CL-H (2012). Frequency distribution analysis of activation times and regional fibrosis in murine Scn5a+/- hearts: The effects of ageing and sex. *Mech Ageing Dev* **133,** 591–599.

Jeevaratnam K, Zhang Y, Guzadhur L, Duehmke RM, Lei M, Grace AA & Huang CL-H (2010). Differences in sino-atrial and atrio-ventricular function with age and sex attributable to the Scn5a+/- mutation in a murine cardiac model. *Acta Physiol (Oxf)* **200,** 23–33.

Jensen PN, Thacker EL, Dublin S, Psaty BM & Heckbert SR (2013). Racial Differences in the Incidence of and Risk Factors for Atrial Fibrillation in Older Adults: The Cardiovascular Health Study. *J Am Geriatr Soc* **61,** 276–280.

Jiang D, Wang R, Xiao B, Kong H, Hunt DJ, Choi P, Zhang L & Chen SRW (2005). Enhanced store overload-induced Ca2+ release and channel sensitivity to luminal Ca2+ activation are common defects of RyR2 mutations linked to ventricular tachycardia and sudden death. *Circ Res* **97,** 1173–1181.

Johnson N, Danilo P, Wit AL & Rosen MR (1986). Characteristics of initiation and termination of catecholamine-induced triggered activity in atrial fibers of the coronary sinus. *Circulation* **74,** 1168–1179.

Jones SA, Boyett MR & Lancaster MK (2007). Declining Into Failure. *Circulation* **115,** 1183–1190.

Jones SA, Lancaster MK & Boyett MR (2004). Ageing-related changes of connexins and conduction within the sinoatrial node. *J Physiol* **560,** 429–437.

Jørgensen HS, Nakayama H, Reith J, Raaschou HO & Olsen TS (1996). Acute stroke with atrial fibrillation. The Copenhagen Stroke Study. *Stroke* **27,** 1765–1769.

Kabunga P, Lau AK, Phan K, Puranik R, Liang C, Davis RL, Sue CM & Sy RW (2015). Systematic review of cardiac electrical disease in Kearns-Sayre syndrome and mitochondrial cytopathy. *Int J Cardiol* **181,** 303–310.

Kakkar AK, Mueller I, Bassand J-P, Fitzmaurice DA, Goldhaber SZ, Goto S, Haas S, Hacke W, Lip GYH, Mantovani LG, Turpie AGG, van Eickels M, Misselwitz F, Rushton-Smith S, Kayani G, Wilkinson P, Verheugt FWA & GARFIELD Registry Investigators (2013). Risk profiles and antithrombotic treatment of patients newly diagnosed with atrial fibrillation at risk of stroke: perspectives from the international, observational, prospective GARFIELD registry. ed. Hernandez A V. *PLoS One* **8,** e63479.

Kalantarian S, Stern TA, Mansour M & Ruskin JN (2013). Cognitive Impairment Associated With Atrial Fibrillation. *Ann Intern Med* **158,** 338.

Kalin A, Usher-Smith J, Jones VJ, Huang CL-H & Sabir IN (2010). Cardiac arrhythmia: a simple conceptual framework. *Trends Cardiovasc Med* **20,** 103–107.

Katritsis D, Ioannidis JP, Anagnostopoulos CE, Sarris GE, Giazitzoglou E, Korovesis S & Camm AJ (2001). Identification and catheter ablation of extracardiac and intracardiac components of ligament of Marshall tissue for treatment of paroxysmal atrial fibrillation. *J Cardiovasc Electrophysiol* **12,** 750–758.

Katzung BG, Hondeghem LM & Grant AO (1975). Letter: Cardiac ventricular automaticity induced by current of injury. *Pflugers Arch* **360,** 193–197.

Kawakami Y, Tsuda M, Takahashi S, Taniguchi N, Esteban CR, Zemmyo M, Furumatsu T, Lotz M, Belmonte JCI & Asahara H (2005). Transcriptional coactivator PGC-1 regulates chondrogenesis via association with Sox9. *Proc Natl Acad Sci* **102,** 2414–2419.

Killeen MJ, Gurung IS, Thomas G, Stokoe KS, Grace AA & Huang CL-H (2007). Separation of early afterdepolarizations from arrhythmogenic substrate in the isolated perfused hypokalaemic murine heart through modifiers of calcium homeostasis. *Acta Physiol* **191,** 43–58.

Killeen MJ, Sabir IN, Grace AA & Huang CL-H (2008). Dispersions of repolarization and ventricular arrhythmogenesis: Lessons from animal models. *Prog Biophys Mol Biol* **98,** 219–229.

Kim B-S, Kim Y-H, Hwang G-S, Pak H-N, Lee SC, Shim WJ, Oh DJ & Ro YM (2002). Action potential duration restitution kinetics in human atrial fibrillation. *J Am Coll Cardiol* **39,** 1329–1336.

Kim YH, Lim DS, Lee JH, Lim D-S, Shim WJ, Ro YM, Park GH, Becker KG, Cho-Chung YS & Kim M-K (2003). Gene expression profiling of oxidative stress on atrial fibrillation in humans. *Exp Mol Med* **35,** 336–349.

King JH, Huang CL-H & Fraser JA (2013*a*). Determinants of myocardial conduction velocity: implications for arrhythmogenesis. *Front Physiol* **4,** 154.

King JH, Wickramarachchi C, Kua K, Du Y, Jeevaratnam K, Matthews HR, Grace AA, Huang CL-H & Fraser JA (2013*b*). Loss of Nav1.5 expression and function in murine atria containing the RyR2-P2328S gain-of-function mutation. *Cardiovasc Res* **99,** 751–759.

King JH, Zhang Y, Lei M, Grace AA, Huang CL-H & Fraser JA (2013*c*). Atrial arrhythmia, triggering events and conduction abnormalities in isolated murine RyR2-P2328S hearts. *Acta Physiol (Oxf)* **207,** 308–323.

Kirchhof P, Kahr PC, Kaese S, Piccini I, Vokshi I, Scheld H-H, Rotering H, Fortmueller L, Laakmann S, Verheule S, Schotten U, Fabritz L & Brown NA (2011). PITX2c Is Expressed in the Adult Left Atrium, and Reducing Pitx2c Expression Promotes Atrial Fibrillation Inducibility and Complex Changes in Gene Expression. *Circ Cardiovasc Genet* **4,** 123–133.

Knollmann BC, Blatt SA, Horton K, De Freitas F, Miller T, Bell M, Housmans PR, Weissman NJ, Morad M & Potter JD (2001*a*). Inotropic stimulation induces cardiac dysfunction in transgenic mice expressing a troponin T (I79N) mutation linked to familial hypertrophic cardiomyopathy. *J Biol Chem* **276,** 10039–10048.

Knollmann BC, Katchman AN & Franz MR (2001*b*). Monophasic action potential recordings from intact mouse heart: validation, regional heterogeneity, and relation to refractoriness. *J Cardiovasc Electrophysiol* **12,** 1286–1294.

Knutti D, Kaul A & Kralli A (2000). A tissue-specific coactivator of steroid receptors, identified in a functional genetic screen. *Mol Cell Biol* **20,** 2411–2422.

Koller BS, Karasik PE, Solomon AJ & Franz MR (1995). Relation between repolarization and refractoriness during programmed electrical stimulation in the human right ventricle. Implications for ventricular tachycardia induction. *Circulation* **91,** 2378–2384.

Korantzopoulos P, Kolettis TM, Galaris D & Goudevenos JA (2007). The role of oxidative stress in the pathogenesis and perpetuation of atrial fibrillation. *Int J Cardiol* **115,** 135–143.

Köster OF, Szigeti GP & Beuckelmann DJ (1999). Characterization of a [Ca2+]i-dependent current in human atrial and ventricular cardiomyocytes in the absence of Na+ and K+. *Cardiovasc Res* **41,** 175–187.

Kostin S, Klein G, Szalay Z, Hein S, Bauer EP & Schaper J (2002). Structural correlate of atrial fibrillation in human patients. *Cardiovasc Res* **54,** 361–379.

Krijthe BP, Kunst A, Benjamin EJ, Lip GYH, Franco OH, Hofman A, Witteman JCM, Stricker BH & Heeringa J (2013). Projections on the number of individuals with atrial fibrillation in the European Union, from 2000 to 2060. *Eur Heart J* **34,** 2746–2751.

Krummen DE, Bayer JD, Ho J, Ho G, Smetak MR, Clopton P, Trayanova NA & Narayan SM (2012). Mechanisms of Human Atrial Fibrillation Initiation: Clinical and Computational Studies of Repolarization Restitution and Activation Latency. *Circ Arrhythmia Electrophysiol* **5,** 1149–1159.

Kucharska-Newton AM, Couper DJ, Pankow JS, Prineas RJ, Rea TD, Sotoodehnia N, Chakravarti A, Folsom AR, Siscovick DS & Rosamond WD (2010). Diabetes and the risk of sudden cardiac death, the Atherosclerosis Risk in Communities study. *Acta Diabetol* **47 Suppl 1,** 161–168.

Kukreja RC, Okabe E, Schrier GM & Hess ML (1988). Oxygen radical-mediated lipid peroxidation and inhibition of Ca2+-ATPase activity of cardiac sarcoplasmic reticulum. *Arch Biochem Biophys* **261,** 447–457.

Kumagai K, Akimitsu S, Kawahira K, Kawanami F, Yamanouchi Y, Hiroki T & Arakawa K (1991). Electrophysiological properties in chronic lone atrial fibrillation. *Circulation* **84,** 1662–1668.

Kumagai K, Ogawa M, Noguchi H, Yasuda T, Nakashima H & Saku K (2004). Electrophysiologic properties of pulmonary veins assessed using a multielectrode basket catheter. *J Am Coll Cardiol* **43,** 2281–2289.

Kurokawa S, Niwano S, Niwano H, Ishikawa S, Kishihara J, Aoyama Y, Kosukegawa T, Masaki Y & Izumi T (2011). Progression of ventricular remodeling and arrhythmia in the primary hyperoxidative state of glutathione-depleted rats. *Circ J* **75,** 1386–1393.

Kusumoto FM, Phillips R & Goldschlager N (2002). Pacing therapy in the elderly. *Am J Geriatr Cardiol* **11,** 305–316.

Lai L-P, Tsai C-C, Su M-J, Lin J-L, Chen Y-S, Tseng Y-Z & Huang SKS (2003). Atrial fibrillation is associated with accumulation of aging-related common type mitochondrial DNA deletion mutation in human atrial tissue. *Chest* **123,** 539–544.

Lai L, Leone TC, Zechner C, Schaeffer PJ, Kelly SM, Flanagan DP, Medeiros DM, Kovacs A & Kelly DP (2008). Transcriptional coactivators PGC-1alpha and PGC-lbeta control overlapping programs required for perinatal maturation of the heart. *Genes Dev* **22,** 1948–1961.

Lai LP, Su MJ, Lin JL, Lin FY, Tsai CH, Chen YS, Huang SK, Tseng YZ & Lien WP (1999). Down-regulation of L-type calcium channel and sarcoplasmic reticular Ca(2+)-ATPase mRNA in human atrial fibrillation without significant change in the mRNA of ryanodine receptor, calsequestrin and phospholamban: an insight into the mechanism of atrial ele. *J Am Coll Cardiol* **33,** 1231–1237.

Lakatta EG & Sollott SJ (2002). Perspectives on mammalian cardiovascular aging: humans to molecules. *Comp Biochem Physiol A Mol Integr Physiol* **132,** 699–721.

Lamirault G, Gaborit N, Le Meur N, Chevalier C, Lande G, Demolombe S, Escande D, Nattel S, Léger JJ & Steenman M (2006). Gene expression profile associated with chronic atrial fibrillation and underlying valvular heart disease in man. *J Mol Cell Cardiol* **40,** 173–184.

Lane RK, Hilsabeck T & Rea SL (2015). The role of mitochondrial dysfunction in age-related diseases. *Biochim Biophys Acta - Bioenerg* **1847,** 1387–1400.

Larsson N-G, Garman JD, Oldfors A, Barsh GS & Clayton DA (1996). A single mouse gene encodes the mitochondrial transcription factor A and a testis–specific nuclear HMG-box protein. *Nat Genet* **13,** 296–302.

Larsson N-G, Wang J, Wilhelmsson H, Oldfors A, Rustin P, Lewandoski M, Barsh GS & Clayton DA (1998). Mitochondrial transcription factor A is necessary for mtDNA maintance and embryogenesis in mice. *Nat Genet* **18,** 231–236.

Lee KS, Marban E & Tsien RW (1985). Inactivation of calcium channels in mammalian heart cells: joint

dependence on membrane potential and intracellular calcium. *J Physiol* **364,** 395–411.

Lee SH, Lin FY, Yu WC, Cheng JJ, Kuan P, Hung CR, Chang MS & Chen SA (1999). Regional differences in the recovery course of tachycardia-induced changes of atrial electrophysiological properties. *Circulation* **99,** 1255–1264.

Lehman JJ, Barger PM, Kovacs A, Saffitz JE, Medeiros DM & Kelly DP (2000). Peroxisome proliferator-activated receptor gamma coactivator-1 promotes cardiac mitochondrial biogenesis. *J Clin Invest* **106,** 847–856.

Lei M, Goddard C, Liu J, Léoni A-L, Royer A, Fung SS-M, Xiao G, Ma A, Zhang H, Charpentier F, Vandenberg JI, Colledge WH, Grace AA & Huang CL-H (2005). Sinus node dysfunction following targeted disruption of the murine cardiac sodium channel gene Scn5a. *J Physiol* **567,** 387–400.

Lelliott CJ et al. (2006). Ablation of PGC-1β results in defective mitochondrial activity, thermogenesis, hepatic function, and cardiac performance ed. Barsh GS. *PLoS Biol* **4,** e369.

Lenegre J (1964). Etiology and pathology of bilateral bundle branch block in relation to complete heart block. *Prog Cardiovasc Dis* **6,** 409–444.

Leone TC & Kelly DP (2011). Transcriptional control of cardiac fuel metabolism and mitochondrial function. *Cold Spring Harb Symp Quant Biol* **76,** 175–182.

Lesnefsky EJ, Williams GR, Rubinstein JD, Hogue TS, Horwitz LD & Reiter MJ (1991). Hydrogen peroxide decreases effective refractory period in the isolated heart. *Free Radic Biol Med* **11,** 529–535.

Lev M (1964). Anatomic basis for atrioventricular block. *Am J Med* **37,** 742–748.

Lewis T (1921). Oliver-Sharpey Lectures ON THE NATURE OF FLUTTER AND FIBRILLATION OF THE AURICLE. *Br Med J* **1,** 551–555.

Li D, Fareh S, Leung TK & Nattel S (1999). Promotion of atrial fibrillation by heart failure in dogs: atrial remodeling of a different sort. *Circulation* **100,** 87–95.

Li N et al. (2014). Ryanodine receptor-mediated calcium leak drives progressive development of an atrial fibrillation substrate in a transgenic mouse model. *Circulation* **129,** 1276–1285.

Li W, Jin D, Hata M, Takai S, Yamanishi K, Shen W, El-Darawish Y, Yamanishi H & Okamura H (2016). Dysfunction of mitochondria and deformed gap junctions in the heart of IL-18-deficient mice. *Am J Physiol Heart Circ Physiol* **311,** H313-25.

Liang X, Xie H, Zhu P-H, Hu J, Zhao Q, Wang C-S & Yang C (2008). Ryanodine receptor-mediated Ca2+ events in atrial myocytes of patients with atrial fibrillation. *Cardiology* **111,** 102–110.

Lin J, Handschin C & Spiegelman BM (2005). Metabolic control through the PGC-1 family of transcription coactivators. *Cell Metab* **1,** 361–370.

Lin J, Lopez EF, Jin Y, Van Remmen H, Bauch T, Han H-C & Lindsey ML (2008). Age-related cardiac muscle sarcopenia: Combining experimental and mathematical modeling to identify

mechanisms. *Exp Gerontol* **43,** 296–306.

Lin PH, Lee SH, Su CP & Wei YH (2003). Oxidative damage to mitochondrial DNA in atrial muscle of patients with atrial fibrillation. *Free Radic Biol Med* **35,** 1310–1318.

Lin X, Wu N, Shi Y, Wang S, Tan K, Shen Y, Dai H & Zhong J (2015). Association between transforming growth factor β 1 and atrial fibrillation in essential hypertensive patients. *Clin Exp Hypertens* **37,** 82–87.

Lin Y-K, Lai M-S, Chen Y-C, Cheng C-C, Huang J-H, Chen S-A, Chen Y-J & Lin C-I (2012). Hypoxia and reoxygenation modulate the arrhythmogenic activity of the pulmonary vein and atrium. *Clin Sci (Lond)* **122,** 121–132.

Ling G & Gerard RW (1949). The normal membrane potential of frog sartorius fibers. *J Cell Comp Physiol* **34,** 383–396.

Lip GY, Bawden L, Hodson R, Rutland E, Snatchfold J & Beevers DG (1998). Atrial fibrillation amongst the Indo-Asian general practice population. The West Birmingham Atrial Fibrillation Project. *Int J Cardiol* **65,** 187–192.

Lip GY & Beevers DG (1995). ABC of atrial fibrillation. History, epidemiology, and importance of atrial fibrillation. *BMJ* **311,** 1361–1363.

Litovsky SH & Antzelevitch C (1988). Transient outward current prominent in canine ventricular epicardium but not endocardium. *Circ Res* **62,** 116–126.

Liu DW, Gintant GA & Antzelevitch C (1993). Ionic bases for electrophysiological distinctions among epicardial, midmyocardial, and endocardial myocytes from the free wall of the canine left ventricle. *Circ Res* **72,** 671–687.

Liu G, Iden JB, Kovithavongs K, Gulamhusein R, Duff HJ & Kavanagh KM (2004). In vivo temporal and spatial distribution of depolarization and repolarization and the illusive murine T wave. *J Physiol* **555,** 267–279.

Liu M, Liu H & Dudley SC (2010). Reactive oxygen species originating from mitochondria regulate the cardiac sodium channel. *Circ Res* **107,** 967–974.

Liu M, Sanyal S, Gao G, Gurung IS, Zhu X, Gaconnet G, Kerchner LJ, Shang LL, Huang CL-H, Grace A, London B & Dudley SC (2009). Cardiac Na+ current regulation by pyridine nucleotides. *Circ Res* **105,** 737–745.

Lloyd-Jones DM, Wang TJ, Leip EP, Larson MG, Levy D, Vasan RS, D'Agostino RB, Massaro JM, Beiser A, Wolf PA & Benjamin EJ (2004). Lifetime Risk for Development of Atrial Fibrillation: The Framingham Heart Study. *Circulation* **110,** 1042–1046.

London B (2001). Cardiac arrhythmias: from (transgenic) mice to men. *J Cardiovasc Electrophysiol* **12,** 1089–1091.

London B, Wang DW, Hill JA & Bennett PB (1998). The transient outward current in mice lacking the potassium channel gene Kv1.4. *J Physiol* **509,** 171–182.

Lu Z, Cui B, He B, Hu X, Wu W, Wu L, Huang C, Po SS & Jiang H (2011). Distinct restitution properties in vagally mediated atrial fibrillation and six-hour rapid pacing-induced atrial fibrillation. *Cardiovasc Res* **89,** 834–842.

Lübkemeier I, Andrié R, Lickfett L, Bosen F, Stöckigt F, Dobrowolski R, Draffehn AM, Fregeac J, Schultze JL, Bukauskas FF, Schrickel JW & Willecke K (2013). The Connexin40A96S mutation from a patient with atrial fibrillation causes decreased atrial conduction velocities and sustained episodes of induced atrial fibrillation in mice. *J Mol Cell Cardiol* **65,** 19–32.

Mackenzie J (1894). The Significance of the Venous Pulse. *Trans Medico-Chirurgical Soc Edinburgh* **13,** 69–74.

Mackenzie J (1904). Observations on the Inception of the Rhythm of the Heart by the Ventricle: As the cause of Continuous Irregularity of the Heart. *Br Med J* **1,** 529–536.

Mackenzie J (1905). New methods of studying affections of the heart. *Br Med J* **1,** 587–589.

Majeed A, Moser K & Carroll K (2001). Trends in the prevalence and management of atrial fibrillation in general practice in England and Wales, 1994-1998: analysis of data from the general practice research database. *Heart* **86,** 284–288.

Manning AS, Coltart DJ & Hearse DJ (1984). Ischemia and reperfusion-induced arrhythmias in the rat. Effects of xanthine oxidase inhibition with allopurinol. *Circ Res* **55,** 545–548.

Marionneau C, Couette B, Liu J, Li H, Mangoni ME, Nargeot J, Lei M, Escande D & Demolombe S (2005). Specific pattern of ionic channel gene expression associated with pacemaker activity in the mouse heart. *J Physiol* **562,** 223–234.

Martin CA, Grace AA & Huang CL-H (2011*a*). Refractory dispersion promotes conduction disturbance and arrhythmias in a Scn5a (+/-) mouse model. *Pflugers Arch* **462,** 495–504.

Martin CA, Guzadhur L, Grace AA, Lei M & Huang CL-H (2011*b*). Mapping of reentrant spontaneous polymorphic ventricular tachycardia in a Scn5a+/- mouse model. *Am J Physiol Heart Circ Physiol* **300,** H1853–H1862.

Martin CA, Matthews GDK & Huang CL-H (2012*a*). Sudden cardiac death and inherited channelopathy: the basic electrophysiology of the myocyte and myocardium in ion channel disease. *Heart* **98,** 536–543.

Martin CA, Siedlecka U, Kemmerich K, Lawrence J, Cartledge J, Guzadhur L, Brice N, Grace AA, Schwiening C, Terracciano CM & Huang CL-. H (2012*b*). Reduced Na(+) and higher K(+) channel expression and function contribute to right ventricular origin of arrhythmias in Scn5a+/- mice. *Open Biol* **2,** 120072.

Martin CA, Zhang Y, Grace AA & Huang CL-H (2010*a*). In vivo studies of Scn5a+/− mice modeling Brugada syndrome demonstrate both conduction and repolarization abnormalities. *J Electrocardiol* **43,** 433–439.

Martin CA, Zhang Y, Grace AA & Huang CL-H (2010*b*). Increased right ventricular repolarization gradients promote arrhythmogenesis in a murine model of Brugada Syndrome. *J Cardiovasc Electrophysiol* **21,** 1153–1159.

Marzona I, O'Donnell M, Teo K, Gao P, Anderson C, Bosch J & Yusuf S (2012). Increased risk of cognitive and functional decline in patients with atrial fibrillation: results of the ONTARGET and TRANSCEND studies. *CMAJ* **184,** E329-36.

Masani F (1986). Node-like cells in the myocardial layer of the pulmonary vein of rats: an ultrastructural study. *J Anat* **145,** 133–142.

Massumi RA & Ali N (1970). Accelerated isorhythmic ventricular rhythms. *Am J Cardiol* **26,** 170–185.

Matsuda JJ, Lee H & Shibata EF (1992). Enhancement of rabbit cardiac sodium channels by beta-adrenergic stimulation. *Circ Res* **70,** 199–207.

Matthews GDK, Guzadhur L, Grace A & Huang CL-H (2012). Nonlinearity between action potential alternans and restitution, which both predict ventricular arrhythmic properties in Scn5a+/- and wild-type murine hearts. *J Appl Physiol* **112,** 1847–1863.

Matthews GDK, Guzadhur L, Sabir IN, Grace AA & Huang CL-H (2013). Action potential wavelength restitution predicts alternans and arrhythmia in murine Scn5a+/− hearts. *J Physiol* **591,** 4167–4188.

Matthews GDK, Martin CA, Grace AA, Zhang Y & Huang CL-H (2010). Regional variations in action potential alternans in isolated murine Scn5a (+/-) hearts during dynamic pacing. *Acta Physiol (Oxf)* **200,** 129–146.

Mayer J (1906). *Rhythmical Pulsation in Scyphomedusae*. Carnegie Institution of Washington, Washington, D.C. : Available at: https://www.biodiversitylibrary.org/item/76072 [Accessed September 29, 2018].

McManus DD, Hsu G, Sung SH, Saczynski JS, Smith DH, Magid DJ, Gurwitz JH, Goldberg RJ, Go AS & Cardiovascular Research Network PRESERVE Study (2013). Atrial Fibrillation and Outcomes in Heart Failure With Preserved Versus Reduced Left Ventricular Ejection Fraction. *J Am Heart Assoc* **2,** e005694–e005694.

McMichael J (1982). History of atrial fibrillation 1628-1819 Harvey - de Senac - Laënnec. *Br Heart J* **48,** 193–197.

McWilliam JA (1887). Fibrillar Contraction of the Heart. *J Physiol* **8,** 296–310.

De Mello WC (1983). The role of cAMP and Ca on the modulation of junctional conductance: an integrated hypothesis. *Cell Biol Int Rep* **7,** 1033–1040.

Melnyk P, Ehrlich JR, Pourrier M, Villeneuve L, Cha T-J & Nattel S (2005). Comparison of ion channel distribution and expression in cardiomyocytes of canine pulmonary veins versus left atrium. *Cardiovasc Res* **65,** 104–116.

Mendez C, Mueller WJ & Urguiaga X (1970). Propagation of impulses across the Prukinje fiber-muscle junctions in the dog heart. *Circ Res* **26,** 135–150.

Menezes AR, Lavie CJ, Dinicolantonio JJ, O'Keefe J, Morin DP, Khatib S, Abi-Samra FM, Messerli FH & Milani R V (2013*a*). Cardiometabolic risk factors and atrial fibrillation. *Rev Cardiovasc Med* **14,** e73-81.

Menezes AR, Lavie CJ, DiNicolantonio JJ, O'Keefe J, Morin DP, Khatib S & Milani R V. (2013*b*). Atrial Fibrillation in the 21st Century: A Current Understanding of Risk Factors and Primary Prevention Strategies. *Mayo Clin Proc* **88,** 394–409.

Michael LF, Wu Z, Cheatham RB, Puigserver P, Adelmant G, Lehman JJ, Kelly DP & Spiegelman BM (2001). Restoration of insulin-sensitive glucose transporter (GLUT4) gene expression in muscle cells by the transcriptional coactivator PGC-1. *Proc Natl Acad Sci U S A* **98,** 3820–3825.

Middeldorp ME, Pathak RK, Meredith M, Mehta AB, Elliott AD, Mahajan R, Twomey D, Gallagher C, Hendriks JML, Linz D, McEvoy RD, Abhayaratna WP, Kalman JM, Lau DH & Sanders P (2018). PREVEntion and regReSsive Effect of weight-loss and risk factor modification on Atrial Fibrillation: the REVERSE-AF study. *EP Eur*; DOI: 10.1093/europace/euy117.

Mihm MJ, Yu F, Carnes CA, Reiser PJ, McCarthy PM, Van Wagoner DR & Bauer JA (2001). Impaired myofibrillar energetics and oxidative injury during human atrial fibrillation. *Circulation* **104,** 174–180.

Milberg P, Reinsch N, Wasmer K, Monnig G, Stypmann J, Osada N, Breithardt G, Haverkamp W & Eckardt L (2005). Transmural dispersion of repolarization as a key factor of arrhythmogenicity in a novel intact heart model of LQT3. *Cardiovasc Res* **65,** 397–404.

Milton RL & Caldwell JH (1990). Na current in membrane blebs: implications for channel mobility and patch clamp recording. *J Neurosci* **10,** 885–893.

Mines GR (1913). On dynamic equilibrium in the heart. *J Physiol* **46,** 349–383.

Mitchell GF, Jeron A & Koren G (1998). Measurement of heart rate and Q-T interval in the conscious mouse. *Am J Physiol*; DOI: n.a.

Miyamoto K, Tsuchiya T, Narita S, Yamaguchi T, Nagamoto Y, Ando S -i., Hayashida K, Tanioka Y & Takahashi N (2009). Bipolar electrogram amplitudes in the left atrium are related to local conduction velocity in patients with atrial fibrillation. *Europace* **11,** 1597–1605.

Miyasaka Y, Barnes ME, Bailey KR, Cha SS, Gersh BJ, Seward JB & Tsang TSM (2007). Mortality Trends in Patients Diagnosed With First Atrial Fibrillation. *J Am Coll Cardiol* **49,** 986–992.

Miyasaka Y, Barnes ME, Gersh BJ, Cha SS, Bailey KR, Abhayaratna WP, Seward JB & Tsang TSM (2006). Secular Trends in Incidence of Atrial Fibrillation in Olmsted County, Minnesota, 1980 to 2000, and Implications on the Projections for Future Prevalence. *Circulation* **114,** 119–125.

Moe GK (1956). Cardiac arrhythmias; introductory remarks. *Ann N Y Acad Sci* **64,** 540–542.

Moe GK & Abildskov JA (1959). Atrial fibrillation as a self-sustaining arrhythmia independent of focal discharge. *Am Heart J* **58,** 59–70.

Moe GK, Rheinboldt WC & Abildskov JA (1964). A COMPUTER MODEL OF ATRIAL FIBRILLATION. *Am Heart J* **67,** 200–220.

Montaigne D, Marechal X, Lefebvre P, Modine T, Fayad G, Dehondt H, Hurt C, Coisne A, Koussa M, Remy-Jouet I, Zerimech F, Boulanger E, Lacroix D, Staels B & Neviere R (2013). Mitochondrial Dysfunction as an Arrhythmogenic Substrate. *J Am Coll Cardiol* **62,** 1466–1473.

Mootha VK et al. (2003). PGC-1α-responsive genes involved in oxidative phosphorylation are coordinately downregulated in human diabetes. *Nat Genet*; DOI: 10.1038/ng1180.

Morel E, Meyronet D, Thivolet-Bejuy F & Chevalier P (2008). Identification and distribution of interstitial Cajal cells in human pulmonary veins. *Hear Rhythm* **5,** 1063–1067.

Mori M, Konno T, Ozawa T, Murata M, Imoto K & Nagayama K (2000). Novel interaction of the voltage-dependent sodium channel (VDSC) with calmodulin: does VDSC acquire calmodulin-mediated Ca2+-sensitivity? *Biochemistry* **39,** 1316–1323.

Morillo CA, Klein GJ, Jones DL & Guiraudon CM (1995). Chronic rapid atrial pacing. Structural, functional, and electrophysiological characteristics of a new model of sustained atrial fibrillation. *Circulation* **91,** 1588–1595.

Moss AJ & Kass RS (2005). Long QT syndrome: from channels to cardiac arrhythmias. *J Clin Invest* **115,** 2018–2024.

Mozaffarian D, Furberg CD, Psaty BM & Siscovick D (2008). Physical Activity and Incidence of Atrial Fibrillation in Older Adults: The Cardiovascular Health Study. *Circulation* **118,** 800–807.

Murphy BJ, Rogers J, Perdichizzi AP, Colvin AA & Catterall WA (1996). cAMP-dependent phosphorylation of two sites in the alpha subunit of the cardiac sodium channel. *J Biol Chem* **271,** 28837–28843.

Näbauer M, Beuckelmann DJ, Uberfuhr P & Steinbeck G (1996). Regional differences in current density and rate-dependent properties of the transient outward current in subepicardial and subendocardial myocytes of human left ventricle. *Circulation* **93,** 168–177.

Nakada K, Inoue K, Ono T, Isobe K, Ogura A, Goto Y-I, Nonaka I & Hayashi J-I (2001). Inter-mitochondrial complementation: Mitochondria-specific system preventing mice from expression of disease phenotypes by mutant mtDNA. *Nat Med* **7,** 934–940.

Nanthakumar K, Lau YR, Plumb VJ, Epstein AE & Kay GN (2004). Electrophysiological Findings in Adolescents With Atrial Fibrillation Who Have Structurally Normal Hearts. *Circulation* **110,** 117–123.

Narayan SM, Bode F, Karasik PL & Franz MR (2002). Alternans of atrial action potentials during atrial flutter as a precursor to atrial fibrillation. *Circulation* **106,** 1968–1973.

Narayan SM, Kazi D, Krummen DE & Rappel W-J (2008). Repolarization and Activation Restitution Near Human Pulmonary Veins and Atrial Fibrillation Initiation. *J Am Coll Cardiol* **52,** 1222–1230.

Narayan SM, Krummen DE, Shivkumar K, Clopton P, Rappel W-J & Miller JM (2012). Treatment of Atrial Fibrillation by the Ablation of Localized Sources. *J Am Coll Cardiol* **60,** 628–636.

Nearing BD, Huang AH & Verrier RL (1991). Dynamic tracking of cardiac vulnerability by complex demodulation of the T wave. *Science* **252,** 437–440.

Neef S, Dybkova N, Sossalla S, Ort KR, Fluschnik N, Neumann K, Seipelt R, Schöndube FA, Hasenfuss G & Maier LS (2010). CaMKII-dependent diastolic SR Ca2+ leak and elevated diastolic Ca2+ levels in right atrial myocardium of patients with atrial fibrillation. *Circ Res* **106,**

1134–1144.

Nerbonne JM & Guo W (2002). Heterogeneous expression of voltage-gated potassium channels in the heart: roles in normal excitation and arrhythmias. *J Cardiovasc Electrophysiol* **13,** 406–409.

Nerbonne JM & Kass RS (2005). Molecular Physiology of Cardiac Repolarization. *Physiol Rev* **85,** 1205–1253.

Neuberger H-R, Schotten U, Verheule S, Eijsbouts S, Blaauw Y, van Hunnik A & Allessie M (2005). Development of a substrate of atrial fibrillation during chronic atrioventricular block in the goat. *Circulation* **111,** 30–37.

Nguyen BL, Fishbein MC, Chen LS, Chen P-S & Masroor S (2009). Histopathological substrate for chronic atrial fibrillation in humans. *Hear Rhythm* **6,** 454–460.

Nichols GA, Reinier K & Chugh SS (2009). Independent contribution of diabetes to increased prevalence and incidence of atrial fibrillation. *Diabetes Care* **32,** 1851–1856.

Ning F, Luo L, Ahmad S, Valli H, Jeevaratnam K, Wang T, Guzadhur L, Yang D, Fraser J, Huang C-H, Ma A & Salvage S (2016). The RyR2-P2328S mutation downregulates Na(v)1.5 producing arrhythmic substrate in murine ventricles. *Pflugers Arch* **468,** 655–665.

Nisbet AM, Camelliti P, Walker NL, Burton FL, Cobbe SM, Kohl P & Smith GL (2016). Prolongation of atrio-ventricular node conduction in a rabbit model of ischaemic cardiomyopathy: Role of fibrosis and connexin remodelling. *J Mol Cell Cardiol* **94,** 54–64.

Nolasco JB & Dahlen RW (1968). A graphic method for the study of alternation in cardiac action potentials. *J Appl Physiol* **25,** 191–196.

Noma A (1983). ATP-regulated K+ channels in cardiac muscle. *Nature* **305,** 147–148.

O'Rourke B (2007). Mitochondrial ion channels. *Annu Rev Physiol* **69,** 19–49.

Ohara T, Qu Z, Lee M-H, Ohara K, Omichi C, Mandel WJ, Chen P-S & Karagueuzian HS (2002). Increased vulnerability to inducible atrial fibrillation caused by partial cellular uncoupling with heptanol. *Am J Physiol Heart Circ Physiol* **283,** H1116-22.

Olson TM, Michels V V, Ballew JD, Reyna SP, Karst ML, Herron KJ, Horton SC, Rodeheffer RJ & Anderson JL (2005). Sodium Channel Mutations and Susceptibility to Heart Failure and Atrial Fibrillation. *JAMA* **293,** 447.

Orlandi A, Francesconi A, Marcelleni M, Ferlosio A & Spagnoli L (2004). Role of ageing and coronary atherosclerosis in the development of cardiac fibrosis in the rabbit. *Cardiovasc Res* **64,** 544–552.

Padeletti L, Michelucci A, Giovannini T, Porciani M, Bamoshmoosh M, Mezzani A, Chelucci A, Pieragnoli P & Gensini G (1995). Wavelength Index at Three Atrial Sites in Patients with Paroxysmal Atrial Fibrillation. *Pacing Clin Electrophysiol* **18,** 1266–1271.

Pandit S V., Berenfeld O, Anumonwo JMB, Zaritski RM, Kneller J, Nattel S & Jalife J (2005). Ionic Determinants of Functional Reentry in a 2-D Model of Human Atrial Cells During Simulated Chronic Atrial Fibrillation. *Biophys J* **88,** 3806–3821.

Pandit S V. & Jalife J (2013). Rotors and the dynamics of cardiac fibrillation. *Circ Res* **112,** 849–862.

Pandozi C, Bianconi L, Villani M, Gentilucci G, Castro A, Altamura G, Jesi AP, Lamberti F, Ammirati F & Santini M (1998). Electrophysiological characteristics of the human atria after cardioversion of persistent atrial fibrillation. *Circulation*; DOI: 10.1161/01.CIR.98.25.2860.

Papadatos GA, Wallerstein PMR, Head CEG, Ratcliff R, Brady P a, Benndorf K, Saumarez RC, Trezise AEO, Huang CL-H, Vandenberg JI, Colledge WH & Grace A a (2002). Slowed conduction and ventricular tachycardia after targeted disruption of the cardiac sodium channel gene Scn5a. *Proc Natl Acad Sci U S A* **99,** 6210–6215.

Papp Z, Sipido KR, Callewaert G & Carmeliet E (1995). Two components of [Ca2+]i-activated Cl- current during large [Ca2+]i transients in single rabbit heart Purkinje cells. *J Physiol* **483 (Pt 2),** 319–330.

Park JH, Pak HN, Kim SK, Jang JK, Choi JI, Lim HE, Hwang C & Kim YH (2009). Electrophysiologic characteristics of complex fractionated atrial electrograms in patients with atrial fibrillation. *J Cardiovasc Electrophysiol* **20,** 266–272.

Pastore JM, Girouard SD, Laurita KR, Akar FG & Rosenbaum DS (1999). Mechanism linking T-wave alternans to the genesis of cardiac fibrillation. *Circulation* **99,** 1385–1394.

Patti M-E & Corvera S (2010). The Role of Mitochondria in the Pathogenesis of Type 2 Diabetes. *Endocr Rev* **31,** 364–395.

Paydak H, Kall JG, Burke MC, Rubenstein D, Kopp DE, Verdino RJ & Wilber DJ (1998). Atrial fibrillation after radiofrequency ablation of type I atrial flutter: time to onset, determinants, and clinical course. *Circulation* **98,** 315–322.

Pérez-Hernández M, Matamoros M, Barana A, Amorós I, Gómez R, Núñez M, Sacristán S, Pinto Á, Fernández-Avilés F, Tamargo J, Delpón E & Caballero R (2016). Pitx2c increases in atrial myocytes from chronic atrial fibrillation patients enhancing IKs and decreasing ICa,L. *Cardiovasc Res* **109,** 431–441.

Perez-Lugones A, McMahon JT, Ratliff NB, Saliba WI, Schweikert RA, Marrouche NF, Saad EB, Navia JL, McCarthy PM, Tchou P, Gillinov AM & Natale A (2003). Evidence of specialized conduction cells in human pulmonary veins of patients with atrial fibrillation. *J Cardiovasc Electrophysiol* **14,** 803–809.

Porter MJ, Morton JB, Denman R, Lin AC, Tierney S, Santucci PA, Cai JJ, Madsen N & Wilber DJ (2004). Influence of age and gender on the mechanism of supraventricular tachycardia. *Hear Rhythm* **1,** 393–396.

Prinzmetal M & Corday E (1950). Mechanism of the auricular arrhythmias. *Circulation* **1,** 241–245.

Priori SG, Pandit S V., Rivolta I, Berenfeld O, Ronchetti E, Dhamoon A, Napolitano C, Anumonwo J, Di Barletta MR, Gudapakkam S, Bosi G, Stramba-Badiale M & Jalife J (2005). A novel form of short QT syndrome (SQT3) is caused by a mutation in the KCNJ2 gene. *Circ Res* **96,** 800–807.

Puigserver P, Rhee J, Donovan J, Walkey CJ, Yoon JC, Oriente F, Kitamura Y, Altomonte J, Dong H, Accili D & Spiegelman BM (2003). Insulin-regulated hepatic gluconeogenesis through FOXO1–

PGC-1α interaction. *Nature* **423,** 550–555.

Puigserver P, Wu Z, Park CW, Graves R, Wright M & Spiegelman BM (1998). A cold-inducible coactivator of nuclear receptors linked to adaptive thermogenesis. *Cell* **92,** 829–839.

Qu Y, Rogers JC, Tanada TN, Catterall WA & Scheuer T (1996). Phosphorylation of S1505 in the cardiac Na+ channel inactivation gate is required for modulation by protein kinase C. *J Gen Physiol* **108,** 375–379.

Qu Z, Kil J, Xie F, Garfinkel A & Weiss JN (2000). Scroll wave dynamics in a three-dimensional cardiac tissue model: roles of restitution, thickness, and fiber rotation. *Biophys J* **78,** 2761–2775.

R Core Team (2015). R: A Language and Environment for Statistical Computing.

Reilly SN, Jayaram R, Nahar K, Antoniades C, Verheule S, Channon KM, Alp NJ, Schotten U & Casadei B (2011). Atrial sources of reactive oxygen species vary with the duration and substrate of atrial fibrillation: implications for the antiarrhythmic effect of statins. *Circulation* **124,** 1107–1117.

Remme CA, Verkerk AO, Nuyens D, van Ginneken ACG, van Brunschot S, Belterman CNW, Wilders R, van Roon MA, Tan HL, Wilde AAM, Carmeliet P, de Bakker JMT, Veldkamp MW & Bezzina CR (2006). Overlap Syndrome of Cardiac Sodium Channel Disease in Mice Carrying the Equivalent Mutation of Human SCN5A-1795insD. *Circulation* **114,** 2584–2594.

Rentschler S, Vaidya DM, Tamaddon H, Degenhardt K, Sassoon D, Morley GE, Jalife J & Fishman GI (2001). Visualization and functional characterization of the developing murine cardiac conduction system. *Development* **128,** 1785–1792.

Rhee J, Inoue Y, Yoon JC, Puigserver P, Fan M, Gonzalez FJ & Spiegelman BM (2003). Regulation of hepatic fasting response by PPAR coactivator-1 (PGC-1): Requirement for hepatocyte nuclear factor 4 in gluconeogenesis. *Proc Natl Acad Sci* **100,** 4012–4017.

Riccio ML, Koller ML & Gilmour RF (1999). Electrical Restitution and Spatiotemporal Organization During Ventricular Fibrillation. *Circ Res*.

Riehle C & Abel ED (2012). PGC-1 proteins and heart failure. *Trends Cardiovasc Med* **22,** 98–105.

Ringer S (1883). A further Contribution regarding the influence of the different Constituents of the Blood on the Contraction of the Heart. *J Physiol* **4,** 29–42.3.

Rodrigo R, Korantzopoulos P, Cereceda M, Asenjo R, Zamorano J, Villalabeitia E, Baeza C, Aguayo R, Castillo R, Carrasco R & Gormaz JG (2013). A Randomized Controlled Trial to Prevent Post-Operative Atrial Fibrillation by Antioxidant Reinforcement. *J Am Coll Cardiol* **62,** 1457–1465.

Rosen MR, Gelband H, Merker C & Hoffman BF (1973). Mechanisms of digitalis toxicity. Effects of ouabain on phase four of canine Purkinje fiber transmembrane potentials. *Circulation* **47,** 681–689.

Rosenbaum DS, Jackson LE, Smith JM, Garan H, Ruskin JN & Cohen RJ (1994). Electrical alternans and vulnerability to ventricular arrhythmias. *N Engl J Med* **330,** 235–241.

Rosenkranz S, Flesch M, Amann K, Haeuseler C, Kilter H, Seeland U, Schlüter K-D & Böhm M (2002). Alterations of β-adrenergic signaling and cardiac hypertrophy in transgenic mice overexpressing TGF-β 1. *Am J Physiol - Hear Circ Physiol* **283,** H1253–H1262.

Ruigómez A, Johansson S, Wallander MA & Rodríguez LAG (2002). Incidence of chronic atrial fibrillation in general practice and its treatment pattern. *J Clin Epidemiol* **55,** 358–363.

Russell LK, Finck BN & Kelly DP (2005). Mouse models of mitochondrial dysfunction and heart failure. *J Mol Cell Cardiol* **38,** 81–91.

Russell LK, Mansfield CM, Lehman JJ, Kovacs A, Courtois M, Saffitz JE, Medeiros DM, Valencik ML, McDonald JA & Kelly DP (2004). Cardiac-specific induction of the transcriptional coactivator peroxisome proliferator-activated receptor gamma coactivator-1alpha promotes mitochondrial biogenesis and reversible cardiomyopathy in a developmental stage-dependent manner. *Circ Res* **94,** 525–533.

Ryan AK, Blumberg B, Rodriguez-Esteban C, Yonei-Tamura S, Tamura K, Tsukui T, de la Peña J, Sabbagh W, Greenwald J, Choe S, Norris DP, Robertson EJ, Evans RM, Rosenfeld MG & Izpisúa Belmonte JC (1998). Pitx2 determines left-right asymmetry of internal organs in vertebrates. *Nature* **394,** 545–551.

Sabir IN, Fraser JA, Cass TR, Grace AA & Huang CL-H (2007*a*). A quantitative analysis of the effect of cycle length on arrhythmogenicity in hypokalaemic Langendorff-perfused murine hearts. *Pflugers Arch* **454,** 925–936.

Sabir IN, Fraser JA, Killeen MJ, Grace AA & Huang CL-H (2007*b*). The contribution of refractoriness to arrhythmic substrate in hypokalemic Langendorff-perfused murine hearts. *Pflugers Arch* **454,** 209–222.

Sabir IN, Killeen MJ, Goddard CA, Thomas G, Gray S, Grace AA & Huang CL-H (2007*c*). Transient alterations in transmural repolarization gradients and arrhythmogenicity in hypokalaemic Langendorff-perfused murine hearts. *J Physiol* **581,** 277–289.

Sabir IN, Killeen MJ, Grace AA & Huang CL-H (2008*a*). Ventricular arrhythmogenesis: insights from murine models. *Prog Biophys Mol Biol* **98,** 208–218.

Sabir IN, Li LM, Grace AA & Huang CL-H (2008*b*). Restitution analysis of alternans and its relationship to arrhythmogenicity in hypokalaemic Langendorff-perfused murine hearts. *Pflugers Arch Eur J Physiol* **455,** 653–666.

Sabir IN, Li LM, Jones VJ, Goddard CA, Grace AA & Huang CL-H (2008*c*). Criteria for arrhythmogenicity in genetically-modified Langendorff-perfused murine hearts modelling the congenital long QT syndrome type 3 and the Brugada syndrome. *Pflugers Arch Eur J Physiol* **455,** 637–651.

Saito T, Waki K & Becker AE (2000). Left atrial myocardial extension onto pulmonary veins in humans: anatomic observations relevant for atrial arrhythmias. *J Cardiovasc Electrophysiol* **11,** 888–894.

Saitoh H, Bailey JC & Surawicz B (1988). Alternans of action potential duration after abrupt shortening of cycle length: differences between dog Purkinje and ventricular muscle fibers. *Circ*

Res **62,** 1027–1040.

Salvage S, Chandrasekharan, KH Jeevaratnam K, Dulhunty A, Thompson A, Jackson A & Huang C-H (2017). Multiple targets for flecainide action: implications for cardiac arrhythmogenesis. *Br J Pharmacol*.

Salvage SC, King JH, Chandrasekharan KH, Jafferji DIG, Guzadhur L, Matthews HR, Huang CL-H & Fraser JA (2015). Flecainide exerts paradoxical effects on sodium currents and atrial arrhythmia in murine RyR2-P2328S hearts. *Acta Physiol* **214,** 361–375.

Sanguinetti MC & Jurkiewicz NK (1990). Two components of cardiac delayed rectifier K+ current. Differential sensitivity to block by class III antiarrhythmic agents. *J Gen Physiol* **96,** 195–215.

Sato D, Xie L-H, Sovari AA, Tran DX, Morita N, Xie F, Karagueuzian H, Garfinkel A, Weiss JN & Qu Z (2009). Synchronization of chaotic early afterdepolarizations in the genesis of cardiac arrhythmias. *Proc Natl Acad Sci* **106,** 2983–2988.

Scarpulla RC (2002). Nuclear activators and coactivators in mammalian mitochondrial biogenesis. *Biochim Biophys Acta* **1576,** 1–14.

Schaper J, Meiser E & Stämmler G (1985). Ultrastructural morphometric analysis of myocardium from dogs, rats, hamsters, mice, and from human hearts. *Circ Res* **56,** 377–391.

Scherf D, Schaffer AI & Blumenfeld S (1953). Mechanism of flutter and fibrillation. *AMA Arch Intern Med* **91,** 333–352.

Scherf D & Terranova R (1949). Mechanism of auricular flutter and fibrillation. *Am J Physiol Content* **159,** 137–142.

Schnabel RB, Sullivan LM, Levy D, Pencina MJ, Massaro JM, D'Agostino RB, Newton-Cheh C, Yamamoto JF, Magnani JW, Tadros TM, Kannel WB, Wang TJ, Ellinor PT, Wolf PA, Vasan RS & Benjamin EJ (2009). Development of a risk score for atrial fibrillation (Framingham Heart Study): a community-based cohort study. *Lancet* **373,** 739–745.

Seppet E, Eimre M, Peet N, Paju K, Orlova E, Ress M, Kõvask S, Piirsoo A, Saks VA, Gellerich FN, Zierz S & Seppet EK (2005). Compartmentation of energy metabolism in atrial myocardium of patients undergoing cardiac surgery. *Mol Cell Biochem* **270,** 49–61.

Shan J, Xie W, Betzenhauser M, Reiken S, Chen B-X, Wronska A & Marks AR (2012). Calcium leak through ryanodine receptors leads to atrial fibrillation in 3 mouse models of catecholaminergic polymorphic ventricular tachycardia. *Circ Res* **111,** 708–717.

Shi R, Li Z-H, Chen D, Wu Q-C, Zhou X-L & Tie H-T (2018). Sole and combined vitamin C supplementation can prevent postoperative atrial fibrillation after cardiac surgery: A systematic review and meta-analysis of randomized controlled trials. *Clin Cardiol* **41,** 871–878.

Siasos G, Tsigkou V, Kosmopoulos M, Theodosiadis D, Simantiris S, Tagkou NM, Tsimpiktsioglou A, Stampouloglou PK, Oikonomou E, Mourouzis K, Philippou A, Vavuranakis M, Stefanadis C, Tousoulis D & Papavassiliou AG (2018). Mitochondria and cardiovascular diseases-from pathophysiology to treatment. *Ann Transl Med* **6,** 256.

Silverman ME (1989). William Withering and An Account of the Foxglove. *Clin Cardiol* **12,** 415–418.

Silverman ME (1994). From rebellious palpitations to the discovery of auricular fibrillation: contributions of Mackenzie, Lewis and Einthoven. *Am J Cardiol* **73,** 384–389.

Slagsvold KH, Johnsen AB, Rognmo O, Høydal M, Wisløff U & Wahba A (2014). Comparison of left versus right atrial myocardium in patients with sinus rhythm or atrial fibrillation - an assessment of mitochondrial function and microRNA expression. *Physiol Rep*; DOI: 10.14814/phy2.12124.

Smyth JW, Hong TT, Gao D, Vogan JM, Jensen BC, Fong TS, Simpson PC, Stainier DYR, Chi NC & Shaw RM (2010). Limited forward trafficking of connexin 43 reduces cell-cell coupling in stressed human and mouse myocardium. *J Clin Invest* **120,** 266–279.

Sonoda J, Mehl IR, Chong L-W, Nofsinger RR & Evans RM (2007). PGC-1beta controls mitochondrial metabolism to modulate circadian activity, adaptive thermogenesis, and hepatic steatosis. *Proc Natl Acad Sci U S A* **104,** 5223–5228.

Sossalla S, Kallmeyer B, Wagner S, Mazur M, Maurer U, Toischer K, Schmitto JD, Seipelt R, Schöndube FA, Hasenfuss G, Belardinelli L & Maier LS (2010). Altered Na(+) currents in atrial fibrillation effects of ranolazine on arrhythmias and contractility in human atrial myocardium. *J Am Coll Cardiol* **55,** 2330–2342.

Sovari AA, Rutledge CA, Jeong E-M, Dolmatova E, Arasu D, Liu H, Vahdani N, Gu L, Zandieh S, Xiao L, Bonini MG, Duffy HS & Dudley SC (2013). Mitochondria Oxidative Stress, Connexin43 Remodeling, and Sudden Arrhythmic Death. *Circ Arrhythmia Electrophysiol* **6,** 623–631.

Spach MS & Boineau JP (1997). Microfibrosis produces electrical load variations due to loss of side-to-side cell connections: a major mechanism of structural heart disease arrhythmias. *Pacing Clin Electrophysiol* **20,** 397–413.

Spach MS, Dolber PC & Heidlage JF (1988). Influence of the passive anisotropic properties on directional differences in propagation following modification of the sodium conductance in human atrial muscle. A model of reentry based on anisotropic discontinuous propagation. *Circ Res* **62,** 811–832.

Spach MS, Miller WT, Dolber PC, Kootsey JM, Sommer JR & Mosher CE (1982). The functional role of structural complexities in the propagation of depolarization in the atrium of the dog. Cardiac conduction disturbances due to discontinuities of effective axial resistivity. *Circ Res* **50,** 175–191.

Spector P (2013). Principles of cardiac electric propagation and their implications for re-entrant arrhythmias. *Circ Arrhythm Electrophysiol* **6,** 655–661.

Stiles MK, John B, Wong CX, Kuklik P, Brooks AG, Lau DH, Dimitri H, Roberts-Thomson KC, Wilson L, De Sciscio P, Young GD & Sanders P (2009). Paroxysmal lone atrial fibrillation is associated with an abnormal atrial substrate: characterizing the "second factor". *J Am Coll Cardiol* **53,** 1182–1191.

Stokoe KS, Balasubramaniam R, Goddard CA, Colledge WH, Grace AA & Huang CL-H (2007). Effects of flecainide and quinidine on arrhythmogenic properties of *Scn5a* +/− murine hearts modelling the Brugada syndrome. *J Physiol* **581,** 255–275.

Stühmer W, Roberts WM & Almers W (1983). The Loose Patch Clamp. In *Single-Channel Recording*, ed. Sakmann B & Neher E, pp. 123–132. Springer US.

Sullivan DE, Ferris M, Pociask D & Brody AR (2008). The Latent Form of TGFβ 1 is Induced by TNFα Through an ERK Specific Pathway and is Activated by Asbestos-Derived Reactive Oxygen Species *In Vitro* and *In Vivo*. *J Immunotoxicol* **5,** 145–149.

Sultan A, Lüker J, Andresen D, Kuck KH, Hoffmann E, Brachmann J, Hochadel M, Willems S, Eckardt L, Lewalter T, Senges J & Steven D (2017). Predictors of Atrial Fibrillation Recurrence after Catheter Ablation: Data from the German Ablation Registry. *Sci Rep* **7,** 16678.

Sun N, Youle RJ & Finkel T (2016). The Mitochondrial Basis of Aging. *Mol Cell* **61,** 654–666.

Tada H, Oral H, Ozaydin M, Greenstein R, Pelosi F, Knight BP, Strickberger SA & Morady F (2002). Response of pulmonary vein potentials to premature stimulation. *J Cardiovasc Electrophysiol* **13,** 33–37.

Taggart P, Sutton PM, Boyett MR, Lab M & Swanton H (1996). Human ventricular action potential duration during short and long cycles. Rapid modulation by ischemia. *Circulation* **94,** 2526–2534.

Tan HL, Kupershmidt S, Zhang R, Stepanovic S, Roden DM, Wilde AAM, Anderson ME & Balser JR (2002). A calcium sensor in the sodium channel modulates cardiac excitability. *Nature* **415,** 442–447.

Tawara S (1906). *Das Reizleitungenssystem des Säugetierherzens : eine anatomisch-histologische Studie über das Atrioventrikularbündel und die Purkinjeschen Fäden : Tawara, S. (Sunao), 1873-1952 : Free Download, Borrow, and Streaming : Internet Archive*. Available at: https://archive.org/details/dasreizleitungen00tawa [Accessed September 27, 2018].

Tedrow UB, Conen D, Ridker PM, Cook NR, Koplan BA, Manson JE, Buring JE & Albert CM (2010). The long- and short-term impact of elevated body mass index on the risk of new atrial fibrillation the WHS (women's health study). *JAmCollCardiol* **55,** 2319–2327.

Tellez JO, Mączewski M, Yanni J, Sutyagin P, Mackiewicz U, Atkinson A, Inada S, Beresewicz A, Billeter R, Dobrzynski H & Boyett MR (2011). Ageing-dependent remodelling of ion channel and Ca 2+ clock genes underlying sino-atrial node pacemaking. *Exp Physiol* **96,** 1163–1178.

Terentyev D, Györke I, Belevych AE, Terentyeva R, Sridhar A, Nishijima Y, De Blanco EC, Khanna S, Sen CK, Cardounel AJ, Carnes CA & Györke S (2008). Redox modification of ryanodine receptors contributes to sarcoplasmic reticulum Ca2+ leak in chronic heart failure. *Circ Res* **103,** 1466–1472.

Tessier S, Karczewski P, Krause EG, Pansard Y, Acar C, Lang-Lazdunski M, Mercadier JJ & Hatem SN (1999). Regulation of the transient outward K(+) current by Ca(2+)/calmodulin-dependent protein kinases II in human atrial myocytes. *Circ Res* **85,** 810–819.

Thery C, Gosselin B, Lekieffre J & Warembourg H (1977). Pathology of sinoatrial node. Correlations with electrocardiographic findings in 111 patients. *Am Heart J* **93,** 735–740.

Thomas G, Gurung IS, Killeen MJ, Hakim P, Goddard CA, Mahaut-Smith MP, Colledge WH, Grace AA & Huang CL-H (2007). Effects of L-type Ca(2+) channel antagonism on ventricular

arrhythmogenesis in murine hearts containing a modification in the Scn5a gene modelling human long QT syndrome 3. *J Physiol* **578,** 85–97.

Tsai CF, Tai CT, Hsieh MH, Lin WS, Yu WC, Ueng KC, Ding YA, Chang MS & Chen SA (2000). Initiation of atrial fibrillation by ectopic beats originating from the superior vena cava: electrophysiological characteristics and results of radiofrequency ablation. *Circulation* **102,** 67–74.

Tsuboi M, Hisatome I, Morisaki T, Tanaka M, Tomikura Y, Takeda S, Shimoyama M, Ohtahara A, Ogino K, Igawa O, Shigemasa C, Ohgi S & Nanba E (2001). Mitochondrial DNA deletion associated with the reduction of adenine nucleotides in human atrium and atrial fibrillation. *Eur J Clin Invest* **31,** 489–496.

Tutuianu C, Szilagy J, Pap R & Sághy L (2015). Very Long-Term Results Of Atrial Fibrillation Ablation Confirm That This Therapy Is Really Effective. *J Atr Fibrillation* **8,** 1226.

Usher-Smith JA, Xu W, Fraser JA & Huang CL-H (2006). Alterations in calcium homeostasis reduce membrane excitability in amphibian skeletal muscle. *Pflügers Arch - Eur J Physiol* **453,** 211–221.

Vaidya D, Morley GE, Samie FH & Jalife J (1999). Reentry and fibrillation in the mouse heart. A challenge to the critical mass hypothesis. *Circ Res* **85,** 174–181.

Vajda S, Baczkó I & Leprán I (2007). Selective cardiac plasma-membrane K(ATP) channel inhibition is defibrillatory and improves survival during acute myocardial ischemia and reperfusion. *Eur J Pharmacol* **577,** 115–123.

Valli H, Ahmad S, Sriharan S, Dean LD, Grace AA, Jeevaratnam K, Matthews HR & Huang CL-H (2018). Epac-induced ryanodine receptor type 2 activation inhibits sodium currents in atrial and ventricular murine cardiomyocytes. *Clin Exp Pharmacol Physiol* **45,** 278–292.

Varró A, Nánási PP & Lathrop DA (1993). Potassium currents in isolated human atrial and ventricular cardiocytes. *Acta Physiol Scand* **149,** 133–142.

van Veen TAB, Stein M, Royer A, Le Quang K, Charpentier F, Colledge WH, Huang CL-H, Wilders R, Grace AA, Escande D, de Bakker JMT & van Rijen HVM (2005). Impaired Impulse Propagation in Scn5a-Knockout Mice: Combined Contribution of Excitability, Connexin Expression, and Tissue Architecture in Relation to Aging. *Circulation* **112,** 1927–1935.

Vega RB, Huss JM & Kelly DP (2000). The coactivator PGC-1 cooperates with peroxisome proliferator-activated receptor alpha in transcriptional control of nuclear genes encoding mitochondrial fatty acid oxidation enzymes. *Mol Cell Biol* **20,** 1868–1876.

Venetucci LA, Trafford AW, O'Neill SC & Eisner DA (2007). Na/Ca exchange: regulator of intracellular calcium and source of arrhythmias in the heart. *Ann N Y Acad Sci* **1099,** 315–325.

Verheule S, Sat T, Everett IV T, Engle SK, Otten D, Rubart-Von Der Lohe M, Nakajima HO, Nakajima H, Field LJ & Olgin JE (2004). Increased vulnerability to atrial fibrillation in transgenic mice with selective atrial fibrosis caused by overexpression of TGF-β1. *Circ Res* **94,** 1458–1465.

Verma A, Jiang C, Betts TR, Chen J, Deisenhofer I, Mantovan R, Macle L, Morillo CA, Haverkamp W, Weerasooriya R, Albenque J-P, Nardi S, Menardi E, Novak P, Sanders P & STAR AF II Investigators (2015). Approaches to Catheter Ablation for Persistent Atrial Fibrillation. *N Engl J*

Med **372,** 1812–1822.

Verrier RL & Nearing BD (1994). Electrophysiologic basis for T wave alternans as an index of vulnerability to ventricular fibrillation. *J Cardiovasc Electrophysiol* **5,** 445–461.

Vest JA, Wehrens XHT, Reiken SR, Lehnart SE, Dobrev D, Chandra P, Danilo P, Ravens U, Rosen MR & Marks AR (2005). Defective cardiac ryanodine receptor regulation during atrial fibrillation. *Circulation* **111,** 2025–2032.

Vianna CR, Huntgeburth M, Coppari R, Choi CS, Lin J, Krauss S, Barbatelli G, Tzameli I, Kim Y-B, Cinti S, Shulman GI, Spiegelman BM & Lowell BB (2006). Hypomorphic mutation of PGC-1beta causes mitochondrial dysfunction and liver insulin resistance. *Cell Metab* **4,** 453–464.

Vidaillet H, Granada JF, Chyou P o-H, Maassen K, Ortiz M, Pulido JN, Sharma P, Smith PN & Hayes J (2002). A population-based study of mortality among patients with atrial fibrillation or flutter. *Am J Med* **113,** 365–370.

Virbasius CA, Virbasius J V & Scarpulla RC (1993). NRF-1, an activator involved in nuclear-mitochondrial interactions, utilizes a new DNA-binding domain conserved in a family of developmental regulators. *Genes Dev* **7,** 2431–2445.

Wagner S, Hacker E, Grandi E, Weber SL, Dybkova N, Sossalla S, Sowa T, Fabritz L, Kirchhof P, Bers DM & Maier LS (2009). Ca/calmodulin kinase II differentially modulates potassium currents. *Circ Arrhythm Electrophysiol* **2,** 285–294.

Wagner S, Ruff HM, Weber SL, Bellmann S, Sowa T, Schulte T, Anderson ME, Grandi E, Bers DM, Backs J, Belardinelli L & Maier LS (2011). Reactive oxygen species-activated Ca/calmodulin kinase IIδ is required for late I(Na) augmentation leading to cellular Na and Ca overload. *Circ Res* **108,** 555–565.

Van Wagoner DR, Pond AL, Lamorgese M, Rossie SS, McCarthy PM & Nerbonne JM (1999). Atrial L-type Ca2+ currents and human atrial fibrillation. *Circ Res* **85,** 428–436.

Van Wagoner DR, Pond AL, McCarthy PM, Trimmer JS & Nerbonne JM (1997). Outward K+ current densities and Kv1.5 expression are reduced in chronic human atrial fibrillation. *Circ Res* **80,** 772–781.

Wan X, Laurita KR, Pruvot EJ & Rosenbaum DS (2005). Molecular correlates of repolarization alternans in cardiac myocytes. *J Mol Cell Cardiol* **39,** 419–428.

Wanahita N, Messerli FH, Bangalore S, Gami AS, Somers VK & Steinberg JS (2008). Atrial fibrillation and obesity—results of a meta-analysis. *Am Heart J* **155,** 310–315.

Wang J, Klysik E, Sood S, Johnson RL, Wehrens XHT & Martin JF (2010). Pitx2 prevents susceptibility to atrial arrhythmias by inhibiting left-sided pacemaker specification. *Proc Natl Acad Sci* **107,** 9753–9758.

Wang J, Wang H, Zhang Y, Gao H, Nattel S & Wang Z (2004). Impairment of HERG K(+) channel function by tumor necrosis factor-alpha: role of reactive oxygen species as a mediator. *J BiolChem* **279,** 13289–13292.

Wang J, Wilhelmsson H, Graff C, Li H, Oldfors A, Rustin P, Brüning JC, Kahn CR, Clayton DA, Barsh GS, Thorén P & Larsson NG (1999). Dilated cardiomyopathy and atrioventricular conduction blocks induced by heart-specific inactivation of mitochondrial DNA gene expression. *Nat Genet* **21,** 133–137.

Wang TJ, Larson MG, Levy D, Vasan RS, Leip EP, Wolf PA, D'Agostino RB, Murabito JM, Kannel WB & Benjamin EJ (2003). Temporal relations of atrial fibrillation and congestive heart failure and their joint influence on mortality: the Framingham Heart Study. *Circulation* **107,** 2920–2925.

Wang Y, Cheng J, Joyner RW, Wagner MB & Hill JA (2006). Remodeling of Early-Phase Repolarization: A Mechanism of Abnormal Impulse Conduction in Heart Failure. *Circulation* **113,** 1849–1856.

Watanabe H, Chopra N, Laver D, Hwang HS, Davies SS, Roach DE, Duff HJ, Roden DM, Wilde AAM & Knollmann BC (2009). Flecainide prevents catecholaminergic polymorphic ventricular tachycardia in mice and humans. *Nat Med* **15,** 380–383.

Watanabe H, Tanabe N, Watanabe T, Darbar D, Roden DM, Sasaki S & Aizawa Y (2008). Metabolic syndrome and risk of development of atrial fibrillation: the Niigata preventive medicine study. *Circulation* **117,** 1255–1260.

Watanabe MA, Fenton FH, Evans SJ, Hastings HM & Karma A (2001). Mechanisms for discordant alternans. *J Cardiovasc Electrophysiol* **12,** 196–206.

Wehrens XH, Kirchhoff S & Doevendans PA (2000). Mouse electrocardiography: an interval of thirty years. *Cardiovasc Res* **45,** 231–237.

Weidmann S (1993). Cardiac Action Potentials, Membrane Currents, and Some Personal Reminiscences. *Annu Rev Physiol* **55,** 1–18.

Weiss JN, Garfinkel A, Karagueuzian HS, Chen P-S & Qu Z (2010). Early afterdepolarizations and cardiac arrhythmias. *Hear Rhythm* **7,** 1891–1899.

Weiss JN, Qu Z, Chen PS, Lin SF, Karagueuzian HS, Hayashi H, Garfinkel A & Karma A (2005). The dynamics of cardiac fibrillation. *Circulation* **112,** 1232–1240.

van der Werf C, Kannankeril PJ, Sacher F, Krahn AD, Viskin S, Leenhardt A, Shimizu W, Sumitomo N, Fish FA, Bhuiyan ZA, Willems AR, van der Veen MJ, Watanabe H, Laborderie J, Haïssaguerre M, Knollmann BC & Wilde AAM (2011). Flecainide Therapy Reduces Exercise-Induced Ventricular Arrhythmias in Patients With Catecholaminergic Polymorphic Ventricular Tachycardia. *J Am Coll Cardiol* **57,** 2244–2254.

Wijffels MC, Kirchhof CJ, Dorland R & Allessie MA (1995). Atrial fibrillation begets atrial fibrillation. A study in awake chronically instrumented goats. *Circulation* **92,** 1954–1968.

Wingo TL, Shah VN, Anderson ME, Lybrand TP, Chazin WJ & Balser JR (2004). An EF-hand in the sodium channel couples intracellular calcium to cardiac excitability. *Nat Struct Mol Biol* **11,** 219–225.

Wit AL & Cranefield PF (1978). Reentrant excitation as a cause of cardiac arrhythmias. *Am J Physiol Circ Physiol* **235,** H1–H17.

Wolf PA, Dawber TR, Thomas HE & Kannel WB (1978). Epidemiologic assessment of chronic atrial fibrillation and risk of stroke: the Framingham study. *Neurology* **28,** 973–977.

Wu EQ, Birnbaum HG, Mareva M, Tuttle E, Castor AR, Jackman W & Ruskin J (2005*a*). Economic burden and co-morbidities of atrial fibrillation in a privately insured population. *Curr Med Res Opin* **21,** 1693–1699.

Wu G, Huang C, Tang Y, Jiang H, Wan J, Chen H, Xie Q & Huang Z (2005*b*). Changes of IK, ATP current density and allosteric modulation during chronic atrial fibrillation. *Chin Med J (Engl)* **118,** 1161–1166.

Wu J, Zhang Y, Zhang X, Cheng L, Lammers WJ, Grace AA, Fraser JA, Zhang H, Huang CL-H & Lei M (2012). Altered sinoatrial node function and intra-atrial conduction in murine gain-of-function Scn5a+/ KPQ hearts suggest an overlap syndrome. *AJP Hear Circ Physiol* **302,** H1510–H1523.

Wu Z, Puigserver P, Andersson U, Zhang C, Adelmant G, Mootha V, Troy A, Cinti S, Lowell B, Scarpulla RC & Spiegelman BM (1999). Mechanisms controlling mitochondrial biogenesis and respiration through the thermogenic coactivator PGC-1. *Cell* **98,** 115–124.

Xie W, Santulli G, Reiken SR, Yuan Q, Osborne BW, Chen B-X & Marks AR (2015). Mitochondrial oxidative stress promotes atrial fibrillation. *Sci Rep* **5,** 11427.

Xie Y, Garfinkel A, Camelliti P, Kohl P, Weiss JN & Qu Z (2009). Effects of fibroblast-myocyte coupling on cardiac conduction and vulnerability to reentry: A computational study. *Hear Rhythm* **6,** 1641–1649.

Yamazaki M, Filgueiras-Rama D, Berenfeld O & Kalifa J (2012). Ectopic and reentrant activation patterns in the posterior left atrium during stretch-related atrial fibrillation. *Prog Biophys Mol Biol* **110,** 269–277.

Yan GX & Antzelevitch C (1998). Cellular basis for the normal T wave and the electrocardiographic manifestations of the long-QT syndrome. *Circulation* **98,** 1928–1936.

Yan X, Ma J & Zhang P (2009). Modulation of KATP currents in rat ventricular myocytes by hypoxia and a redox reaction. *Acta Pharmacol Sin* **30,** 1399–1414.

Yang K-C, Bonini MG & Dudley SC (2014). Mitochondria and arrhythmias. *Free Radic Biol Med* **71,** 351–361.

Yang S, Yang Z, Wu C, Li W & Xu H (2015). [Electrophysiological properties and mechanism of aging for the susceptibility of left atrium to arrhythmogenesis in rabbits]. *Zhonghua Yi Xue Za Zhi* **95,** 2302–2306.

Yanni J, Tellez JO, Sutyagin PV, Boyett MR & Dobrzynski H (2010). Structural remodelling of the sinoatrial node in obese old rats. *J Mol Cell Cardiol* **48,** 653–662.

Yeung C-Y, Lam K-FKS-L, Li S-W, Lam K-FKS-L, Tse H-F & Siu C-W (2012). Sudden cardiac death after myocardial infarction in type 2 diabetic patients with no residual myocardial ischemia. *Diabetes Care*; DOI: 10.2337/dc12-0118.

Ypey DL, van Meerwijk WPM, Umar S, Pijnappels DA, Schalij MJ & van der Laarse A (2013). No

TitleDepolarization-induced automaticity in rat ventricular cardiomyocytes is based on the gating properties of L-type calcium and slow Kv channels. *Eur Biophys J*; DOI: 10.1007/s00249-012-0866-9.

Yu WC, Lee SH, Tai CT, Tsai CF, Hsieh MH, Chen CC, Ding YA, Chang MS & Chen SA (1999). Reversal of atrial electrical remodeling following cardioversion of long-standing atrial fibrillation in man. *Cardiovasc Res* **42,** 470–476.

Zaitsev A V, Berenfeld O, Mironov SF, Jalife J & Pertsov AM (2000). Distribution of excitation frequencies on the epicardial and endocardial surfaces of fibrillating ventricular wall of the sheep heart. *Circ Res* **86,** 408–417.

Zeng J & Rudy Y (1995). Early afterdepolarizations in cardiac myocytes: mechanism and rate dependence. *Biophys J* **68,** 949–964.

Zhang X, Zhang S, Li Y, Detrano RC, Chen K, Li X, Zhao L, Benjamin EJ & Wu Y (2009*a*). Association of obesity and atrial fibrillation among middle-aged and elderly Chinese. *Int J Obes* **33,** 1318–1325.

Zhang Y, Castellani LW, Sinal CJ, Gonzalez FJ & Edwards PA (2004). Peroxisome proliferator-activated receptor-gamma coactivator 1alpha (PGC-1alpha) regulates triglyceride metabolism by activation of the nuclear receptor FXR. *Genes Dev* **18,** 157–169.

Zhang Y, Fraser JA, Jeevaratnam K, Hao X, Hothi SS, Grace AA, Lei M & Huang CL-H (2011). Acute atrial arrhythmogenicity and altered Ca(2+) homeostasis in murine RyR2-P2328S hearts. *Cardiovasc Res* **89,** 794–804.

Zhang Y, Guzadhur L, Jeevaratnam K, Salvage SC, Matthews GD, Lammers WJ, Lei M, Huang CL-H & Fraser JA (2014*a*). Arrhythmic substrate, slowed propagation and increased dispersion in conduction direction in the right ventricular outflow tract of murine Scn5a+/- hearts. *Acta Physiol* **211,** 559–573.

Zhang Y, Schwiening C, Killeen MJ, Zhang Y, Ma A, Lei M, Grace AA & Huang CL-H (2009*b*). Pharmacological changes in cellular Ca $^{2+}$ homeostasis parallel initiation of atrial arrhythmogenesis in murine langendorff-perfused hearts. *Clin Exp Pharmacol Physiol* **36,** 969–980.

Zhang Y, Wu J, Jeevaratnam K, King JH, Guzadhur L, REN X, GRACE AA, Lei M, Huang CL-HL-H & Fraser JA (2013). Conduction slowing contributes to spontaneous ventricular arrhythmias in intrinsically active murine RyR2-P2328S hearts. *J Cardiovasc Electrophysiol* **24,** 210–218.

Zhang Y, Wu J, King JH, Huang CL-H & Fraser JA (2014*b*). Measurement and interpretation of electrocardiographic QT intervals in murine hearts. *Am J Physiol Heart Circ Physiol* **306,** H1553-7.

Zheng Y, Xia Y, Carlson J, Kongstad O & Yuan S (2016). Atrial average conduction velocity in patients with and without paroxysmal atrial fibrillation. *Clin Physiol Funct Imaging*n/a-n/a.

Zoni-Berisso M, Lercari F, Carazza T & Domenicucci S (2014). Epidemiology of atrial fibrillation: European perspective. *Clin Epidemiol* **6,** 213–220.